UNIVERSITY OF SOUTHAMPTON

Faculty of Natural and Environmental Sciences

School of Biological Sciences

Volume 1 of 1

DNA Damage Response and Repair in Mouse Oocytes

by

Josie Kate Collins

Thesis for the degree of Doctor of Philosophy

August 2016

UNIVERSITY OF SOUTHAMPTON

ABSTRACT

FACULTY OF NATURAL AND ENVIRONMENTAL SCIENCES

School of Biological Sciences

Thesis for the degree of Doctor of Philosophy

DNA DAMAGE RESPONSE AND REPAIR IN MOUSE OOCYTES

By Josie Kate Collins

This thesis investigates the response of mouse oocytes to DNA damage, and their ability to repair such damage. The effect on the progression through the first meiotic division is examined, using a variety of agents to induce DNA damage, with a particular focus on germinal vesicle breakdown and polar body extrusion. It is shown that although oocytes with DNA damage can readily resume meiosis, there is a mechanism that exists to prevent the formation of a potentially fertilisable egg with DNA damage, by arresting at metaphase I. The pathways that lead to this arrest are also explored; specifically the activities of the Spindle Assembly Checkpoint (SAC) and the Anaphase Promoting Complex (APC). Using pharmacological inhibitors coupled with time-lapse fluorescence microscopy it is shown that the DNA damage induced arrest is mediated by the SAC, which in turn inhibits the APC. It is also shown that oocytes are able to detect and signal DNA damage through the phosphorylation of histone H2AX. The ability of the oocyte to repair DNA damage is demonstrated using an immunofluorescence based assay. The role of major DNA damage response proteins, ATM and ATR, is explored using pharmacological inhibitors and genetically modified mice. These proteins are shown to reduce the signalling of DNA damage in oocytes but do not appear to function in activating the SAC, to induce an arrest, in response to DNA damage. These findings highlight an important mechanism that exists to prevent a fertilisable egg with DNA damage from being produced. Such an egg, if fertilised, could lead to defective embryo development or miscarriage. More specifically, it has shown that the SAC may also have a novel and alternative function in oocytes. Altogether this work has implications for the maintenance of female fertility during the treatment of cancer, but also during the age-related decline in fertility.

Table of Contents

List of Tables

List of Figures

DECLARATION OF AUTHORSHIP

I, Josie Kate Collins

declare that this thesis and the work presented in it are my own and has been generated by me as the result of my own original research.

DNA Damage Response and Repair in Mouse Oocytes

I confirm that:

1. This work was done wholly or mainly while in candidature for a research degree at this University;
2. Where any part of this thesis has previously been submitted for a degree or any other qualification at this University or any other institution, this has been clearly stated;
3. Where I have consulted the published work of others, this is always clearly attributed;
4. Where I have quoted from the work of others, the source is always given. With the exception of such quotations, this thesis is entirely my own work;
5. I have acknowledged all main sources of help;
6. Where the thesis is based on work done by myself jointly with others, I have made clear exactly what was done by others and what I have contributed myself;
7. [Delete as appropriate] None of this work has been published before submission [or] Parts of this work have been published as: [please list references below]:

Signed: .....

Date: .....

Acknowledgements

I would like to take this opportunity to thank Prof. Keith Jones for his supervision and the advice he has provided throughout my PhD.

I also want to thank my family, in particular my Mum and my Nan, for their never-ending belief in me and for all of the encouragement and support they have given.

Thank you to all of the members of the Jones' Lab for their guidance and company throughout my PhD.

Finally, I thank Adam, for all of his kindness, support and for always being understanding. Without him, I don't know how I would have made it through.

Definitions and Abbreviations

A-T - Ataxia-telangiectasia

AT-LD - Ataxia-telangiectasia like disease

ATM - Ataxia Telangiectasia Mutated

ATR - Ataxia Telangiectasia and Rad3 Related

ATRIP - ATR interacting protein

APC - Anaphase Promoting Complex

BER - Base excision repair

BLM - Bloom Helicase

BUB1 - Budding Uninhibited by Benzimidazoles 1

BUBR1 - Mitotic Checkpoint Serine/Threonine Kinase B

cAMP - Cyclic adenosine monophosphate

CDK - Cyclin dependant kinase

cGMP - Cyclic guanosine monophosphate

CHK1 - Checkpoint Kinase 1

CHK2 - Checkpoint Kinase 2

CPD - Cyclobutane Pyrimidine Dimer

CO - Crossover

COC- Cumulus Oocyte Complex

DDB1 - DNA damage binding protein 1

DDB2 - DNA damage binding protein 2

DDR - DNA Damage Response

DMC1 - DNA Meiotic Recombinase 1

DNA-PK - DNA-dependent protein kinase

DSB - Double Strand Break

EME1 - Essential Meiotic Structure-specific Endonuclease 1

FHA - Forkhead-associated domain

FSH - Follicle-stimulating hormone

GPCR - G-protein-coupled receptor

GST - Glutathione S-transferase

GV - Germinal Vesicle

GVBD - Germinal Vesicle Breakdown

HJ - Holliday Junction

HR - Homologous Recombination

HR23B - RAD23 homolog B

IR - Ionising Radiation

LC3 - Microtubule associated protein 1/ light chain 3

LH - Luteinising hormone

MAD2 - Mitotic Arrest Deficient 2

MCC - Mitotic checkpoint complex

MDM2 – Mouse double minute 2 homolog

MEF - Mouse embryonic fibroblast

MI - Meiosis I

MII - Meiosis II

MLH1 - MutL Homolog 1

MLH3 - MutL Homolog 3

MMC - Mitomycin C

MMR - Mismatch repair

MND1 - Meiotic Nuclear Divisions 1

MPS1- Monopolar Spindle 1

MRN - MRE11/RAD50/NBS1

MSH4 - MutS Holmolog 4

MSH5 - MutS Homolog 5

MTOC – Microtubule-organising centre

NBS - Nijmegen breakage syndrome

NCO – Non-crossover

NCS - Neocarzinostatin

NHEJ - Non-homologous end joining

NER - Nucleotide excision repair

PB - Polar Body

PBE - Polar Body Extrusion

PDE3 - Phosphodiesterase 3

PGCs - Primordial Germ Cells

PI3K - Phosphoinositide 3-kinase

PKA - Protein kinase A

POF - Premature Ovarian Failure

RNF212 - Ring Finger Protein 212

ROS - Reactive Oxygen Species

RA - Retanoic acid

RPA - Replication protein A

SAC - Spindle Assembly Checkpoint

SC - Synaptonemal complex

SCD - S/T-Q cluster domain

SGO2 - Shugoshin 2

ssDNA - single stranded DNA

TFIIH - Transcription factor II Human

TOPBP1 - DNA Topoisomerase DNA II Binding Protein 1

UV - Ultraviolet

XLF - XRCC4-like factor

XPA - Xeroderma pigmentosum group A

XPB - Xeroderma pigmentosum group B

XPC - Xeroderma pigmentosum group C

XPD - Xeroderma pigmentosum group D

XPF - Xeroderma pigmentosum group F

XPG - Xeroderma pigmentosum group G

Chapter 1: Introduction

This thesis focuses on the DNA damage response and repair of DNA damage in mouse oocytes. Therefore, the aim of this introduction is to provide an overview of a variety of topics that are of interest for this project. I will introduce the different types of DNA damage that can be encountered and the responses that can be elicited in somatic cells, as well as an overview of different repair mechanisms that can be used to rid the cell of such damage. I will also give an overview of oocyte development and what is currently known about their response to DNA damage.

1.1 The DNA Damage Response

DNA damage is common occurrence in the life of a somatic cell and can be dangerous if not resolved accordingly. Due to this, ways to deal with such insults have evolved over time. There are several responses to DNA damage which include, but are not limited to, the arrest of the cell cycle or apoptosis. Checkpoints can occur at several points throughout the cell cycle such as the G1/S, intra-S and G2/M transitions (Sancar et al. 2004). Whereas apoptosis is usually induced when damage is severe and cannot be repaired (Roos and Kaina 2006, Roos and Kaina 2013, Sancar et al. 2004). The majority of our knowledge on the DNA Damage response (DDR) and the checkpoint arrests involved is based on extensive investigation in somatic cells. In contrast relatively little is known concerning the response to, or repair of, DNA damage at the different stages in oocyte development.

1.2 Types of DNA damage

There are a variety of sources that can contribute to damaging the DNA within a cell. The most common source of DNA damage arises endogenously as a result of replication errors, spontaneous depurination or deamination of bases, or damaging factors produced as a by-product of metabolism (Helleday et al. 2014, Kryston et al. 2011). The types of damage that can be caused as a result of this includes base-pair mismatches, insertions or deletions (Sancar et al. 2004, Shiloh 2003). Also base alterations, such as the formation of 8-oxo-Guanosine, are caused by the generation of reactive oxygen species (ROS) during metabolic processes (Kryston et al. 2011). Endogenously produced ROS has also been suggested to be able to generate double strand breaks (DSBs) in DNA (Woodbine et al. 2011).

However, there are also a diverse range of exogenous sources that can induce DNA damage which includes both chemical and physical agents that are often used for the treatment of cancer. I will now provide a brief description of some of these agents that are used throughout this thesis, as well as the types of lesion they induce.

1.2.1 Etoposide

Etoposide became readily available as a commercial chemotherapy agent in the 1960's. Despite this it took nearly two decades to discover the target of the drug, Topoisomerase II; an enzyme needed to maintain and alter the topology of DNA. It is able to introduce or remove coils from the DNA double helix by introducing a DSB in the backbone of DNA (Burden and Osheroff 1998).

When used for the treatment of cancer, Etoposide works by causing an increase in the number of DSB in DNA, inducing an apoptotic response in cancer cells. Etoposide does not work by inhibiting the catalytic domain of Topoisomerase II; instead it works by increasing the prevalence of Topoisomerase II-DNA cleavage complexes (Nitiss 2009, Hande 1998). This becomes an issue when DNA replication machinery and helicases come into contact with the complex that they need to traverse. As a result of this interaction, topoisomerase II is removed from the complex, which leaves behind a permanent double strand break capped with topoisomerase II, a lesion that is highly resistant to repair.

1.2.2 Ionising Radiation

We are exposed to ionising radiation (IR) on a daily basis, however, much higher and more concentrated exposures occur during medical procedures such as diagnostic imaging and during the treatment of cancer. IR can be split into two main groups; photon or particle radiation. Photon radiation such as x-ray and gamma ray is the most common form used in the treatment of cancer (Baskar et al. 2012).

DNA damage results from either the direct or indirect action of the radiation on DNA (Desouky et al. 2015). IR can directly alter the molecular structure of DNA but it is the indirect actions of IR that causes most of the damage in cells exposed to photon radiation. IR is able to produce a range of reactive ROS, including the OH free radical (Desouky et al. 2015); a highly reactive molecule which is important in the induction of double strand breaks (Gates 2009). However, base alterations such as those caused by endogenous ROS are also likely to be formed as a result of ionising radiation.

1.2.3 Bleomycin sulphate

Bleomycins are a group of antibiotics from *Streptomyces verticillus* and are commonly used to treat a variety of tumours (Hecht 2000). A mix of Bleomycin sulfate salts is used during cancer therapy, predominantly Bleomycin A2 and Bleomycin B2, in a treatment called Blenoxane. Bleomycins induce DNA degradation in the presence of metal ions like Fe^{2+} or Cu^{+} and also require oxygen. These antibiotic drugs act as IR mimetics, meaning they are able to create the free radicals that are important in the process of DSB induction (Povirk 1996, Hecht 2000, Chen and Stubbe 2004).

1.2.4 Ultraviolet Radiation

Although it is not used for cancer treatment, ultraviolet (UV) radiation is considered one of the most damaging agents known, and is a key player in the cause of skin cancer (de Gruijl et al. 2001). The Earth's only source of protection from solar UV radiation is the ozone layer, but since its man-made partial degradation there has been a large increase in UV exposure at the Earth's surface (Sivasakthivel and Reddy 2011). There are three groups of UV radiation categorised by their associated wavelengths; 1. UV-A at 315-400nm, 2. UV-B at 280-315nm and 3. UV-C at a wavelength less than 280nm (Rastogi et al. 2010).

UV is not deeply penetrating, and so cannot be absorbed further than the skin (de Gruijl et al. 2001). It is therefore not necessarily a concern for human fertility. However, there are many species on Earth, particularly amphibian species, who lay their eggs in the surrounding environment leaving them exposed to damaging agents such as water pollution or UV radiation. There is some evidence to suggest that amphibian species may be at risk due to increased UV radiation (Palen et al. 2005). Despite its inability to affect mammalian reproduction it is still a useful tool for monitoring the effects of different types of DNA damage on mammalian oocytes due to its efficacy being fairly consistent.

DNA damage induced by UV radiation comes in several forms. Pyrimidine bases are preferentially damaged to form dimers, as a result of UV being absorbed by a double bond causing it to react with neighbouring bases. If 2 new covalent bonds form between carbon 5 and carbon 6 of two pyrimdine bases, this forms a cyclobutane pyrimidine dimer (CPD) (Goodsell 2001). If only a single bond forms between carbon 4 and carbon 6 the two bases the resulting lesion is called a 6-4-photoproduct (Goodsell 2001). These dimers are able to distort the DNA helix by disturbing helix curvature and can induce helical bending at the lesion itself (Rastogi et al. 2010). As well as this, UV can also form protein-DNA

crosslinks, oxidative damage to bases and single strand breaks in DNA (Sinha and Hader 2002, Rastogi et al. 2010, de Gruijl et al. 2001). UV-B in particular has been suggested to induce DNA double strand breaks primarily through the formation of ROS but also as a secondary effect during the repair of UV-induced dimers (Rastogi et al. 2010).

1.3 Major DNA Damage Response components

In order to establish a checkpoint arrest many components are involved in complex signalling cascades and are often split into the following categories; sensors, mediators, transducers and effectors. Sensors tend to be shared among the three DNA damage checkpoints (G1/S, Intra-S and G2/M), as are the transducers (Sancar et al. 2004). It is the effectors that create the individuality of each checkpoint arrest. The components of the pathways that are put into action is dependent on several factors including the type of DNA damage, duration of exposure or extent of the damage, whether it is a meiotic or mitotic cell, and the stage of the cell cycle when the damage occurs (Bartek and Lukas 2001, Sancar et al. 2004). Before going into the details of the checkpoint arrests an understanding of the major players in sensing and signalling DNA damage is important.

1.3.1 ATM Kinase

Ataxia telangiectasia mutated (ATM) is one of the major kinases required for the *in vivo* response to DNA DSBs (McKinnon 2012, Shiloh and Ziv 2013). ATM is a large protein, at 350kDa, and is related to the phosphoinositide 3-kinase (PI3K) family (Shiloh and Ziv 2013). Due to it kinase ability it phosphorylates its substrates at serine and threonine residues (Shiloh and Ziv 2013). This allows it to activate many branches of the DDR.

The involvement of ATM and its importance in the DDR is best demonstrated in patients suffering from the rare genetic disorder ataxia telangiectasia (A-T) in which ATM is mutated (McKinnon 2004, McKinnon 2012). Patients suffer from a variety of symptoms, including infertility, but one of interest to this project is that the appropriate response to DNA DSBs fails to be initiated leading to radiosensitivity (McKinnon 2004).

In order for ATM to activate downstream substrates such as Checkpoint Kinase 2 (CHK2) and p53 (Shiloh and Ziv 2013), it first needs to be catalytically activated (summarised in Figure 1.1). Autophosphorylation and dissociation from inactive dimer to monomer is required for ATM kinase activation *in vivo* (Bakkenist and Kastan 2003). Cells exposed to IR incorporated high levels of radioactive phosphate into both endogenous and exogenous

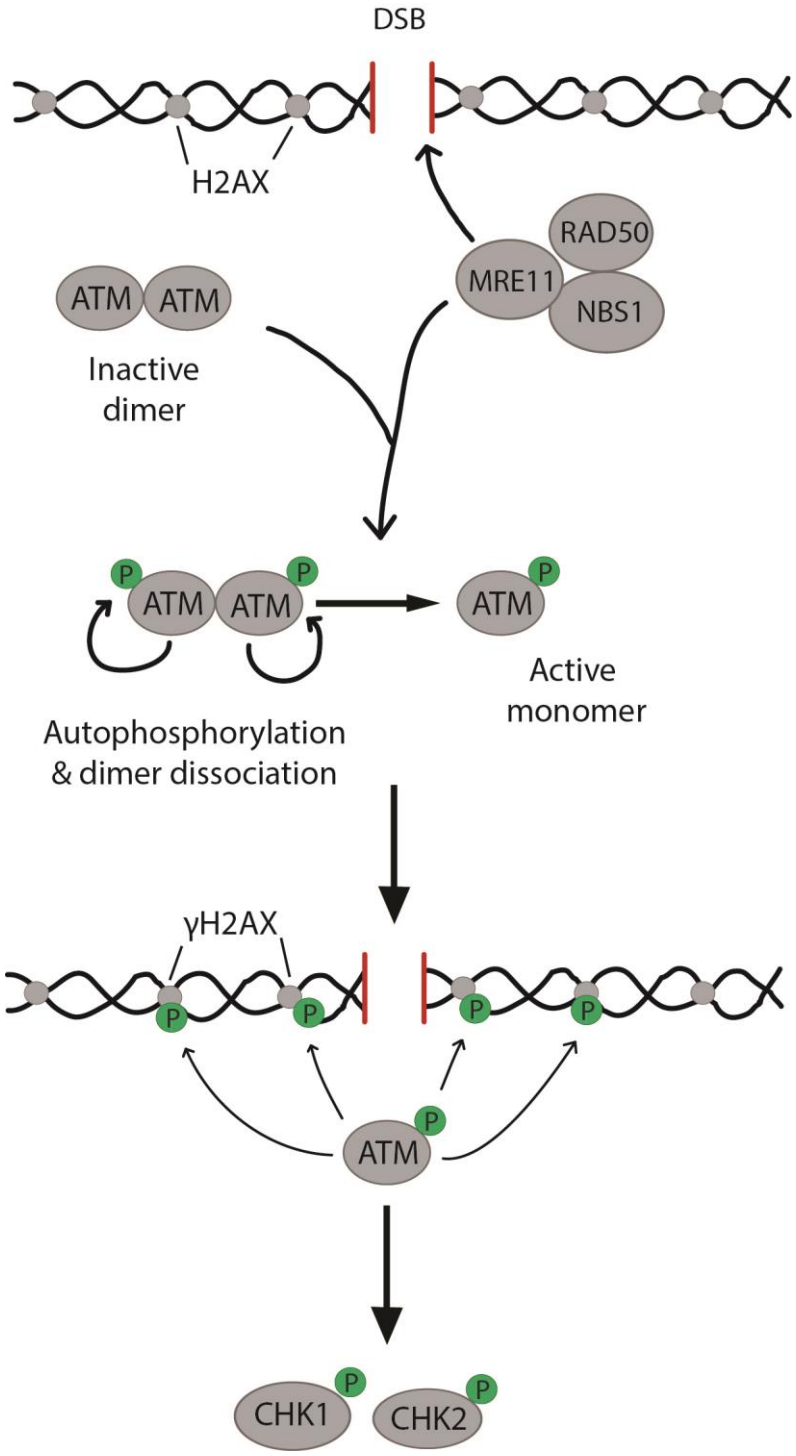

Figure 1-1 Summary of events during the activation of ATM

Prior to activation ATM is held in an inactive dimer. DNA DSBs are initially sensed, possibly by the MRN complex, and ATM is activated by autophosphoryation of serine 1981. This causes the inactive dimer to dissociate into the fully active ATM monomer. Activate ATM is then able to phosphorylate downstream substrates such as H2AX, CHK1 and CHK2.

sources of ATM. Assessment of this phenomenon by gel electrophoresis and chromatography identified the specific residue that is phosphorylated; Serine 1981. Also specific antibodies to this residue revealed that it is rapidly phosphorylated to a maximum within just one hour of IR exposure (Bakkenist and Kastan 2003). The necessity for dissociation has also been supported by *in vitro* evidence (Lee and Paull 2005). However, one study revealed that autophosphorylation of serine 1981 was not needed for monomerisation *in vitro* (Dupre et al. 2006). Despite this autophosphorylation is needed to retain ATM at the site of damage and to mount a proper response to DNA double strand breaks (So et al. 2009).

ATM activation also requires the MRE11-RAD50-NBS1 (MRN) complex (Lee and Paull 2007, Shiloh and Ziv 2013). Mutations within the complex produce a phenotype similar to that of A-T patients. Hypomorphic mutation of the *Mre11* gene leads to AT-like disease (AT-LD) and mutation of the *Nbs1* gene causes Nijmegen Breakage Syndrome (NBS) (van den Bosch et al. 2003). NBS is characterised by microcephaly, altered growth and susceptibility to tumours (Taylor et al. 2004, Digweed and Sperling 2004). Using cell lines from patients suffering these diseases it was shown that nuclear retention and activation of ATM after DNA damage was perturbed (Uziel et al. 2003). As well as this the activation of downstream targets was also negatively affected. By reconstituting defective cells with exogenous MRN, normal ATM phosphorylation and activation of downstream targets was rescued (Uziel et al. 2003).

Once activated ATM kinase is responsible for phosphorylating and activating many branches of the DDR. Its major substrates include CHK2 (Matsuoka et al. 2000), Checkpoint Kinase 1 (CHK1) (Gatei et al. 2003) and p53 (Banin et al. 1998, Kodama et al. 2010, Saito et al. 2002). These proteins then have the role of activating distinct mediators which give the DNA damage checkpoint their individuality, the details of which will be discussed in later sections.

1.3.2 ATR Kinase

Ataxia telangiectasia and Rad3 related (ATR) kinase is not only important for the DDR in response to various types of DNA damage, but also for eliciting the correct response to stalled replication forks during S-Phase (Marechal and Zou 2013). Due to its role in DNA replication it is an essential gene, the loss of which leads to embryonic lethality in mice (Brown and Baltimore 2000). A splicing mutation of ATR leads to a rare condition called

Seckel Syndrome in humans, which results in severe perturbations in foetal development and impaired DNA damage response to UV (O'Driscoll et al. 2003).

The structure that stalled replication forks and the products of DNA repair all have in common is single stranded DNA (ssDNA) and it is thought to be this that leads to ATR activation and signalling (summarised in Figure 1.2). ssDNA becomes coated with Replication Protein A (RPA) (Cimprich and Cortez 2008, Marechal and Zou 2015, Shiotani and Zou 2009) and RPA-ssDNA is then recognised by the binding partner of ATR, the ATR interacting protein (ATRIP) (Cimprich and Cortez 2008, Marechal and Zou 2013, Namiki and Zou 2006, Shiotani and Zou 2009) via its N-terminal domain (Ball et al. 2005). Although not essential for the activation of ATR, ATRIP is needed for the correct localisation of ATR to sites of DNA damage (Ball et al. 2005, Cimprich and Cortez 2008). In order for ATR to become properly activated several other proteins are also required. RAD17 recruits a complex known as the 9-1-1 complex, which is made up of RAD9, RAD1 and HUS1, to the sites of DNA damage (Marechal and Zou 2013, Shiotani and Zou 2009). However, another protein is also needed in mammalian cells; this factor is called DNA Topoisomerase II Binding Protein I (TOPBP1) (Kumagai et al. 2006, Shiotani and Zou 2009). Interactions between RAD9 of the 9-1-1 complex and TOPBP1 have been demonstrated, and this is thought to be one way that the activation of ATR occurs at sites of damage (Cimprich and Cortez 2008, Shiotani and Zou 2009). RPA-ssDNA is also integral for the correct localisation of TOPBP1 in Xenopus egg extract (Acevedo et al. 2016). Once activated at stalled replication forks or sites of damage repair, ATR is able to phosphorylate a range of substrates including its own regulatory elements, but the main substrate is CHK1 (Shiotani and Zou 2009).

1.3.3 CHK1/CHK2

CHK1 and CHK2 are the downstream substrates of ATR and ATM respectively, although there is now thought to be a substantial amount of crosstalk between the two pathways. CHK2 was discovered in 1998 (Matsuoka et al. 1998), and it is a 65kDa serine/threonine kinase (Zannini et al. 2014). It has 3 domains that are integral to its activation and signalling; 1. SQ/TQ cluster domain (SCD), 2. Fork-head associated (FHA) domain, and 3. C-terminal kinase domain. Due to the high concentration of serine and threonine residues in the SCD domain, this is where most phosphorylation by ATM or ATR takes place (Zannini et al. 2014). The FHA domain is important for protein interactions and a group of residues located within the kinase domain form what is known as the activation loop; this

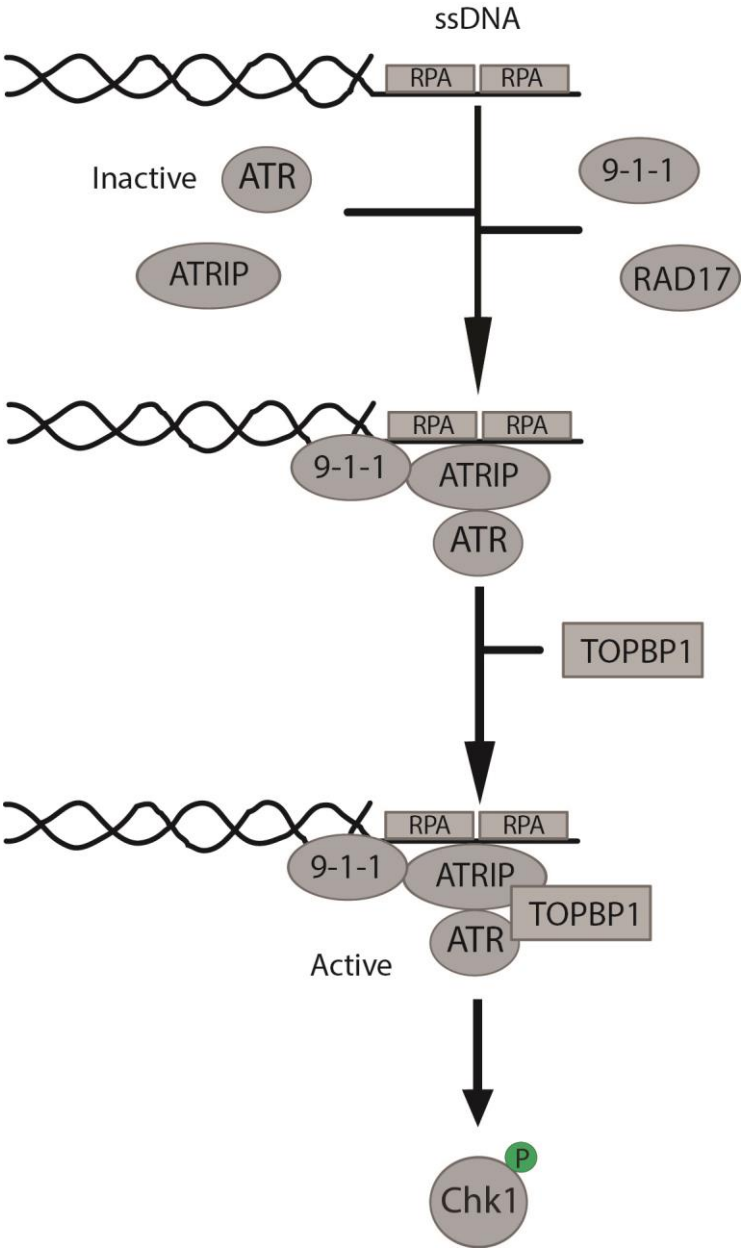

Figure 1-2 Summary of events during the activation of ATR

In order for ATR to be activated ssDNA bound by RPA is needed to act as a platform to which other proteins can bind. ATR bound to its binding partner, ATRIP, localise to the RPA bound ssDNA with the aid of RAD17 and the 9-1-1 complex. However, for full activation of ATR, TOPBP1 is also required.

needs to be phosphorylated to activate the catalytic function (Zannini et al. 2014). CHK2 activation is summarised in Figure 1.3.

Inactive CHK2 is present as a monomer within cells, however when DNA damage has been detected CHK2 monomers form a dimer. Dimerisation is due to ATM phosphorylating CHK2 (Ahn et al. 2000, Zannini et al. 2014). This modification was demonstrated using *in vitro* kinase assays where wild type or kinase-dead ATM was challenged with wild-type and mutant GST-CHK2 (Ahn et al. 2000). Wild-type ATM was able to phosphorylate CHK2 whereas the kinase dead ATM did not. Furthermore, by mutating individual serine or threonine candidates Ahn *et al*. (2000) revealed that the residue to be phosphorylated was threonine 68 (T68) and also confirmed this *in vivo* using ATM-/- mouse embryonic fibroblasts (MEFs). Phosphorylating CHK2 facilitates the interaction of its SCD domain with the FHA domain of another CHK2 monomer (Ahn et al. 2002, Xu et al. 2002, Zannini et al. 2014). This interaction was demonstrated by Ahn *et al.* (2002) using HCT15 cell extracts expressing FLAG-tagged wild type or mutant CHK2, where T68 had been changed to alanine. The extracts were then analysed *in vitro* using GST-FHA binding assay. Only wild type CHK2 was able to interact with the GST-FHA. After dimerisation CHK2 is autophosphorylated within the kinase domain (X. Guo et al. 2010, Lee and Chung 2001, Zannini et al. 2014). Two residues within this domain have been shown to be important for activating the kinase in humans; threonine 383 and threonine 387 (Lee and Chung 2001). When these residues were mutated to alanine a striking reduction in kinase activity was reported. However, in more recent years the phosphorylation status of additional residues including Ser372, Thr378, Thr389 and Tyr390, have also been shown to effect CHK2 activity when mutated (X. Guo et al. 2010). These modifications lead to dissociation of the dimers into fully active monomers (Zannini et al. 2014).

CHK1 is one of the main substrates of ATR (Shiotani and Zou 2009), however it has been shown to be activated by ATM as well in response to ionising radiation (Gatei et al. 2003). Like CHK2, CHK1 is a serine/threonine protein kinase (Tapia-Alveal et al. 2009, Zhang and Hunter 2014). CHK1 activation is made up of a series of complex events that is quite different to the activation of CHK2 (Summarised in Figure 1.4). Phosphorylation events are still very important for the activation of CHK1, which is regulated by its association with the multi-unit platform of ATR, ATRIP, TOPBP1 and 9-1-1 that forms at stalled replication forks or sites of DNA repair (Shiotani and Zou 2009, Tapia-Alveal et al. 2009, Zhang and Hunter 2014) (see 1.3.2). The phosphorylation of several residues, including

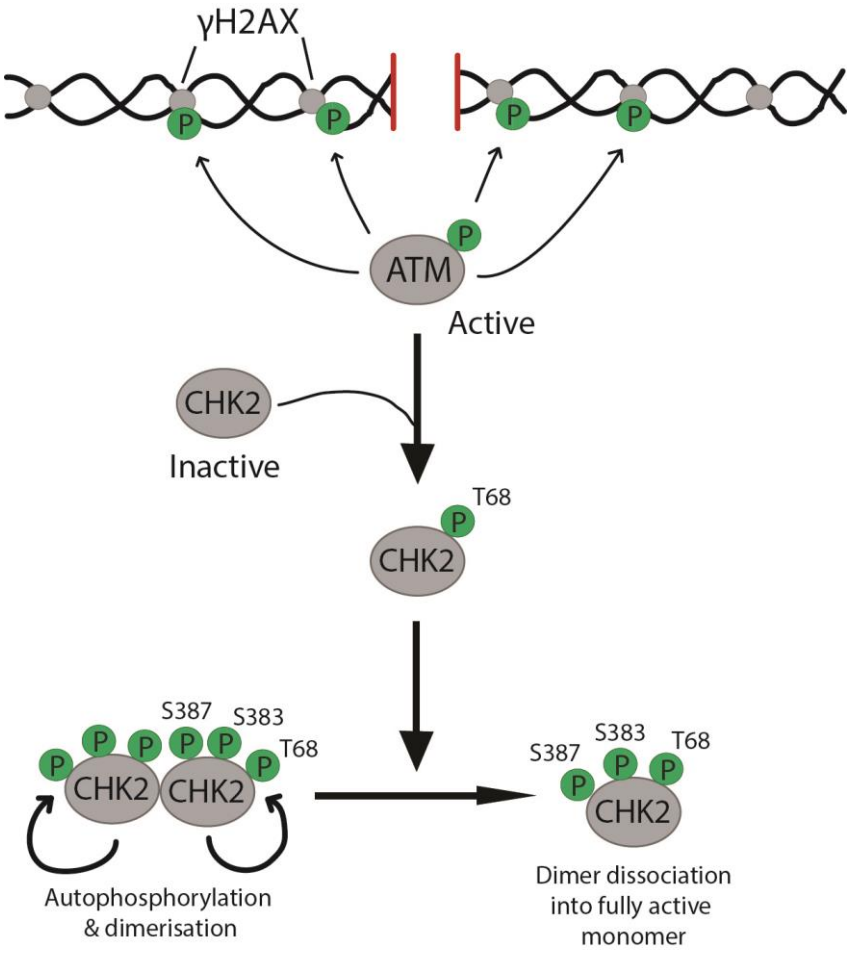

Figure 1-3 Summary of events during the activation of CHK2

The activation of CHK2 requires initial phosphorylation by ATM kinase on threonine 68. This allows for CHK2 to pair up with another CHK2 monomer, and in turn this causes autophosphorylation at a variety of residues. Modification of these residues leads to a conformational change and dissociation of the dimer into fully active monomer.

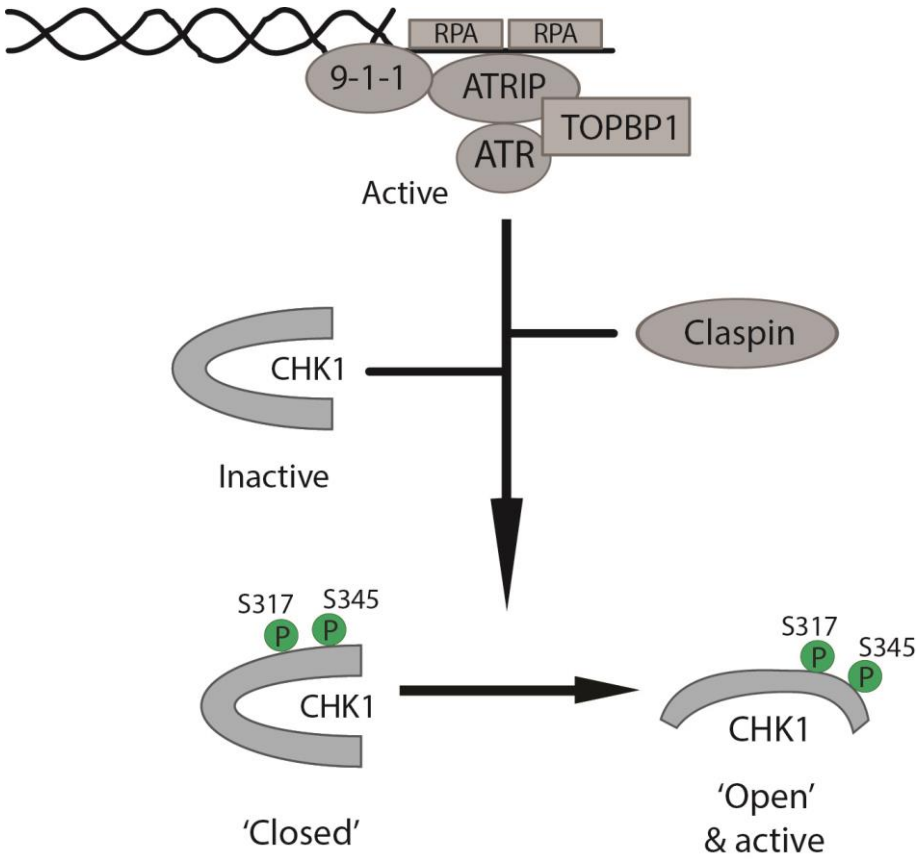

Figure 1-4 Summary of events during the activation of CHK1

When CHK1 is not required an in-built mechanism of inactivation is used by holding the protein in a 'closed' conformation. After DNA damage is detected both ATR and Claspin are required to carry out the phosphorylation of CHK1. These modifications are thought to disrupt the interactions within the 'closed' CHK1 enabling a conformational change to an 'open' and active form.

serine 317 and serine 345, by ATR has been extensively demonstrated (Capasso et al. 2002, Tapia-Alveal et al. 2009, Zhang and Hunter 2014, Zhao and Piwnica-Worms 2001). Mutating S345 or S317 to alanine residues is known to abrogate checkpoint activation (Zhang and Hunter 2014, Zhao and Piwnica-Worms 2001), and CHK1 failed to show the usual mobility shift when analysed by gel electrophoresis (Capasso et al. 2002). An additional component that is needed for correct CHK1 phosphorylation is Claspin (Kumagai et al. 2004, Liu et al. 2006, Zhang and Hunter 2014). Using RNA interference and analysis using phospho-specific antibodies against certain residues within CHK1, Liu et al. (2006) showed that the phosphorylation of serine 317 and serine 345 was prevented when TOPBP1 and Claspin were knocked-down. Specifically, they showed that TOPBP1 is needed for the interaction of Claspin and CHK1, as TOPBP1 depletion interrupted this interaction (Liu et al. 2006).

However, as well as phosphorylation events being important for the activation of this kinase, CHK1 also has an in-built regulatory mechanism known as auto-inhibition. This means that when CHK1 is not required, in the absence of DNA damage, it is held in a closed conformation. This conformation is permitted by interactions between the N- and C-terminal domains (Katsuragi and Sagata 2004, Tapia-Alveal et al. 2009, Zhang and Hunter 2014). It is thought the phosphorylating events can disrupt this interaction, releasing the kinase domain (Katsuragi and Sagata 2004). As the kinase domain is constitutively active the disruption between the two domains stimulates CHK1 catalytic activity (Tapia-Alveal et al. 2009, Zhang and Hunter 2014).

1.4 DNA Damage Checkpoints

As already mentioned there are several points throughout the cell cycle that a DNA damage checkpoint can be activated, namely at the G1/S transition, during S-phase, or at the G2/M transition (Figure 1.5). These checkpoints arrest the cell cycle preventing any further progression, which allows for a cell to initiate repair mechanisms to rid itself of the damage. Below is a brief description of the signalling pathways that lead to checkpoint arrest in somatic cells.

1.4.1 G1/S

The role of the G1/S checkpoint is to stop cells with damaged DNA entering S phase, and so committing to a new round of cell division, by inhibiting the initiation of DNA replication, and can also induce apoptosis if damage is severe (Sancar et al. 2004).

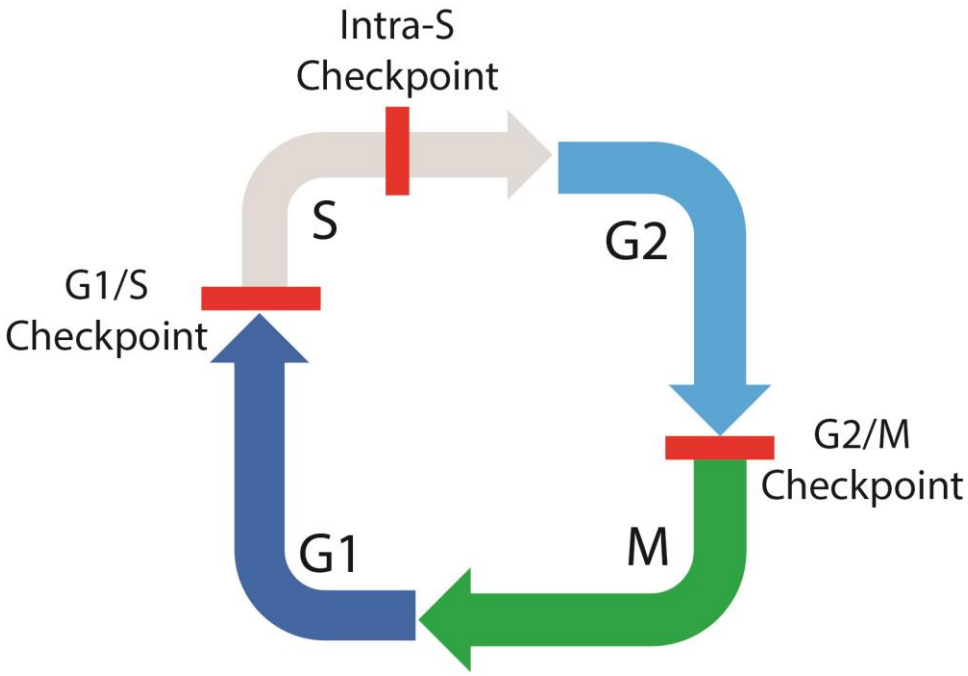

Figure 1-5 DNA Damage Checkpoints throughout the mitotic cell cycle

Arrests in the cell cycle can occur at the G1/S transition, during S-phase or at the G2/M transition.

A cascade of phosphorylation events is initiated culminating in the inactivation of CDC25A via its exclusion from the nucleus and degradation by proteolysis (Summarised in Figure 1.6). In order for the phosphatase to be inactivated it is now clear that the ubiquitin proteasome pathway is involved (Molinari et al. 2000). As well as this, CHK1/2 phosphorylation of CDC25A at serine123 is required (Bartek and Lukas 2001). In the absence of CDC25A, CDK2 is inactive. The downstream result of this is that CDC45 cannot be phosphorylated, a signal needed for the initiation of replication (Sancar et al. 2004, Bartek and Lukas 2001).

The maintenance pathway is slow in comparison and takes several hours to become apparent after damage. Again, ATM and ATR kinases are involved depending on the damaging agent (Bartek and Lukas 2001). However, unlike the initiation of the arrest the transcription factor, p53, is required for a prolonged arrest. p53 is highly unstable and is readily degraded under normal conditions. Its instability is due to a protein called Mouse double minute 2 homolog (MDM2); a ubiquitin ligase that binds to p53 and targets the transcription factor for degradation (Bartek and Lukas 2001). The phosphorylation of p53 at serine 15 directly by ATM/ATR aids its activation. Also, serine 20 is phosphorylated by CHK1/CHK2 which again has activating properties (Sancar et al. 2004) and leads to the dissociation of p53 and MDM2 *in vitro* and p53 stabilisation *in vivo* (Chehab et al. 1999). Another important phosphorylation event is that of MDM2 on serine 395 which prevents nuclear export of p53 (Bartek and Lukas 2001). An impact of p53 nuclear retention is the activation and up-regulation of the p21 gene (Bartek and Lukas 2001), encoding a protein that inhibits several complexes key to S phase. For instance, the CDK4-cyclin D complex usually phosphorylates Rb which releases it from E2F, a transcription factor required for the expression of key S phase genes (Sancar et al. 2004).

1.4.2 Intra-S

The Intra-S checkpoint is caused by DNA damage induced at S-phase or damage that escaped G1. In order to produce an arrest during S-phase the series of events is very similar to that of the maintenance of a G1/S checkpoint. When the damage sensed is a DSB ATM activates CHK2. In turn this leads to the inhibitory phosphorylation of CDC25A (Houtgraaf et al. 2006, Sancar et al. 2004). As already mentioned in section 1.4.1, in the absence of CDC25A, CDK2 is inactive. The result is that CDC45 cannot bind to chromatin and this also prevents the association of DNA polymerase and the formation of the pre-replication complex (Houtgraaf et al. 2006, Sancar et al. 2004, Willis and Rhind 2009).

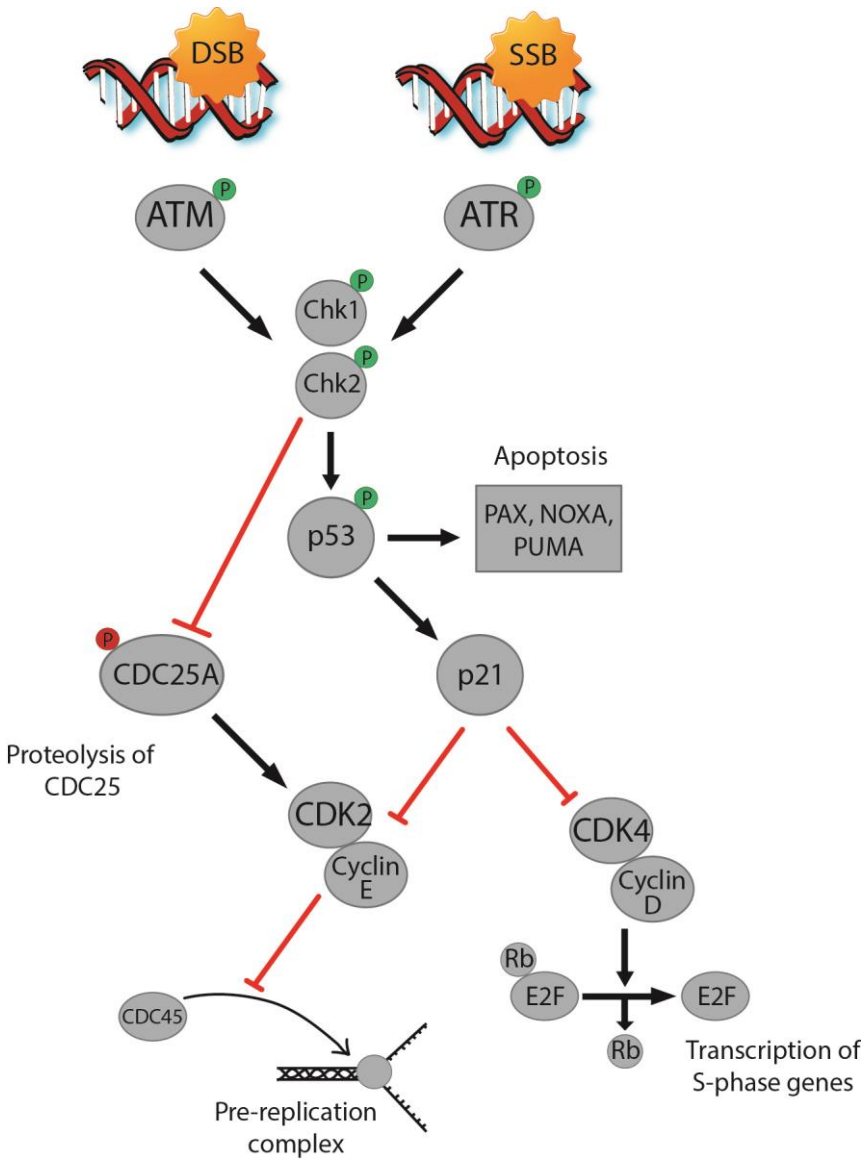

Figure 1-6 Summary of events during the G1/S Checkpoint

DNA damage leads to the activation of ATM and ATR. These kinases can then activate downstream substrates such as CHK1 and CHK2. Phosphorylation of CDC25A by CHK1 and CHK2 leads to the degradation of this protein, which is needed to initiate the formation of the pre-replication complex. Also ATM/ATR and CHK1/CHK2 activate the p53 transcription factor. p53 upregulates p21 which is an inhibitor of CDK complexes needed for S-phase entry.

The same result is initiated in response to UV damage or stalled replication forks, however under these conditions ATR activates CHK1 which in turn inhibits the activity of CDC25A (Sancar et al. 2004).

1.4.3 G2/M

In order for a cell to enter M-phase the CDK1-Cyclin B1 complex needs to accumulate (Gavet and Pines 2010, Stark and Taylor 2004). Therefore regulation of this complex is the last point at which a cell can stop entry into mitosis if conditions are not right. Such regulatory elements include WEE1 kinase and CDC25C phosphatase. WEE1 is responsible for inhibitory phosphorylation of CDK1 which prevents the binding of cyclin B1, whereas CDC25C removes such inhibitory modifications (Stark and Taylor 2004, Timofeev et al. 2010). The G2/M checkpoint is activated when DNA damage is sensed by a cell (summarised on Figure 1.7); as with the G1/S and Intra-S checkpoints ATM and ATR are activated and in turn this activates CHK2 and CHK1 (Sancar et al. 2004). The checkpoint kinases then phosphorylate CDC25C which inhibits its phosphatase activity on CDK1 by causing it to bind to a protein called 14-3-3; this association sequesters CDC25C in the cytoplasm (Burgoyne et al. 2007, Donzelli and Draetta 2003, Sancar et al. 2004, Zhang and Hunter 2014, Zhou and Elledge 2000). The activity of WEE1 is also up-regulated and CDK1 is phosphorylated on tyrosine 15 preventing the association with cyclin B1 (Burgoyne et al. 2007, Sancar et al. 2004, Stark and Taylor 2004, Zhang and Hunter 2014). Without a functional CDK1-Cyclin B complex, nuclear envelope break cannot occur and entry into mitosis is inhibited.

1.5 DNA Damage Repair

There are many types of repair mechanisms that have evolved to deal with insults to DNA. Not all mechanisms available to a cell are relevant to this thesis but it is worth noting the existence of base excision repair (BER), nucleotide excision repair (NER), mismatch repair (MMR), and double strand break repair (Dexheimer 2013, Sancar et al. 2004). DNA damage induced by spontaneous reactions or replication errors are commonly repaired by BER and MMR respectively (Dexheimer 2013) (Dexheimer 2013). DNA damage resulting from exposure to UV light is repaired by NER (Dexheimer 2013, Nouspikel 2009, Scharer 2013). Finally, DSBs induced by IR or anticancer drugs are repaired by one of two mechanisms; homologous recombination (HR) or non-homologous end joining (NHEJ)

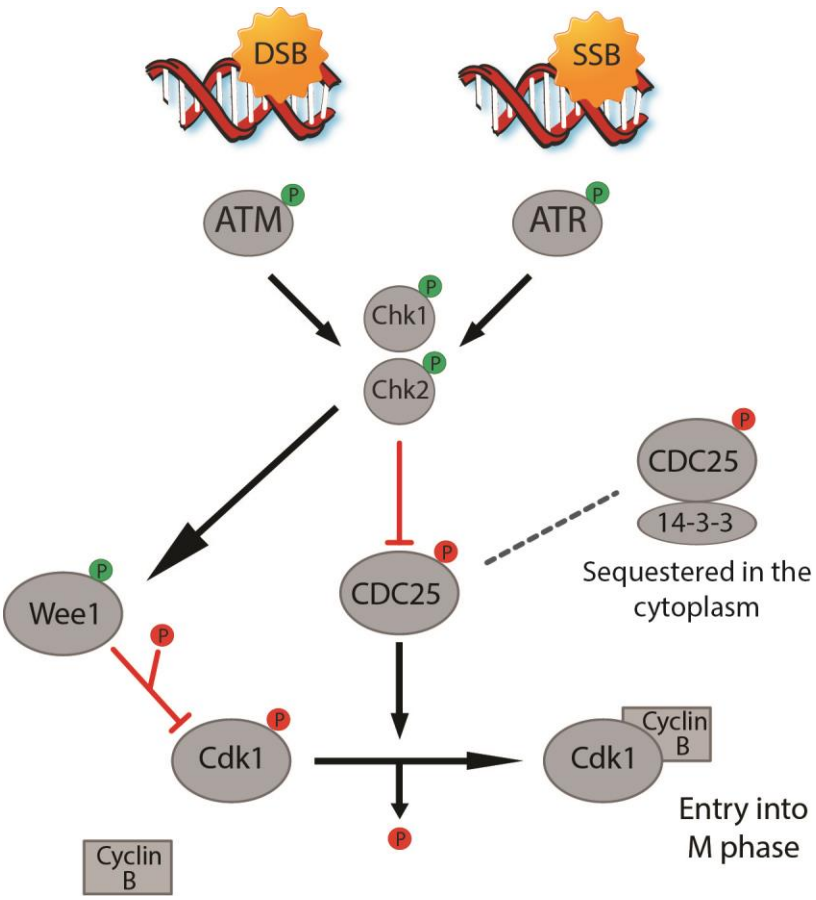

Figure 1-7 Signalling events during the G2/M Checkpoint

DNA damage leads to the activation of ATM and ATR. As with the G1/S checkpoint, these kinases activate CHK1 and CHK2. CHK1/CHK2 is responsible for inhibiting the action of CDC25 phosphatases. CDC25 normally act to remove inhibitory phosphate groups from CDK1, which prevent it binding to cyclin B1. The CDK1-cyclin B complex is essential for M-phase entry.

(Dexheimer 2013, Sancar et al. 2004). Due to the nature of the drugs used throughout this thesis the repair of DSBs and UV damage will be the focus of the following section.

1.5.1 DSB Repair: Homologous Recombination

HR is considered an error free method of dealing with DNA DSBs as it uses an undamaged sister chromatid as a template. Due to the requirement of a sister chromatid, HR is limited to two phases of the cell cycle; S- and G2-phases (Dexheimer 2013).

The process of HR is often split into three main sections; (1) presynaptic, (2) synaptic and (3) postsynaptic (Dexheimer 2013, Filippo et al. 2008, Krejci et al. 2012, Sung et al. 2003). During the presynaptic phase the first step that is taken is the resection of the DNA ends created by the DSB. The MRN complex, CtIP and Bloom helicase (BLM) work together to trim the 5' of the DNA end, and create overhangs of ssDNA (Dexheimer 2013, Filippo et al. 2008, Lamarche et al. 2010, Sartori et al. 2007). As mentioned in section 1.3.2 ssDNA is bound by RPA, and so these overhangs become coated in the protein (Dexheimer 2013). This interaction has multifaceted effects on the presynaptic phase due to its ability to regulate the binding of RAD51. Firstly, it can eliminate secondary structures from long lengths of ssDNA allowing RAD51 to bind (Filippo et al. 2008, Krejci et al. 2012, Sung et al. 2003). However, RPA can also act as a physical barrier preventing such binding, and in turn ensures RAD51 association with the ssDNA occurs in a timely manner (Filippo et al. 2008, Krejci et al. 2012, Sung et al. 2003). The binding of RAD51 creates the presynaptic filament; a nucleoprotein filament containing ~6 RAD51 molecules for every ~18 nucleotide bases (Filippo et al. 2008, Krejci et al. 2012, Sung et al. 2003). Due to the inhibitory effects of RPA on RAD51 binding several HR mediators are needed to form the presynaptic filament. In mammals, BRCA2 is thought to be one of the main mediators of RAD51 binding (Chatterjee et al. 2016, Filippo et al. 2008, Forget and Kowalczykowski 2010, Krejci et al. 2012, Liu et al. 2010). However, several other mammalian mediators have been identified over the years. RAD51 paralogues known to influence the presynaptic filament include RAD51B, RAD51C, RAD51D, XRCC2 and XRCC3 (Dexheimer 2013, Filippo et al. 2008, Krejci et al. 2012).

Synapsis is characterised by the formation of connections between the DNA of the presynaptic filament and the DNA of its sister chromatid. The chromatid is held briefly to test for homology, if unsuccessful it is released and a new part is tested. When homology is found the filament and the homologous DNA duplex are bound together by Watson-Crick bonds and become intertwined into a structure known as the D-loop (Filippo et al. 2008,

Krejci et al. 2012, Sung et al. 2003). Strand invasion and D-loop formation is aided by RAD45 and RAD54B which function in chromatin remodelling and coiling (Krejci et al. 2012). RAD54 proteins also function in later stages of HR by facilitating the removal of RAD51 (Filippo et al. 2008, Forget and Kowalczykowski 2010, Krejci et al. 2012, Sung et al. 2003).

Once the D-loop has formed DNA polymerase is needed to extend the 3'end of the invading strand in a process called DNA strand exchange or DNA branch migration (Filippo et al. 2008, Krejci et al. 2012, Sung et al. 2003). This is then ligated by DNA ligase I to form a structure known as a Holliday Junction (HJ). The HJ is resolved by crossover or non-crossover methods depending on the circumstances. In somatic cells HR repair is rarely associated with the formation of crossovers (Heyer et al. 2010). Crossovers are avoided by dissolving HJs carried out by BLM helicase (Dexheimer 2013, Seki et al. 2006, Swuec and Costa 2014), and is thought to be the favoured way to deal with HJs in mitosis.

1.5.2 DSB Repair: Non-Homologous End Joining

NHEJ has the ability to function at any stage of the cell cycle, as unlike HR it does not require the presence of a sister chromatid. Instead NHEJ works by simply ligating DNA ends together regardless of whether they are from the same chromosome. One of the first events during this type of repair is the recognition of the DSB and binding of the end by the KU heterodimer (Britton et al. 2013, Davis and Chen 2013, Dexheimer 2013, Fell and Schild-Poulter 2015). This dimer is made up of two subunits; KU70 and KU80 (Davis and Chen 2013, Dexheimer 2013, Fell and Schild-Poulter 2015). The binding of the KU complex acts as a platform to which other NHEJ proteins can localise. Also KU80 is suggested to have a role in stabilising the DNA ends, thus preventing their local movement (Soutoglou et al. 2007). The next component to be recruited to the DSB is the catalytic subunit of DNA-dependent protein kinase (DNA-PK) (Davis and Chen 2013, Dexheimer 2013, Fell and Schild-Poulter 2015). DNA-PK activity is very important for DNA repair and MEFs deficient for the kinase are hypersensitive to IR (Taccioli et al. 1998). When bound it causes the inward movement of the KU complex towards the DNA and also activates the kinase function of DNA-PK (Davis and Chen 2013, Dexheimer 2013).

In order for the DNA ends to be re-ligated there may be a requirement for DNA end processing; factors such as Artemis or DNA polymerase are known to be involved in this (Davis and Chen 2013, Dexheimer 2013, Fell and Schild-Poulter 2015). Artemis is an

endonuclease known to process overhangs, thus creating blunt ends to ligate (Davis and Chen 2013). Its activation has been shown to be reliant on the autophosphorylation of DNA-PK, which is believed to make the DNA accessible to Artemis (Goodarzi et al. 2006).

Also recruited to the site of DNA damage is the XRCC4-DNA ligase IV complex (Britton et al. 2013, Mari et al. 2006), through its interactions with the KU complex (Costantini et al. 2007, Fell and Schild-Poulter 2015). XRCC4 has been suggested to act as a tether between the KU complex and DNA ligase IV (Mari et al. 2006). Another NHEJ factor important for the localisation and activity of DNA ligase IV is XLF, again through interactions with KU70/80 (Ahnesorg et al. 2006, Fell and Schild-Poulter 2015, Yano et al. 2008). DNA ligase IV can then ligate the DNA ends thus repairing the DSB (Davis and Chen 2013, Dexheimer 2013, Fell and Schild-Poulter 2015).

1.5.3 UV Damage Repair: Nucleotide Excision Repair

Nucleotide excision repair (NER) is deployed as a way of ridding a cell of the DNA damage induced by UV exposure, namely CPDs and 6-4 photoproducts (Dexheimer 2013, Scharer 2013) (Section 1.2.4). The process of NER is summarised in Figure 1.8. Firstly, the DNA helix surrounding the lesion needs to be unwound. To begin with a complex of XPC/HR23B/CEN2 is localised to the site of DNA damage (Dexheimer 2013, Nouspikel 2009, Petruseva et al. 2014, Scharer 2013). The requirement for HR23B was shown *in vitro* using cell free extracts (Sugasawa et al. 1996). Extracts were obtained from Xeroderma pigmentosum group C (XPC) deficient cells and HR23B was depleted. Using purified human recombinant XPC and HR23B the NER activity within the extract was rescued. However, recombinant XPC alone was not efficient at restoring NER (Sugasawa et al. 1996). CEN2 has been shown to enhance NER *in vivo* using XPC deficient cells that express wild-type or a mutant version of XPC that cannot bind CEN2 (Nishi et al. 2005). Using this system Nishi *et al*. (2005) revealed that although NER could take place in the absence of CEN2, its presence greatly enhanced the ability of the cell to repair 6-4 photoproducts. This enhancement was suggested to be due to the ability of CEN2 to increase the efficiency of XPC DNA binding (Nishi et al. 2005). The XPC/HR23B complex does not have a high affinity to DNA damage that causes more subtle alterations in the helical structure such as CPDs, therefore another factors known as the UV-damage-binding proteins 1 and 2 (UV-DDB1/2) are required (Fitch et al. 2003, Nouspikel 2009, Scharer 2013).

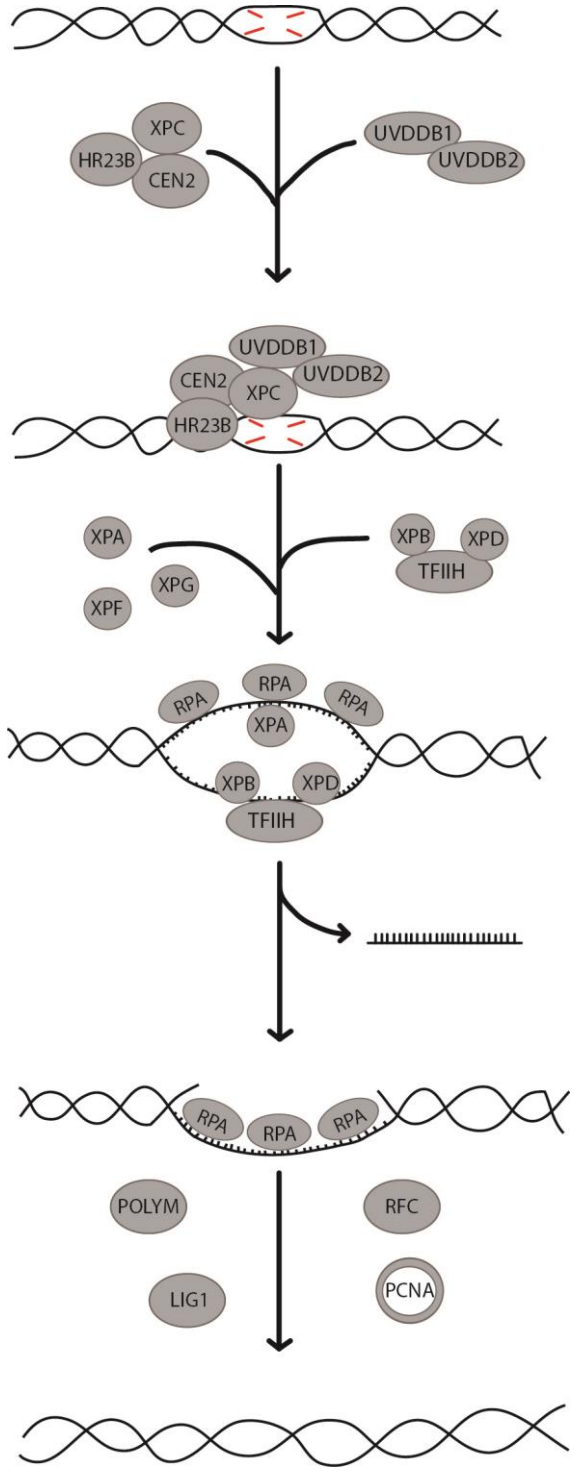

Figure 1-8 Summary of events during NER

To repair damage caused by UV exposure, the lesion in detected and bound by a large complex of proteins including XPC/CEN2/HR23B as well as UV-DDB1 and 2. TFIIH, alongside the endonucleases XPF and XPG mediate the opening and cleavage of around 30 nucleotides that carries the lesion. This section of DNA is then re-synthesised by DNA polymerase and the remaining nick is filled by DNA ligase I.

This was highlighted using immunofluorescence; the UV-DDB subunit p48 could localise to CPDs or 6-4 photoproducts whereas very few cells showed a co-localisation of XPC with CPDs when p48 was absent (Fitch et al. 2003). Overexpression of p48 in these cells allowed XPC to co-localise with CPDs.

This is then followed by binding of TFIIH, a multi-protein complex crucial for NER (Dexheimer 2013, Nouspikel 2009, Petruseva et al. 2014, Scharer 2013). Xeroderma pigmentosum group B (XPB) and Xeroderma pigmentosum group D (XPD) are two helicases from this complex that are needed for opening up damaged DNA (Coin et al. 2007). However, it is only the ATPase activity of XPB in combination with the helicase activity of XPD that facilitate this action (Coin et al. 2007). The DNA helix is unwound to form a bubble of about 30 nucleotides that encompasses the lesion (Dexheimer 2013, Nouspikel 2009, Petruseva et al. 2014, Scharer 2013).

By opening up the DNA helix, ssDNA is exposed and leads to the recruitment of RPA (Nouspikel 2009, Dexheimer 2013, Scharer 2013, Petruseva et al. 2014). Using yeast two hybrid screening, interactions between RPA and Xeroderma pigmentosum group A (XPA) have been demonstrated (Li et al. 1995, Matsuda et al. 1995). Thus XPA is then recruited to the RPA coated DNA which has an important role in stabilising the complex needed for the removal of the nucleotides containing the lesion (Petruseva et al. 2014)

Next the DNA needs to be cleaved in order to remove the damaged area. This involves the endonucleases Xeroderma pigmentosum group G (XPG), which cleaves 3' to the DNA damage, and Xeroderma pigmentosum group F (XPF), that cleaves the 5' (Nouspikel 2009, Dexheimer 2013, Scharer 2013, Petruseva et al. 2014). Next the length of DNA that has just been removed needs to be re-synthesised. DNA polymerase δ or ε use the undamaged strand as a template for this resynthesis (Nouspikel 2009, Dexheimer 2013, Petruseva et al. 2014), and this is aided by RFC and PCNA complexes (Scharer 2013, Petruseva et al. 2014). The final step in NER is to repair the remaining nick in the DNA strand which is catalysed by DNA ligase I (Nouspikel 2009, Dexheimer 2013, Scharer 2013, Petruseva et al. 2014).

1.6 Oocyte Development

Meiosis is a type of cell division in which DNA replication (or S phase) only occurs once followed by two consecutive cell divisions, generating haploid daughter cells not genetically identical to the mother cell. In order for meiosis to begin primordial germ cells

(PGCs) need to migrate to the gonad during foetal development. Once the PGCs have arrived meiosis is initiated and chromosomes pair and undergo meiotic recombination which acts to tether the sister chromosomes, creating a bivalent structure, but also to increase genetic diversity. Once recombination is complete oocytes arrest in prophase I; this arrest can last for many years in humans (Chiang et al. 2012, Mehlmann 2005). Oocytes will resume meiosis when exposed to the correct hormonal signals. The oocyte then undergoes germinal vesicle breakdown (GVBD) where the nuclear membrane breaks down and chromatin condenses. The spindle apparatus forms during prometaphase and bivalents begin to attach to the spindle. During meiosis I, which is summarised in Figure 1.9, bivalents align at the metaphase plate. Once anaphase is triggered the homologous chromosomes are pulled to either pole of the spindle generating the first polar body. The polar body should contain half the genetic material that was originally held within the oocyte. In meiosis the spindle migrates towards the cortex of the oocyte producing an asymmetrical division so that the volume of the polar body is much less than that of the oocyte (Maro and Verlhac 2002). After the polar body is extruded meiosis II commences straight away, without an intervening interphase or S-phase, but this time arrests at metaphase II. The oocyte remains at this stage until activation upon fertilisation by a single sperm (Jones 2008).

1.6.1 Primordial Germ Cell Selection and Migration

Gametes arise from a pool of founder cells known as PGCs. A small number of epiblast cells are induced to become PGCs by extraembryonic tissues (Strome and Updike 2015). At around embryonic day 5.75 (E5.75) in mice WNT3 and BMP4 signalling from extraembryonic cells cause mesodermal genes to be switched off and germ cell development genes to be switched on; such genes includes *Blimp1/Prdm1*, *Prdm14*, and *Ap2γ* (Strome and Updike 2015). One role of these genes is to reset the epiblast cells to germ line. This is done through the demethylation of DNA and histones. Following this, these cells move through the embryo from the epiblast to the allantois where further selection occurs at around E10.5-11-5 in mice (Bowles and Koopman 2007) and week 3-4 in human (De Felici 2013). After this they rapidly divide and migrate through the hindgut to the genital ridges where the gonads will form (Bowles and Koopman 2007). Once the PGCs arrive they continue to proliferate from days E11.5-13.5 in mice.

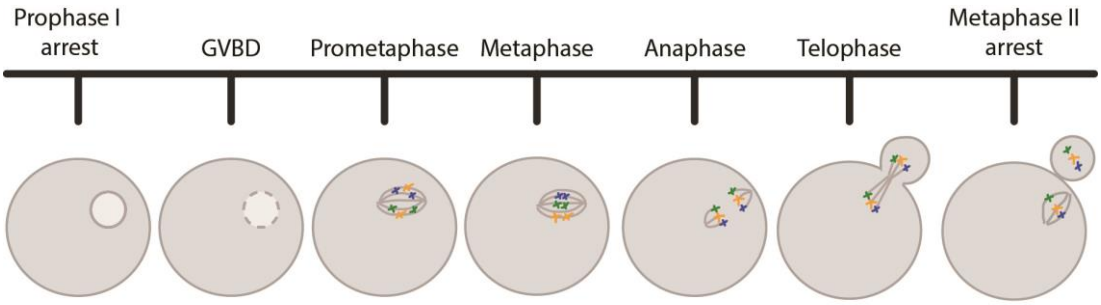

Figure 1-9 Overview of Oocyte Maturation

The resumption of meiosis is characterised by the breakdown of the nuclear envelope, also known as germinal vesicle breakdown. During prometaphase the meiotic spindle forms and bivalents begin to be captured by the spindle apparatus. By metaphase all bivalents should be aligned along the metaphase plate. Due to the bipolar attachment to the spindle, bivalents are physically separated during anaphase. The chromosomes reach the spindle poles by telophase and the first polar body begins to form. Following cytokinesis, the polar body is extruded and should contain half of the original genetic material. The oocyte continues to progress through meiosis until it reaches metaphase II, where it remains arrested until fertilisation.

1.6.2 Initiation of Meiosis and Recombination

In females, meiosis is initiated at around E13.5 in mice (Bowles and Koopman 2007) and around week 10 in humans (De Felici 2013). This is in contrast to males where the process is triggered at puberty. The initiation of meiosis in females is due to the production of retinoic acid (RA) in combination with the inability to degrade it. In mice the necessity of RA has been shown to be due to its requirement for the expression of certain genes (Bowles et al. 2006, Koubova et al. 2006). Koubova et al. (2006) used an antagonist of the RA receptor to prevent the expression of RA activated genes in E11.5 ovaries. In ovaries cultured in this drug, the expression of STRA8 (Koubova et al. 2006) and also the cohesin, REC8 (Koubova et al. 2014) was prevented. STRA8 was shown to be essential for signalling meiotic prophase condensation, as *Stra8* null mice did not display condensed chromatin despite being in the presence of RA (Koubova et al. 2006). Additionally it has also been reported that *Stra8-/-* mice fail to form a synaptonemal complex (SC) or programmed double strand breaks (Bowles and Koopman 2007). Males possess a cytochrome encoded by the *Cyp26bl* gene that allows for RA to be degraded and thus entry into meiosis I is avoided (Bowles et al. 2006, Koubova et al. 2006, Bowles and Koopman 2007, Koubova et al. 2014).

Once meiosis is initiated, oocytes undergo a series of events prior to arresting during prophase I. One main event of meiotic prophase I is the pairing of homologous chromosomes through the formation of the SC (Handel and Schimenti 2010). The other main event, which is aided by the presence of the SC, is the physical tethering of homologous chromosomes through meiotic recombination (Baudat et al. 2013, Handel and Schimenti 2010). This process allows for the crossover of genetic information but is also crucial for the correct segregation of chromosomes during meiosis. The absence of a single crossover between homologous chromosomes greatly increases the incidence of aneuploidy (Ferguson et al. 2007, Handel and Schimenti 2010).

The SC begins to form in leptotene which aligns the homologous chromosomes and at the same time DSBs are induced by the topoisomerase-like SPO11 (Baudat et al. 2013, Baudat et al. 2000, Mahadevaiah et al. 2001, Romanienko and Camerini-Otero 2000). Other proteins involved in the formation of DSBs include MEI4, MEI1 and REC114 (Baudat et al. 2013, Kumar et al. 2010, Kumar et al. 2015, Libby et al. 2003). By zygotene this pairing is complete. Synapsis begins at this point and the SC is fully formed by the end of pachytene. Throughout this time the DSBs induced by SPO11 are identified and signalled for repair by recombination (the mechanism of which will be discussed in detail in section

1.8.1). Once recombination is complete at the diplotene stage, desynapsis occurs and involves the removal of the SC (Handel and Schimenti 2010). The product of this is that homologous chromosomes are tethered together by at least one crossover, or chiasmata. Oocytes then remain arrested in prophase I at the diplotene stage until hormonal signalling during postnatal life (Sánchez and Smitz 2012).

1.6.3 Follicle Development

As already mentioned in section 1.6.1 once PGCs arrive in the gonad they continue to proliferate mitotically until E13.5 in mice. The cell division that takes place occurs in the absence of cytokinesis to form clusters of PGCs known as germ cell nests (Sánchez and Smitz 2012). Meiosis is initiated at E13.5 (in mice) and recombination takes place prior to the formation of follicles within the ovary. Around the time that the oocytes arrest in prophase I, germ cell nests begin to breakdown to mark the start of follicle formation (Pepling and Spradling 2001, Sánchez and Smitz 2012). The regulation of this breakdown is poorly understood but it is thought to involve a variety of factors including steroid hormone signalling as well as proteins such as GDF9, BMP19 and FOXL2 (Sánchez and Smitz 2012). During germ cell nest breakdown there is a large reduction in the number of oocytes that remain in the ovary, as those oocytes that are not surrounded by somatic cells undergo apoptosis (Pepling and Spradling 2001, Sánchez and Smitz 2012). By labelling the germ cells Pepling and Spradling (2001) revealed that during just a two day window the number of germ cells was reduced from 6000 per ovary to 2000.

All of the oocytes that remain are arrested in prophase and are held within a primordial follicle. A primordial follicle consists of the oocyte surrounded by just a single layer of flattened somatic cells called granulosa (Sánchez and Smitz 2012). Primordial follicles are then recruited to begin folliculogenesis, which is the process of growth and development of the follicle ready for ovulation, and also coincides with an oocyte obtaining meiotic competency. The transcription factor FOXO3A expressed in mouse oocytes has been shown to prevent primordial follicle activation (Castrillon et al. 2003, Sánchez and Smitz 2012) and is negatively regulated by AKT (Hsueh et al. 2015). The necessity for FOXO3 in supressing follicle activation was demonstrated using knockout mice (Castrillon et al. 2003). *Foxo3a-/-* mice exhibit early depletion of follicles and as a result are sterile by 15 weeks of age, and this was shown to be due to a global activation of primordial follicles (Castrillon et al. 2003). Thus to allow activation of the follicle to occur FOXO3A down-regulation is required. The activity of its regulator, AKT, is controlled by PI3K/PTEN

signalling (Reddy et al. 2008, Sánchez and Smitz 2012) and in the absence of PTEN, AKT is activated which inhibits FOXO3 by phosphorylation (Sánchez and Smitz 2012). Similar to mice lacking FOXO3A, all of the primordial follicles become activated within the ovaries of *Pten-/-* mice (Reddy et al. 2008). Reddy et al (2008) showed that in the *Pten-/-* mice AKT was activated further supporting the involvement of the PTEN/PI3K signalling pathway in follicle activation.

To be able to develop beyond the primordial follicle stage the oocyte expression of the transcription factors, NOBOX and SOHLH1, is essential (Sánchez and Smitz 2012). These transcription factors allow the development of the primordial follicle to primary follicle, where the flattened granulosa become cuboidal in shape. Thus when they are knocked-out by genetic manipulation in mice progression beyond the primordial stage is prevented (Pangas et al. 2006, Rajkovic et al. 2004). By the late primary stage in mice ovarian cells are recruited to form the theca; however, this layer becomes apparent at a later stage in other mammalian species (Fortune 2003).

Proliferation of the granulosa to produce a secondary follicle does not require hormonal signalling and instead relies on the factors present in the ovary that are produced by the oocyte and their surrounding granulosa and theca. These proteins include GDF9 and BMP15, as well as the transcription factor TBP2 (Sánchez and Smitz 2012).

In order for a follicle to develop from the preantral to antral stage, factors such as GDF9 and BMP15 are still required. However, this developmental transition also requires hormonal signalling (Sánchez and Smitz 2012). Mice that do not express follicle stimulating hormone (FSH) or the FSH receptor do not reach the antral stage (Burns et al. 2001, Dierich et al. 1998). The characteristic changes that occur between the preantral and antral stage is the rapid division of the granulosa cells, which increases follicle size, but also the formation of the antral cavity and the differentiation of the granulosa into cumulus and mural cells (Sánchez and Smitz 2012). Being able to respond to FSH is also important for continued development as it drives the expression of the luteinising hormone (LH) receptor (Burns et al. 2001), so that ovulation can be induced by the surge of LH.

1.6.4 Prophase Arrest and Resumption

During folliculogenesis the oocyte grows to its full size, from about 20µm to 80µm in mice and 100µm in humans, it remains arrested in prophase of the first meiotic cycle (Mehlmann 2005) (Summarised in Figure 1.10). As well as growth, obtaining meiotic

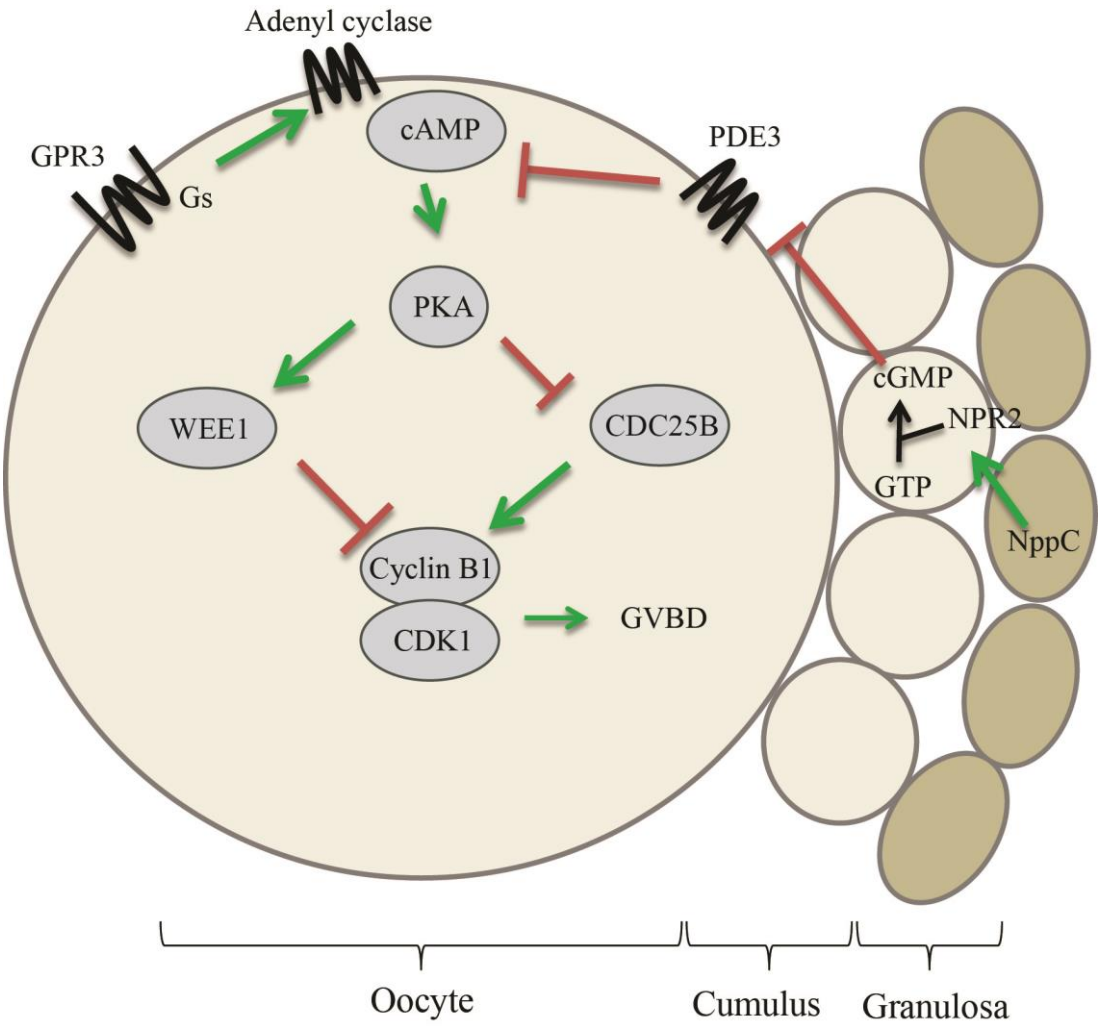

Figure 1-10 Maintenance of GV arrest in oocytes

cAMP is required for the activation of PKA. In turn PKA is responsible for regulating WEE1 kinase and the phosphatase CDC25B. Maintaining the GV arrest needs CDC25B to be inactivate, so that there is no removal of inhibitory phosphates from CDK1. WEE1 provides the inhibitory phosphorylation. This means that active CDK1-Cyclin B1 cannot form and meiotic resumption does not take place.

competence is essential for an oocyte; this coincides with factors, such as CDK1, reaching a threshold level (deVantery et al. 1996). In previous years it had been difficult to study the mechanisms of arrest and resumption in oocytes due to the effect of the surrounding cumulus and granulosa cells but methods of microinjection were developed and it has proven to be indispensable to studies on oocyte maturation. As a result it is well-known that follicular cells surrounding the oocyte are needed to maintain arrest and that the resumption of meiosis requires a surge of luteinising hormone (LH).

In order for oocytes to remain arrested several conditions have to be met including the maintenance of cyclic AMP (cAMP) and cyclic GMP (cGMP) levels. These cyclic nucleotides enable a cascade of events within the oocyte to ensure the germinal vesicle (GV – alternative name for the nucleus) is maintained. Adenylyl cyclase is responsible for the production of cAMP, the activation of which is reliant on a G protein coupled receptor (GPCR) and its corresponding stimulatory G protein (G_s) (Mehlmann et al. 2002, Mehlmann et al. 2004). Inhibition of the G_s in mouse oocytes causes precocious GVBD, whereas inhibiting alternative G proteins have no such effect (Mehlmann et al. 2002). The corresponding receptor was later identified by the same group. They searched a cDNA library for GPCRs where GPR3 emerged as a potential candidate due to its ability to elevate cAMP levels in cultured cells. GPR3 presence was confirmed in oocytes by RT-PCR and following this *Gpr3-/-* mice were generated to study its involvement in oocyte maturation. Oocytes from *Gpr3-/-* mice had only metaphase chromosomes when retrieved from mature follicles in contrast to wild type oocytes that were all prophase arrested (Mehlmann et al. 2004). cAMP activates protein kinase A (PKA) which leads to the inhibitory phosphorylation of CDK1, rendering the CDK1-cyclin B1 complex inactive. It does so by regulating the activity of CDC25, a phosphatase that removes inhibitory phosphate groups, and WEE1, the kinase that provides these inhibitory modifications (Jones 2008, Mehlmann 2005).

The involvement of cGMP in maintaining GV arrest is attributed to its ability to aid in keeping cAMP levels high. In recent years it has been found that granulosa cells express natriuretic peptide precursor C (NppC) and cumulus cells express NppC receptor 2 (NPR2) a guanylyl cyclase that produces cGMP (Zhang et al. 2010). Cumulus cell expression of NPR2 mRNA was coupled with the expression of oocyte factors such as GDF9, BMP15 and FGF8B. *Nppc* expression allowed levels of cGMP to increase in cumulus cells and oocytes, keeping cAMP levels up by inhibiting a phosphodiesterase, PDE3A. Oocytes from NppC and/or NPR2 mutant mice do not maintain prophase arrest (Zhang et al. 2010).

The movement of cyclic factors like cGMP, is reliant on the presence of gap junction connexin 43 in the cumulus cells and connexin 37 in the oocyte surface (Richard and Baltz 2014).

The surge of LH at ovulation stimulates a decrease in cAMP and resumption of meiosis through the activation of PDE3A. Milrinone is a pharmacological inhibitor of PDE3 (Boswell-Smith et al. 2006) and can be added to culture media to prevent oocytes undergoing GVBD (Jensen et al. 2002). It is a useful tool in oocyte research as it gives the user control of the starting point of maturation and synchronises the oocytes. *Pde3-/-* female mice are infertile suggesting its involvement in oocyte quality or maturation (Masciarelli et al. 2004). Oocytes from these mice had high levels of cAMP, and did not undergo spontaneous GVBD when removed from follicles which was the cause of their infertility. When studied *in vitro* LH caused a decrease in cAMP by effecting the two proteins mentioned above; NppC and NPR2 (Robinson et al. 2011). Within 20 minutes of LH addition a decrease in guanylyl activity of NPR2 was measurable and this decrease in activity was not coupled to a reduction in the protein itself. Also, by 2 hours after LH addition the amount of NppC available to bind to its receptor had significantly dropped (Robinson et al. 2011). The decreased cAMP signalling prevents PKA from inhibiting CDC25B, resulting in the activation of the CDK1-cyclin B complex.

1.6.5 Prometaphase: Spindle Formation

The purpose of meiosis I is to physically separate bivalents so that one homolog is held within the oocyte and the other is expelled into the polar body. To do this a bipolar spindle is required and bivalents need to be captured and aligned on this apparatus. The spindle itself is made up of hollow tubular structures formed from the polymerisation of α and β tubulin (Dumont and Desai 2012, Severson et al. 2016). It is worth noting here that during mitosis the assembly of the spindle requires centrosomes. At the centre of the centrosomes is a pair of very stable structures called centrioles. Located within this structure are γ-tubulin ring complexes that allow for the polymerisation of tubulin to form microtubules (Severson et al. 2016). In contrast to this, spindle assembly in oocytes progresses without requirement for centrioles.

Many of the finer details regarding spindle assembly in mouse oocytes is still unknown, however it is thought to involve a variety of proteins, some of which function in mitotic spindle assembly. Most of our current knowledge on this topic has come from live imaging studies on mouse oocytes where it had been shown that multiple microtubule organising

centres (MTOCs), made up of γ-tubulin, pericentrin and CEP192, are needed for spindle assembly in mouse oocytes (Clift and Schuh 2015, Schuh and Ellenberg 2007, Severson et al. 2016). Other proteins including NEDD1 are also localised to the MTOCs and have been shown to be crucial for correct spindle assembly (Ma et al. 2010). Originally it was thought that MTOCs formed a 'ball' structure and that some MTOCs are ejected from the structure and coalesces to form a bipolar spindle (Schuh and Ellenberg 2007). However, more recently using CEP192-GFP live imaging the ball structures were not seen and instead chromosomes and MTOCs were mixed together after GVBD (Clift and Schuh 2015). Prior to GVBD the MTOCs have been shown to be stretched, that requires the dynein motor protein BICD2, and are then fragmented after GVBD, by the kinesin KIFIIB, allowing the formation of many small MTOC foci that later coalesces (Clift and Schuh 2015). The exact mechanisms involved in MTOC merging are still unknown. The sorting of MTOCs to allow for a bipolar spindle to form (Breuer et al. 2010). The large increase in microtubules from the MTOCs has also been shown to be reliant on Ran-GTPase activity (Schuh and Ellenberg 2007).

The formation of the spindle allows for bivalents to begin to be captured by the dynamic microtubule structures. In meiosis, the two sister kinetochores of one chromosome within the bivalent are captured by a microtubule from one pole, rather than each kinetochore being captured by microtubules from opposite poles as occurs in mitosis (Watanabe 2012). Instead the opposite pole captures the pair of kinetochores on the other homolog. This bipolar attachment allows the homologous chromosomes to be pulled to opposite poles at the onset of anaphase (Watanabe 2012).

1.6.6 Metaphase I to Metaphase II Transition

Once oocytes have resumed meiosis and the spindle is formed, the next major event is the metaphase to anaphase transition, as this allows for bivalents to reductionally segregate into sister chromatid pairs. In both mitosis and meiosis there are several key proteins needed for this transition including the Anaphase Promoting Complex (APC) and separase (Homer 2013, Terret and Jallepalli 2006). There are also many other regulatory elements that help to control the activity of the APC and separase so that anaphase occurs when bivalents are correctly attached to the spindle. Once this transition is complete, telophase and cytokinesis follow and can be identified by the extrusion of the polar body.

Bivalents are maintained by a structure called cohesin (Nasmyth and Haering 2009, Tachibana-Konwalski et al. 2010). To allow the physical separation of bivalents cohesin is

cleaved by the protease separase (Kudo et al. 2009, Kudo et al. 2006, Terret et al. 2003, Terret and Jallepalli 2006). Separase activity is controlled by a variety of measures including CDK1-dependent phosphorylation (Gorr et al. 2006) and the chaperone binding protein securin (Terret et al. 2003). Securin loss, as well as a decrease in CDK1 activity by lowering cyclin B1 levels, is essential (Herbert et al. 2003). The reduction of these proteins is mediated by the Anaphase Promoting Complex (APC) (Homer 2013, Thornton and Toczyski 2003, Pines 2011). The APC has two activators, CDH1 and CDC20, which allow it to have several specific roles throughout the cell cycle. In meiosis, APC^{CDH1} is required for aiding prophase arrest (Homer 2013, Homer et al. 2009, Reis et al. 2006) however, as the levels of CDK1-Cyclin B1 increase the activity of APC^{CDH1} is swapped for that of APC^{CDC20} (Reis et al. 2007). Once this complex is active the APC^{CDC20} degrades cyclin B1, which decreases the levels of active CDK1. In turn this helps to activate separase. Also, once active, separase appears to inhibit CDK1 further; when mouse oocytes were microinjected with antibodies against the CDK1 binding domains of separase, polar body extrusion (PBE) was dramatically decreased (Gorr et al. 2006).

To ensure only the segregation of homologous chromosomes occurs during meiosis I the cleavage of cohesin is spatially limited (Brooker and Berkowitz 2014). REC8, a meiotic cohesin, is cleaved to allow separation both at meiosis I and II; however it is protected from cleavage at the centromeres during meiosis I. The protection of centromeric REC8 is carried out by Shugoshin 2 (SGO2) and protein phosphatase PP2A-B (Kitajima et al. 2006). These proteins act to prevent the phosphorylation of cohesin; a modification that promotes the dissociation of cohesin from chromatin. The phosphorylation is carried out by cohesin kinase 1 in meiosis (Ishiguro et al. 2010, Katis et al. 2010).

In mitosis the APC is tightly regulated by the spindle assembly checkpoint (SAC) (Musacchio 2015, Sudakin et al. 2001). Many SAC components were first identified in yeast, and have since been identified in mammals including MAD1, MAD2, MPS1 and BUBR1. These proteins assemble at the kinetochores of non-attached chromosomes (Abrieu et al. 2001, Chen 2002, Waters et al. 1998) and the formation of the mitotic checkpoint complex (MCC) readily inhibits the APC. This complex is formed of MAD2, BUB3, and BUBR1, which in turn sequesters the APC co-activator CDC20, rendering the APC inactive (Foley and Kapoor 2013, Musacchio 2015, Sudakin et al. 2001). During mitosis MSP1 is one of the most upstream proteins during MCC signalling and localises to unattached kinetochores (Abrieu et al. 2001, Foley and Kapoor 2013); it is responsible for phosphorylating the kinetochore which in turn creates docking sites for most of the SAC

proteins (Foley and Kapoor 2013). More specifically BUB1 is recruited to the sites of phosphorylation and BUB1 localisation to the kinetochore is needed for BUB3 and BUBR1 to bind (Yamagishi et al. 2012). MAD1 is particularly important for the formation of MAD2-CDC20 complexes (De Antoni et al. 2005). It is thought that MAD2 in the cytosol is converted from an open to closed form that is then bound to CDC20 (De Antoni et al. 2005, Kulukian et al. 2009). This is catalysed by a complex of closed MAD2 bound to MAD1 at the kinetochore (De Antoni et al. 2005). The interaction of MAD2 with kinetochore bound MAD1 has been shown to be aided by MPS1 (Hewitt et al. 2010, Tipton et al. 2013). The conformational changes in MAD2 enable it to sequester CDC20 and the soluble MAD2-CDC20 complex is then bound by BUBR1 (Kulukian et al. 2009). BUBR1 also functions by associating with the kinetochores of unattached chromosomes to aid the localisation of other SAC proteins (Chen 2002).

Similarly, these proteins appear to have a conserved role in meiosis (Sun and Kim 2012) and readily accumulate at the kinetochore of non-attached bivalents (Hached et al. 2011, Wassmann et al. 2003, Wei et al. 2010). However, the oocyte SAC is not as effective at preventing mis-segregation events (Kouznetsova et al. 2007, Gui and Homer 2012, Kolano et al. 2012, Lane et al. 2012, Sebestova et al. 2012) and this causes oocytes to be susceptible to aneuploidy (Jones and Lane 2013). Over the years it has been shown that the oocyte SAC is insufficient at responding to the presence of univalent chromosomes generated in the XO mouse (LeMaire-Adkins et al. 1997) , *Sycp3-/-* mice (Kouznetsova et al. 2007) or during ageing (Sebestova et al. 2012). Despite this oocytes from these studies retained the ability to respond to spindle depolymerising agent, Nocodazole (Kouznetsova et al. 2007, Sebestova et al. 2012). It has also been demonstrated in several studies that oocytes are also unable to initiate a robust SAC response to non-aligned bivalents (Gui and Homer 2012, Kolano et al. 2012, Lane et al. 2012). In oocytes that have been genetically modified, so that bivalent attachment occurs but with a decrease in tension, severe alignment defects are seen (Kolano et al. 2012). Regardless of this misalignment there was no prevention or delay in the onset of anaphase (Kolano et al. 2012). In wild-type oocytes the degradation of cyclin-B1 has been shown to begin despite the presence of non-aligned bivalents, and that the presence of the aberrant bivalents did not affect anaphase onset or PBE (Lane et al. 2012). Thus, with the SAC being largely ineffective at preventing mis-segregation bodes the question of whether it has alternative roles in meiosis.

As already mentioned at the beginning of this section, once anaphase is complete oocytes progress through telophase and cytokinesis and continue into meiosis II, where they arrest

at metaphase (Madgwick and Jones 2007). Oocytes remain arrested at metaphase II until fertilisation resumes meiosis (Clift and Schuh 2013).

1.7 Oocyte responses to DNA damage

The ethical constraint of using human oocytes for research has meant that animal models have been the main way to study oocytes. It is well documented that primordial follicle stage oocytes with DNA damage readily undergo apoptosis (Kerr et al. 2012a, Livera et al. 2008, Roness et al. 2014, Suh et al. 2006). However, the response of fully grown GV oocytes to DNA damage is still largely unexplored.

1.7.1 TAp63α in Oocytes

As discussed in section 1.4.1 the G1/S checkpoint prevents cells committing to a new round of mitosis with damaged DNA. As well as maintaining a checkpoint arrest, p53 is also responsible for the initiation of apoptosis in severely damaged cells (Nowsheen and Yang 2012, Roos and Kaina 2013). Similarly, it is well known that primordial follicle stage oocytes with damaged DNA readily undergo apoptosis (Kerr et al. 2012a, Livera et al. 2008, Roness et al. 2014, Suh et al. 2006).

Mice lacking the p53 transcription factor are prone to spontaneous and induced tumours, showing that p53 acts as the 'guardian of the genome' in somatic cells (Donehower et al. 1992). Interestingly, results obtained from *p53-/-* oocytes suggested that it is not essential for inducing apoptosis in the female germ line if exposed to DNA damage (Suh et al. 2006). Other candidates from the p53 family include p63 and p73 (Levrero et al. 2000). The mRNA of p63 and p73 can be differentially spliced providing the opportunity for numerous functions. Indeed in oocytes one 'guardian' is an alternative member of the p53 family, trans-activating p63 (TAp63) (Kerr et al. 2012b, Livera et al. 2008, Suh et al. 2006). TAp63 has 3 forms; α, β and γ. TAp63α is the full length variety of this protein, whereas β and γ are either truncated or have several exons added or removed (Levrero et al. 2000). Experiments using PCR and studies on knockout mice revealed that the prevalent form of this transcription factor in oocytes is TAp63α (Livera et al. 2008).

The expression profile of TAp63 has been mapped throughout oocyte development in mice. There is virtually no expression at E16.5. Similarly, at E18.5, roughly one day before birth, only about 20% of oocytes express TAp63. However, by postnatal day 5 (P5) practically all oocytes express the transcription factor (Kim and Suh 2014, Suh et al. 2006).

There appears to be a lack of TAp63 expression that allows embryonic oocytes to evade apoptosis, whereas oocytes retrieved from the ovaries of 5 day old mice die within just a few days of exposure to IR (Kim and Suh 2014). In agreement with this *TAp63-/-* oocytes within primordial follicles are much more resistant to gamma irradiation (Suh et al. 2006).

Following DNA damage TAp63 is activated by a series of phosphorylation events mediated by proteins including ATM and CHK2 (Bolcun-Filas et al. 2014, Livera et al. 2008, Suh et al. 2006). These phosphorylation events cause a mobility shift of TAp63 seen on immunoblots after IR exposure when assessed, and phosphatase treatment prevents this TAp63 mobility shift (Livera et al. 2008, Suh et al. 2006). This shift is only seen from postnatal day 5 (P5) onwards, compared to no shift seen in new born oocytes (Kim and Suh 2014), suggesting that the kinases responsible for these modifications are inhibited prior to P5. ATM kinase has been specifically shown to mediate TAp63 activation; treatment with pharmacological inhibitors of ATM - KU55933 and Wortmannin - prevented apoptosis in damaged follicles (Kim and Suh 2014). CHK2 has also recently been shown to be involved in oocyte apoptosis after irradiation (Bolcun-Filas et al. 2014). The absence of CHK2 (*Chk2-/-*) in the ovaries of mice caused TAp63 to remain un-phosphorylated after IR exposure, and allowed oocytes to evade apoptosis.

The downstream signalling of the p53 family once they have been activated has been extensively studied over the years. In somatic cells, p53 activation leads to the initiation of apoptosis by increasing the expression of NOXA, PUMA and BAX (Basu and Haldar 1998, Harris and Levine 2005, Roos and Kaina 2013). These pro-apoptotic factors are members of the BCL2 family that are responsible for activating capase-9, a crucial protein during apoptosis (Elmore 2007). In the case of the oocyte, TAp63 is essential for the expression of NOXA and PUMA in 5 day old mice (Kerr et al. 2012b). *Puma-/-*, *Noxa-/-* and *Puma-/-Noxa-/-* ovaries have many primordial follicles after ionising radiation treatment compared to wild-type controls, where follicles are rapidly depleted. This suggests that PUMA and NOXA expression is what drives primordial follicle apoptosis after DNA damage. Not only are these follicles protected, the knockout also aided in the preservation of fertility indicated by the production of multiple litters without gross abnormalities (Kerr et al. 2012b). This also suggests that these oocytes have the ability to repair damage to their DNA over time (Kerr et al. 2012b). As well as the preservation of fertility, NOXA and PUMA knockout mice have no increased susceptibility to cancer, thus highlighting a potential medical application in reducing the prevalence of oocyte loss in women undergoing cancer therapy.

All of the above suggests that, similar to somatic cells, the p53 family, ATM and CHK2 are crucial for the elimination of postnatal oocytes with DNA damage. Also, that eliminating these components or those downstream of p63 can prevent cell death. Further study is required to elucidate the finer details of the pathway leading to oocyte apoptosis. It is also unclear how and whether such preventative measures could be targeted to the oocyte without interfering with cancer treatment.

1.7.2 DNA Damage Response in Fully Grown GV Oocytes

Primordial and primary follicle expression of TAp63 is high (Section 1.7.1) but this expression is dramatically lost when recruited for ovulation (Suh et al. 2006). Thus it was unknown how fully grown and meiotically competent oocytes would respond to DNA damage and has not been comprehensively studied. However, prior to beginning my PhD studies, two research groups had begun to explore this. Due to the similarities between the G2/M checkpoint in somatic cells and the maintenance of prophase arrest in oocytes (Solc et al. 2010) it was assumed that oocytes would remain GV arrested after exposure to DNA damaging agents. However, this was shown not to be the case in one study, as fully grown GV oocytes would readily enter M-phase despite having damaged DNA (Marangos and Carroll 2012). DNA damage has been suggested to have a negative effect on the rate of PBE in oocytes (Yuen et al. 2012) and it is possible that there may be an arrest or checkpoint induced during meiosis I. When oocytes were treated with the IR mimetic, Neocarzinostatin (NCS), there was a significant inhibition in the completion of meiosis I and a large decrease in polar body formation from ~80% to just 7% (Yuen et al. 2012). Therefore, much more work was required to properly characterise the response of fully grown GV oocytes to DNA damage and the mechanisms that may be involved. This forms the background on which the bulk of my thesis was based upon as will be reflected in the thesis aims (Section 1.10).

1.8 DNA Damage Repair in Oocytes

1.8.1 Repair of Programmed DSBs during Early Prophase

As already mentioned in section 1.6.2 it is essential that at least one of the DSBs that are induced by SPO11 during prophase is repaired as a crossover with the homologous chromosome. The method of repair for programmed DSBs follows a very similar pathway

to HR (described in section 1.5.1); however there are some variations and meiosis-specific proteins involved as will be highlighted below.

Meiotic DSBs are highlighted by the phosphorylation of H2AX that flank the damage site (Baudat et al. 2013, Mahadevaiah et al. 2001). As with homologous recombination that takes place in somatic cells with DNA damage, the ends of the DSB need to be processed (Neale et al. 2005). During meiosis this processing is predicted to involve the MRN complex, CtlP and BLM (Baudat et al. 2013). RPA binds to the ssDNA which is then bound by recombinase proteins. In meiosis, RAD51 is one of these proteins, however there is also a meiosis-specific recombinase recruited as well; DMC1 (Baudat et al. 2013, Youds and Boulton 2011). Interestingly, *Dmc1-/-* males and females are sterile due to a lack of synapsis suggesting that both RAD51 and DMC1 are needed to ensure timely meiotic recombination (Pittman et al. 1998). The meiosis specific HOP2 and MND1 may promote recombination through stabilisation of the presynaptic filament, but also by facilitating strand invasion and D-loop formation, and also stimulating the activity of the recombinases (Baudat et al. 2013, Krejci et al. 2012, Petukhova et al. 2005, Petukhova et al. 2003, Pezza et al. 2014). As with HR, mediators are required to enhance the activity of the recombinases; BRCA2 is needed for the recruitment and activity of RAD51 and DMC1 (Baudat et al. 2013, Thorslund et al. 2007, Youds and Boulton 2011). Using a mouse model deficient in BRCA2 it has been shown that despite the formation of DSBs via SPO11, the phosphorylation of H2AX and the recruitment of RPA to chromosomes, without BRCA2 the formation of RAD51 and DMC1 foci was negligible in spermatocytes (Sharan et al. 2004).

Similar to HR, strand invasion and D-loop formation follows, and the arrangement of the other DSB end begins to start the differentiation between the formation of a crossover (CO) or non-crossover (NCO) product. However, the exact mechanisms leading to choosing one or the other is still not completely clear. It is also believed that the decision is made very early on in the recombination process. The promotion of a CO is thought to be carried out by factors including, but not limited to, MSH4, MSH5, MER3 and RNF212 (Baudat et al. 2013, Youds and Boulton 2011). Genetic knockout of any of these factors leads to aberrations in crossover formation and they are thought to function in stabilising recombination intermediates (Baudat et al. 2013, de Vries et al. 1999, Edelmann et al. 1999, Kneitz et al. 2000, Reynolds et al. 2013). RNF212 localises to just a small subset of recombination sites, suggesting its role in CO formation (Reynolds et al. 2013). Furthermore, it has been shown to stabilise the MLH1/MLH3 at these sites (Reynolds et al.

2013). MLH1 and MLH3 (also known as MutLγ) are endonucleases specifically involved in CO formation during meiosis (Baker et al. 1996, Baudat et al. 2013, Hunter 2015, Lipkin et al. 2002). *Mlh1-/-* male and female mice are completely sterile further implementing their role in meiosis (Baker et al. 1996, Edelmann et al. 1996). Similarly, *Mlh3-/-* mice are also sterile (Lipkin et al. 2002). Lipkin et al. (2002) suggested that this could be due to the necessity of MLH3 for MLH1 localisation to meiotic chromosomes in spermatocytes.

Resolvases, including MUS81/EME1 and GEN1/SLX1/SLX4, are able to use their endonuclease activity to resolve holliday junctions into either CO or NCO products during HR (Chan and West 2015, Matos and West 2014, Wyatt et al. 2013). MUS81 is thought to only contribute to a small number of CO during meiosis, with a majority induced by MLH1/MLH3 (Holloway et al. 2008). Holliday junctions can also be dissolved by BLM helicase to form NCOs (Seki et al. 2006, Swuec and Costa 2014). The involvement of BLM in NCO formation was highlighted by the fact that a deficiency of this helicase led to increased numbers of chiasmata (Holloway et al. 2010).

1.8.2 Repair of DNA Damage from Exogenous Sources

As already discussed oocytes carry out the repair of programmed DSBs that are initiated during prophase (Section 1.8.1). There are also some studies that suggest that oocytes can repair DNA damage caused by exogenous sources. Many of the early publications that studied the oocytes' ability to repair DNA damage, caused by exogenous sources, focused on the responses of Xenopus oocytes (Sweigert and Carroll 1990, Matsumoto and Bogenhagen 1991), although some studies did use the mouse model (Masui and Pedersen 1975). In one study Xenopus extracts were shown to be able to repair synthetic DNA containing damage that is commonly formed during base excision repair (Matsumoto and Bogenhagen 1991). Xenopus oocytes injected with plasmids that had been irradiated with X-rays were shown to initiate repair through recombination (Sweigert and Carroll 1990). Using mouse oocytes it had also been shown that GV oocytes irradiated with UV initiated unscheduled DNA synthesis and incorporated radioactive thymidine, suggesting repair was taking place. Interestingly, this study revealed that levels of thymidine incorporation was highest in GV stage oocytes compared to metaphase I or metaphase II stage oocytes (Masui and Pedersen 1975), suggesting GV oocytes have a greater ability for repair.

The use of more modern techniques, such as microarrays, on human oocytes has allowed levels of mRNA expression to be monitored. This revealed that oocytes express most DNA

repair proteins at medium to high levels. The mRNA expression of NER proteins such as XPC, and XPA were high in GV (Menezo et al. 2007) and metaphase II oocytes (Jaroudi et al. 2009). This was also shown for mRNA that encodes proteins involved in homologous recombination, such as RPA and the RAD proteins (Menezo et al. 2007, Jaroudi et al. 2009).

The ability of metaphase II oocytes to repair DNA damage has also been more extensively studied in the last decade (Kujjo et al. 2010, Perez et al. 2007). Metaphase II oocytes obtained from the inbred strain, AKR/J, exhibited high rates of apoptosis (Perez et al. 2007). This was found to be due to genetic instability and by microinjecting these oocytes with the HR factor, RAD51, levels of DNA damage were decreased and apoptosis was suppressed. In another strain of mouse, B6C3F1, rates of apoptosis after DNA damage induction could be increased or decreased by immunodepleting or microinjecting human RAD51 protein respectively (Kujjo et al. 2010). This highlighted the importance of DNA repair in oocyte survival. Also, using the comet assay metaphase II oocytes obtained from young ICR mice were shown to have high levels of spontaneous DNA damage upon collection, but after 6 hours much of this damage had been repaired (Kujjo et al. 2010).

Taken together this implies that oocytes at many stages in development possess the machinery to make them capable of carrying out most repair mechanisms. However, to the best of my knowledge, there have been very few publications to specifically assay and characterise the repair ability of fully grown GV mouse oocytes. Therefore, there is much more work to be done on oocytes at this stage.

1.9 DNA Damage Exposure throughout Reproductive Life

1.9.1 Cancer Therapy and Female Fertility

There are a now a wide variety of drugs available used in the treatment of cancer including Etoposide, Mitomycin C (MMC), Bleomycin sulphate, Neocarzinostatin (NCS) and Ionising radiation (IR). These agents work by causing a range of lesions to the DNA of cancer cells leading to apoptosis. However, the pathways activated that culminate in cancer cell death are also of concern for other cells within the body, including germ line cells.

With the large number of effective anti-cancer treatments available, survival rates among cancer sufferers has increased (Aziz and Rowland 2003, Dillman and McClure 2014). Due to this a new problem emerging is the long-term effects of such life-saving treatments,

including the loss of fertility in men and women alike. These aggressive cancer treatments cause the lifetime supply of oocytes within the ovary to be killed off resulting in premature ovarian failure (POF) in women (Maltaris et al. 2007). POF is identified as the lack of menstruation, oestrogen deficiency and elevated gonadotropin levels under the age of 40 (Shelling 2010). The pathway leading to widespread oocyte death was discussed in section 1.7.1.

One of the more established methods of preserving fertility in women is to cryopreserve embryos and oocytes (ASRM 2013, Maltaris et al. 2007, Roness et al. 2014, Skaznik-Wikiel et al. 2015). However, cryopreservation is not an option for all patients. There are several limitations of this technique including the fact that a partner, or willingness to use a sperm donor, is needed to produce the embryos. Also cryopreservation methods are only applicable to post-pubertal women. Therefore, there are currently no well-established methods for preserving fertility in pre-pubertal girls (Skaznik-Wikiel et al. 2015). One option, still at the experiment stage, is to cryopreserve ovarian tissue; however, there are a large number of risks associated with this including the reintroduction of potentially cancerous tissue (Maltaris et al. 2007, Skaznik-Wikiel et al. 2015). For post-pubertal women, an alternative to cryopreservation is the hormonal suppression of ovaries during treatment, but the use of these drugs may interfere with cancer treatment or could lead to the survival of oocytes with damaged DNA (Roness et al. 2014). By understanding the mechanisms of oocyte death or resistance to DNA damaging agents I hope to gain insight into new ways female fertility could be preserved.

1.9.2 Ageing and Female Fertility

Oocytes are unique in the fact that they can remain inert for several decades and it is well established that fertility declines with age. This decline in fertility is associated with an increase in the occurrence of aneuploid oocytes produced during the first meiotic division (Jones 2008, Chiang et al. 2012, Jones and Lane 2012, Jones and Lane 2013). Increases in the rate of aneuploid meiotic division is thought to be mediated by several factors including the deterioration of cohesin complexes tethering chromosomes together (Lister et al. 2010, Chiang et al. 2012, Jones and Lane 2012, Tsutsumi et al. 2014) and a decline in the efficiency of the SAC to detect errors (Baker et al. 2004, Chiang et al. 2012, Jones and Lane 2012, Jones and Lane 2013). Using live cell imaging of oocytes obtained from an aged mouse colony it was shown that a higher proportion of oocytes progressed to metaphase II but that most of these exhibited severe segregation errors (Lister et al. 2010).

Using immunofluorescence to detect the cohesin protein REC8 it was shown that these erroneous divisions were partly due to a reduction in REC8 at chromosome arms and centromeres (Lister et al. 2010). Also mice with mutations in both alleles of *BubR1* display age-related phenotypes at a much younger age including an accelerated reduction in fertility (Baker et al. 2004). Barker et al. (2004) also showed that oocytes from naturally aged mice have much lower levels of BUBR1 compared to young oocytes.

The long prophase arrest also provides an opportunity for the accumulation of DNA damage from endogenous sources, including metabolic by-products such as ROS (Jones and Lane 2012). In recent years it has been shown that oocytes may experience a decline in the ability to repair DNA damage during the ageing process (Kujjo et al. 2010, Oktay et al. 2015, Titus et al. 2013), suggesting that DNA damage could be another factor contributing to age-related fertility issues. In particular DSBs have been shown to accumulate in oocytes from primordial follicles with age and that this correlates with a reduction in key DNA damage repair proteins including BRCA1, MRE11, RAD51 and ATM (Titus et al. 2013). By understanding the ways fully grown oocytes respond to DNA damage it could allow further advances in maintaining fertility and preventing age-related declines in pregnancy success.

1.10 Thesis Aims

1.10.1 Does DNA damage affect later stages of Meiosis I

It has been suggested that oocytes do not possess a robust response to DNA damage at the G2/M checkpoint (Marangos and Carroll 2012) (Section 1.7.2), however, little is known about how later stages of meiosis I are effected by exogenous sources of DNA damage. One would assume there is a mechanism to prevent the production of embryos with damaged DNA. Therefore, it was of interest to characterise the oocyte DNA damage response. This will be addressed in Chapter 3.

1.10.2 The Role of the Spindle Assembly Checkpoint in the Oocyte DNA Damage Response

Having established the oocyte response to DNA damage and the discovery that damaged oocytes arrest, or considerably delay, at metaphase I prompted the questions of what causes this to happen. The well-known ability of the SAC to inhibit cell cycle progression at metaphase (Section 1.6.4) made it a likely candidate for the involvement in the oocyte

DNA damage induced arrest. Therefore, the involvement of the SAC in the arrest was investigated. This will be addressed in Chapter 4.

1.10.3 Can fully-grown GV oocytes carry out repair of DNA damage?

It is well established that oocytes possess the machinery required to repair DNA damage in the context of programmed DSB's that take place during early prophase (Section 1.8.1). There is also some literature to suggest this ability to repair DSB's may also translate to repairing damage caused by exogenous sources (Section 1.8.2). However, there is little on record with regard to the ability of fully grown GV stage oocytes to repair damage to their DNA. This will be addressed in Chapter 5.

1.10.4 Key proteins involved in the oocyte DNA Damage Response

Many proteins have been established as key players in the DNA damage response in somatic cells (Section 1.3). With the large gap in the literature regarding oocyte responses to DNA damage, it was of interest to begin to elucidate whether well-known DDR proteins, such as ATM and ATR kinases (Section 1.3.1 and 1.3.2), are also involved in the DNA damage-induced metaphase arrest in oocytes. This will be addressed in Chapter 6.

Chapter 2: Materials and Methods

2.1 Mouse Handling and Dissection

2.1.1 Ethics

All mice used were in accordance with the local and UK government regulations on the use of animals in research.

2.1.2 Mice

3-4 week old C57BL/6 female mice were used in most of the experiments detailed in this thesis (Charles River and Biomedical Research Facility, Southampton General Hospital). Some experimental data in Chapter 6 used genetically modified mice, that were conditional knockouts for ATM kinase and ATR kinase (*Atm-/- Atr-/-*; gift from Dr James Turner, MRC National Institute for Medical Research, London). These mice were used at 4-7 weeks of age. All breeding and genotyping of these mice was carried out at the MRC National Institute for Medical Research, London. The knockouts were produced on a mixed background of 129, C57BL/6 and MF1. In order to create a knockout specific to the oocyte the Cre-LoxP system was used; where Cre expression coincided with the expression of DDX4, a protein specific to germ cells.

2.1.3 Hormonal Priming

To increase the yield of germinal vesicle (GV) stage oocytes and decrease the number of mice required for each experiment, females were injected with 10IU of Pregnant Mare Serum Gonadotrophin (PMSG-Intervet®, Centaur Services, UK) 48 hours prior to collection. Mice were held by the loose skin on the back of their neck and the PMSG-Intervet® was injected in to the peritoneal cavity. Mice were checked for general welfare 24 hours later.

2.1.4 Dissection and Ovary Collection

When required mice were culled using the cervical dislocation method. The abdominal region was rinsed with 75% ethanol prior to dissection. Using large dissection scissors the abdominal cavity was exposed. As a follow up after cervical dislocation, to confirm the

cull, the heart was severed several times using the large dissection scissors. Using a small pair of dissection scissors the ovaries were removed from surrounding adipose tissue and the oviducts. Ovaries were placed into warm M2 media containing milrinone (0.5mM; Sigma, UK).

2.2 Oocyte Handling and Collection

2.2.1 Manufacture of Handling Pipettes

Glass pipettes (Corning, UK) used to handle and strip oocytes of cumulus cells were made by hand. Glass pipettes were heated over the flame of a portable Bunsen burner until moveable, then removed from the flame and pulled in opposite directions with varying force to create pipettes with different diameters. Excess glass was broken off so the pipette could be stored.

2.2.2 GV Oocyte Handling and Collection

All handling and collection procedures were performed on a stereo microscope (SZ40, Olympus, Japan) with variable zoom. Also, a heated stage (MATS-U4020WF, Tokai Hit, Japan) set to 37°C was used to mimic *in vivo* physiological temperature. Ovaries collected from culled mice were punctured with a hypodermic needle (30 gauge, ½ inch needle) repeatedly in order to release cumulus oocyte complexes (COCs) into the M2 media. To strip the cumulus cells from the oocytes, glass handling pipettes were broken to an appropriate diameter (~85µm). The COCs were drawn into and out of the pipette quickly. This was repeated 3-4 times to ensure all cumulus cells were removed. Then using a handling pipette with a larger diameter (~90-100µm) the oocytes were transferred to a fresh droplet of M2 containing milrinone. This was performed in a dark room, and in as minimal time as possible; around 30 minutes to process 2 mice.

2.3 Oocyte Culture

In all experiments, unless stated, oocytes were allowed to undergo *in vitro* maturation (IVM) for 16 hours after being washed out of milrinone. This corresponds to a total of ~15 hours after germinal vesicle breakdown (GVBD). In some experiments where the spindle assembly checkpoint was to be inhibited oocytes were cultured in media for 11 hours and then Reversine (0.1µM, Sigma, UK) was added. Following IVM, oocyte maturation was scored by the presence or absence of a polar body at the times specified.

2.3.1 M2 Media

M2 media (Appendix B) was made in-lab fortnightly from individual components and batch tested for oocyte maturation before experimental use. This media was always used for oocyte handling and overnight maturation when MEM media was not required. To prevent evaporation of M2 media during experiments it was always covered with mineral oil (Sigma, UK). Mineral oil and M2 were always pre-warmed to 37°C.

When oocytes needed to be cultured overnight in the presence of various drugs mineral oil could not be used due to the possibility of the drugs leaching into the oil. Instead, 1ml of M2 media was added to 1.5ml Eppendorf tubes and kept on the heated block. No oil was required as minimal evaporation of media occurred under these conditions. This was used as an alternative to MEM when there was variation in batch quality (mentioned below).

2.3.2 MEM Media

A small number of experiments were performed using MEM to culture oocytes overnight. It was brought in commercially as a powder (Amsbio, UK) and made up fortnightly (Appendix B). Unlike M2, MEM does not contain HEPES, thus had to be kept in the incubator at 37°C with 5% CO_2 to maintain a normal pH. MEM could be used, when mineral oil could not be added to cover the media, by humidifying the incubator. However, there was some batch-to-batch variation in MEM; as a result MEM was only used for a small number of experiments.

2.4 Etoposide

2.4.1 Etoposide Preparation

Powdered Etoposide (Sigma, UK) was dissolved into DMSO (Sigma, UK) to obtain a stock solution of 25mg/ml. Aliquots of 1µl, 2µl, and 4µl were stored at -20°C. These aliquots were then used to create a working concentration in M2 media, suitable for the experiment to be carried out (2.5µg/ml to 100µg/ml; Table 1).

2.4.2 Etoposide Treatment

Depending on the working concentration desired, Etoposide was diluted in 500µl of M2 media in an Eppendorf. A petri dish with a 500µl droplet of M2 media covered in mineral oil was pre-warmed. Oocytes were added to the droplet and then the 500µl of M2

containing Etoposide was added to mark the start of the treatment. Oocytes were treated for 15 minutes.

Table 1. Working concentrations of Etoposide

Volume of 25mg/ml Etoposide (µl)	Total volume of media (ml)	Working concentration (µg/ml)
0.1	1	2.5
0.2	1	5
0.6	1	15
1	1	25
2	1	50
4	1	100

2.5 Bleomycin sulphate

2.5.1 Bleomycin sulphate Preparation

Powdered Bleomycin (Abcam, UK and Sigma, UK) was dissolved in DMSO to obtain a stock concentration of 50mM. Aliquots of 1µl were stored at -20°C. These aliquots were then used to create a working concentration in M2 media suitable for the experiment to be carried out (0.1µM to 30µM; Table 2). Regardless of the working concentration desired a single aliquot of Bleomycin sulphate was diluted in M2 media to a concentration of 0.5mM (1:100).

Table 2. Working concentrations of Bleomycin sulphate

Volume of 0.5mM Bleomycin (µl)	Total volume of media (ml)	Working concentration (µM)
0.2	1	0.1
0.6	1	0.3
2	1	1
6	1	3
20	1	10
60	1	30

2.5.2 Bleomycin sulphate Treatment

Depending on the working concentration desired 0.5mM Bleomycin sulphate was diluted in 500µl of M2 media in an Eppendorf. A petri dish with a 500µl droplet of M2 media

covered in mineral oil was pre-warmed. Oocytes were added to the droplet and then the 500µl of M2 containing Bleomycin sulphate was added to mark the start of the treatment. Oocytes were treated for 15 minutes.

2.6 UV Irradiation

2.6.1 UV Treatment

Oocytes were placed in a 100µl droplet of M2 media containing milrinone and exposed to UV-B at 300nm using a UV transilluminator (Macrovue UV20, Hoefer) for specific periods of time in order to generate a dose-response (1-30 seconds).

2.7 Ionising Radiation

2.7.1 Ionising Radiation Treatment

In order to expose oocytes to ionising radiation, they were placed inside 1.5ml Eppendorf tubes with 1ml of M2 media and transported to Southampton General Hospital using a portable incubator set to 37°C. The oocytes were placed into the Gammacell 1000 Elite (Nordion International Inc., Ontario, Canada) for set periods of time. The source of radiation in this machine is Caesium^{137} and on the days these experiments were carried out a dose of 25Gy required 11 minutes of exposure; therefore the dose rate was calculated to be 0.038Gy/s. From this dose rate the exposure times required for desired doses of ionising radiation could be calculated (Table 3) using the following equation:

$$Exposure\ time\ (s) = Desired\ Dose(Gy) \div Dose\ rate(Gy\ per\ sec)$$

Table 3. Calculating the exposure time for doses of IR

Desired dose (Gy)	Dose rate (Gy/s)	Exposure time (s)
0.4	0.038	10
1.2	0.038	32
3.9	0.038	103
12.3	0.038	325

2.8 MPS1 Inhibition

To inhibit the spindle assembly checkpoint various components could be targeted. One component assessed was MPS1. In order to inhibit MPS1, a pharmacological inhibitor, called Reversine was used. Reversine (Sigma, UK) was stored in DMSO (Sigma,UK) at a concentration of 0.1mM this was then diluted to 1µM (1:100). 6.6µl of Reversine was then added to 66µl of M2 to obtain a working concentration of 100nM. Reversine was added to media at 11 hours after GVBD. Maturation success was assessed by the presence of the first polar body. Oocytes were monitored every 30 minutes after Reversine had been added. The structural formula for Reversine can be seen below:

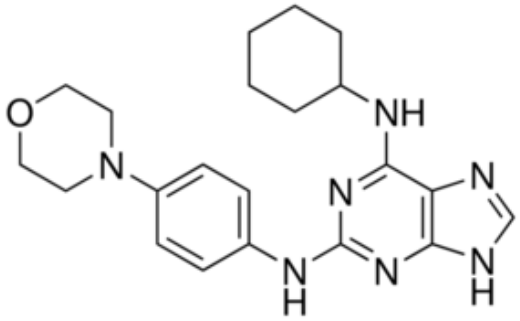

2.9 ATM Inhibition

2.9.1 ATM Inhibitor Preparation

KU55933 (Calbiochem, US), a potent and specific inhibitor of ATM kinase was dissolved in DMSO (Sigma,UK) to obtain a stock solution of 10mM. Aliquots of 1µl were stored at -20°C. These aliquots were used to create a working concentration in media, suitable for the experiment to be carried out (10 and 40µM). Several batches were used throughout experiments. Batches used will be specified in text. The structural formula of KU55933 can be seen below:

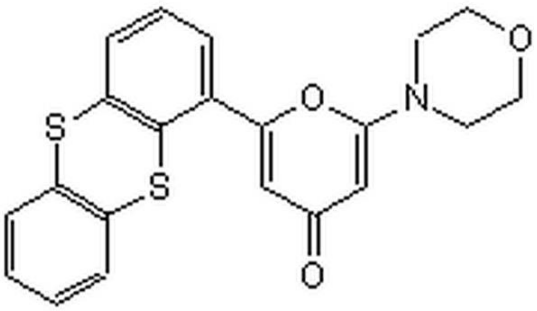

2.9.2 KU55933 Treatment

Depending on the concentration desired stock KU55933 was added to M2 or MEM media. KU55933 was used throughout the duration of the experiment including, during treatment with the DNA damaging agent and throughout IVM. During treatments with damaging agents, the stock KU55933 was added to 500µl of M2 media in an Eppendorf. A petri dish with a 500µl droplet of M2 media covered in mineral oil was pre-warmed. Oocytes were added to the droplet and then 500µl of M2 containing the DNA damaging agent and KU55933 was added to mark the start of the treatment. For the IVM, no mineral oil could be used due to the lipid soluble nature of the drug. Therefore, KU55933 was added to 1ml of media held within 1.5ml Eppendorf tubes as described in section 2.3.1.

2.10 ATR Inhibition

2.10.1 ATR Inhibitor Preparation

ATR inhibitor II (ATRi) (Calbiochem, US), a potent and specific inhibitor of ATR kinase was dissolved in DMSO (Sigma, UK) to obtain a stock solution of 10mM. Aliquots of 1µl were stored at -20°C. These aliquots were used to create a working concentration of 10µM. The structural formula of ATR inhibitor II can be seen below:

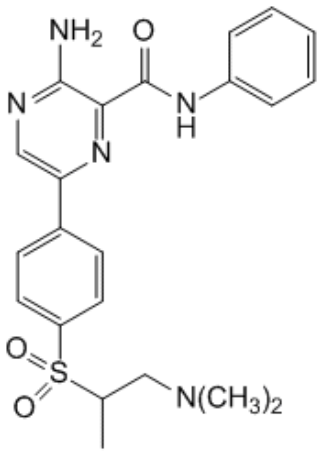

2.10.2 ATR Inhibitor Treatment

Depending on the concentration desired stock ATR inhibitor II was added to M2 media. ATR inhibitor II was used throughout the duration of the experiment including, during the treatment with the DNA damaging agent and throughout IVM. During treatments with DNA damaging agents, the stock ATR inhibitor II was added to 500µl of M2 media in a small Eppendorf. A petri dish with a 500µl droplet of M2 media covered in mineral oil was

pre-warmed. Oocytes were added to the droplet and then the 500µl of M2 containing the DNA damaging agents and ATR inhibitor II were added to mark the start of the treatment. For the IVM, no mineral oil could be used due to the lipid soluble nature of the drug. Therefore, ATRi was added to 1ml of media held within 1.5ml Eppendorf tubes as described in section 2.3.1.

2.11 Oocyte Fixation

All fixations were performed using a 96 well plate. Oocytes were washed with PHEM buffer (Appendix B) to remove any traces of M2 media. Oocytes were moved into a well containing fixing solution (Appendix B) and incubated for 30 minutes at room temperature. Oocytes were washed three times in PHEM buffer for 5 minutes in each well. Following this oocytes were permeabilised using a solution containing Triton X-100, a detergent, and incubated at room temperature for 15 minutes. For oocytes to be stained with MAD2 antibody, permeabilisation was performed overnight at 4°C. Again, oocytes were washed three times in PHEM buffer for 5 minutes in each well. Oocytes could then be stored in 200µl of PBS and kept at 4°C for up to two weeks. For longer term storage of oocytes Sodium Azide (0.02%) was used to supplement the PBS.

2.12 Immunofluorescence

2.12.1 Immunofluorescence Procedure

All immunofluorescence procedures were performed using a 96 well plate and oocytes were transferred through the wells containing 200µl of different solutions as required. Prior to incubation with primary antibody oocytes were kept in blocking solution (Appendix B) overnight at 4°C. This was to prevent non-specific binding and background staining. Oocytes were washed from the blocking solution into a specific washing solution used throughout the immunofluorescence procedure (Appendix B). Oocytes were incubated in primary antibody diluted in blocking solution at 4ºC. Oocytes stained with the MAD2 antibody had to be incubated at 4°C overnight, followed by CREST antibody staining the following day (also overnight at 4°C). For all other primary antibodies 1 hour at 37°C was sufficient. Following three washes for 5 minutes in each well, oocytes were incubated with secondary antibody for 1 hour at 37ºC or 2 hours at room temperature. This incubation needed to be maintained in a dark environment by wrapping the 96 well plates in tin foil. Another three washes were required to remove the secondary antibody. Oocytes were

counterstained with Hoechst (Sigma, UK; 20µg/ml) or DAPI (Sigma, UK; 20µg/ml) diluted in PBS for 5-10 minutes. After this a final wash in PBS was performed.

To mount oocytes onto 12 well 5.2mm numbered diagnostic microscope slides (Thermo Scientific, UK), 1µl of Citifluor (Citifluor Ltd, UK) was placed into the centre of each well. Oocytes were drawn into a handling pipette in minimal media and then transferred to the micro drop of Citifluor. Four small pillars were made out of VALAP (Appendix B) in order to place a glass coverslip on top of the slide. The cover slip was carefully pushed downwards, spreading the VALAP, until pressing down on the oocytes just enough to prevent them from moving. This was then fixed in place using nail varnish. Slides were then stored in the dark at 4ºC.

2.12.2 Antibodies

Microtubules were labelled using a mouse anti α-tubulin (1:400; Life Technologies) and detected with a goat anti-mouse Alexa-633 or Alexa-488 (1:1000; Life Technologies, UK).

Kinetochores were detected using CREST (1:400; Immunovision, US), antibodies derived from patients with an auto-immune disorder against the centromere. To detect this antibody goat anti-human Alexa 555 (Life Technologies, UK) was used.

DNA damage was monitored using an antibody against the popular biomarker, phosphorylated H2AX (γH2AX). This rabbit anti-γH2AX antibody (1:200; Abcam, UK) was detected using a goat anti-rabbit Alexa-633 (1:1000; Life Technologies, UK).

Rabbit anti-Xenopus MAD2 antibody (1:400) was a kind gift from Dr R.H. Chen (Taipei, Taiwan). A goat anti-rabbit Alexa-633 was used to detect this antibody.

2.13 Microinjection

2.13.1 Injection Pipette Manufacture

Microinjection pipettes were pulled from borosilicate glass pipettes (0.84mm inner diameter, 1.5mm outer diameter) with an internal filament (World Precision Instruments, UK) using a Flaming-Brown micropipette puller (Model P97; Sutter Instrument Co, USA). In order to generate a microinjection pipette with a fine tip the parameters on the pipette puller were altered as required. The tip of the pipette was then gently broken against the edge of lint free tissue (KimTech, Kimberly Clark Professional, USA). To assess the

suitability of the pipette it was then examined under a compound microscope. The pipettes were then stored until required and re-assessed prior to use.

2.13.2 Loading Syringe Preparation

In order to load cRNA into the microinjection pipette loading syringes had to be made by hand. 1ml plastic syringes (BD Plastipak, UK) were melted over a Bunsen burner flame until moveable. At this point the syringe was removed from the flame and pulled to create a long thin tip. The syringe was then held still to allow the plastic to set. The tips of the syringes were then cut to around 15cm. Prior to use the tips of the syringes were cut again to about 3-5cm long to ensure a clean even tip remained for loading.

2.13.3 cRNA Manufacture

In order to make cRNA, predesigned and sequenced plasmids had been previously transformed into bacteria and cultured on agar plates overnight at 37°C. Once colonies had been confirmed to contain the plasmid and gene of interest the bacteria were then cultured again overnight. A portion of these cultures were stored in glycerol and kept at -80°C for future use. The rest of the culture was centrifuged to create a plasmid pellet. This pellet was re-suspended and DNA was collected using a Promega Miniprep kit. The plasmid DNA could then be stored at -20°C in nuclease free water. Restriction enzymes are used to create linear plasmid and DNA was purified by Phenol/Chloroform extraction and precipitated for *in vitro* transcription.

cRNA was transcribed *in vitro* from purified linear dsDNA templates. mMessage T7 RNA kits (Ambion, Life Technologies, UK) or T3 RNA polymerase kits (Promega, UK) were used for the *in vitro* transcription reaction. cRNA was suspended in nuclease-free water and the concentration of RNA products were determined by photospectroscopy and diluted accordingly for microinjection. In this thesis there were a variety of cRNA products used including securin tagged with yellow fluorescent protein (securin-YFP), Histone 2B tagged with mCherry (Histone 2B-mCherry) and CENP C tagged with green fluorescent protein (CENPC-GFP).

2.13.4 Microinjection

An imaging chamber was created using a cylinder with a 22mm cover slip sealed to it using VALAP (Appendix B) in order to create a water tight chamber on a TE300 inverted

microscope (Nikon, Japan). To this 1ml of M2 media, containing milrinone, was placed into the chamber and covered with mineral oil. The media and oil was allowed to warm to 37°C within a heating unit (Intracel, UK). The holding pipette was fitted to the micromanipulator (Narashige, Japan) and manoeuvred into the heated chamber so that it was resting on the coverslip at the bottom; the 10x objective was focused accordingly. Denuded oocytes were then placed into the chamber next to the holding pipette. 10-20 oocytes were transferred to allow keep light exposure to a minimum. Once oocytes were in place the injection pipette was prepared. cRNA was defrosted and diluted to an appropriate concentration (250-1000ng/µl) using nuclease free water. Using a specially prepared syringe, about 0.3µl of cRNA was loaded into the pipette. Air bubbles were removed and cRNA encouraged into the pipette tip by gentle centrifugation or flicking. After larger air bubbles were dislodged the injection pipette was fitted to the micromanipulator and moved into focus next to the oocytes and holding pipette. Remaining air bubbles were removed by increasing the pressure to 60-80psi and applying this pressure for a short period of time. Pressure was reduced to 20-30psi, and the time pressure was released for was set to 100-200ms. Using these settings on the Pneumatic PicoPump (World Precision Instruments, UK) ensured cRNA microinjections of an adequate and consistent size.

During the injection procedure the 20x objective lens was used. A single oocyte was positioned on the holding pipette by applying gentle suction and the injection pipette was positioned just above the oocyte. The injection pipette was lowered, so that the zona pellucida was broken through and the oocyte was entered, at all times making sure that contact with the nucleus was avoided. A brief pressure was applied to release the injection; with a size similar to that of the nucleus. The injection pipette was swiftly removed from the oocyte.

Once all oocytes from a batch had been injected they were transferred back into a pre-warmed droplet of M2 media containing milrinone and allowed to rest for at least 1 hour before checking the presence or absence of fluorescence.

2.14 Confocal Microscopy: The Fundamentals

Fluorescence is when a sample can absorb light of one wavelength and then emit light of a different wavelength. This is due to the fact that electrons can be excited to a higher energy state and if the energy is not absorbed by surrounding molecules it will be emitted as light of a longer wavelength. This principle is applied in biological research by imaging

specimens that have been labelled with fluorescent dyes or proteins. As such these dyes and proteins have specific excitation and emission wavelengths (Table 4). In confocal microscopy several lasers are used as the light source; throughout this thesis I used four lasers (Table 5).

Table 4. Maximum absorbance and emission wavelengths of fluorescent dyes and proteins

Fluorescent Dye/Protein	Excitation maximum (nm)	Emission maximum (nm)
DAPI	359	461
Hoechst	352	461
Alexa fluor-488	495	519
Alexa fluor-555	555	565
Alexa fluor-633	632	647
mCherry	587	610
YFP	514	527
GFP	484	507

Table 5. Wavelengths of lasers used to image specific fluorochromes

Laser wavelength (nm)	Fluorophore
405	DAPI, Hoechst
488	GFP, Alexa fluor-488
514	YFP, Alexa fluor-555
594	mCherry
633	Alexa fluor-633

In order to generate an image using confocal microscopy the laser beams have to rapidly scan across a sample in a series of lines. Previously dichromatic mirrors were integral to the imaging process as they reflect higher energy low wavelengths from the laser to allow light to pass through the objective to the sample. The lower energy higher wavelength light emitted from the sample can be transmitted through the dichromatic mirrors. The light is then detected by a photomultiplier (PMT). Prior to reaching the PMT, light is focused onto a pinhole. The pinhole blocks out of focus light passing through to the PMT to give a clearer and more detailed image. The detector is attached to a computer to build up the image pixel by pixel. However, the confocal microscope I have used during the production of this thesis does not use chromatic mirrors; instead it utilises an alternative method of beam splitting called Acousto-optical Beam Splitting (AOBS). The beam splitter consists

of a Tellurium dioxide crystal that can diffract light of different wavelengths depending on its density. The density of the crystal can be altered by applying a mechanical radio-frequency wave. The idea is that a mechanical wave that would deflect the desired excitation colour is used so this light is then fed through to the objective lens to the sample. The emitted light travels through the crystal without any loss to the detector. This is the better option as there is no mechanical movement of parts or alignment of mirrors required. Due to AOBS being programmable changes in illumination parameters can be carried out rapidly.

2.15 Imaging

Fixed samples were imaged using the 60x oil immersion objective on a Leica SP8 confocal microscope fitted with hybrid detectors. Single stack and z-stack images were taken at 512x512 pixel resolution. To prevent bleed through fluorescence being detected fluorochromes with similar emission spectra (Figure 2.1) were imaged sequentially when required.

When quantifying the levels of γH2AX, a ~30µm z-stack (z-slice of 1µm) of the nucleus was taken and the laser settings were not altered throughout the experiment. These images were taken using the 60x objectives with a zoom factor of 2 to obtain an overview of the whole oocyte and a zoom factor of 5 when focusing on just the nucleus.

During time-lapse imaging either the 20x or 40x objectives was used and single stack images were taken to monitor Securin-YFP fluorescence. Chromosome tracking was used in experiments where the dynamics of chromosomes were to be investigated after oocytes had been microinjected with Histone 2B-mCherry and CENPC-GFP.

2.16 Image Analysis

2.16.1 γH2AX Quantification

All images were processed using Image J software (NIH, USA). To determine the nuclear γH2AX fluorescence both nuclear fluorescence intensity, as well as a cytoplasmic background reading needed to be recorded for each oocyte and recorded in Microsoft Excel. Images were opened in Image J and an optical slice where the area of the nucleus was clear and in focus was selected. Using this slice regions of interest (ROI) were defined using the circular tool on Image J; one for the area of the nucleus and one of the same size

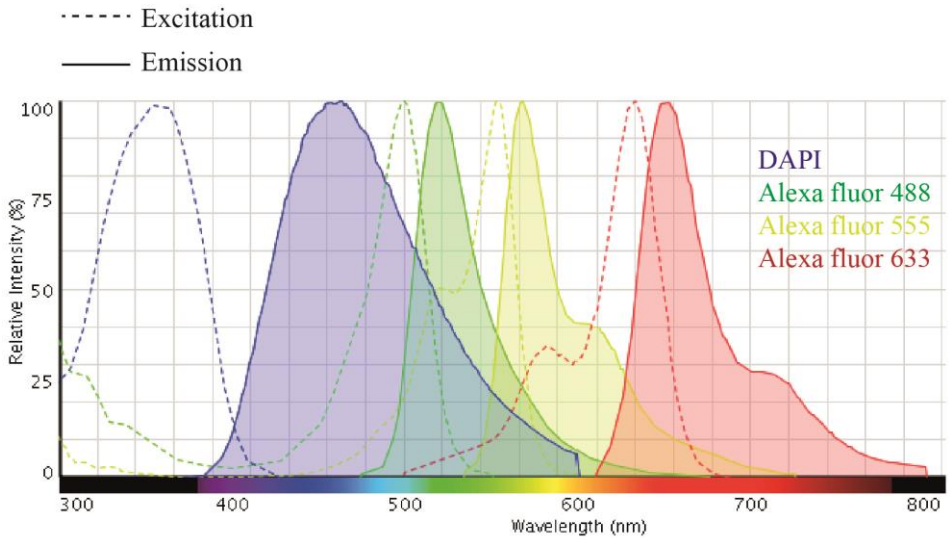

Figure 2-1 Excitation and emission spectra for fluorochromes used in this thesis

The spectra for DAPI, Alexa fluor 488 and Alexa fluor 555 have considerable overlap. These fluorochromes were imaged in a sequential manner to avoid bleed through fluorescence being detected. This was generated using the Fluorescence SpectraViewer available online from Thermo Fisher Scientific.

was placed in the cytoplasm of the oocyte to obtain the background reading (Figure 2.2A). Once these ROIs had been defined the image was opened as a z-stack of the γH2AX channel (Figure 2.2B). Using the 'multi-measure' tool the area and mean fluorescence for each ROI were measured and then exported into Excel. This was repeated for each individual oocyte, by moving and adjusting the size of the ROIs as required.

2.16.2 Securin-YFP Degradation

The images obtained from time lapse imaging were opened in Image J as a stack and then defined regions were marked where fluorescence was to be measured (Figure 2.3A). One region was centred on an area that did not contain an injected oocyte and was used to take a background reading. The average intensity for each region of interest was recorded for all time points (Figure 2.3B) and the raw data was transferred to an Excel spreadsheet.

Firstly the background reading was subtracted from each oocyte for the corresponding time point (Figure 2.3C). The traces were normalised so that the maximum fluorescence was set to 100 (Figure 2.3D). Then the time was adjusted to account for GVBD so that GVBD was time '0' (Figure 2.3E). For display purposes the period between 10-13 hours after GVBD were needed; this required the traces to be normalised to the value at 10 hours after GVBD.

Two time periods were of interest with regards to the degradation rate of securin; before and after Reversine (see section 2.8) had been added to culture media. The rate of securin degradation prior to Reversine addition was calculated for individual oocytes from the fluorescence readings taken between 4 and 10 hours after GVBD (Figure 2.3E). Minimum and maximum fluorescence values and the time these occurred were recorded for each oocyte. The rate of degradation was calculated using the following equation:

$$(\max value - \min value) \div (t \min - t\ max)$$

t = time point

The rate of degradation after the addition of Reversine to culture media was also calculated using the above equation. However, the time period of interest was 11.25 to 12.25 hours after GVBD (Figure 2.3E) when the Reversine was added; therefore fluorescence readings were used for this set period for individual oocytes. When all degradation rates had been calculated mean degradation rates (and standard deviations) could be obtained for both time periods.

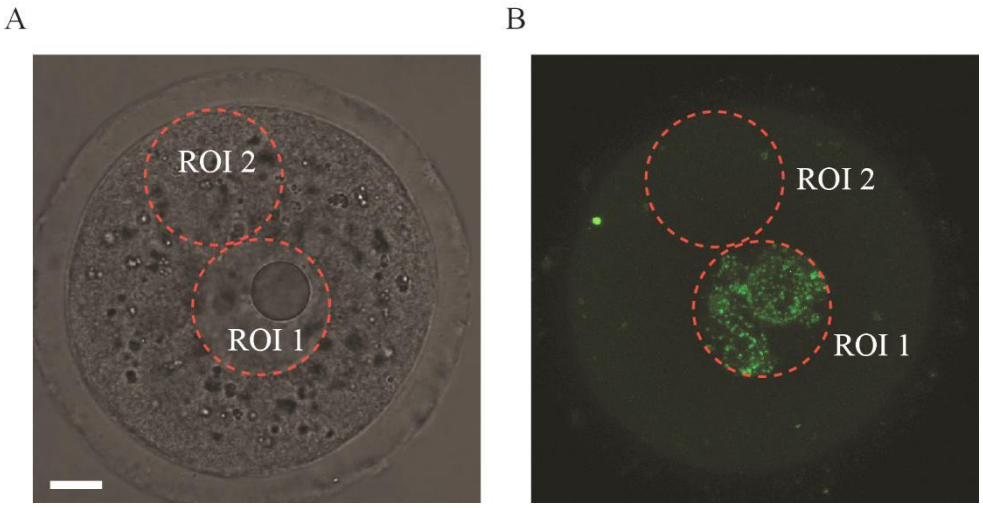

Figure 2-2 Analysing γH2AX fluorescence in oocytes

(A) A single optical selection of an oocyte in which the area of the nucleus is clear and visible. Regions of interest (ROI) were selected using the circle drawing tool on ImageJ. (B) A z-stack of the oocyte in 'A' showing only the γH2AX channel. The positions of ROI1 and ROI2 were logged so that these areas could be measured on the z-stack image. Scale bar, 10μm.

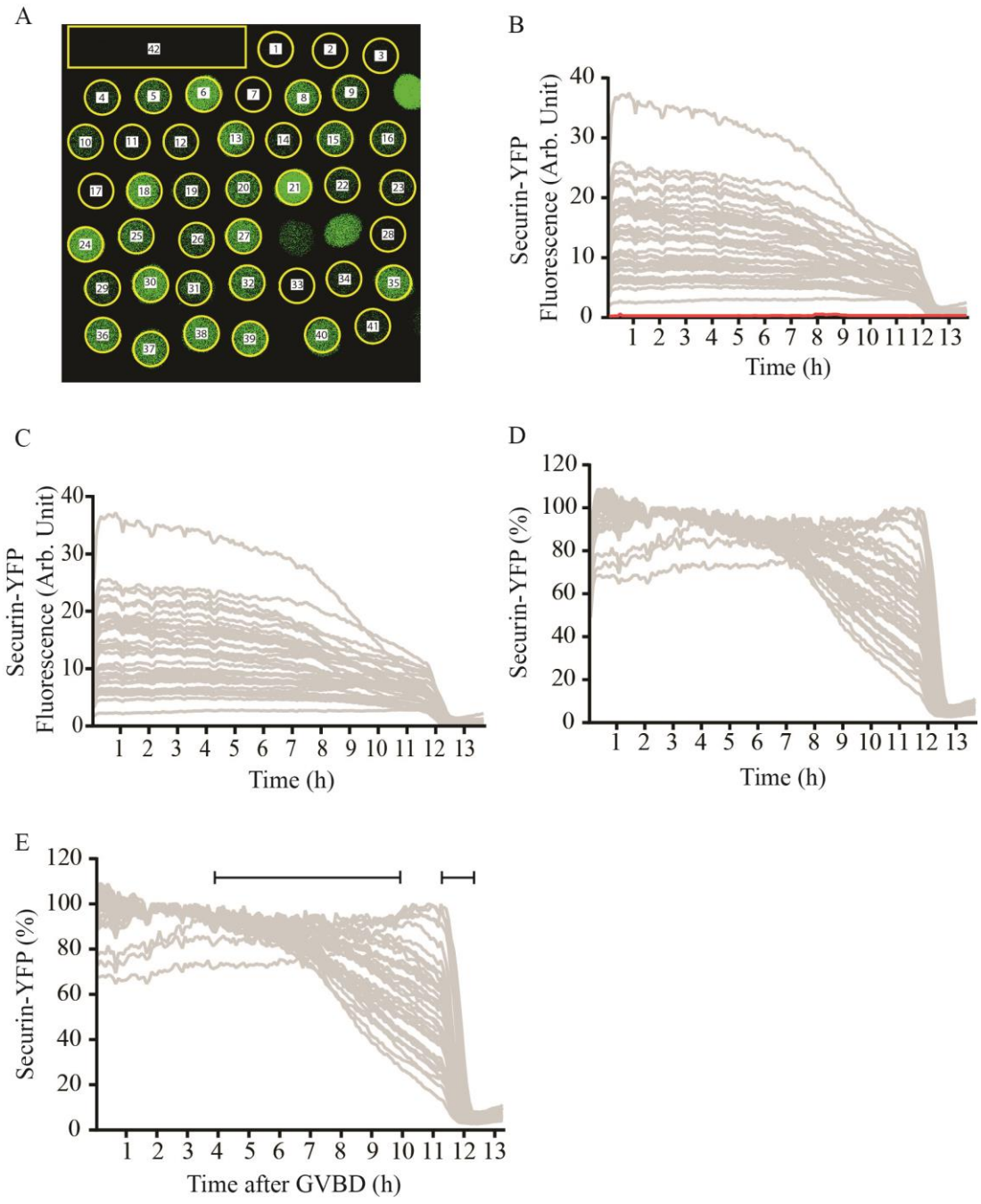

Figure 2-3 Securin-YFP Analysis

(A) Image shows oocytes microinjected with securin-YFP (green). Regions of interest (ROI) were assigned to oocytes and background reading (yellow lines). (B) Raw securin-YFP fluorescence readings during time-lapse for each ROI. Red line represents background securin-YFP fluorescence. (C) Securin-YFP fluorescence after background subtraction. (D) Securin-YFP normalised to the maximum value for each oocyte. (E) Securin-YFP fluorescence after adjusting for GVBD. The black lines represent the time periods where securin degradation rate were calculated.

2.16.3 Chromosome Alignment Analysis

To assess the extent that DNA damage caused the clustering of chromatin at the spindle poles, oocytes were fixed after IVM, stained with antibody against tubulin and counterstained with Hoechst/DAPI. Using z-stack images, a fluorescence plot for Hoechst/DAPI was generated on Image J. The area selected was based on the location of the spindle. Due to the plot being read from left to right all oocytes needed to be in a horizontal orientation with one pole on the left and the other on the right (Figure 2.4A, B). The region to be measured was set using the square tool on Image J. The individual data points from the plot were normalised to the maximum value for that oocyte (Figure 2.4C). The peaks on the plot represent areas of high fluorescence, and so the occurrence of chromatin. On most controls, one peak is seen located in the middle of the spindle, where the chromosomes should align. However, if chromatin was at the spindle poles, extra peaks could be seen. Therefore when analysing the normalised fluorescence plot anything with more than the central peak was scored as having chromatin at the spindle poles.

2.16.4 MAD2 Analysis

Oocytes were fixed at 7 hours after GVBD and stained using the CREST and MAD2 antibodies. The ratio of MAD2/CREST was calculated using a Macro designed for ImageJ. Macros are a saved sequence of instructions or commands to allow a task to be automated. The images were opened in ImageJ and using the CREST signal the position of pairs of kinetochores were logged. The macro marks the image with an open circle and when the slice is reached where the kinetochore was logged it turns into a solid circle. As well as this each pair of kinetochores is numbered, ensuring each kinetochore is only logged once. The macro then calculates the CREST and MAD2 signal intensity along with a background reading. A background subtraction for both MAD2 and CREST is performed and the ratio of MAD2/CREST is calculated. This data was then exported to Excel.

2.16.5 Analysis of Spindle Parameters

Spindle length and width were determined using a Macro made for ImageJ. Images that displayed α-tubulin staining were opened as a z-stack. The area of interest (the spindle) was defined using the ‘square’ tool and the macro then 3D rendered the image. It then recorded the maximum length and width of the spindle. This data was then exported into Excel and analysed using GraphPad Prism.

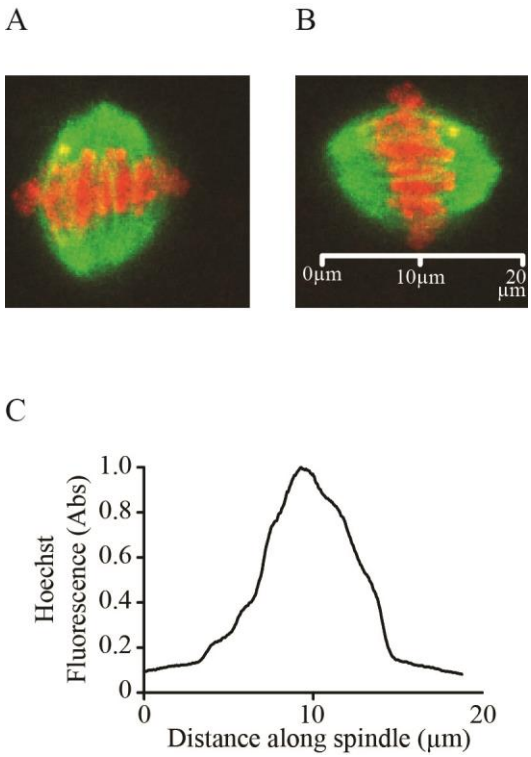

Figure 2-4 Analysis of chromatin clustering towards the spindle poles

(A) Representative oocyte displaying tubulin and Hoechst staining. This oocyte is in the wrong orientation for plotting Hoechst fluorescence. The image needs to be rotated by about 90º. (B) The image has been rotated so that Hoechst fluorescence can be read from one spindle pole to the other (left to right). (C) The Hoechst fluorescence plot for the oocyte shown in 'B', read from one end of the spindle to the other. The x-axis matches the scale bar used in 'B'.

2.17 Statistical Analysis

All statistical analysis was performed using Prism software (GraphPad Software, Inc). Categorical data was analysed using chi squared (Fisher's Exact test). Continuous data was first assessed for normality using the 'Column Statistics' tool on GraphPad. If all groups of data passed the normality test it was then analysed using by Analysis of Variance (ANOVA) with Tukey's post hoc analysis or t-test. When data did not pass the normality test it was analysed using either Mann-Whitney or Kruskal-Wallis with Dunn's post hoc analysis.

Chapter 3: The DNA Damage Response in GV Oocytes

3.1 Introduction

Marangos and Carroll (2012) showed that fully grown GV oocytes do not possess a robust G2/M checkpoint (see Chapter 1.7.2) and can readily re-enter meiosis I. It had also previously been suggested that DNA double strand breaks (DSBs) may impair the progression of oocytes through the remainder of meiosis I (Yuen et al. 2012). Therefore, in this chapter I wanted to characterise the response of fully grown GV oocytes to DNA damage, as these oocytes are temporally closer to producing an embryo, than those from primordial follicles. As a starting point, I needed to find a method to score oocyte maturation success and an *in vitro* maturation (IVM) protocol that permitted a satisfactory rate of maturation. I also needed to establish a method of treating oocytes with DNA damaging agents prior to IVM.

Throughout this chapter I used a variety of DNA damaging agents, both physical and chemical, including Etoposide, Bleomycin sulphate, UV-B and ionising radiation. Etoposide is a topoisomerase inhibitor, capable of inducing DNA DSBs (Chapter 1.2.1). This DNA damaging agent was used by Marangos and Carroll (2012) during their investigation into the effect of DNA DSBs on meiotic resumption. It was logical to use this drug in my study to add continuity to our knowledge of oocyte responses to DNA damage. In order to establish that the responses seen in oocytes were a result of DNA damage in general and not unique to Etoposide, other damaging agents were also used. Ionising radiation, is also able to induce DNA DSBs, but through a different mechanism to that of Etoposide. It is capable of directly altering the structure of DNA, however most damage is caused by the production of free radicals that attack the DNA structure (Chapter 1.2.2). Bleomycin sulphate, is an antibiotic drug often used to treat tumours by inducing DNA DSBs, due to its ability to produce free radicals similar to that of ionising radiation (Chapter 1.2.3). Finally, UV-B was used as a second physical damaging agent, alongside ionising radiation. The damage induced by UV exposure can take a variety of forms from base alterations to DSBs (Chapter 1.2.4).

Once my methods and protocols had been decided I wanted to confirm the findings of Marangos and Carroll (2013), that oocytes do not possess a robust G2/M checkpoint. This was done by treating oocytes with Etoposide, Bleomycin or UV-B and then monitoring the

oocytes under the microscope for the presence or absence of the GV, as this is visual confirmation of the resumption of meiosis.

Once these preliminary measures were complete I investigated the ability of oocytes to respond to DNA damage at a later point in meiosis I. Oocytes were treated with DNA damaging agents, and then allowed to undergo an IVM and the success of this maturation period was assessed after 16 hours. Also, the timing of DNA damage induction and oocyte response was observed. This was assessed by treating the oocytes with DNA damaging agents either whilst they were GV arrested, as in previous experiments, or after meiosis had been resumed. A final aspect that I looked into was whether extending the IVM period, far beyond that of my normal protocol, had any effect on the oocyte response to DNA damage. Therefore, this chapter solely focuses on how DNA damage affects oocyte maturation rates under a variety of experimental conditions.

3.2 Results

3.2.1 Experimental Designs for investigating the effect of DNA Damage on Meiosis I

To better understand the effect of DNA damage on the progression of an oocyte through meiosis I several experimental designs were used (Figure 3.1). To establish if DNA damage has any effect on GVBD, fully grown GV arrested oocytes were treated with DNA damaging agents. These oocytes were then released from milrinone, a drug that keeps them arrested at the GV stage by inhibiting PDE3 (Chapter 1.6.4). Oocytes were monitored every 10 minutes for the disappearance of the GV, visual confirmation of meiotic resumption; this was carried out for a period of 90 minutes in total (Figure 3.1A).

To monitor the effect of DNA damage on the completion of meiosis I, oocytes were treated with DNA damaging agents whilst GV arrested and immediately released from milrinone. This was followed by an IVM of 16 hours (GVBD + 15 hours), in the dark at 37ºC, and after this polar body extrusion (PBE), visual confirmation of the completion of meiosis I, was assessed (Figure 3.1B).

To understand whether the timing of DNA damage induction has any effect on the completion of meiosis I GV arrested oocytes were released from milrinone immediately after collection. These oocytes underwent GVBD and were then treated with DNA damaging agents 1 hour later. PBE was assessed after the standard 16 hour IVM (Figure 3.1C).

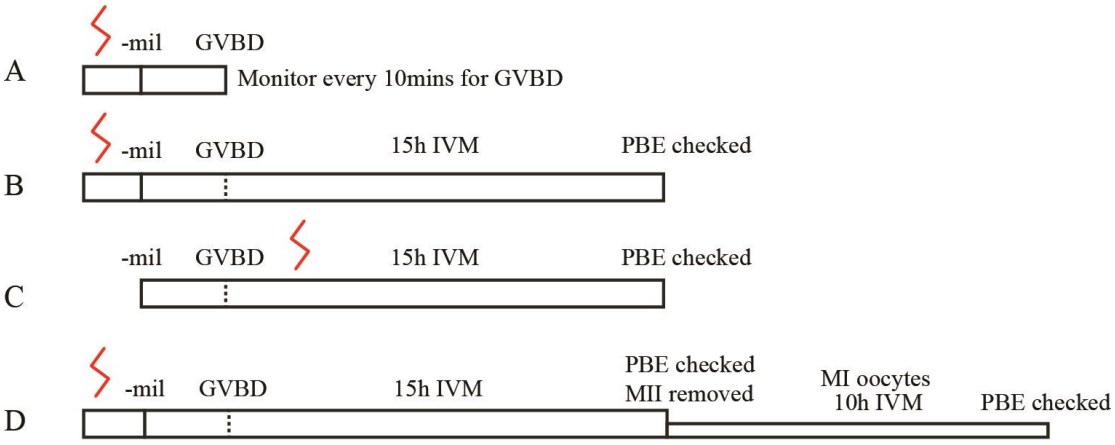

Figure 3-1 Experimental designs for examining the effect of DNA damage on oocyte maturation

(A) DNA damage induced whilst GV arrested, and then oocytes were monitored every 10 minutes for GVBD, for a total of 1.5 hours. (B) DNA damage induced whilst GV arrested, followed by a standard length IVM of 16h (GVBD+15h). PBE checked at 16h after release from milrinone. (C) Oocytes washed from milrinone immediately after collection and DNA damage induced 1h after GVBD. A standard IVM (GVBD+15h) was used for these oocytes. (D) DNA damage induced whilst GV arrested, followed by standard length IVM (GVBD+15h). When PBE checked oocytes arrested in meiosis II (MII) removed from pool. Oocytes arrested in meiosis I (MI) had a further 10h IVM and after a total of 25h (GVBD+24h) a final PBE count performed. Red line indicates induction of DNA damage.

Finally, to see if the length of IVM had any effect on maturation success after DNA damage induction, oocytes were treated whilst GV arrested and released from milrinone. These oocytes were then cultured *in vitro* for 16 hours. PBE was checked at this point and any oocytes with a polar body were removed from the pool. Oocytes without a polar body, and therefore arrested in meiosis I, had a further 10 hours of IVM. A final PBE assessment was taken at a total of 24 hours after GVBD (Figure 3.1D).

3.2.2 Spontaneous arrest is seen in undamaged oocytes

Oocyte maturation rates are often reported at between 70-80% (Yuen et al. 2012). However, this still leaves a large proportion of oocytes that spontaneously arrest in meiosis I. To monitor maturation rates throughout this thesis oocytes were assessed for the presence of a polar body, to provide visual confirmation of the completion of meiosis I. Examples of a mature oocyte and one arrested in meiosis I are shown in Figure 3.2A and B respectively.

When the maturation data of undamaged oocytes from a series of experiments are combined, giving a sample size of over 1000 oocytes, ~80% of oocytes reached the metaphase II stage (Figure 3.2C). To investigate the cause of the spontaneous arrest seen in ~20% of oocytes, I examined the chromatin conformation in individual GV oocytes. Over 90% of fixed oocytes had the surrounded nucleolus (SN) chromatin conformation, indicative of meiotic competence (Monti et al. 2013) (Figure 3.2D, E). This suggested that the cause of meiotic arrest after GVBD was not lack of meiotic competence and instead must be due to some other alternative, possibly endogenous DNA damage.

3.2.3 DNA damage induced in GV oocytes does not block GVBD

As it had already been seen in one study that only high exposure to Etoposide prevents oocytes from undergoing GVBD (Marangos and Carroll 2012), it was important to show that such results could be reproduced using the experimental design shown in Figure 3.1A. GV arrested oocytes were treated with 25 µg/ml Etoposide, 1µM Bleomycin or 15 seconds of UV-B exposure, released from milrinone and were monitored every 10 minutes for the disappearance of the GV to highlight the timing of GVBD. For these three DNA damaging agents normal rates and timings of GVBD were seen (Figure 3.3). By monitoring the disappearance of the GV, it was found that the mean time that 50% of the oocytes underwent GVBD by was altered by less than 10 minutes when DNA damage had been induced. At 50 minutes after release from milrinone the percentage of oocytes with DNA

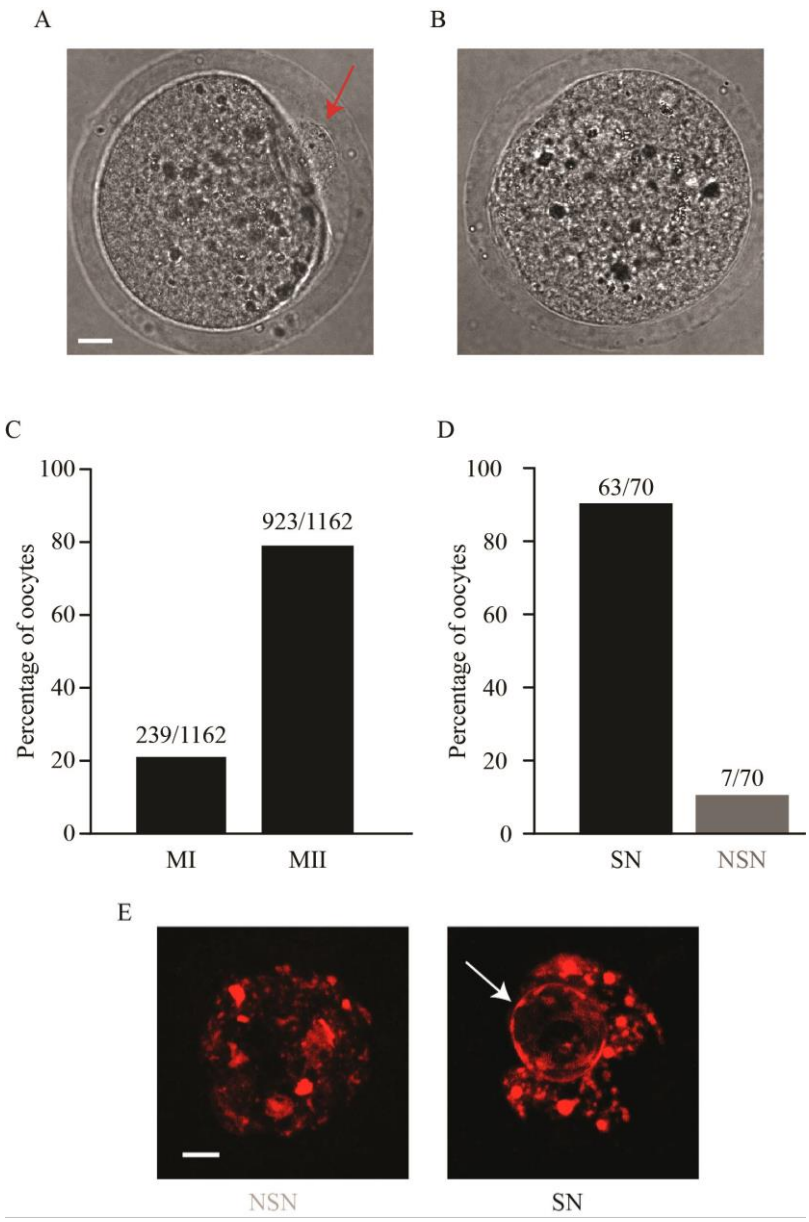

Figure 3-2 Maturation rates in undamaged oocytes

(A) Representative metaphase II oocyte. The extruded polar body can be clearly seen, indicated by the red arrow. (B) Representative oocyte arrested in meiosis I. Note how no polar body can be seen (C) Maturation rates seen in vehicle treated oocytes after IVM of 16 hours (GVBD+15h). Proportion of oocytes arrested at meiosis I (MI) and meiosis II (MII) are depicted. (D) Percentage of oocytes with surrounded nucleolus (SN) or non-surrounded nucleolus (NSN) chromatin conformation. (E) Representative oocytes displaying either SN or NSN chromatin conformation. White arrow highlights the nucleolus. Numbers of oocytes used are as stated. Scale bars, 10µm.

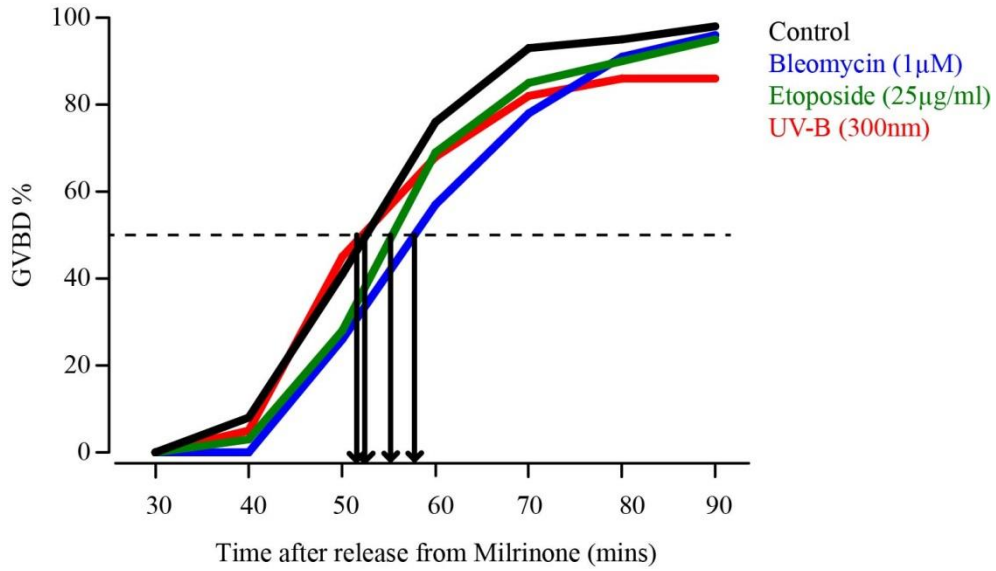

Figure 3-3 Timing of germinal vesicle breakdown was not altered by DNA damage

Timing of GVBD in GV oocytes treated with 0.1% DMSO (n=59); 25µg/ml Etoposide (n=39); 1µM Bleomycin sulphate (n=23); or 15 seconds of UV-B exposure (n=22). Mean timing of 50% of oocytes undergoing GVBD shown by black arrows.

damage that had undergone GVBD was lower than that of undamaged oocytes but this did not reach statistical significance (Control, 41%, n=59; Etoposide, 28%, n=39, P=0.2819; Bleomycin, 26%, n=23, P=0.3149; UV-B, 45%, n=22, P=0.8016 compared to 'Control', Fishers exact test; Figure 3.3). Nevertheless, within 90 minutes over 85% of all oocytes, both un-damaged and damaged, had undergone GVBD. The other DNA damaging agent - ionising radiation- used throughout this thesis was not tested due to the feasibility of the experiment. The Gammacell 1000 Elite (Nordion International Inc., Ontario, Canada), used to treat oocytes with ionising radiation, was based off-site. This meant that there would not have been time to have treated the oocytes and begin the monitoring process before GVBD may have begun. This would have given an incomplete picture of GVBD in ionising radiation treated oocytes, so this treatment was omitted from this experiment.

3.2.4 DNA damage induced in GV oocytes causes an arrest in meiosis I

The lack of effect on GVBD in DNA damaged oocytes led to an investigation into whether such lesions to DNA could alter the progression through meiosis I. To determine this, GV oocytes were handled according to the experimental design in Figure 3.1B. Four different DNA damaging agents were used during these experiments at a range of exposure times or concentrations. After a total of 16 hours of IVM, maturation success was calculated by identifying oocytes with the presence of a polar body (see Figure 3.2A). The absence of a polar body (see Figure 3.2B) was recorded as arrested in meiosis I (MI).

Treatment of oocytes with 2.5µg/ml of Etoposide did not cause a significant increase in MI arrest (Control, 22%, n=462; 2.5µg/ml Etoposide, 24%, n=37; P=0.8377, Fishers exact test; Figure 3.4A). However, in oocytes treated with Etoposide concentrations of 5-100µg/ml, whilst GV arrested, the ability to progress to meiosis II was significantly reduced, marked by an increase in the percentage of oocytes that arrested in MI. The proportion of oocytes that arrested in MI increased in a dose dependant manner. Of the oocytes treated with 5µg/ml Etoposide, 43% arrested in MI (n=40, P=0.0064 compared to '0', Fishers exact test), whereas 76% of oocytes were arrested after treatment with 50µg/ml (n=140, P< 0.001 compared to '0', Fishers Exact test).

Similar results were seen for oocytes treated with Bleomycin (Figure 3.4B). 34% of the oocytes treated with 0.3µM Bleomycin were found to arrest in MI (n=56, P=0.0134 compared to '0', Fishers exact test). Again the proportion of oocytes to arrest in MI increased in a dose dependent manner. About 41% of oocytes arrested in MI after treatment with 1µM Bleomycin (n=751, P<0.001 compared to '0', Fishers exact test) and

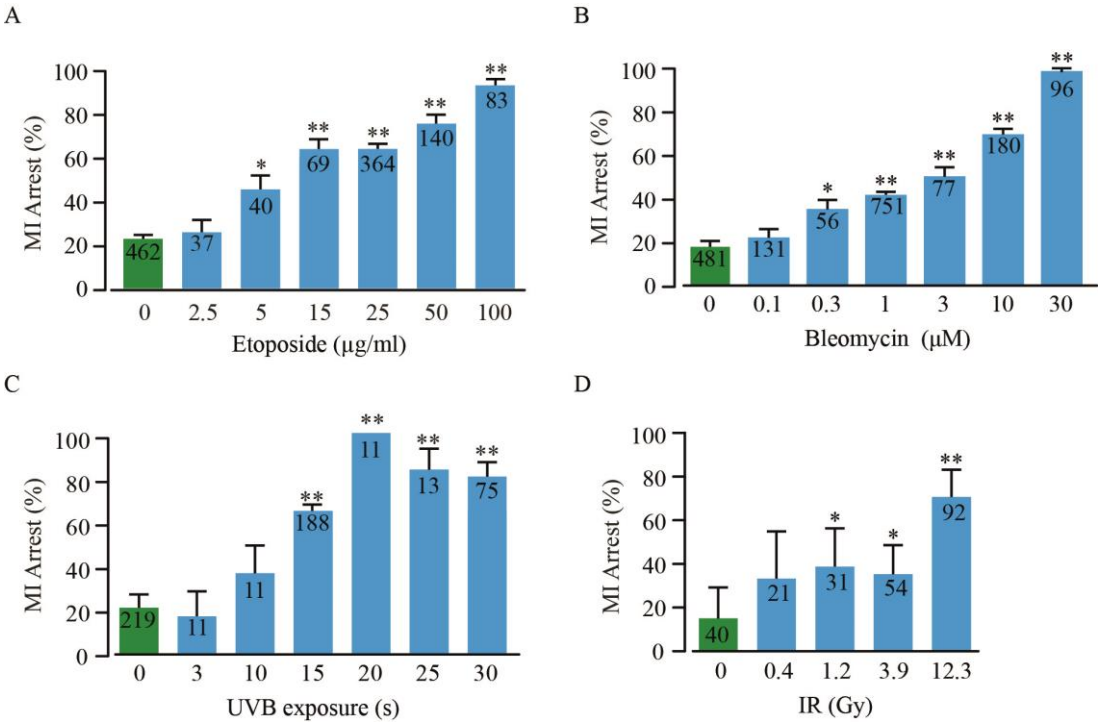

Figure 3-4 DNA damage causes oocytes to arrest in meiosis I

All oocytes in this experiment were treated whilst arrested at the GV stage, and then underwent a standard 16 hour IVM (GVBD+15h). (A) MI arrest rates of GV oocytes treated with varying concentrations of Etoposide for 15 minutes. (B) MI arrest rates of GV oocytes treated with varying concentrations of Bleomycin sulphate for 15 minutes. (C) MI arrest rates of GV oocytes exposed to UV-B (300nm) for specific periods of time. (D) MI arrest rates of GV oocytes exposed to ionising radiation for specific periods of time to create the desired dose (Gy). Numbers of oocytes used are indicated.*, $p<0.05$; **, $p<0.001$ compared to the respective control group (Fisher's Exact test). Error bars are standard error. Pooled from between 2 and 15 mice per treatment.

this increased to 98% of oocytes arresting after treatment with 30µM Bleomycin (n=96, P<0.001 compared to '0', Fishers exact test).

Arrest rates in oocytes exposed to 3 and 10 seconds of UV-B (300nm) did not significantly differ to those of un-exposed oocytes (0s, 21%, n=219; 3s, 18%, n=11, P= 1.000; 10s, 36%, n=11, P=0.2535, Fishers exact test, Figure 3.4C). However, 15 seconds of UV-B exposure caused 66% of oocytes to arrest in MI (n=188, P< 0.001 compared to '0', Fishers exact test, Figure 3.4C). Further increases in MI arrest were seen when longer UV-B exposure times were used (25s, 85%, n=13, P<0.001 compared to '0'; 30s, 81%, n=75, P<0.001 compared to '0', Fishers exact test, Figure 3.4C).

Exposure of oocytes to 0.4Gy caused 33% to arrest in meiosis I, however this did not reach significance when compared to un-exposed oocytes (0, 15%, n=40; 0.4Gy, 33%, n=21, P=0.1127 compared to '0', Fishers exact test, Figure 3.4D). However, 1.2Gy of ionising radiation caused 39% to arrest in MI (n=31, P=0.0295 compared to '0', Fishers exact test, Figure 3.4D) and this increased to 66% of oocytes arresting in MI after exposure to 12.3Gy ionising radiation (n=92, P<0.001 compared to '0', Fishers exact test, Figure 3.4D).

3.2.5 DNA damage induced after GVBD causes an arrest in meiosis I

Having established that damaging the DNA of oocytes whilst at the GV stage caused an arrest after GVBD, it was also checked whether inducing DNA damage after GVBD had any effect on the arrest seen using experimental design shown in Figure 3.1C. Only three of the DNA damaging agents used throughout this thesis was tested (Etoposide, Bleomycin sulphate, and UV-B). Ionising radiation was not used during these experiments due to the equipment required for this treatment not being on site, as discussed in Section 3.2.3. In order to make a comprehensive comparison of the effect of treatment timing experiments in which oocytes had either been treated before GVBD, or after GVBD, were run side-by-side. PBE was assessed after a total of 16 hours IVM. Treating oocytes with these DNA damaging agents 1 hour after GVBD still led to oocytes arresting in meiosis I (Figure 3.5).

In oocytes treated with 25µg/ml Etoposide at the GV stage 75% were arrested in MI after 16 hours IVM, compared to only 24% of control oocytes (- Etop, n=191; + Etop, n=145, P<0.001 compared to -Etop, Fishers exact test, Figure 3.5A). The ability to arrest in MI was still present even when oocytes were treated with 25µg/ml Etoposide 1 hour after GVBD; 79% of Etoposide treated oocytes were arrested in MI compared to 24% of control

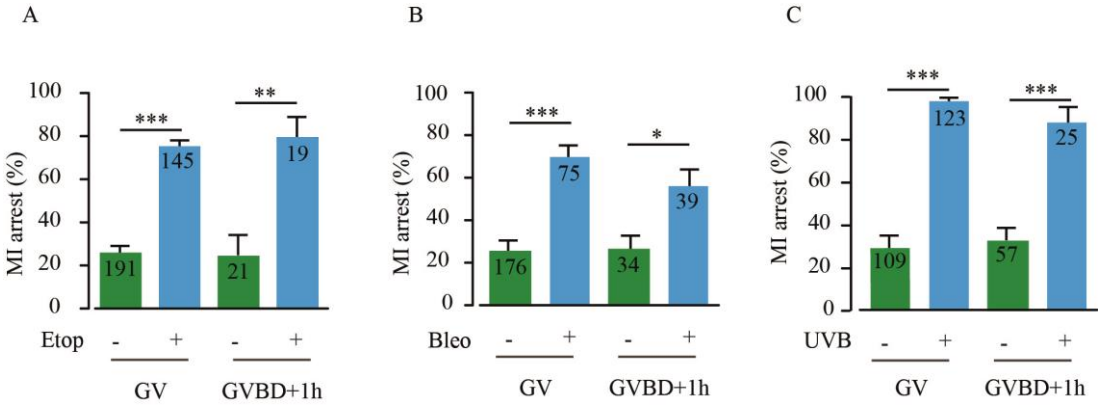

Figure 3-5 DNA damage induction after GVBD caused an arrest in meiosis I

All oocytes in these experiments were treated either during GV arrest or 1 hour after GVBD. (A) MI arrest rates of oocytes treated with 25µg/ml Etoposide. (B) MI arrest rates of oocytes treated with 1µM Bleomycin sulphate. (C) MI arrest rates of oocytes treated with 30 seconds of UV-B. Numbers of oocytes used are indicated. A and B are compared against vehicle addition (0.1% DMSO); C is compared against no UV-B exposure. *, $p<0.05$; **, $p<0.01$; ***, $p<0.0001$ (Fisher's Exact test). Error bars are standard error. Pooled from between 2 and 6 mice per treatment.

oocytes (-Etop, n=21; + Etop, n=19, P=0.0012 compared to -Etop, Fishers exact test, Figure 3.5A).

A similar result was seen in oocytes treated with bleomycin before and after GVBD (Figure 3.5B). Oocytes treated with 1µM Bleomycin at the GV stage had an MI arrest rate of 72% compared to only 22% seen in control oocytes (-Bleo, n=176; +Bleo, n=75, P<0.001 compared to -Bleo, Fishers exact test). Again, the ability to arrest in MI was retained in oocytes treated with 1µM Bleomycin 1 hour after GVBD; 56% of Bleomycin treated oocytes were arrested in MI compared to 26% of control oocytes (-Bleo, n=34; +Bleo, n=39, P=0.017 compared to -Bleo, Fishers exact test).

Oocytes exposed to 30 seconds of UV-B were also just as sensitive whether the treatment occurred before or after GVBD (Figure 3.5C). In those oocytes exposed to UV-B prior to GVBD, 99% arrested in MI after IVM compared to 26% of un-exposed oocytes (-UVB, n=109; +UVB, n=123, P<0.001 compared to -UVB, Fishers exact test). Similar arrest rates were seen when oocytes were exposed to UV-B 1 hour after GVBD; 88% of the treated oocytes were arrested in MI compared to 32% of unexposed oocytes (-UVB, n=57; +UVB, n=25, P<0.001 compared to -UVB, Fishers exact test).

3.2.6 A prolonged IVM after treatment can have an effect on arrest rates

It was important to investigate whether the response seen after DNA damage was a robust arrest in the cell cycle, or simply a delay in the transition to MII. To study this the experimental design as shown in Figure 3.1D was used; oocytes were released from milrinone after treatment and allowed to undergo IVM for 15 hours after GVBD. Those oocytes that were arrested in meiosis I were allowed to undergo a further 10 hours of IVM before a final PBE score was taken.

Indeed, for Etoposide, UV-B and IR treated oocytes the DNA damage appeared to cause a robust arrest, with a majority of oocytes (60-92%) remaining arrested in meiosis I. Interestingly, 93% of oocytes treated with Bleomycin that had been arrested at 15h after GVBD had undergone PBE by 25 hours after GVBD (Figure 3.6).

3.3 Discussion

In this chapter, the induction of DNA damage, both physical and chemical, did not significantly affect the rate or timing of GVBD in oocytes. Instead oocytes were able to resume meiosis I as normal. However, the presence of DNA damage, regardless of the

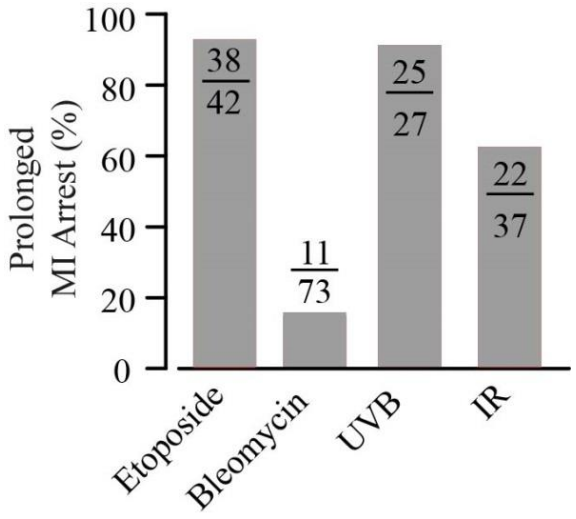

Figure 3-6 Prolonged MI arrest rates in oocytes with DNA damage

Following DNA damage induction at the GV-stage, oocytes in these experiments were initially arrested in meiosis I when checked 15 hours after GVBD, and then cultured for a further 10 hours before being assessed for PBE. Treatments were 25µg/ml Etoposide (15 mins), 1µM Bleomycin sulphate (15 mins), 15 seconds of UV-B exposure or 12.3 Gy of ionising radiation. Numbers of oocytes used are indicated. Pooled from between 2 and 4 mice per treatment.

timing of damage induction, led to oocytes arresting during meiosis I and prevented the formation of polar bodies. The arrest induced by DNA damage appeared to be robust in most of the damaging agents tested, except Bleomycin where a majority of oocytes had been able to extrude polar bodies after a total of 25h IVM.

3.3.1 Oocytes do not have a robust G2/M checkpoint

There are several commonalities of the oocyte prophase arrest and the G2/M checkpoint seen in somatic cells (Solc et al. 2010), and due to this it was assumed that the oocyte may be able to initiate a G2/M checkpoint when exposed to genotoxic agents and maintain the GV state. However, the first study that looked into the effect of DNA double strand breaks in fully grown GV oocytes revealed that in stark contrast to mitotic cells, oocytes do not induce a robust G2/M checkpoint and can resume meiosis after exposure to Etoposide (Marangos and Carroll 2012). Only very high concentrations of Etoposide or doxorubicin delayed M phase entry, but did not prevent it.

The absence of an efficient DNA damage checkpoint in prophase arrested oocytes appears to be due to a lack of ATM kinase activation, also known to be one of the major components of the DDR in somatic cells (Chapter 1.3.1). Very high levels of DNA damage were able to induce ATM activation culminating in the CHK1-dependent inhibitory phosphorylation of CDC25B, a key player in activating CDK1-Cyclin B1, and prevented of GVBD (Marangos and Carroll 2012). The lack of ATM activation in oocytes, compared to somatic cells, was suggested to be due to low levels of ATM expression or the specific chromatin configuration in oocytes.

Indeed, when GV stage oocytes were exposed to a variety of DNA damaging agents the process of GVBD was not affected, and only a small delay was seen (Figure 3.3). More recently published work has also highlighted the lack of a G2/M checkpoint in porcine oocytes where treatment with Etoposide did not alter the ability to undergo or the kinetics of GVBD (Wang et al. 2015a), suggesting that the relative insensitivity of oocytes at this stage may occur in all mammalian species.

However, there are some differences between my results and those reported among other studies. These differences are most likely due to differences in experimental design, such as treatment protocols and mouse strain (Table 6). I have shown that over 80% of oocytes had undergone GVBD within 90 minutes of release from milrinone after treatment with 25µg/ml Etoposide (Figure 3.3). In contrast, less than half of the oocytes had undergone

GVBD within 2 hours, when treated with the same concentration of Etoposide by Marangos and Carroll (2012). Here the difference is probably due to the fact I used a 15 minute exposure to the Etoposide, versus 3 hours used by Marangos and Carroll (2012). Regardless of this though, the overall conclusion, that oocytes do not possess a robust G2/M checkpoint, is still the same, as even when oocytes are treated with 25µg/ml Etoposide for 3 hours over 80% undergo GVBD when examined 20 hours after release from milrinone (Marangos and Carroll 2012).

Table 6. Protocols used to study the G2/M checkpoint in oocytes

	Treatment	Examination Protocol	Mouse Strain
My protocol	25µg/ml Etoposide 15 mins 1µM Bleomycin 15 mins	Every 10 mins for 1.5 hours	C57Bl/6
Marangos and Carrol (2012)	5-100µg/ml Etoposide 3 hours	Every 60 mins for 5 hours & re-examined at 20 hours	MF1
Ma et al. (2013)	5-40µM Bleomycin 1 hour	Every 30 mins for 4 hours	Not specified

One study has even suggested that DNA damaging oocytes can significantly reduce GVBD when treated with Bleomycin or inducing DSBs using laser beam microdissection (Ma et al. 2013). Again the difference seen here is probably due to differences in treatment and monitoring protocols (Table 6). Ma et al. (2013) exposed GV oocytes to much higher concentrations of Bleomycin and for a longer treatment time; therefore the levels of damage induced would be far greater. Also, GVBD rates were monitored up to 4 hours only, rather than the re-examination at 20h carried out by Marangos and Carroll (2012), where they may have seen a greater number of oocytes had undergone GVBD.

Although the treatment protocol is most likely the cause of the difference seen between my results (Figure 3.3) and those previously reported, another factor that could have added to variation is the strain of mouse used (Table 6). The mouse strain used was not reported by Ma et al. (2013) and the MF1 strain was used by Marangos and Carroll (2012), in contrast to the C57Bl/6 strain that I used throughout this thesis. In several reports it has been shown that metaphase II (MII) eggs collected from several strains of mice have varied responses to DNA damage (Kujjo et al. 2010, Perez et al. 2007). In these studies, MII oocytes from the AKR mouse strain were much more sensitive to DNA damage and readily underwent

apoptosis in response to such insults. The susceptibility was thought to be due to a reduced ability to carry out DNA damage repair. Microinjection of recombinant RAD51, a protein essential for DNA DSB repair by homologous recombination (see Chapter 1.5.1), improved survival rates in these oocytes (Kujjo et al. 2010). Therefore, it could be that sensitivity of different strains to DNA damage may also contribute to variation in results reported.

Interestingly, a recent study has suggested that the cumulus cells surrounding the oocyte may give rise to a DNA damage response different to that of denuded oocytes. Oocytes in COCs do not undergo GVBD as readily as denuded oocytes when treated with DNA damaging agents. The mechanistic pathway leading to this response is thought to be an upregulation in cAMP (Sun et al. 2015). As already discussed high levels of cAMP in oocytes hold the oocyte at prophase until the LH surge at ovulation (Chapter 1.6.4). Thus, it is possible that a different situation may be seen in oocytes *in vivo* compared to the *in vitro* experiments on denuded oocytes.

3.3.2 Why do undamaged oocytes spontaneously arrest?

Carrying out IVM experiments throughout this thesis has allowed me to show that PBE is seen in about 80% of undamaged oocytes after 16 hours of *in vitro* culture (Figure 3.2A). This percentage agrees with published literature where PBE is often reported as at least 70% (Holt et al. 2012, Marangos et al. 2015, Yuen et al. 2012). Interestingly, this still leaves about 20% of oocytes that arrest in meiosis I for no apparent reason.

There are many possibilities that could cause oocytes to arrest in meiosis I spontaneously. Firstly, it could have been that oocytes retrieved during collections were still too immature and meiotically incompetent. This possibility was addressed by studying the chromatin configuration of GV oocytes that had been processed for immunofluorescence. The configuration of chromatin, with regards to the nucleoli, in GV oocytes has been suggested to be a good marker of meiotic competency and later embryonic development (Zuccotti et al. 2005). The surrounding nucleolus (SN) formation is where chromatin can be clearly seen associated with the nucleoli, as shown in Figure 3.2E. It is associated with competency and embryos will often develop to the blastocyst stage (Zuccotti et al. 2005). Whereas the non-surrounding nucleolus (NSN), shown in Figure 3.2E, is where chromatin is much more dispersed within the nucleus. Oocytes with this type of chromatin often arrest at the embryonic 2-cell stage after fertilisation (Zuccotti et al. 2005). Interestingly, in an intricate study by Inoue et al. (2008), they found that it was in fact cytoplasmic contents

of NSN oocytes that impeded meiotic development. On the other hand, embryonic development was more dependent on the material in the GV. They found this by transferring the GVs of NSN and SN oocytes into the enucleated SN and NSN oocytes respectively (Inoue et al. 2008). Nevertheless, oocytes with the NSN chromatin configuration still have poor meiotic and developmental outcomes. Of the oocytes stained with Hoechst and assessed here in my study, around 90% had the SN formation (Figure 3.2B). This means that there are around 10% of oocytes that would likely arrest in meiosis I despite having the SN configuration, and immaturity is unlikely to be the cause of the spontaneous arrest that is consistently seen in oocytes.

Another possibility is that DNA damage within oocytes caused by endogenous factors could contribute towards the spontaneous arrest. One factor known to induce DNA damage is oxidative stress (Kryston et al. 2011). Oxidative stress that arises endogenously can be caused by cellular signalling, as a by-product of metabolic processes or during inflammation (Kryston et al. 2011). As discussed in Chapter 1.2, free radicals, like reactive oxygen species (ROS) are responsible for oxidative damage to DNA, which can include base alterations, SSBs and DSBs (Kryston et al. 2011). DSBs have been specifically shown to arise endogenously in human cell lines and mouse embryonic fibroblasts (MEFs) under non-replicating conditions (Woodbine et al. 2011), as would be seen in the oocyte. Also intra-follicular concentrations of 8-hydroxy-2'-deoxyguanosine (8-OHdG), a common base alteration induced by oxidative stress, have been correlated with an increased number of degenerate oocytes in human IVF patients (Tamura et al. 2008). In this same study it was shown that mouse oocytes with induced oxidative stress, using hydrogen peroxide (H_2O_2) treatment, have reduced PBE rates and that these rates could also partially rescued using antioxidant treatment. Oxidative stress may therefore be a contributing factor to oocyte maturation rates, by inducing DNA damage. Further study would be required to fully understand why oocytes arrest in meiosis I despite having no prior treatment and appearing meiotically competent.

3.3.3 Oocytes have a specific checkpoint during M-phase

By evading a G2/M checkpoint, oocytes are able to resume meiosis I with damaged DNA. Also the fact that oocytes will spontaneously arrest in meiosis I (Figure 3.2), possibly due to endogenous DNA damage, led me to explore in more detail how oocytes respond to DNA damage. It is now clear that a mechanism exists to prevent the formation of a metaphase II egg with DNA damage.

Oocytes were shown to arrest in meiosis I after treatment with many DNA damaging agents including IR, UV-B, Etoposide and Bleomycin (Figure 3.4). This supports the findings of Yuen et al. (2012) where Neocarzinostatin (NCS) reduced the percentage of oocytes extruding polar bodies and Ma et al. (2013) in which PBE was delayed after treatment with Bleomycin and laser micro-beam dissection. The results reported in Figure 3.4 are also in agreement with very recent studies in which PBE rates in mouse oocytes were negatively affected by treatment with Etoposide, as well as Phleomycin and Doxorubicin (Marangos et al. 2015). An arrest in meiosis I after DNA damage has also been revealed in other mammalian systems including pigs (Wang et al. 2015a).

The ability of oocytes to arrest in response to DNA damage during the meiotic M phase is quite surprising due to the fact that mitotic cells are not able to establish a full DDR during the equivalent M-phase. It has been shown that mitotic cells can induce early signalling events such as ATM activation, H2AX phosphorylation and the recruitment of MDC1 and the MRN complex to these sites. However, the recruitment and interactions of repair factors such as RNF8, RNF168, BRCA1 and 53BP1 does not occur (Giunta et al. 2010, Heijink et al. 2013, Orthwein et al. 2014). As well as this, the activation of downstream proteins by ATM kinase, such as CHK2, does not occur during M-phase (Giunta et al. 2010). The ability of oocytes to respond to DNA damage during M phase was specifically addressed in Figure 3.5, as oocytes treated with damaging agents after GVBD were still able to arrest in meiosis I. The suppression of a full DDR during M phase in somatic cells is thought to prevent genomic instability. Instead somatic cells will progress through M phase and arrest at G1 of the next cell cycle, once a full DDR can be deployed (Giunta et al. 2010).

The induction of a DDR during the mitotic M-phase has been shown to increase the occurrence of lagging chromosomes during anaphase, due to the stabilisation of kinetochore-microtubule association (Bakhoum et al. 2014). Anaphase bridge formation has been reported to be promoted by DNA repair pathways when cells were treated with Etoposide (Terasawa et al. 2014). Also, restoring DNA repair during mitosis has been suggested to increase the occurrence of telomere fusions (Orthwein et al. 2014). Telomeres are the ends of chromosome arms, and must be distinguished from a double strand break, to keep these ends from being linked to other chromosomes in repair processes. Telomere fusions are described as the covalent ligation of these chromosome ends. Therefore, the DDR is supressed at the telomeres by a complex known as shelterin, with TRF2 being an important component of this complex (Cesare 2014). Telomeres have three states; (1)

closed, where the DDR is fully suppressed (2) intermediate, where an ATM dependent DDR can be activated, but non-homologous end-joining (NHEJ) is suppressed by the presence of some TRF2 (3) uncapped, without enough TRF2 present telomere fusions occur by NHEJ. It is not completely understood why allowing DSB repair during mitosis leads to telomere fusions, but it is thought that intermediate state sister chromatid telomeres may be fusing during DSB repair that is usually suppressed during M-phase (Orthwein et al. 2014).

3.3.4 Oocytes may 'slip' out of the arrest after treatment with some DNA damaging agents

To find out whether the response seen in oocytes was a robust arrest or simply a delay in the cell cycle, oocytes were allowed to mature *in vitro* for an extended period of time. For the majority, DNA damage led to a fairly robust arrest in meiosis I. However, many Bleomycin treated oocytes that had been arrested at 15 hours were able to extrude the first polar body by 24 hours (Figure 3.6). There are several possible explanations for this phenomenon. One reason for these oocytes being able to progress through to meiosis II is that the damage to the DNA was repaired whilst the oocytes were arrested in meiosis I. If DSBs had been repaired during the arrest period, deactivation of the DDR may have permitted the progression to meiosis II. As mentioned in Section 3.3.3 somatic cells cannot initiate a full DDR during M phase. DDR proteins such as ATM are activated and recruited but repair processes are not to avoid genetic instability (Giunta et al. 2010). However, it has been suggested that both metaphase I and II oocytes can repair DNA damage (Kujjo et al. 2010, Mayer et al. 2016). Despite this, it is unlikely to be the cause of PBE rescue in bleomycin treated oocytes, because if oocytes were able to repair DSBs caused by Bleomycin one would expect a rescue of PBE in other treatments used in this chapter as well.

Mitotic cells that are treated with spindle poisons such as Nocodazole, will delay exit from mitosis by activating the spindle assembly checkpoint (SAC). The SAC's canonical function is to inhibit the Anaphase Promoting Complex (APC) under conditions where chromosomes are not correctly attached to the spindle (Chapter 1.6.6). However, it has been shown that rat kangaroo and human RPE1 cells can escape the delay and exit mitosis (Brito and Rieder 2006, Dalton and Yang 2009). This phenomenon is called 'mitotic slippage'. The length of the delay until cells exit mitosis is related to the concentration of the spindle poison used and is caused by a slow degradation of key APC substrates, like

cyclin B1 (Brito and Rieder 2006). Brito and Rieder (2006) suggested that the cause of this is that the SAC cannot effectively inhibit all APCs. Also, DNA damage induced by Doxorubicin or ionising radiation in mitotic cells can often result in defects in maintaining a checkpoint arrest (Vakifahmetoglu et al. 2008). However, such events usually lead to apoptosis further downstream (Dalton and Yang 2009, Vakifahmetoglu et al. 2008). Therefore, one possibility is that the oocytes treated with Bleomycin underwent an initial period of arrest which was then 'escaped' from.

If this was the case the quality of the oocytes formed would be of great concern as 'slippage' in mitotic cells is often associated with aneuploidy, cell death and even an increase in DNA damage (Dalton and Yang 2009). Taking this into account if Bleomycin treated oocytes slipped out of the DNA damage induced meiotic arrest, it would be highly unlikely that they would be of good quality.

Regardless of the mechanisms that led to Bleomycin treated oocytes progressing to meiosis II, an important and unanswered question remains. Would these oocytes be of a good enough quality to be successfully fertilised after a total of 25 hours IVM? The normal window for fertilisation is 12-18 hours after GVBD in mice (Jones 1998). Therefore an additional 7-13 hours of IVM could potentially have negative effects on development. Indeed it has been shown that post ovulatory ageing has many effects on oocytes, including increased ROS and a decrease in fertilisation ability, within just 8 hours of postovulatory aging (Lord and Aitken 2013). Thus, it would be interesting to explore this response further to find out when exactly PBE takes place during the extended IVM.

Similarly oocytes treated with ionising radiation did not all remain arrested in MI, although the completion of MI was not seen in as high proportion as in Bleomycin treated oocytes. This suggests there could be a spectrum of responses seen when other drugs or agents are used and raises the question of whether this is a response unique to Bleomycin, or if similar effects would be seen when oocytes were treated with other available drugs such as doxorubicin.

3.3.5 Conclusions

It will be interesting to find out the specific stage at which oocytes arrest after treatment with DNA damaging agents as this could begin to highlight the mechanisms involved. One reason for an arrest in meiosis I could be due to the SAC, as it is a well-established mediator of a metaphase arrest in somatic cells and oocytes alike (Musacchio 2015, Sun

and Kim 2012). Activation of such a checkpoint could be due to DNA fragmentation after exposure to damaging agents, as fragments have previously been reported in NCS treated oocytes (Yuen et al. 2012). This will be addressed in Chapter 4.

Chapter 4: The role of the Spindle Assembly Checkpoint in the Oocyte DNA Damage Response

4.1 Introduction

Having established that oocytes do not initiate a response to DNA damage whilst GV arrested, but instead arrest during meiosis I (Chapter 3), I wanted to explore the nature of this arrest. Additionally, it was important to unravel the mechanisms behind the response.

I wanted to establish at which stage in meiosis I oocytes arrested following treatment with DNA damaging agents used throughout Chapter 3. Therefore, immunofluorescence using antibodies against α-tubulin and a DNA counterstain allowed me to analyse the organisation of the chromatin within the oocyte. This also meant I could investigate whether DNA damage had any effects on spindle formation or structure, as well as some insight into chromosome alignment. I also assessed whether DNA damage could induce DNA fragmentation in oocytes. This was carried out using time-lapse confocal imaging on oocytes microinjected with H2B-mCherry and CENPC-GFP.

As well as chromosome and spindle integrity, I investigated the possible involvement of the Spindle Assembly Checkpoint (SAC) in the DNA damage induced arrest. This was done because the SAC is well reported as an inducer of an arrest at the metaphase to anaphase transition in somatic cells and oocytes alike (Musacchio 2015, Sun and Kim 2012) (Chapter 1.6.6). I did this investigation using a variety of methods; pharmacological inhibition of MPS1 (Chapter 1.6.6), immunofluorescence using antibodies against MAD2 (Chapter 1.6.6), and monitoring the activity of the Anaphase Promoting Complex (APC) using live time-lapse confocal imaging. The role of the APC has been discussed in Chapter 1.6.6.

Therefore, this Chapter focuses on where in meiosis I the oocytes arrest after exposure to DNA damaging agents and whether or not the SAC is involved. As well as this, other potential triggers of the arrest were investigated, including the formation of an abnormal spindle, and DNA fragmentation.

Many of the results presented in this chapter have been published (see Appendix A). Any experimental data from this publication that was not collected by me is stated in Appendix A and will be referred to in the discussion as ‘Collins et al. 2015’.

4.2 Results

4.2.1 Experimental designs for investigating the involvement of the SAC in the oocyte DNA damage induced arrest

To better understand the mechanistic events of the DNA damage induced arrest seen in Chapter 3, several experimental designs were used (Figure 4.1). To establish the stage in meiosis I oocytes arrest at after DNA damage induction experimental design 4.1A was used. Here oocytes were treated with DNA damaging agents, released from milrinone and this was followed by a 16 hours IVM (GVBD+15 hours). At the end of the culture period oocytes were fixed and processed for immunofluorescence. An antibody against α-tubulin was used to show the spindle, and a DNA counterstain to highlight the chromatin, allowing the stage in meiosis I to be identified in individual oocytes.

Having identified the stage that oocytes arrested after DNA damage, the role of the SAC and other cell cycle machinery, such as the APC, was investigated in several ways (Figure 4.1B, C, D). Firstly, DNA damage was induced whilst oocytes were GV arrested, followed by a shortened IVM of 12 hours (GVBD+ 11 hours). PBE was assessed and those oocytes arrested in meiosis I had Reversine added to the culture media. Reversine is a potent and selective inhibitor of MPS1 (Santaguida et al. 2010), a SAC component, and so allowed me to find out whether MPS1 was required for the arrest. After the addition of Reversine, PBE was monitored every 30 minutes for a total of 2 hours (Figure 4.1B). To further explore the role of MPS1 in the DNA damage induced arrest GV oocytes were microinjected with cRNA encoding securin tagged with yellow fluorescent protein (YFP); these oocytes were then allowed to rest for a minimum of 1 hour. By injecting the fluorescently tagged securin the activity of the APC could be monitored. DNA damage was induced whilst oocytes were still GV arrested, followed by a 16 hour IVM. The IVM took place within a heated chamber on a confocal microscope and oocytes were imaged throughout the entire maturation period. A shortened IVM of 12 hours was also used, and Reversine was added to the media at this point, to monitor the effect of MSP1 inhibition of the activity of the APC.

By microinjecting a combination of H2B-mCherry and CENPC-GFP, according to Figure 4.1C, chromosomes and kinetochores could be monitored throughout the IVM and was used to see if DNA damage could induce DNA fragmentation in oocytes.

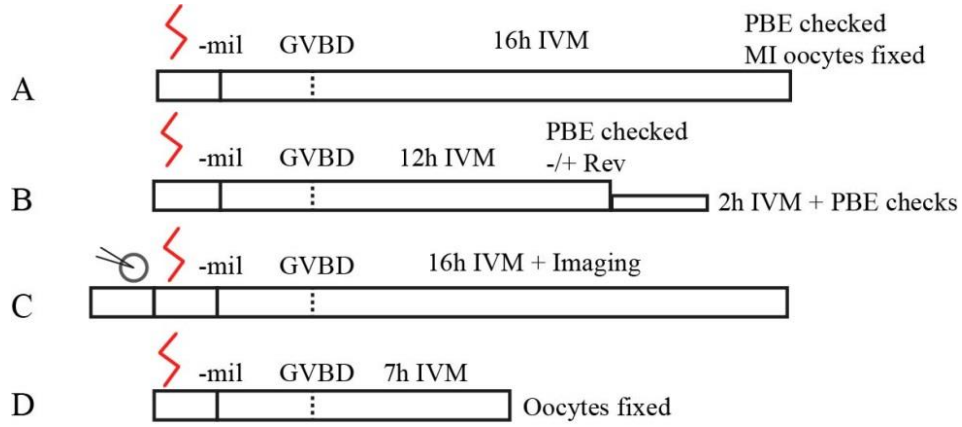

Figure 4-1Experimental designs for investigating the involvement of the SAC in the oocyte response to DNA damage

(A) DNA damage induced whilst GV arrested, followed by standard length IVM of 16h (GVBD+15h). PBE checked at 16h after release from milrinone and arrested oocytes fixed. (B) DNA damage induced whilst GV arrested, followed by a shortened IVM of 12h (GVBD+11h). PBE checked at 12h after release from milrinone. Reversine (Rev) was added to a pool of arrested oocytes and monitored for PBE every 30 minutes for 2h. Oocytes without Reversine were also monitored for PBE during this period. (C) GV oocytes were microinjected with desired cRNA and allowed to rest for a minimum of 1h. DNA damage was induced whilst GV arrested, followed by 16h IVM during which confocal time-lapse imaging took place. (D) DNA damage was induced whilst GV arrested, followed by IVM. Oocytes were fixed at 7h into IVM for immunofluorescence staining. Red line indicates DNA damage induction. Grey symbol indicates microinjection.

To explore the possibility of the SAC protein, MAD2, being involved in the DNA damage induced arrest experimental design 4.1D was used. DNA damage was induced whilst oocytes were GV arrested and then released from milrinone. After 7 hours (GVBD+ 6 hours) of IVM oocytes were fixed and processed for immunofluorescence. These oocytes were then stained using antibodies against MAD2 and CREST, an antibody used to highlight the centromere. The ratio of MAD2 and CREST were then calculated in control and DNA damaged oocytes.

4.2.2 DNA damage causes oocytes to arrest at Metaphase I

With oocytes arresting at some point within meiosis I, it was of interest to find out at which stage these damaged oocytes were arrested. To look into this, the experimental design shown in Figure 4.1A was used. Oocytes exposed to DNA damaging agents whilst GV-arrested, were allowed to undergo a total of 16 hours IVM. After this period oocytes arrested in meiosis I were fixed and permeabilised. Immunofluorescence staining using an α-tubulin antibody and a Hoechst counterstain revealed that both chemical (Etoposide and Bleomycin) and physical treatments (UV-B) caused oocytes to arrest at metaphase I (Figure 4.2). This stage was easily identified as it is defined by a morphological appearance where all chromosomes are aligned along the metaphase plate. Oocytes were not at prometaphase, as the chromosomes would not have been aligned at the equator of the spindle and would have instead been more dispersed along the spindle itself. Also, oocytes appeared to have a normal barrel shaped spindle that had undergone elongation (Figure 4.2), which would not have been the case if the oocytes had arrested very early in prometaphase.

4.2.3 Inhibiting MPS1 can overcome the DNA damage induced arrest

The canonical function of the SAC is to prevent the onset of anaphase until all chromosomes are correctly bi-orientated at the metaphase plate. Under normal circumstances the oocyte SAC is relatively ineffective at causing an arrest even when some bivalents are not correctly attached to the spindle (see Chapter 1.6.6). However, here is a situation where oocytes are substantially arrested at metaphase after DNA damage (Figure 4.2), perhaps suggesting that the SAC may be involved. To observe whether the DNA damage induced metaphase arrest was mediated by the SAC the experimental design shown in Figure 4.1B was used. Reversine, a specific and potent inhibitor of MPS1, a key SAC component, was added to M2 media after 12h IVM (GVBD+11h). Undamaged

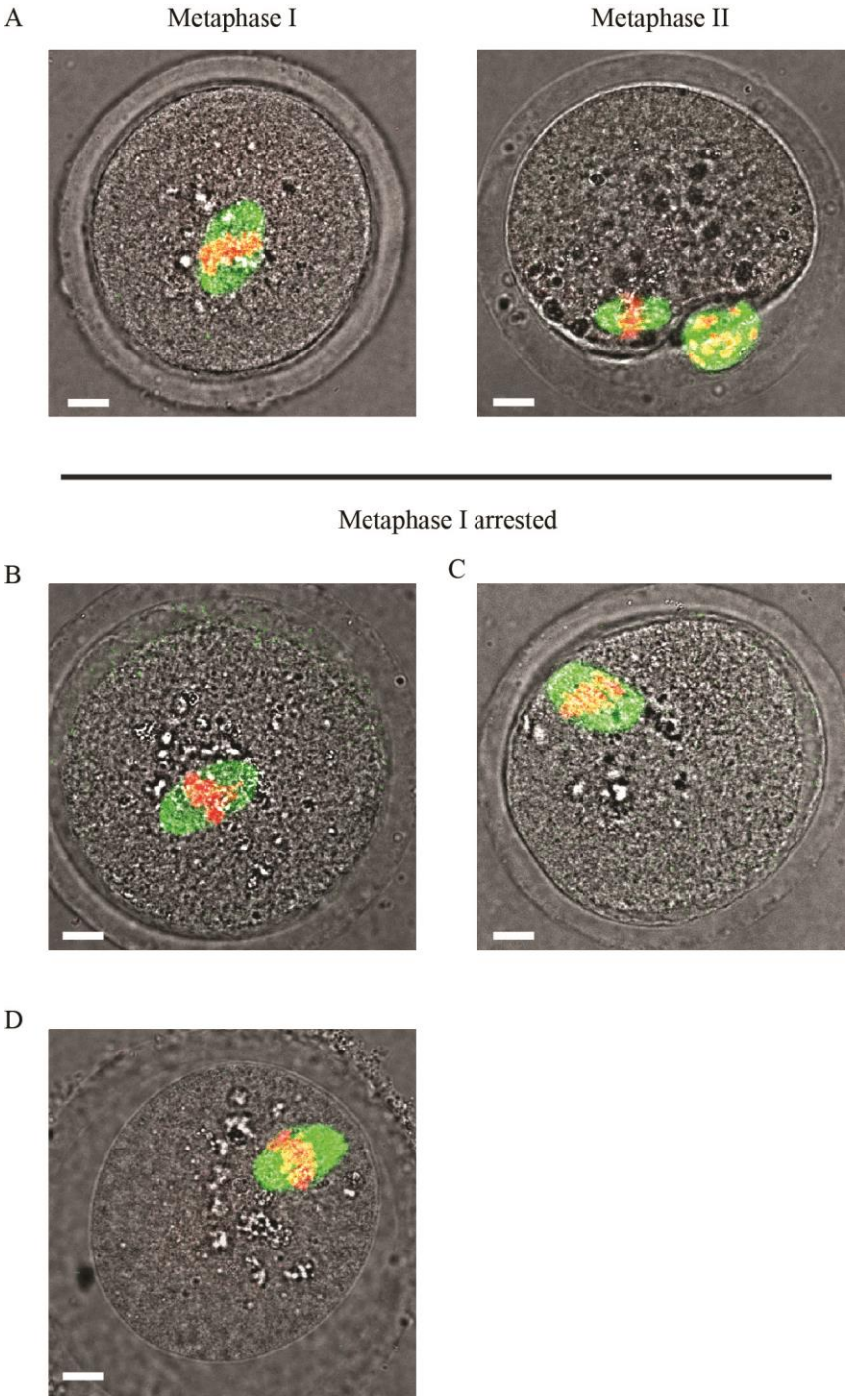

Figure 4-2 DNA damage caused oocytes to arrest at metaphase I of meiosis

All oocytes were fixed for immunofluorescence after a standard length IVM (GVBD+15h). (A) Representative undamaged oocytes arrested either at metaphase I (n=15) or metaphase II (n=72). (B) Representative oocyte treated with 25µg/ml Etoposide arrested at metaphase I (n=42). (C) Representative oocyte treated with 1µM Bleomycin sulphate arrested at metaphase I (n=12). (D) Representative oocyte exposed to 15 seconds of UV-B (300nm) arrested at metaphase I (n=9). Scale bar represents 10µm. Green is α-tubulin. Red is chromatin.

oocytes usually extrude their polar bodies between 8-10 hours after GVBD (Lane et al. 2010). Therefore, this time point was chosen due to it being 2-3 hours after control oocytes had extruded their first polar body and it was unlikely that any further extrusion would occur. Doses and exposure rates used were chosen due to their ability to cause a large proportion of oocytes to arrest at metaphase I and would allow an adequate sample size.

After 30 minutes of Reversine addition, only 2% of Etoposide treated oocytes had extruded a polar body. However, within 1 hour of Reversine addition 74% of oocytes had extruded a polar body, and this increased further to 87% by 2 hours (n= 54; Figure 4.3A, green line). The polar body was clearly identifiable, as shown in Figure 4.3B. Similar was seen in Bleomycin treated oocytes; within 1 hour of Reversine addition 70% of oocytes had extruded a polar body and by 2 hours this increased to 94% (n=50; Figure 4.3A, blue line). 60% of oocytes treated with UV-B had extruded a polar body within 1 hour of reversine being added to the culture media, and this increased to 87% within 2 hours (n=46; Figure 4.3A, red line). Finally, the same trend was seen in oocytes exposed to ionising radiation with over 90% extruding a polar body within just 1 hour of Reversine addition (n=65; Figure 4.3A, yellow line).

To control for the fact that some of the DNA damaged oocytes may have progressed to metaphase II even without Reversine being added to the culture media vehicle (DMSO) was added to DNA damaged oocytes and monitored every 30 minutes. None of the oocytes with DNA damage progressed to metaphase II when Reversine treatment had not been added (n=26; Figure 4.3A, black line).

4.2.4 The Anaphase Promoting Complex is inhibited by the Spindle Assembly Checkpoint in Etoposide treated oocytes

As explained in Chapter 1.6.6 the APC is needed for the degradation of proteins, including securin, to allow the metaphase to anaphase transition to occur. If the SAC is inhibiting the APC during the DNA damage induced arrest the degradation of such proteins should either not be seen, or be very low. Therefore, to establish what role the SAC plays in the DNA damage induced metaphase arrest the experimental design shown in Figure 4.1C was used. Oocytes were microinjected with securin-YFP, so the activity of the APC could be monitored, and treated with Etoposide. After microinjection the oocytes were released from milrinone and imaged on the confocal microscope every 5 minutes throughout maturation. Reversine was added to the culture media after 12 hours of IVM between image acquisitions.

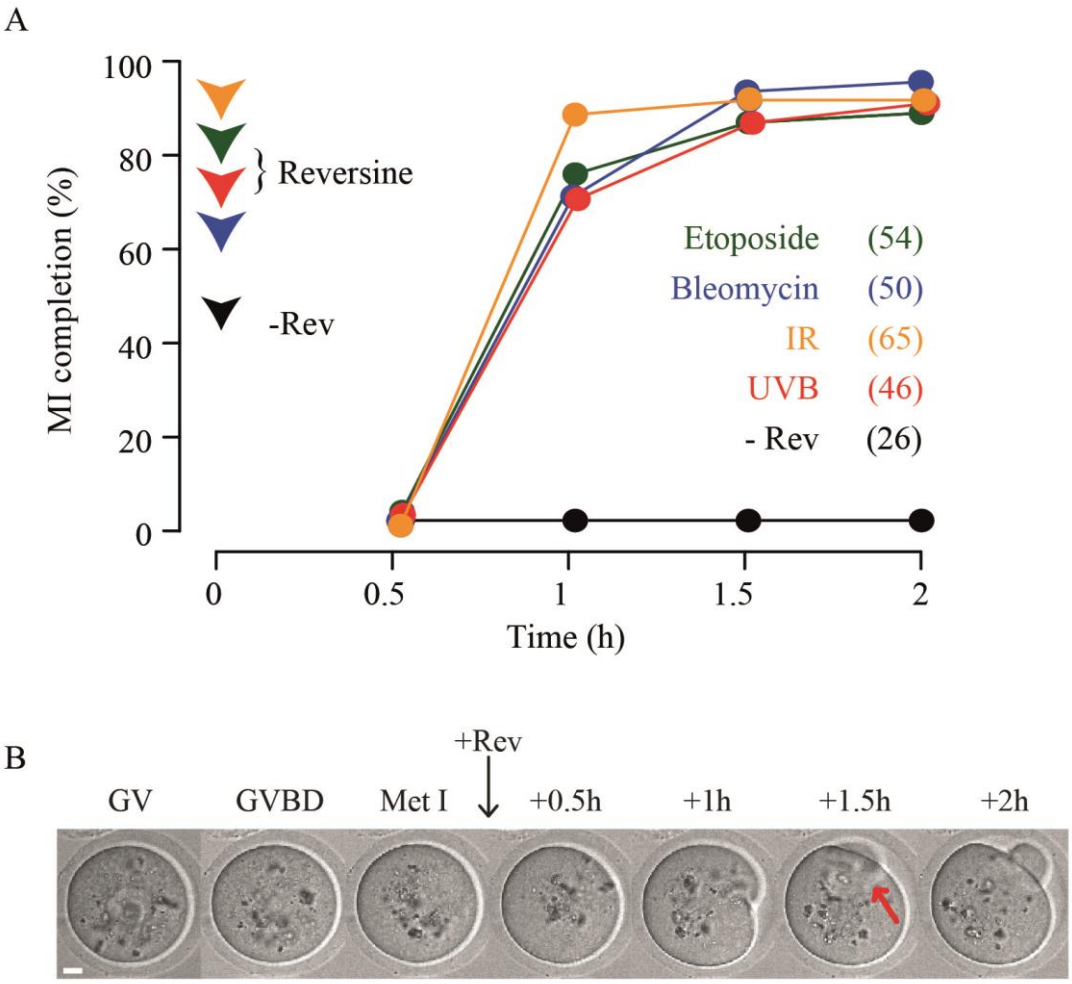

Figure 4-3 Inhibiting MPS1 activity overcame the DNA damage induced metaphase I arrest

(A) Rate of meiosis I completion following the addition of Reversine, at 11h after GVBD. Oocytes were arrested at metaphase I through various methods of DNA damage; 50µg/ml Etoposide, 1µM Bleomycin sulphate, UV-B 15 seconds and 4.5Gy ionising radiation. Numbers of oocytes used are as stated (pooled from 3-4 mice per treatment). As a control, DMSO was added to DNA damaged oocytes, and all of these remained arrested in meiosis I. (B) Representative oocyte treated with Etoposide, followed by Reversine at GVBD+11hours. The polar body had been extruded after 1.5 hours of Reversine addition in this oocyte, as shown by the red arrow. Scale bar, 10µm.

Once the images had been processed (see Materials and Methods 2.16.2) the degradation profile was plotted for individual oocytes, as well as the mean degradation profile (Figure 4.4A). The securin degradation profiles of 35 oocytes are displayed in total, and it can be seen that either no, or relatively little, securin degradation could be seen between 4 and 10 hours after GVBD. However, shortly after Reversine was added to the culture media a sharp decrease was seen (Figure 4.4A).

Indeed, when the degradation rate was calculated for the period between 4 and10 hours after GVBD (see Materials and Methods 2.16.2) prior to Reversine addition the mean degradation rate was low (6±4 %/h, n =35, Figure 4.4B; red dots). Whereas, in the hour following the addition of Reversine (11.25-12.25 hours after GVBD) there was a dramatic increase in the mean securin degradation (47±23 %/h, n=35, Figure 4.4B; green dots). These results suggest that the arrest is mediated by low APC activity, which is likely to be due to an active SAC.

4.2.5 MAD2 staining at the kinetochores is elevated in Bleomycin treated oocytes

The SAC is made up from several components, one of them being the kinetochore associated MAD2. It was possible that the metaphase arrest induced by DNA damage was also related to an increased level of MAD2 recruitment at the kinetochore. To investigate this possibility the experimental design shown in Figure 4.1D was used. As a positive control, Nocodazole (400nM) was added to the culture media 15 minutes before fixing, due to its ability to destabilise kinetochore-microtubule attachments leading to the recruitment of SAC proteins to the kinetochore (Waters et al. 1998, Wei et al. 2010, Yin et al. 2006). To identify the kinetochores oocytes were also stained with the anti-centromeric antibody, CREST. Using Image J the fluorescence level of CREST and MAD2 was measured; the ratio of these two proteins was then calculated in Excel (see Materials and Methods 2.16.4).

In vehicle treated controls the MAD2/CREST ratio was 0.15±0.17, n=236, Figure 4.5B; white bar). This ratio was increased by the addition of 400nM Nocodazole (0.24±0.16, n=144, $P<0.001$ compared to 'Veh', Figure 4.5B; black bar) and when oocytes had been treated with 1µM Bleomycin when GV arrested (0.24±0.16, n=296, $P<0.001$ compared to 'Veh', Figure 4.5B; yellow bar). This supports the notion that at least two SAC proteins (MPS1 and MAD2) are likely to be crucial mediators of the arrest in meiosis I after DNA damage.

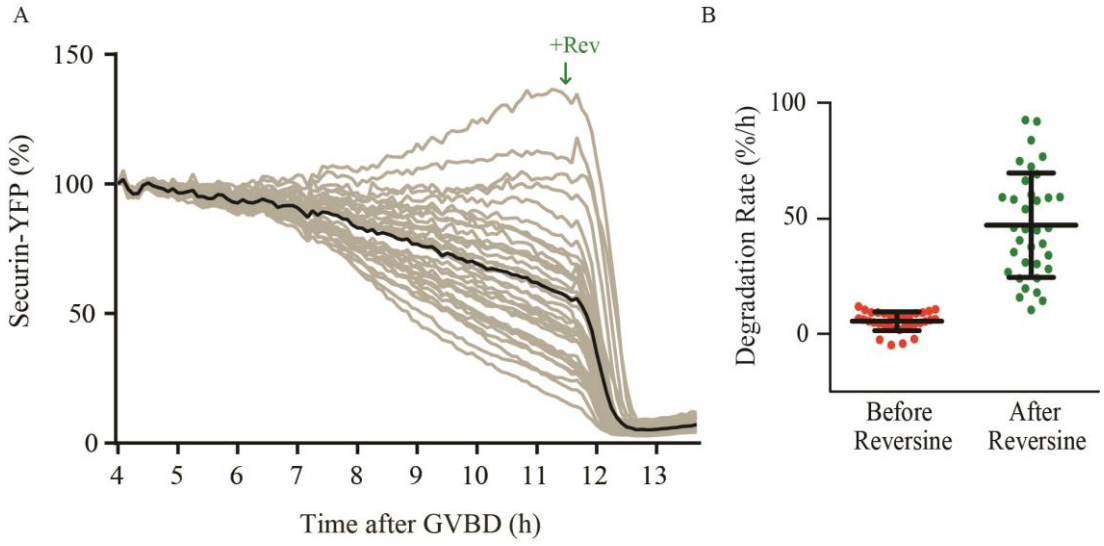

Figure 4-4 The DNA damage induced metaphase arrest involves inhibition of the APC via the SAC

Oocytes were microinjected with securin RNA tagged with YFP and then treated with Etoposide. Fluorescence levels were then monitored throughout the IVM period. 35 oocytes were analysed in total. (A) The securin degradation profile of oocytes treated with 25µg/ml Etoposide after the addition of Reversine. Grey lines depict the profiles of individual oocytes. Black line is the mean securin fluorescence. The time indicated is after GVBD. (B) Calculated degradation rate of securin-YFP in oocytes treated with 25µg/ml Etoposide before (4-10 hours after GVBD) and after Reversine addition (11.25-12.5 hours after GVBD). Each dot represents one oocyte; 35 in total.

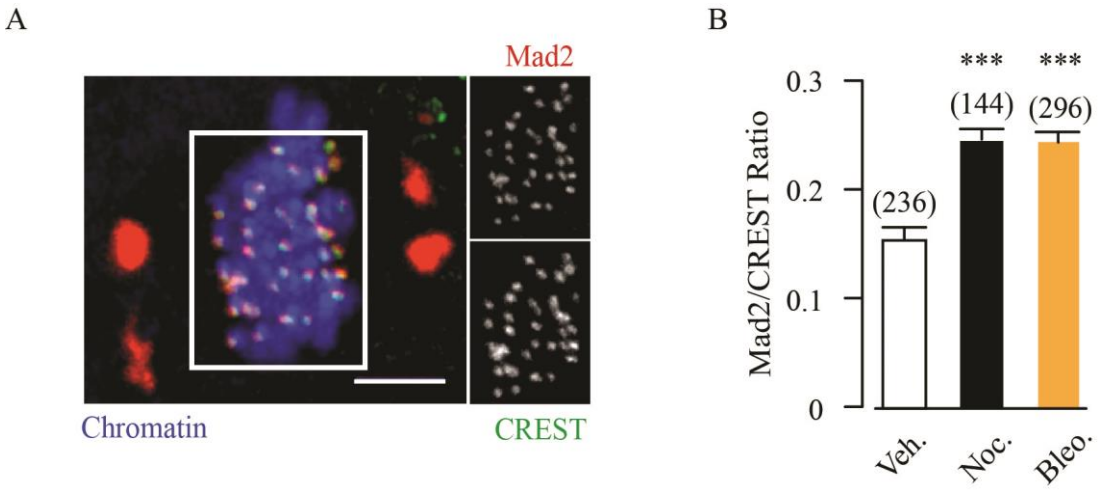

Figure 4-5 Kinetochore MAD2 levels are elevated after treatment with Bleomycin

(A) MAD2 and CREST immunofluorescence, showed co-localisation of the two proteins. MAD2 could also be observed at the spindle poles. (B) MAD2 was quantified at the kinetochore, and expressed as a ratio of against the CREST signal. Number of kinetochores analysed are indicated (pooled from 3 mice per treatment). ***, $p<0.001$(ANOVA); error bars are standard error. Scale bar is 10µm.

4.2.6 DNA damage can cause alterations in spindle parameters

It was next important to investigate why the SAC had been activated after the induction of DNA damage. Spindle parameters, including width and length, were measured to ensure that a normal spindle was formed (see Materials and Methods 2.16.5). There were some differences in spindle length and width when oocytes were treated with Etoposide, UV or Bleomycin.

In oocytes treated with 15µg/ml Etoposide there were no significant alterations to the mean spindle width (0, 12.1±1.9µm, n=14; 15µg/ml, 12.2±2.1µm, n=14, P>0.05 compared to '0'; Figure 4.6A) or length (0, 23.3±3.5µm, n=14; 15µg/ml, 22.1±5.2µm, n=14 , P>0.05 compared to '0', ANOVA with Tukey's post hoc analysis; Figure 4.6B). Small but significant increases in the mean spindle width were seen when oocytes were treated with 25-100µg/ml Etoposide (25µg/ml, 14.8±1.4µm, n=43, P<0.001; 50µg/ml, 14.4±1.8µm, n=34, P<0.001; 100µg/ml, 14.4±1.5µm, n=44, P<0.001 compared to '0', ANOVA with Tukeys post hoc analysis; Figure 4.6A). The mean length of the spindle was only increased significantly by 50-100µg/ml Etoposide (50µg/ml, 27.7±4µm, n=34, P<0.01; 100µg/ml, 26.5±2.1µm, n=44, P<0.05 compared to '0', ANOVA with Tukeys post hoc analysis; Figure 4.6B).

1-3µM Bleomycin caused an increase in mean spindle width (0, 12.1±1.9µm, n=14; 1µM, 14.9±1.2µm, n=12, P<0.001; 3µM, 16±0.8µm, n=10, P<0.001 compared to '0', ANOVA with Tukeys post hoc analysis; Figure 4.7A) and length (0, 23.3±3.5µm, n=14; 1µM, 26.8±1.8µm, n=12, P<0.01; 3µM, 26±1.4µm, n=10, P<0.05 compared to '0', ANOVA with Tukeys post hoc analysis; Figure 4.7B). However, in oocytes treated with 10µM no such differences in mean width (10µM, 13.4±0.7µm, n=9, P>0.05 compared to '0', ANOVA with Tukeys post hoc analysis; Figure 4.7A) or length (10µM, 24.6±2.6µm, n=10, P>0.05 compared to '0', ANOVA with Tukeys post hoc analysis; Figure 4.7B) were seen.

Finally, 25 seconds of UV-B was the only exposure dose to cause a significant increase in the mean width of the spindle (0, 12.1±1.9µm, n=14; 25s, 15.1±1.5µm, n=9, P=0.001 compared to '0', ANOVA with Tukeys post hoc analysis; Figure 4.8A). The length of the spindle was far more sensitive to UVB exposure; as little as 15 seconds of exposure caused a significant increase in the mean spindle length (15s, 30±2.7µm, n=9, P<0.001 compared to '0', ANOVA with Tukeys post hoc analysis; Figure 4.8B). No decreases in spindle length or width were seen for any of the treatments used here in this thesis.

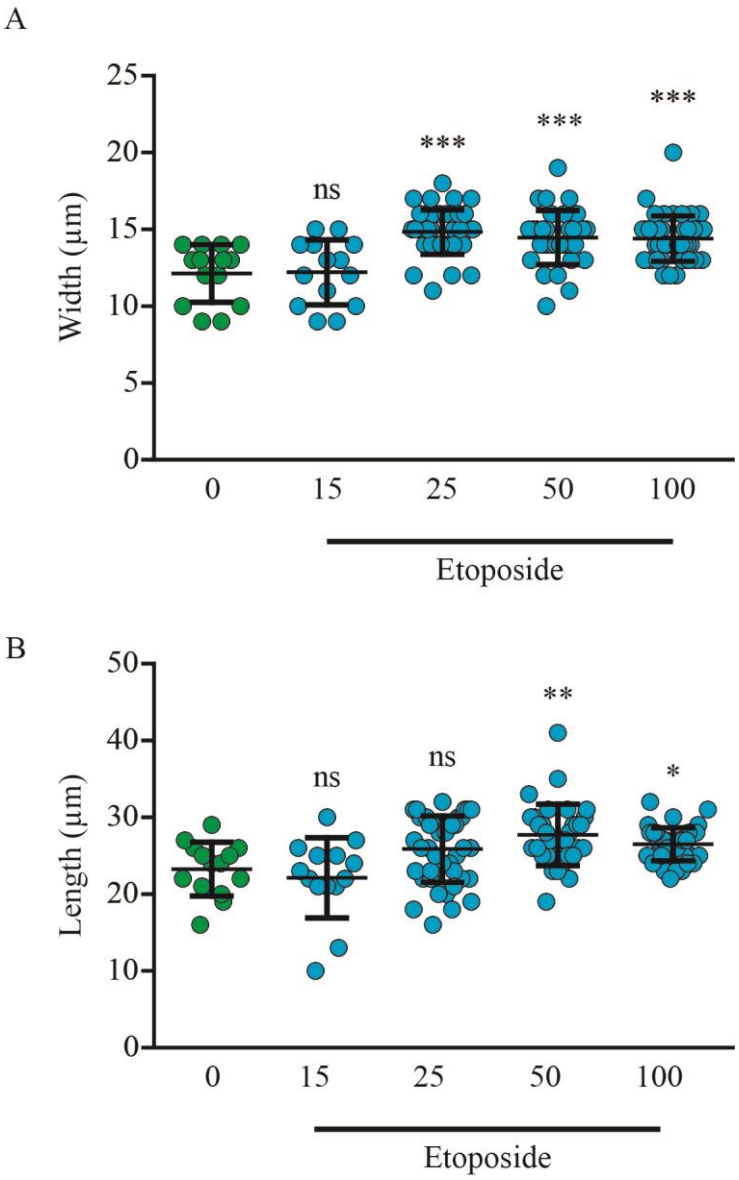

Figure 4-6 Meiotic spindle measurements taken on fixed oocytes treated with Etoposide

(A) Spindle width of oocytes treated with varying concentrations of Etoposide (15-100µg/ml) for 15 minutes whilst GV arrested. (B) Spindle length of oocytes treated with varying concentrations of Etoposide (15-100µg/ml) for 15 minutes whilst GV arrested. Between 14 and 44 oocytes were analysed per dose. Oocytes pooled from between 2 and 6 mice. *, $P<0.05$, **, $P<0.01$, ***, $P<0.001$, ANOVA (with Tukey's post hoc analysis) compared to 'control'.

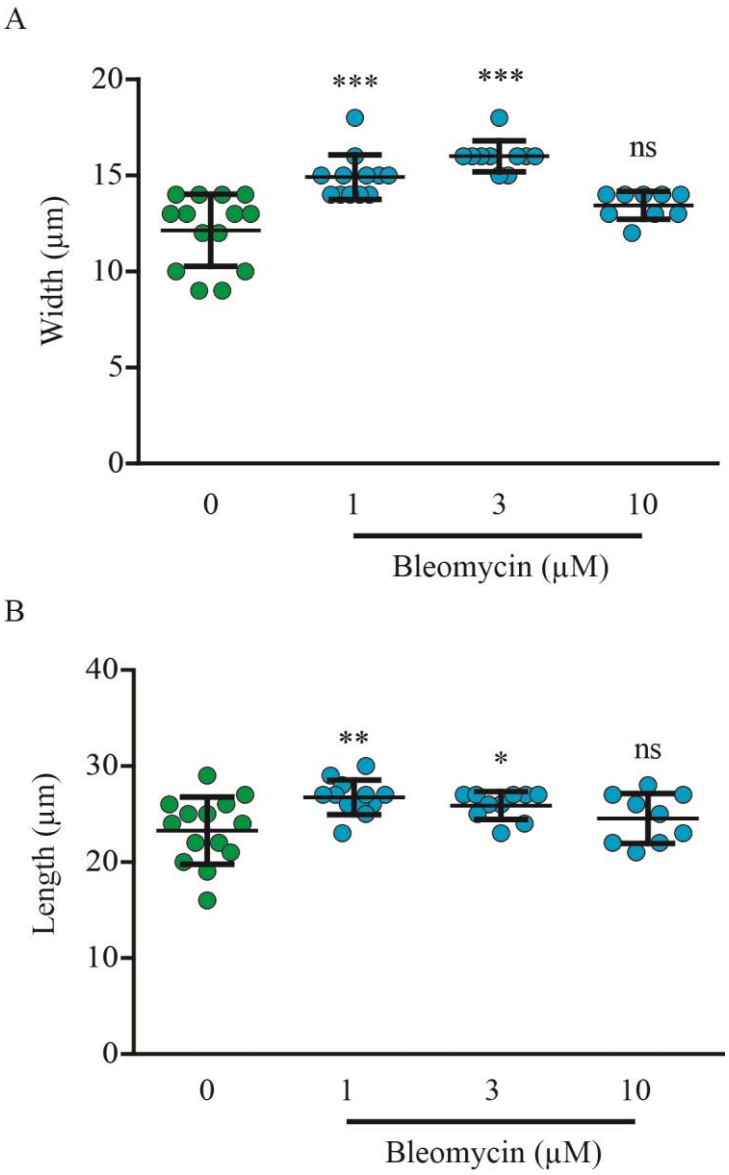

Figure 4-7 Meiotic spindle measurements taken on fixed oocytes treated with Bleomycin

(A) Spindle width of oocytes treated with varying concentrations of Bleomycin (1-10µM) for 15 minutes whilst GV arrested. (B) Spindle length of oocytes treated with varying concentrations of Bleomycin (1-10µM) for 15 minutes whilst GV arrested. Between 9 and 14 oocytes were analysed per dose. Oocytes pooled from between 1 and 2 mice per treatment. *, $P<0.05$, **, $P<0.01$, ***, $P<0.001$ ANOVA (with Tukey's post hoc analysis) compared to 'control'.

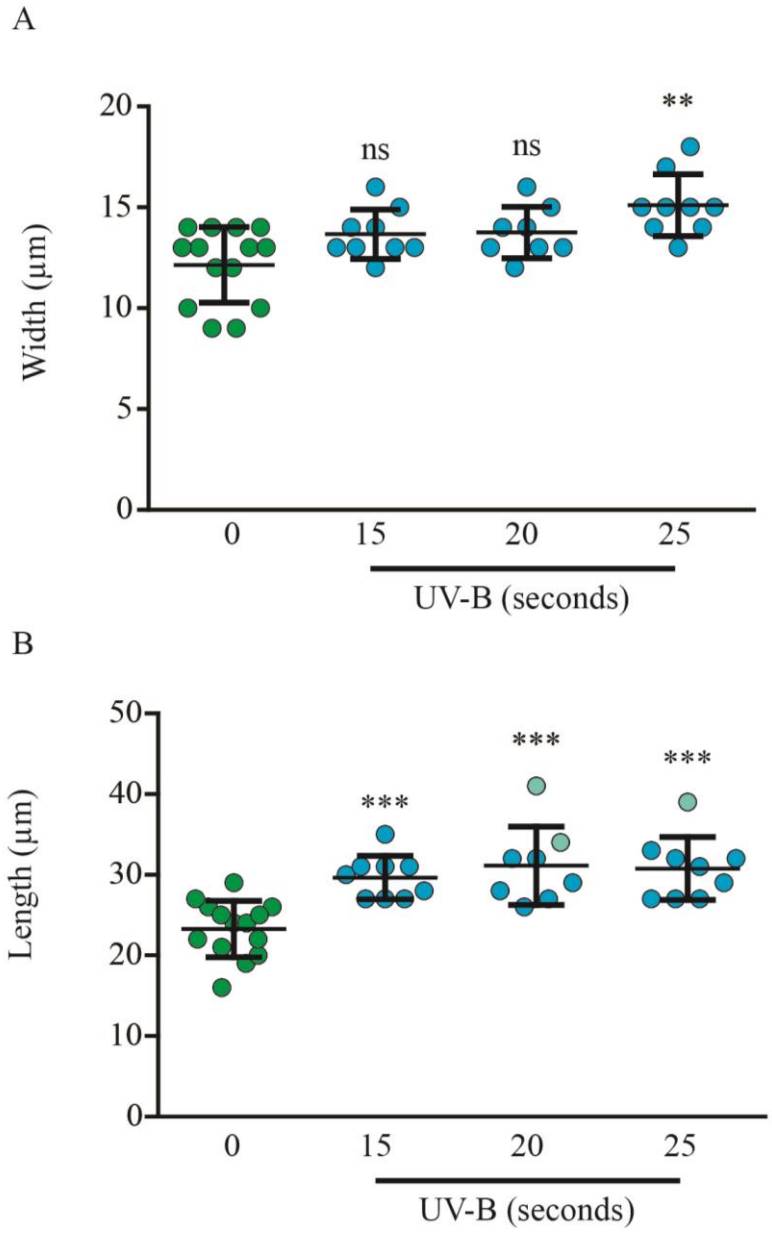

Figure 4-8 Meiotic spindle measurements taken on fixed oocytes exposed to ultraviolet radiation

(A) Spindle width of oocytes exposed to varying periods of UV-B (15-25 seconds) whilst GV arrested. (B) Spindle length of oocytes treated with varying concentrations of UV-B (15-25 seconds) whilst GV arrested. Between 9 and 14 oocytes were analysed per dose. Oocytes pooled from between 1 and 2 mice per treatment. ** P<0.01, ***, P<0.001 ANOVA (with Tukey's post hoc analysis) compared to 'control'.

4.2.7 Chromosome alignment in oocytes damaged with Etoposide or Bleomycin

Fixed samples obtained using experimental design in Figure 4.1A, were used to assess chromosome alignment. Images were analysed to assess whether DNA damage caused chromatin to cluster towards the spindle poles. This was done by using Image J to produce a Hoechst fluorescence plot along the length of the spindle, from pole to pole (see Materials and Methods 2.16.3). Peaks on the fluorescence plots corresponded to high intensities of Hoechst staining, thus allowing me to see where chromatin was aligned along the spindle.

In vehicle treated or un-exposed oocytes the occurrence of this was very low (0, 14%, n=14; Figure 4.9, 4.10 and 4.11). In all concentrations of Etoposide and Bleomycin analysed, the percentage of oocytes with chromatin clustered towards the spindle poles was not significantly different, but did occur in 20-40% of oocytes (Figure 4.9 and 4.10). Also worth noting is that there appears to be a downwards trend in chromosome clustering as the concentration of Etoposide concentration increases, this could be due to increased aggregation of chromatin (described in section 4.2.9).

4.2.8 Chromosome alignment in oocytes damaged with UV-B

DNA damage caused by chemical agents appeared to have only a small effect on chromosome alignment in fixed samples. However, in oocytes exposed to UV-B clustering of chromatin towards either pole was much more pronounced, and appeared to be far more severe (Figure 4.11) than in either Etoposide or Bleomycin treated oocytes (Figure 4.9 and 4.10). Nearly all oocytes exposed to UV-B were shown to have chromatin clustered towards the spindle poles (Figure 4.11C).

4.2.9 Etoposide and UV-B exposure can create fragmented DNA

In order to further study chromosome alignment and the possibility of DNA damage creating fragmented DNA, oocytes were microinjected with H2B-mCherry and CENPC-GFP, according to the experimental design shown in Figure 4.1C. Following microinjection, oocytes were treated with either 15 seconds of UV-B (300nm) or 15 minutes of 25µg/ml Etoposide and then using time lapse imaging were monitored throughout IVM. The time lapse data was then analysed for the presence or absence of DNA fragments. Fragments were found in 40-50% of oocytes examined (Figure 4.12 A, B, C). These fragments often only possessed a single kinetochore (Figure 4.12A) and could be

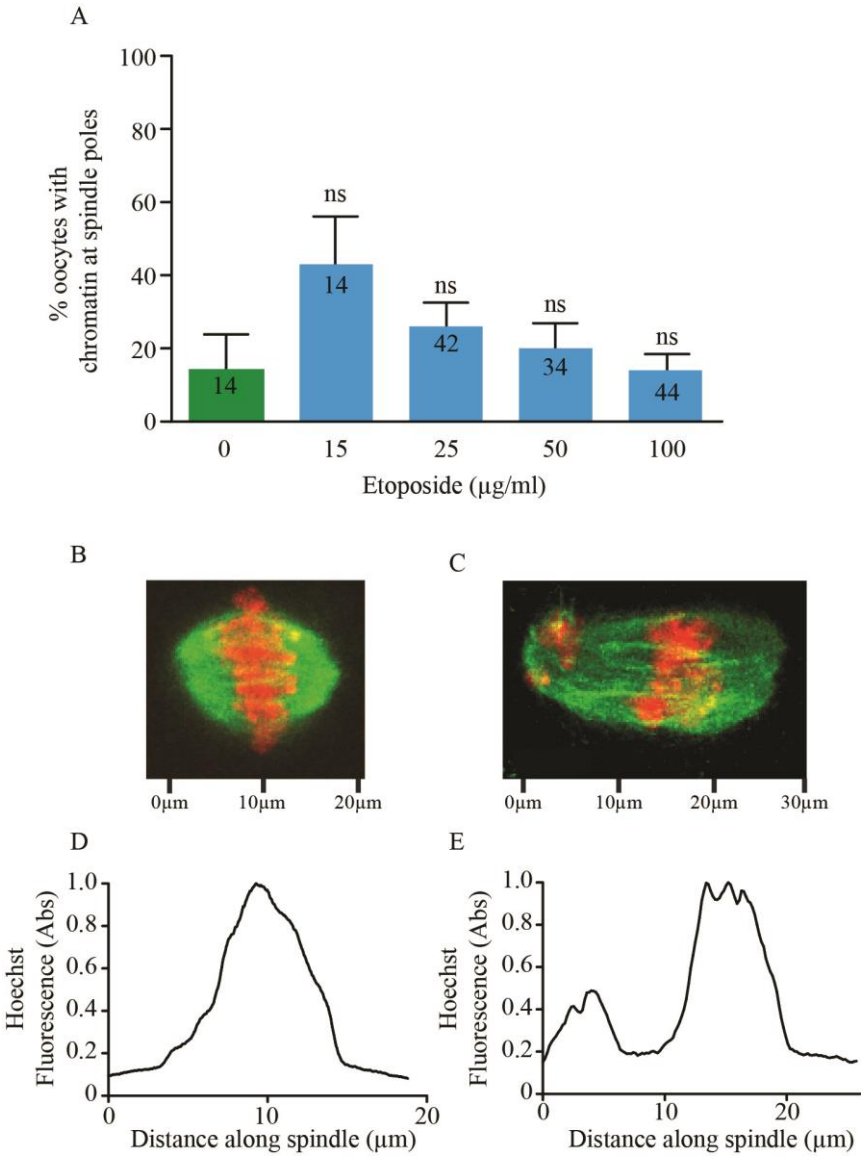

Figure 4-9 Clustering of chromatin at spindle poles in oocytes treated with Etoposide

(A) Percentage of oocytes with chromatin clustered towards the spindle poles after treatment with Etoposide. (B) Oocyte showing no clustering of chromatin after 25µg/ml Etoposide treatment. Sizes shown on x-axis. (C) Representative oocyte showing some clustering of chromatin to the spindle pole after 25µg/ml Etoposide treatment. Sizes shown on x-axis. (D) The fluorescence plot of Hoechst from the oocyte shown in B. The x-axis corresponds to the scale on 'B'. (E) The fluorescence plot of Hoechst from the oocyte shown in C. The x-axis corresponds to the scale on 'C'. Numbers of oocytes used are as indicated (pooled from between 2-6 mice per treatment). ns, $p>0.05$ compared to '0' (Fisher's Exact test. Error bars are standard error.

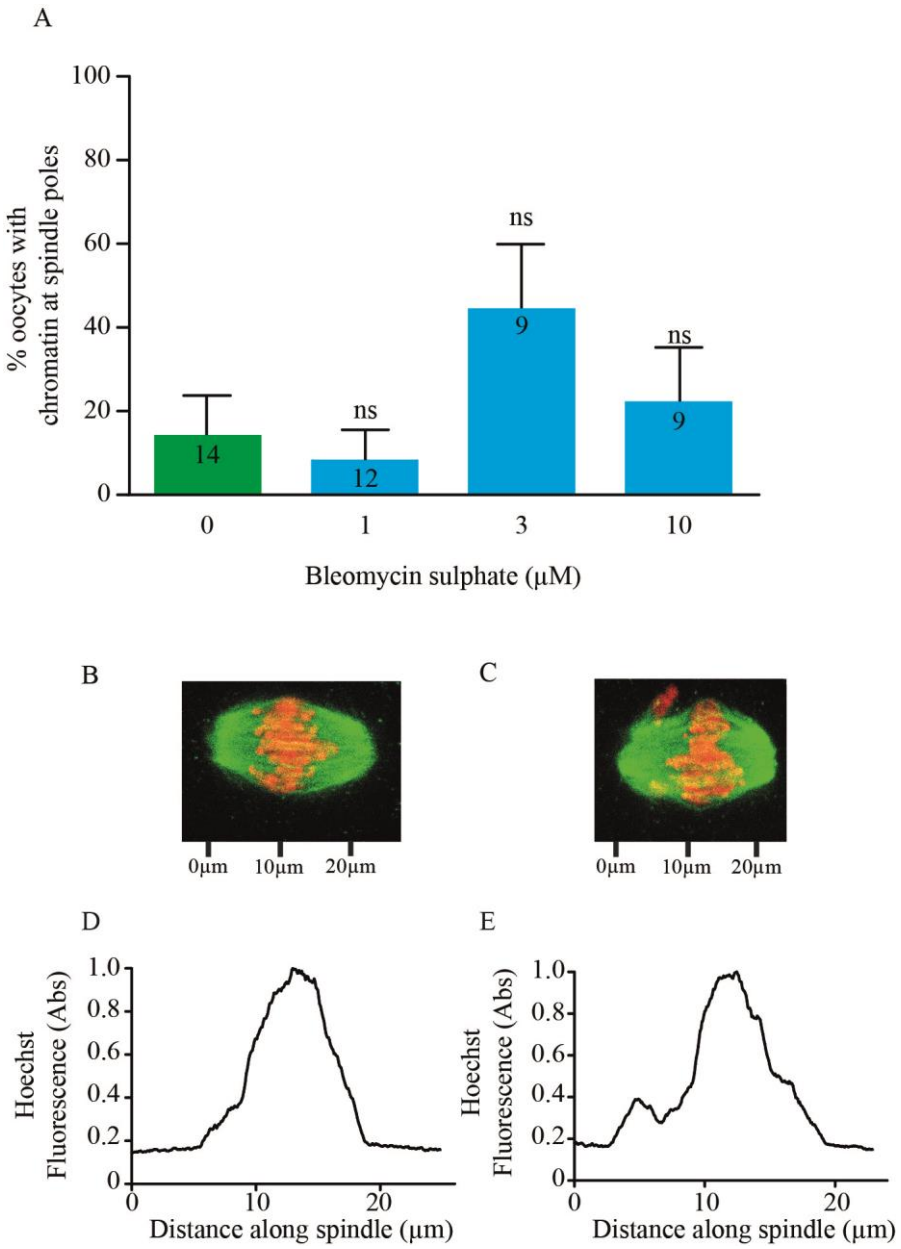

Figure 4-10 Clustering of chromatin at spindle poles in oocytes treated with Bleomycin

(A) Percentage of oocytes with chromatin clustered towards the spindle poles after Bleomycin sulphate treatment. (B) Representative oocyte showing no clustering of chromatin after 1µM Bleomycin. Sizes shown on x-axis. (C) Representative oocyte displaying some clustering of chromatin to the spindle pole after treatment with 1µM Bleomycin. Sizes shown on x-axis. (D) The fluorescence plot of Hoechst from the oocyte shown in B. The x-axis corresponds to the scale on 'B'. (E) The fluorescence plot of Hoechst from the oocyte shown in C. The x-axis corresponds to the scale on 'C'. Numbers of oocytes used are as indicated (pooled from between 2-6 mice per treatment). ns, $p>0.05$ compared to '0' (Fisher's Exact test. Error bars are standard error.

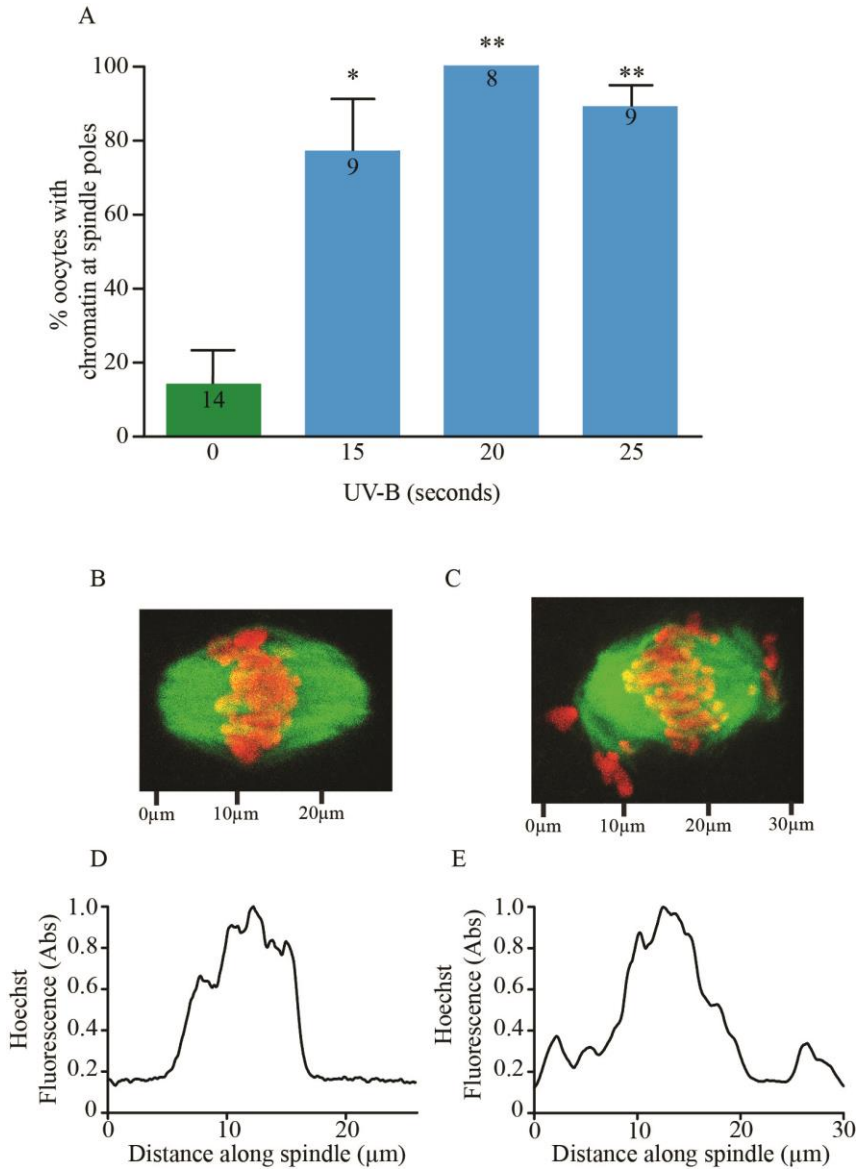

Figure 4-11 Clustering of chromatin to spindle poles in oocytes with physically induced DNA damage

(A) Percentage of oocytes with chromatin clustered towards the spindle poles after exposure to UV-B (300nm). (B) Representative oocyte showing no clustering of chromatin after UV-B exposure (15 seconds). Sizes shown on x-axis. (C) Representative oocyte showing clustering of chromatin towards both spindle poles after UV-B exposure (15 seconds). Sizes shown on x-axis. (D) The fluorescence plot of Hoechst from the oocyte shown in B. The x-axis corresponds to the scale on 'B'. (E) The fluorescence plot of Hoechst from the oocyte shown in C. The x-axis corresponds to the scale on 'C'. Numbers of oocytes used are as indicated. *, $p<0.05$, **$p<0.001$ compared to '0' (Fisher's Exact test). Error bars are standard error.

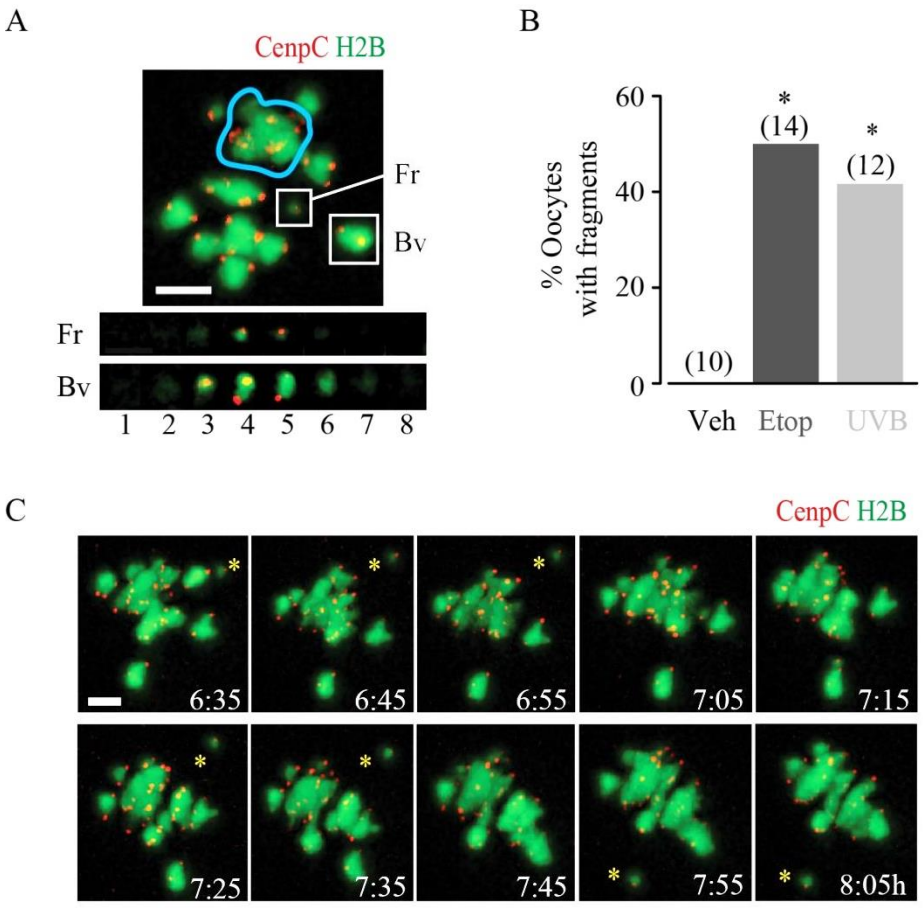

Figure 4-12 DNA Damage causes DNA fragmentation

(A) A chromosome fragment (Fr) generated by 25µg/ml Etoposide. The fragment only possessed a single kinetochore when Z-stack was examined (z-slices numbered 1-8). For a comparison two sister kinetochore pairs on a bivalent are highlighted (Bv). The blue circle highlights an area of 'clumped' DNA. (B) Percentage of oocytes expressing CENP-C and H2B found to have fragmented DNA during time-lapse imaging. Images were taken every 10mins over a 15 hour period. Numbers of oocytes used are as indicated (data pooled from 2 mice for each condition). *, $p<0.05$, Fisher's exact test. (C) Time-lapse of an oocyte expressing CENP-C and H2B, with a fragment possessing a single kinetochore (*). It has erratic movement around the spindle equator. Scale bar is 5µm.

seen to make frantic oscillations across the spindle equator (Figure 4.12C) As well as visible fragments, it was apparent that in Etoposide treated oocytes the chromatin was often ‘clumped’ or ‘tangled’ and it was on occasion hard to decipher individual chromosomes (Figure 4.12 A).

4.3 Discussion

In this chapter, oocytes were shown to arrest at metaphase I after treatment with DNA damaging agent whilst held at the GV stage. The DNA damage protocols used here did not affect the formation of the spindle itself, but did cause some alterations in spindle size under some conditions. It was also clear that inducing DNA damage caused some instances of chromosome mis-alignment and DNA fragmentation but these were unlikely to be the sole cause of the arrest as it did not occur in all oocytes with DNA damage. The metaphase arrest induced by DNA damaged appeared to be dependent on the spindle assembly checkpoint (SAC), but further investigation is required as to how DNA damage causes the activation of the SAC.

4.3.1 Oocytes with DNA damage arrest at Metaphase I

Throughout Chapter 3 it was established that oocytes are not able to initiate any form of G2/M checkpoint using my treatment protocol and that instead oocytes are able to arrest during the first meiotic M phase (Figure 3.4). This has now been shown by other groups in mice (Ma et al. 2013, Marangos et al. 2015, Yuen et al. 2012) and even porcine oocytes (Wang et al. 2015a, Zhang et al. 2014); many of which have been published since my study began.

The next step in understanding this phenomenon was to find out when during meiosis I the oocytes with DNA damage arrest. The discovery of this was important to show what mechanisms may lead to such an arrest and how it could be overcome therapeutically. Oocytes exposed to DNA damaging agents were fixed after IVM (GVBD+ 15h). These were then stained using antibodies against α-tubulin and counterstained using Hoechst. This revealed that oocytes that arrested during meiosis I, after being treated with DNA damaging agents, were halted at metaphase I (Figure 4.2). Metaphase I is easily identified by its morphological appearance where all chromosomes are aligned along the metaphase place. If oocytes had been arrested at prometaphase or anaphase the appearance of the spindle, and organisation of the chromatin, would have been very different. If oocytes had arrested at prometaphase, the chromatin would be condensed but the chromosomes would

have been dispersed along the spindle as all the correct attachments or alignment wouldn't have occurred yet. If the oocytes had been at anaphase when they were fixed two easily identifiable groups of chromatin would have been seen, and these would be being pulled towards either pole of the spindle.

One hypothesis was that the SAC could be responding to a variety of stimuli within the oocytes with damaged DNA. It is well documented that the SAC can mediate an arrest in the cell cycle, at the metaphase to anaphase transition, in both somatic cells and oocytes alike (Musacchio 2015, Sun and Kim 2012). The SAC in mitotic cells is extremely sensitive to non-attachment or mis-alignment of chromosomes (Khodjakov and Pines 2010) as discussed in Chapter 1.6.6. However, it is extensively reported that the oocyte SAC is not as sensitive to such aberrations (Gui and Homer 2012, Kitajima et al. 2011, Kolano et al. 2012, Lane et al. 2012, Nagaoka et al. 2011, Sebestova et al. 2012). With the oocyte SAC being relatively insensitive to chromosome attachment errors, one possibility is that there is a second novel role of the SAC in detecting DNA damage in oocytes.

4.3.2 The metaphase arrest induced by DNA damage is SAC-dependent

The block in meiosis I seen after treatment with Etoposide, UV-B and bleomycin occurs prior to the metaphase to anaphase transition (Figure 4.2). Using a variety of experimental protocols I found that this arrest was dependent upon the SAC. Indeed the dependence on the SAC for the DNA damage induced arrest in oocytes has also recently been shown by another group using the mouse model (Marangos et al. 2015). From my experiments I have shown that several components of the SAC are required for the DNA damage induced arrest including MPS1 (Figure 4.3, 4.4) and MAD2 (Figure 4.5).

To highlight the dependence of the response on MPS1, a pharmacological inhibitor, Reversine, was used to inhibit its activity. MPS1 is a kinase that associates with the kinetochore (Abrieu et al. 2001) and known to function in both the meiotic and mitotic cell cycle (Abrieu et al. 2001, Hached et al. 2011). It has been shown to be essential for spindle checkpoint activation and maintenance; this is due to the fact that it is required to recruit and retain CENPE at the kinetochore (Abrieu et al. 2001, Hewitt et al. 2010). In turn this allows for the recruitment of MAD1 and MAD2 (Abrieu et al. 2001, Hewitt et al. 2010). Both are integral members of the mitotic checkpoint complex (MCC) that sequesters the APC co-activator, CDC20 (Sudakin et al. 2001) (see Chapter 1.6.6). When MPS1 is depleted chromosome alignment and segregation is severely impaired in both mitosis and meiosis I (Hached et al. 2011, Hewitt et al. 2010). By pharmacologically inhibiting MPS1

at 11 hours after GVBD the arrest could be overcome and PBE was rescued (Figure 4.3, 4.4). This time point was chosen as it is several hours after control oocytes normally extrude the first polar body. This allowed me to be sure that the oocytes being treated with Reversine were arrested in meiosis I.

However, there are some possible limitations of using pharmacological inhibition including off-target effects. Also, there may be variability in the effectiveness of the drug over time or sets of experiments. Despite this, Reversine is reported as a potent and selective inhibitor (Santaguida et al. 2010) giving confidence in the results reported here. The discovery that MPS1 is necessary for the arrest is supported by the findings of Marangos and Carroll (2015). Using the specific MPS1 inhibitor AZ3146 they were also able to prevent the arrest of oocytes at metaphase when treated with 100µg/ml of Etoposide (Marangos et al. 2015).

With MPS1 being integral for the SAC-dependent response to DNA damage it was of interest to highlight whether or not other SAC components were also needed. MAD2 has been shown to be an integral member of the SAC over the years. In meiosis, MAD2 is required for the correct timing of APC activation (Homer et al. 2005b) as well as responding to non-attachment (Homer et al. 2005a). It has been shown to localise at the kinetochores of non-attached bivalents in meiosis I (Wassmann et al. 2003, Zhang et al. 2004). In mitosis, MAD2 is a key component of the MCC, where it is required to sequester CDC20 (Sudakin et al. 2001). With MAD2 overexpression leading to a metaphase arrest in oocytes (Wassmann et al. 2003, Homer et al. 2005b, Niault et al. 2007) it made sense to investigate its involvement in the DNA damage induced arrest. Indeed, levels of MAD2 at the kinetochore were elevated after treatment with bleomycin when compared to controls (Figure 4.5). This suggests that, like MPS1, it may also be crucial for the arrest to take place. In support of this, MAD2 dependence has also been shown by microinjecting oocytes with a validated morpholino against MAD2 (Collins et al. 2015). In the case of Etoposide, Bleomycin and UV-B treated oocytes, knocking down MAD2 enabled a significant rescue of PBE. Rescue of PBE by MAD2 depletion has also been shown in oocytes treated with 100µg/ml Etoposide for 1 hour (Marangos et al. 2015), however the progression of these oocytes through to metaphase II was significantly delayed compared to non-Etoposide-treated oocytes with MAD2 depletion. Un-damaged oocytes with MAD2 depletion generally complete meiosis I at a faster rate than non-injected controls, due to the lack of an intact SAC (Homer et al. 2005b, Marangos et al. 2015). This could mean that something else, alongside the SAC, may be contributing towards the M-phase response in

oocytes after DNA damage. Therefore, it would be interesting to observe the kinetics of PBE in oocytes treated with other agents such as Bleomycin and UV-B after MAD2 depletion.

In the future it would be interesting to explore the involvement of other SAC proteins. It has now been observed that BUB1 is required for the oocyte response to DNA damage (Marangos et al. 2015). BUB1 is known to function in oocytes and its knockdown causes premature activation of the APC and accelerated exit from meiosis I, alongside this it also prevents proper biorientation and increases aneuploidy rates (McGuinness et al. 2009, Yin et al. 2006). Similar to MAD2, BUB1 was also found to be strongly localised to the kinetochore in oocytes treated with Etoposide at a time when it is no longer at the kinetochores in control oocytes (Marangos et al. 2015). By microinjecting dominant-negative BUB1 Marangos et al. (2015) were able to rescue PBE in oocytes treated with 100µg/ml Etoposide. They also found that the dominant-negative BUB1 reduced BUBR1 localisation to the kinetochore significantly, which suggests that BUBR1 may also be necessary for the DNA damage induced arrest. There has been some discrepancy between studies that have researched the role of BUBR1 during meiosis I. One study suggested that the depletion of BUBR1 causes oocytes to arrest at metaphase I (Homer et al. 2009), whereas more recently published work implied depletion accelerated progression of meiosis I (Touati et al. 2015, Wei et al. 2010). These discrepancies are likely to be due to differences in the extent of BUBR1 depletion. Regardless of this it is shown to exist and function in oocytes (Homer et al. 2009, Wei et al. 2010, Touati et al. 2015). The complete depletion of BUBR1 by conditional knock-out leads to an acceleration in PBE and causes perturbations in the alignment of chromosomes (Touati et al. 2015). Therefore, it is likely that other SAC components like BUBR1 function in the SAC mediated arrest after DNA damage.

The works presented here and the study by Marangos et al. (2015) directly implements the SAC in the oocytes response to DNA damage. However, I wanted to distinguish what the SAC was responding to in oocytes with DNA damage; whether it was the physical damage to the DNA itself or stimuli that the SAC would canonically respond to such as non-attachment.

4.3.3 Spindle alterations induced by DNA damage

One possible explanation for the DNA damage-induced metaphase arrest in oocytes could have been that the SAC is activated due to severe spindle abnormalities. The spindle is a

microtubule structure that forms in both mitosis and meiosis (Duro and Marston 2015) (Chapter 1.6.5). It allows for chromosomes to be physically separated at anaphase. Without a functional spindle chromosomes would not be able to attach via their kinetochores and this would lead to canonical SAC activation. Indeed it is well known that treating oocytes with high doses of spindle poisons such as Nocodazole, a microtubule depolymerising agent, has negative effects on maturation rate (Holt et al. 2012, Lane et al. 2010, Wassmann et al. 2003).

Some types of DNA damaging agents have been reported to cause spindle abnormalities in porcine oocytes (Wang et al. 2015a) which may lead to a lack of chromosome attachment to the spindle and consequently activate the SAC. UV damage has been shown to affect the microtubule structure upon irradiation (Zaremba et al. 1984). Also spindle alterations have been reported in oocytes from female mice exposed to oxidative environments, known to cause DNA damage, such as cigarette smoke (Camlin et al. 2016, Jennings et al. 2011) and hydrogen peroxide (Choi et al. 2007). Thus a possible explanation for the arrest at metaphase I was that the short exposure to DNA damaging agents, whilst GV arrested, could perturb spindle formation having an impact on chromosome alignment and segregation. However, the images in Figure 4.2 show that a spindle did form with the normal barrel shape. When these spindles were observed in more detail, by examining width and length measurements, some changes could be seen (Figures 4.6, 4.7, 4.8). However, no such changes were reported in mouse oocytes treated with 100µg/ml Etoposide, when fixed and examined at 8 hours after GVBD (Marangos et al. 2015), compared to after 16 hours of IVM in my study. Thus the timing of fixation could contribute to the differences in the occurrence of spindle alterations.

Alterations in spindle size alone were unlikely to be the cause of the arrest after DNA damage induction as, regardless of its size, spindle formation did appear relatively normal. Further details on chromosome dynamics were required to elucidate whether this would be the cause of SAC activation.

4.3.4 DNA damage in oocytes can cause fragmentation and aggregation of DNA

Any agent that causes DNA double strand breaks has the potential to cause fragmentation of DNA. The issue that would arise with fragmented DNA is that it could lead to a loss of one or more kinetochores, which in turn would have an effect on chromosome attachment to the spindle.

Initially the occurrence of DNA fragmentation was assessed using oocytes fixed after IVM. The evidence that would suggest that DNA fragmentation had occurred is the presence of chromatin towards the spindle poles. The clustering of chromatin towards one pole would imply that only one kinetochore was present and functional, as there would not be equal forces from each spindle pole to align the chromosome at the equator. Indeed this phenomenon was seen, but in only ~20-40% of oocytes treated with either Etoposide or Bleomycin (Figure 4.9, 4.10). However, in oocytes treated with as little as 15 seconds of UV-B most oocytes had more severe misalignment and clustering of chromatin at the poles (Figure 4.11). This discrepancy in DNA fragmentation between chemically and physically induced damage could be due to the fact that using fixed samples may be under representative, as only one time point is analysed. Therefore, live time-lapse imaging of oocytes, that had been microinjected with fluorescently tagged histone 2B and CENPC, was used to monitor chromosome dynamics in more detail. Using this method allowed me to identify fragments of chromosomes throughout the whole *in vitro* maturation. Fragments were easily identifiable by their erratic oscillations across the spindle equator. Between, 40-50% of oocytes treated with either UV-B or Etoposide contained fragments (Figure 4.12). Analysing fragments through time lapse imaging was likely to be more accurate as the whole maturation could be analysed rather just one time point at which the oocytes would have been arrested at metaphase for a long period, which could have allowed for additional time for fragmentation.

The ability of DNA damaging agents to cause chromosome fragmentation has been reported by several groups investigating the oocyte response to DNA damage. Neocarzinostatin (NCS) was the first drug reported to induce DNA fragmentation in a dose-dependent manner (Yuen et al. 2012). Severe DNA damage induced using high concentrations of Bleomycin (up to 40μM) caused extensive fragmentation and the dispersal of these fragments amongst the ooplasm (Ma et al. 2013). Kinetochore free fragments have also been identified in about 30% of oocytes treated with 100μg/ml Etoposide (Marangos et al. 2015). In addition to this they also reported reduced chromosome alignment at the metaphase plate, which agrees with the findings presented (Figure 4.9, 4.10, 4.11). The same dose of Etoposide also caused similar aberrations in porcine oocytes (Wang et al. 2015a), suggesting that oocyte DNA will readily fragment after treatment with DNA damaging agents.

The results presented here in combination with the studies mentioned above could mean that oocytes with DNA damage are simply responding to the presence of DNA fragments

that do not properly attach to, or align along, the spindle. However, there are two pieces of evidence that led me to believe DNA fragmentation alone could not be the cause of SAC activation. Firstly, my results show that fragmentation of chromosomes only occurred in 40-50% of oocytes examined in the live imaging, meaning that 50-60% of oocytes treated with DNA damaging agent did not possess such DNA aberrations, yet still arrested at metaphase I. Secondly, it has been thoroughly shown that the oocyte SAC is not as sensitive to non-attachment as in somatic cells (Abrieu et al. 2001, Gui and Homer 2012, Kolano et al. 2012, Kouznetsova et al. 2007, Lane et al. 2012, Sebestova et al. 2012). Indeed up to 8 bivalents not properly biorientated, or under tension, does not prevent the metaphase to anaphase transition in oocytes treated with Nocodazole (Collins et al. 2015). Also, parameters associated with chromosome biorientation, such as bivalent tension, displacement from the metaphase plate and the angle that forms between the bivalent and spindle equator have been analysed. Bivalent stretch, displacement and alignment were consistently better in DNA-damaged oocytes that were arrested compared to nocodazole-treated oocytes that went on to extrude a polar body (Collins et al. 2015). One parameter that was found to be altered in UV-B treated oocytes was bivalent stretch which was thought to be due to UV-B altering the chromatin configuration. Such stretching has also been reported in oocytes treated with very low concentrations of NCS (Mayer et al. 2016).

As well as visible fragments, from live imaging of Etoposide treated oocytes it was apparent that the chromatin was often ‘clumped’, forming aggregations where individual bivalents were not easily made out (Figure 4.12). This finding is supported by the work of Marangos et al. (2015), where they also found that 100µg/ml Etoposide caused the aggregation of DNA to be visible at just 1 hour after GVBD. This phenotype is likely due to the effects of topoisomerase II inhibition, as this enzyme participates in condensation and decatenation of DNA (Cortes et al. 2003, Li et al. 2013, Ramamoorthy et al. 2012). However, aggregations of DNA are unlikely to be the cause of the arrest as oocytes have been shown not to possess a decatenation checkpoint (Li et al. 2013).

4.3.5 Conclusions

The findings presented in this chapter directly implement the Spindle Assembly Checkpoint in the DNA damage induced metaphase arrest. My work, in combination with that of other groups, suggests that the SAC may be activated by the DNA damage itself, rather than the side effects of such aberrations, like misalignment or DNA fragmentation. As a result it will be important to explore the type of damage that is induced by these

agents, and whether oocytes have the ability to detect and repair these insults. If repair occurs, then it could be that the SAC is not activated and maturation is rescued after repair has taken place. This will be the focus of Chapter 5. Having found that the SAC is integral to the arrest induced by DNA damage, it will be interesting to explore what signalling cascades lead to SAC activation and whether any canonical DNA damage response proteins, such as ATM or ATR, are involved. This will be addressed in later Chapter 6.

Chapter 5: Repair of DNA damage in fully-grown GV oocytes

5.1 Introduction

Having found that oocytes are able to arrest in meiosis I (Chapter 3) in a SAC-dependent manner (Chapter 4) in response to DNA damage, in this chapter I wanted to show that oocytes are able to detect and signal the damage in a similar manner to somatic cells. This would also allow further insight into any particular pathways that may be involved in the oocyte response to DNA damage.

Therefore, I needed a method to be able to quantify DNA damage; to do so I utilised an antibody against phosphorylated histone 2AX (γH2AX), a popular biomarker of DNA DSBs. I used this antibody due to the fact that H2AX phosphorylation at serine 139 is one of the most upstream signalling events that takes place after the induction of DNA DSBs (Podhorecka et al. 2010). Oocytes were treated with the four agents used in previous chapters – Etoposide, Bleomycin, ionising radiation and UV-B- whilst they were GV arrested. These oocytes were then fixed, processed for immunofluorescence and stained using the γH2AX antibody. Levels of γH2AX fluorescence within the nucleus were calculated for individual oocytes.

I also wanted to investigate the ability of oocytes to repair DNA DSBs caused by exogenous factors, as it is well known that oocytes can repair programmed DSBs during development (see Chapter 1.8.1). To do this oocytes were treated with DNA damaging agents and held at the GV stage. They were then fixed for immunofluorescence at different time points after DNA damage induction, and stained using the γH2AX antibody. γH2AX fluorescence within the nucleus was calculated for each oocyte allowing me to follow changes to the level of histone phosphorylation over time. I used oocytes damaged both chemically with Etoposide and physically using UV-B to investigate this.

Having analysed the self-repair capability of oocytes it was important to find out if such a repair period after the induction of DNA damage, would rescue oocyte maturation rates. To study this possibility, oocytes were treated with Etoposide at the GV stage and held for 10 hours following treatment. These oocytes were then released from milrinone and

allowed to undergo an *in vitro* maturation. Maturation success was scored by the presence or absence of the first polar body as in previous chapters.

Therefore, this Chapter focuses on the ability of oocytes to detect and signal the damage induced by a range of agents and whether they have the ability to repair such damage. Also, the effect of a resting period for repair on oocyte maturation rates was assessed.

5.2 Results

5.2.1 Experimental designs for investigating oocyte DNA damage repair ability

In order to study the oocytes ability to both recognise and repair DNA damage a variety of protocols were used (Figure 5.1). To simply highlight the fact that oocytes are able to recognise DNA damage, method 5.1A was used, which was to fix GV oocytes immediately after treatment with DNA damaging agent and stained with the γH2AX antibody. Due to slight differences in DNA damage signalling in UV-B treated oocytes, they had to be treated and then held GV arrested for 1 hour prior to fixing (Figure 5.1B). To monitor DNA repair in GV oocytes, groups of oocytes were fixed at set time points over a 10 hour period after treatment with either UV-B or Etoposide. These oocytes were also stained with γH2AX antibody (Figure 5.1C). To see whether the 10 hour recovery period after DNA damage induction would have a positive effect on PBE in DNA damaged oocytes method 5.1D was used. Oocytes were treated whilst GV arrested, held at the GV stage for the set time period using milrinone and maturation success was scored after 12-16hours of IVM.

5.2.2 Quantifying levels of DNA damage

Having found that DNA damage causes an arrest in meiosis I, this suggested that fully grown GV oocytes may have the ability to detect insults to their DNA. One of the most upstream events after DNA damage has taken place is the phosphorylation of histone 2A variant X on serine 139 (γH2AX) and so it is often used as a marker for DNA damage. Thus to study whether oocytes can detect damage to their DNA, GV oocytes were treated with either Etoposide, Bleomycin or ionising radiation and then fixed ready for immunostaining for γH2AX and DNA according to experimental design as shown in Figure 5.1A. Nuclear γH2AX fluorescence was then calculated for each oocyte (see Materials & Methods 2.16.1).

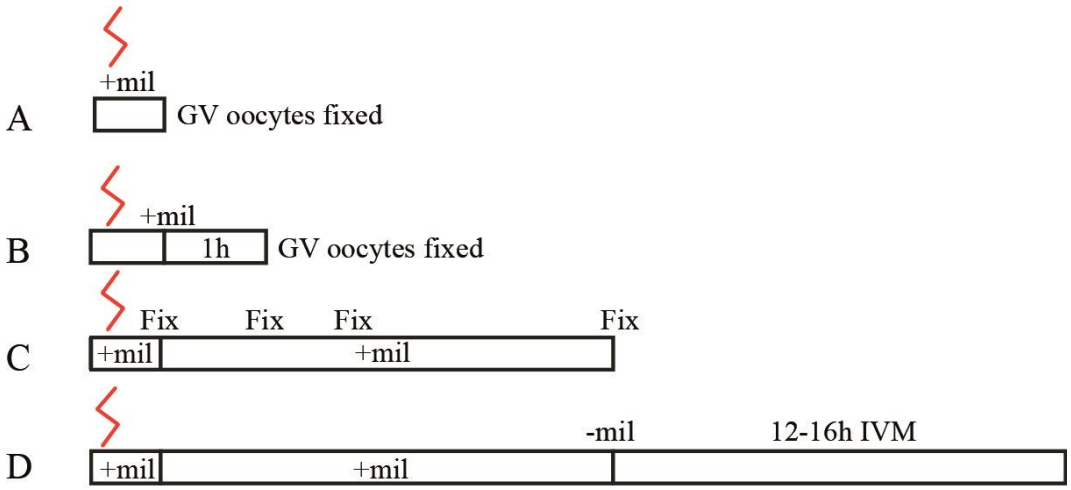

Figure 5-1 Experimental designs for investigating the ability of oocytes to repair DNA damage

(A) DNA damage induced whilst GV arrested and oocytes fixed as soon as possible afterwards (~15mins). (B) DNA damage induced whilst GV arrested and held in milrinone for 1 hour before fixing. (C) DNA damage induced whilst GV arrested and held at the GV stage in milrinone. Pools of oocytes fixed at set time points after treatment (0.3, 1, 3 and 10 hours after treatment). (D) DNA damage induced at the GV stage and held in milrinone for 10 hours, followed by an IVM of 12h-16h.

GV oocytes that were not exposed to Etoposide, Bleomycin or ionising radiation had little or no γH2AX within the nucleus, but when small foci were visible they co-localised with the chromatin (Figure 5.2A, 5.3A, 5.4A). However, numerous γH2AX foci could be seen in the nucleus of oocytes treated with all of the DNA damaging agents mentioned above, and these foci also co-localised with chromatin (Figure 5.2A, 5.3A, 5.4A).

When the mean nuclear γH2AX fluorescence was quantified there were significant increases in GV oocytes fixed immediately after treatment with 25µg/ml Etoposide (Control, 0.2±0.05 Arb. Units, n=10; Etoposide, 1.5±0.7 Arb. Units, n=9, P<0.001 compared to control, unpaired t-test, Figure 5.2B), 1µM Bleomycin (Control, 0.2±0.05 Arb. Units, n=10; Bleomycin, 0.6±0.6 Arb.Units, n=24, P<0.001 compared to control, Mann-Whitney test, Figure 5.3B) and 4.5y of ionising radiation (Control, 0.2±0.1, n=13; IR, 2.5±0.7 Arb.Units, n=15, P<0,001, unpaired t-test, Figure 5.4B).

5.2.3 UV induces H2AX phosphorylation in a delayed manner in GV oocytes

Interestingly, when nuclear γH2AX fluorescence was examined in UV-B exposed oocytes immediately after treatment, there was no visible difference between the staining pattern of UV-B treated oocytes and those that were un-exposed (Figure 5.5A). When mean nuclear γH2AX fluorescence was quantified it confirmed that there was not a significant difference between the exposed and un-exposed at this time point (0.3h control, 6990±2595 Arb.Units, n=36; 0.3h UVB, 7491±2972 Arb.Units, n=41, P>0.05 compared to 0h control, ANOVA with Tukeys post hoc analysis, Figure 5.5B).

I thought it may be possible that there is a delay in the phosphorylation of H2AX after UV-B exposure and the experimental design as shown in Figure 5.1B was used. Indeed, by holding UV-B exposed oocytes at the GV stage for 1 hour after treatment and then fixing, led to a visible increase in the γH2AX foci (Figure 5.5A). When quantified there was a significant increase in mean nuclear γH2AX fluorescence (1h control, 6514±2033 Arb.Units, n=46; 1h UVB, 12531±3377 Arb.Units, n=43, P<0.001 compared to 1h control, ANOVA with Tukeys post hoc analysis, Figure 5.5B).

5.2.4 Oocytes treated with Etoposide can self-repair

As discussed in Chapter 1.6.2 oocytes undergo programmed double strand breaks during early prophase and these have to be repaired. This suggests that oocytes may possess the ability to repair damage caused by exogenous factors as well. In order to examine this

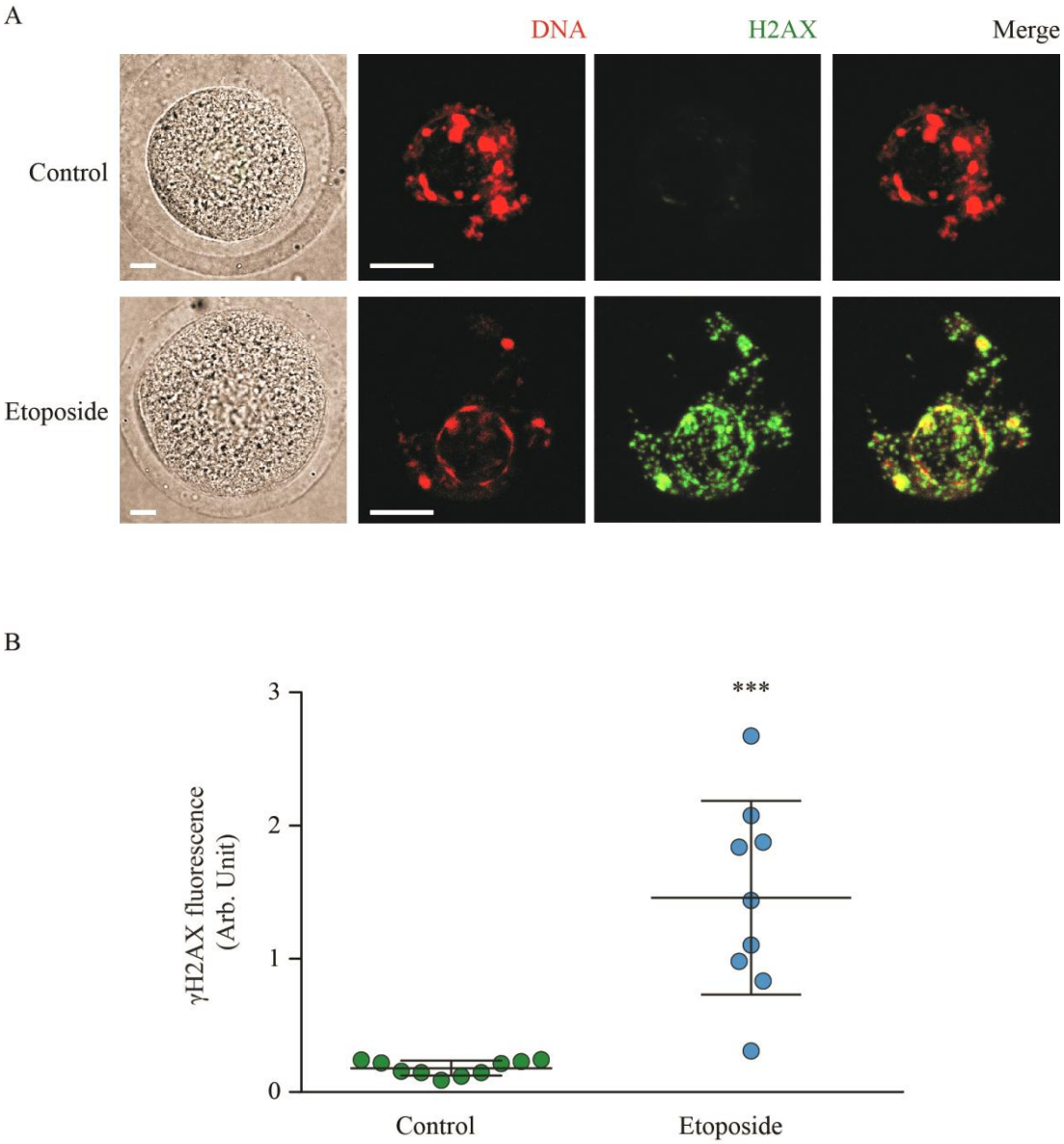

Figure 5-2 Etoposide induces the phosphorylation of H2AX in GV oocytes

(A) Representative γH2AX in a GV oocyte following either no treatment or 25µg/ml Etoposide. Scale bar, 10µm. (B) Nuclear γH2AX fluorescence levels in individual oocytes following treatment with 25µg/ml Etoposide. Data are pooled from 2 mice for each condition. Each data point represents a single oocyte; means and s.d are represented by the horizontal lines. *** P<0.001, compared to control (unpaired t-test).

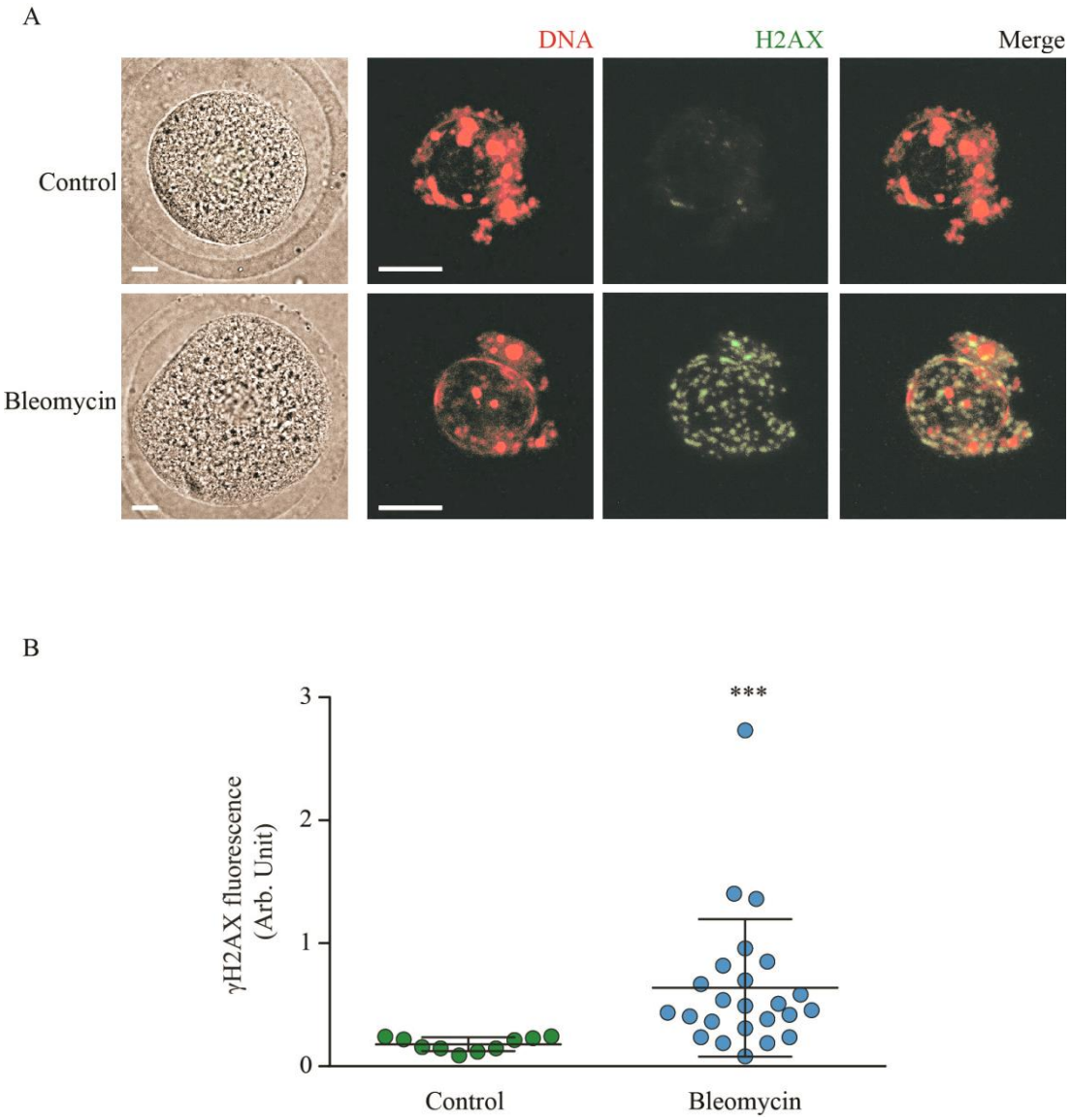

Figure 5-3 Bleomycin induces the phosphorylation of H2AX in GV oocytes

(A) Nuclear γH2AX fluorescence levels in individual oocytes following treatment with 1μM Bleomycin. Data are pooled from 2-3 mice for each condition. Each data point represents a single oocyte; means and s.d are represented by the horizontal lines. *** P<0.001, compared to control (Mann-Whitney test). (B) Representative γH2AX in a GV oocyte following either no treatment or 1μM Bleomycin. Scale bar, 10μm.

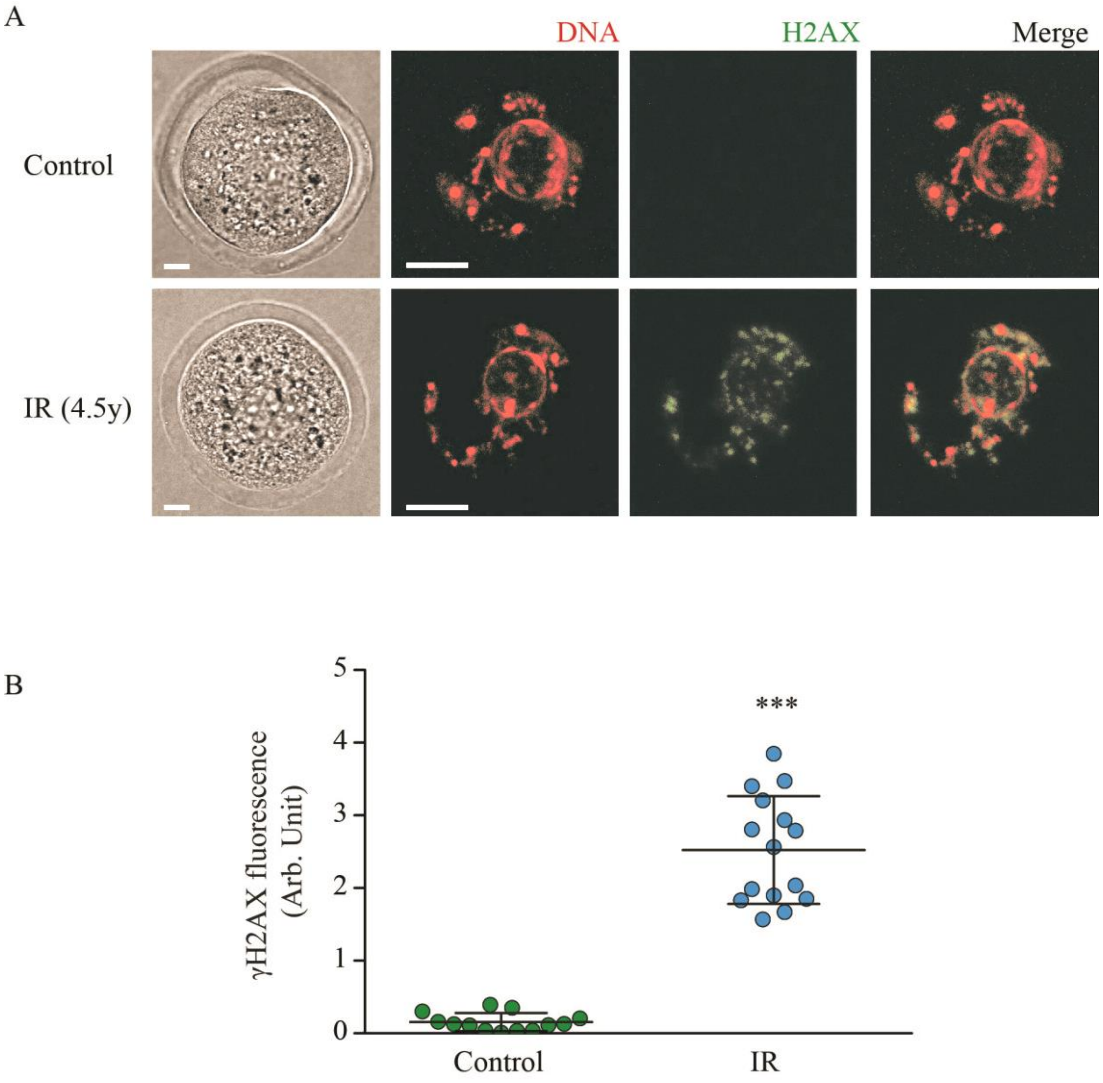

Figure 5-4 Ionising radiation induces the phosphorylation of H2AX in GV oocytes

(A) Nuclear γH2AX fluorescence levels in individual oocytes following treatment with 4.5y IR. Data are pooled from 2-3 mice for each condition. Each data point represents a single oocyte; means and s.d are represented by the horizontal lines. *** P<0.001, compared to control (unpaired t-test). (B) Representative γH2AX in a GV oocyte following either no treatment or 4.5y IR. Scale bar, 10μm.

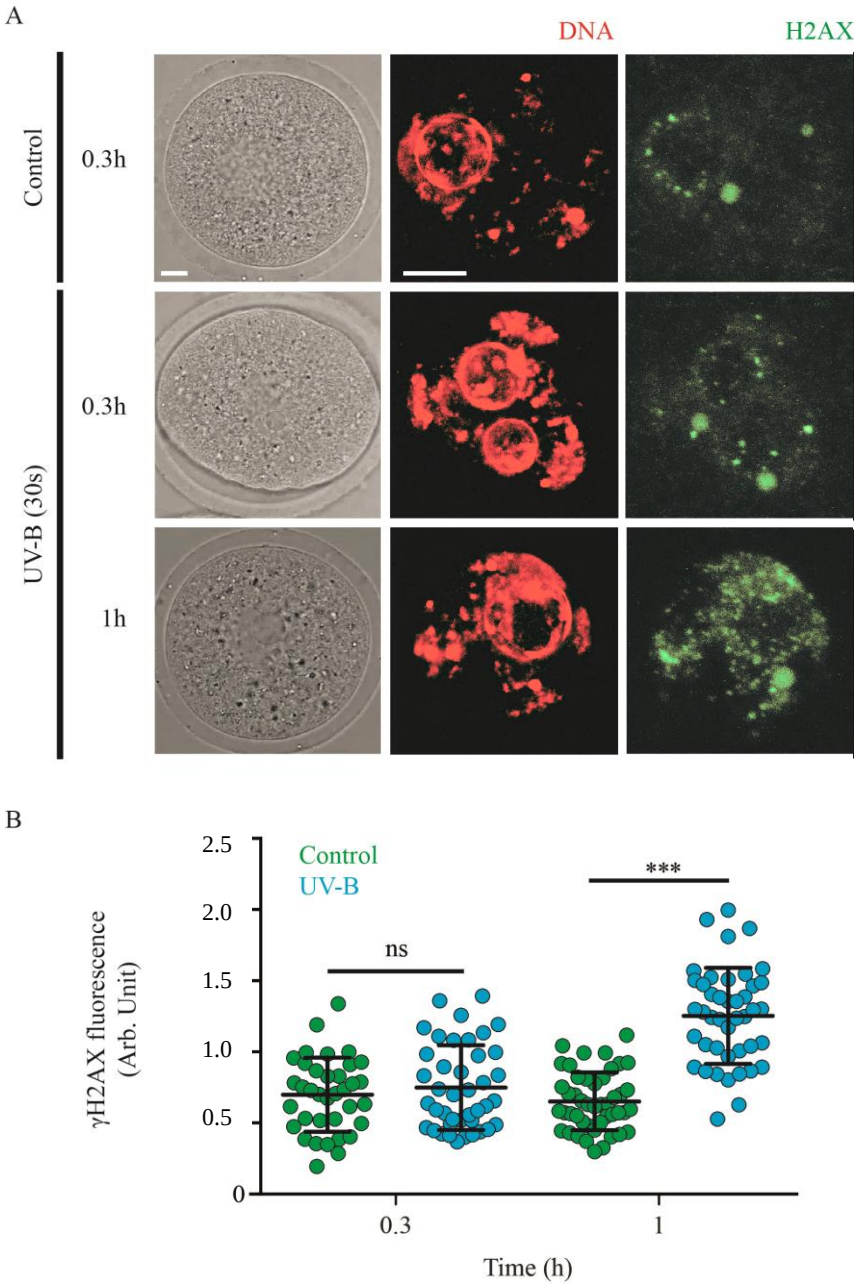

Figure 5-5 UV-B exposure induces the phosphorylation of H2AX in a delayed manner in GV oocytes

(A) Representative γH2AX immunofluorescence in GV oocytes following either no exposure or 30 seconds of UV-B (300nm). UV-B treated oocytes shown here immediately after treatment and 1 hour after treatment. (B) Nuclear γH2AX fluorescence levels in individual oocytes following either none or 30 seconds of UV-B exposure. Oocytes maintained at the GV for times indicated. Oocytes pooled from 5 mice. Each data point represents a single oocyte; means and s.d are represented by the horizontal lines. *** P<0.001, compared to control (ANOVA, Tukey's *post hoc* test). Scale bar, 10μm.

possibility the experimental design as shown in Figure 5.1C was used. GV oocytes were treated with 25µg/ml Etoposide for 15 minutes as in previous chapters. The oocytes were kept in milrinone to maintain GV arrest and groups of oocytes were taken from this pool at different time points after treatment (~20mins, 1h, 3h, 10h) and prepared for immunofluorescence utilising the γH2AX antibody.

The staining pattern for Etoposide treated GV oocytes altered over the 10 hour time period. At ~20mins and 1h after treatment there were a huge number of small foci, of which there was some overlap making individual foci difficult to see (Figure 5.6A). These foci also co-localised with the chromatin. However, by 10 hours after Etoposide treatment the number of foci had been greatly resolved. Also, the remaining foci appeared to be larger and much more distinct than at the earlier time points (Figure 5.6A).

When the mean nuclear γH2AX fluorescence was quantified in undamaged oocytes it was low and remained fairly consistent at the time points studied (0.3h control, 1.2±0.3 Arb.Units, n=16; 1h control, 0.9±0.3 Arb.Units, n=15; 3h control, 0.8±0.2 Arb.Units, n=18; 10h control, 0.8±0.2 Arb.Units, n=13; Figure 5.6B, green dots). Oocytes treated with Etoposide initially had much higher mean nuclear γH2AX fluorescence, which slowly declined over time, but still remained significantly higher than levels in control oocytes for 3 hours after treatment (0.3h Etoposide, 3.9±2.4 Arb.Units, n=18, $P<0.001$ compared to 0.3h control, ANOVA with Tukeys post hoc analysis; 1h Etoposide, 3.1±1.1 Arb.Units, n=19, $P<0.001$ compared to 1h control; 3h Etoposide, 2.0±0.8 Arb.Units, n=18, $P<0.05$ compared to 3h control; Figure 5.6B, green dots). By 10 hours after treatment the mean nuclear γH2AX fluorescence in control and treated oocytes was not significantly different (10h control, 0.8±0.2 Arb.Units, n=13; 10h Etoposide 0.7±0.2 Arb.Units, n=16, $P>0.05$ compared to 10h control, ANOVA with Tukeys post hoc analysis; Figure 5.6B), suggesting repair was taking place.

5.2.5 Repair of UV-B associated damage in GV oocytes

Having discovered the delayed induction of γH2AX in UV-B treated oocytes displayed in Figure 5.5, nuclear γH2AX fluorescence was also followed over a 10 hour period. As with the Etoposide treated oocytes, after UV-B exposure groups of oocytes were taken from the main pool at different time points (~20mins, 1h, 3h, 10h) and processed for immunofluorescence.

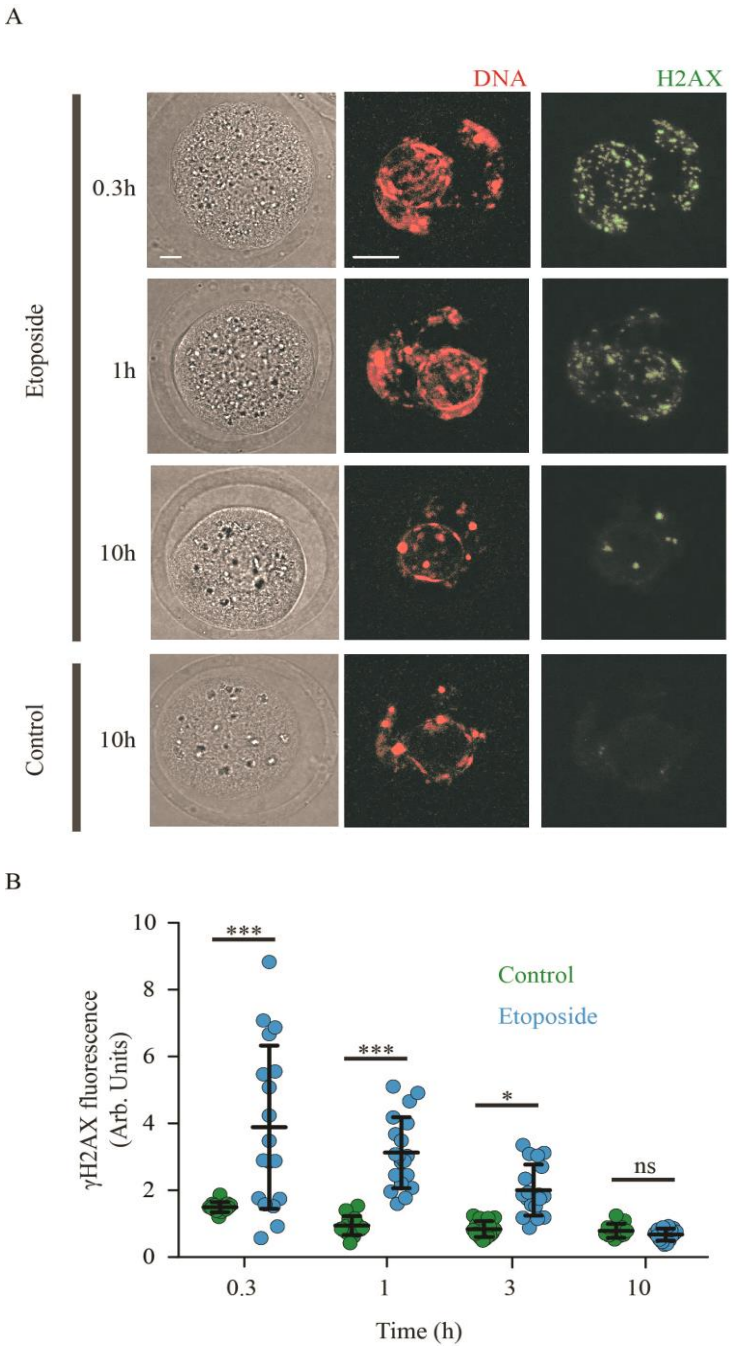

Figure 5-6 GV oocytes initiate repair of DNA damage induced by Etoposide

(A) Representative γH2AX immunofluorescence in GV oocytes following either control or 25µg/ml Etoposide. Etoposide treated oocytes shown here immediately after, 3 hours or 10 hours after treatment. (B) Nuclear γH2AX fluorescence levels in individual oocytes following either control or 25µg/ml Etoposide. Oocytes maintained at the GV stage for times indicated. Oocytes pooled from 4 mice. Each data point represents a single oocyte; means and s.d are represented by the horizontal lines. *, P<0.05, ***, P<0.001 compared to control (ANOVA, Tukey's *post hoc* test). Scale bar, 10µm.

The staining pattern for UV-B exposed GV oocytes altered over the 10 hour time period. As already highlighted in Figure 5.5 at ~20mins after exposure very little γH2AX could be seen; only a few small foci could be seen and these were also apparent in controls when examined at all stages (Figure 5.7A; only control at 10h is displayed as oocytes were similar from all time points examined). γH2AX foci were much more abundant at 1, 3 and 10 hours after UV-B exposure and there was no obvious visible change in the size of the foci either (Figure 5.7A).

When nuclear γH2AX was quantified, it showed that in contrast to Etoposide treated oocytes (Figure 5.6) UV-B exposed oocytes do not reach a peak in γH2AX fluorescence until 3 hours after treatment (3h UV-B, 39774±6568 Arb.Units, n=23; Figure 5.7B). By 10 hours after UV-B exposure γH2AX levels had begun to decrease, but were still much higher than that of controls from the same time point (10h control, 10355±2634 Arb.Units, n=24; 10h UV-B, 25509±9814 Arb.Units, n=23, $P<0.001$ compared to 10h control, ANOVA with Tukeys post hoc analysis; Figure 5.7B).

5.2.6 Self-repair can cause small increases in PBE in DNA damaged oocytes

Having found that oocytes treated with Etoposide are able to repair a significant amount of DNA damage within a 10 hour period, visualised by the reduction in γH2AX fluorescence (Figure 5.6), it was of interest to see if this translated into a rescue of PBE. To assess this the experimental design as shown in Figure 5.1D was used. Holding undamaged oocytes at the GV stage had no effect on maturation when compared to those that did not have the holding period; rates in both cases were at least 60% (Figure 5.8, green bars). As already established, treatment with Etoposide significantly reduced maturation rates in oocytes. However, by including a 10 hour holding period at the GV stage after treatment, allowed for a small but significant increase in polar body extrusion (Etoposide -10h hold, 7%, n=367; Etoposide +10hold, 19%, n=280, $P<0.001$ compared to Etoposide -10h hold, Fishers exact test; Figure 5.8, blue bars).

5.3 Discussion

In this chapter GV oocytes were shown to be able to detect and signal DNA damage induced by Etoposide, Bleomycin and ionising radiation, through the phosphorylation of H2AX. However, the phosphorylation of H2AX in UV-B treated oocytes was shown to be induced in a delayed manner. Using the γH2AX antibody it was also clear that oocytes treated with Etoposide could resolve these foci over a 10 hour holding period, suggesting

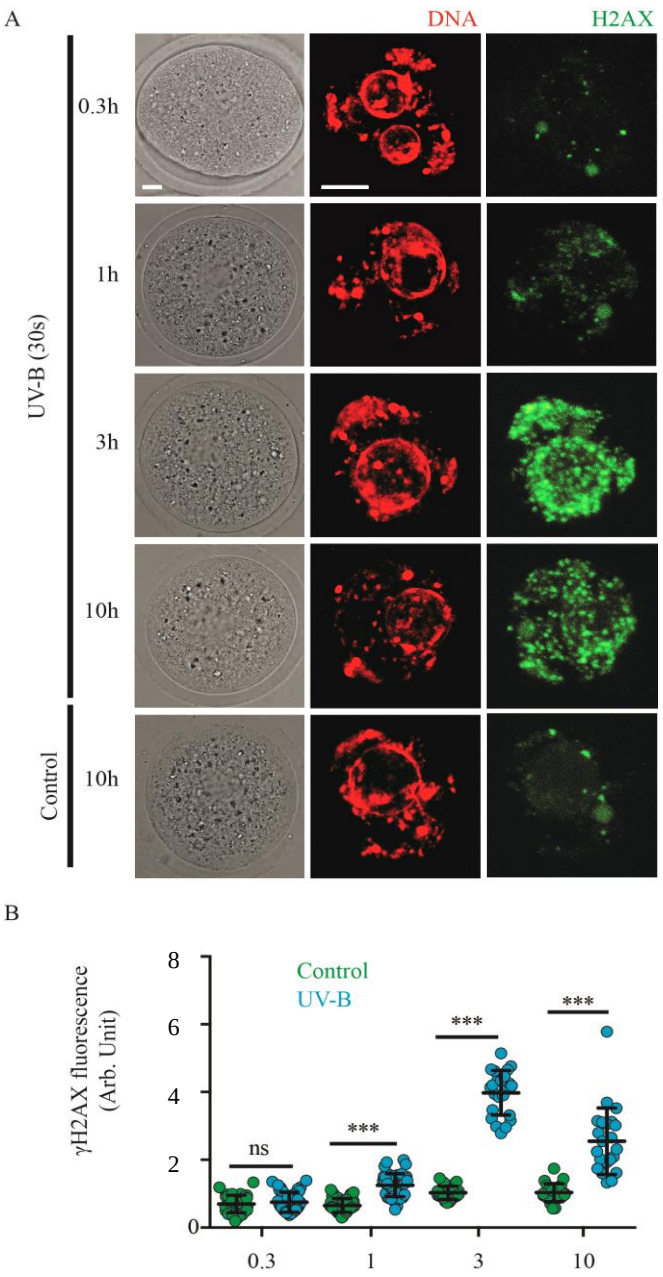

Figure 5-7 GV oocytes do not initiate efficient repair of UV-B associated damage

(A) Representative γH2AX immunofluorescence in GV oocytes following either control or 30 seconds of UV-B. UV-B treated oocytes shown here immediately after, 1 hour, 3 hours, or 10 hours after treatment. (B) Nuclear γH2AX fluorescence levels in individual oocytes following either control or 30 seconds of UV-B. Oocytes maintained at the GV for times indicated. Oocytes pooled from 5 mice. Each data point represents a single oocyte; means and s.d are represented by the horizontal lines. *** P<0.001, compared to control (ANOVA, Tukey's *post hoc* test). Scale bar, 10μm.

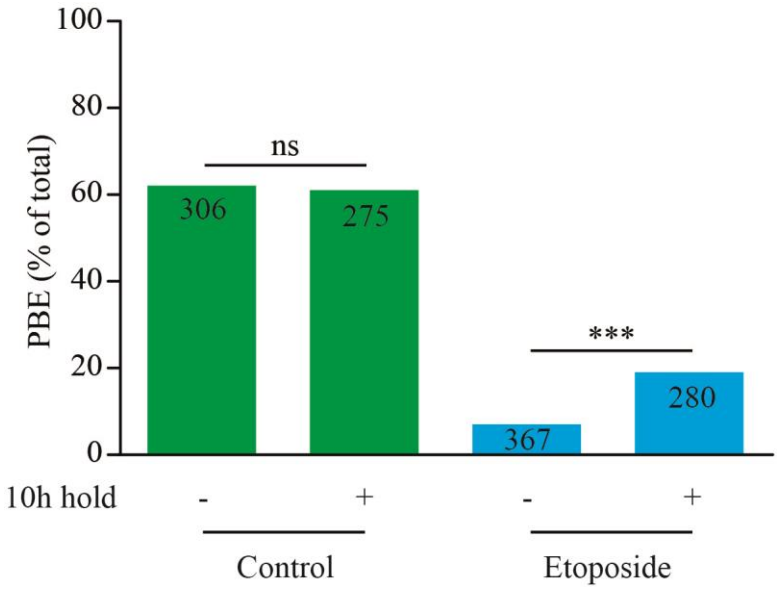

Figure 5-8 A 10h hold period can improve the maturation rates in DNA damaged oocytes

Oocyte maturation rates in oocytes treated with control or 25 µg/ml Etoposide that were either immediately released for IVM, or held for 10h at the GV stage prior to release. PBE was assessed after 12-16h after IVM. Pooled from 5 mice per treatment. ***, P<0.001 compared to Etoposide -10h hold period (Fishers Exact test).

that repair had taken place. However, oocytes exposed to UV-B could not. In fact these oocytes did not reach a peak in fluorescence until 3 hours after treatment, perhaps highlighting a different method of DSB induction after exposure to UV-B. The effect of DNA repair on maturation success was also investigated using Etoposide treated oocytes; this revealed that a repair period whilst GV arrested could translate into a mild rescue of PBE.

5.3.1 Oocytes can detect and signal DNA damage induced by exogenous sources

The phosphorylation of H2AX is one of the most upstream signalling events after DNA double strand breaks have been formed in somatic cells (Podhorecka et al. 2010). This modification allows for the accumulation of other DDR proteins required to initiate a cell cycle arrest and DNA damage repair (Kinner et al. 2008, Podhorecka et al. 2010).

As discussed in detail in Chapter 1.6.2, during early prophase the oocyte undergoes a series of programmed DSBs in order for meiotic recombination and crossover formation to occur. It is also known that these DSBs are detected and signalled for repair (Mahadevaiah et al. 2001). If these breaks are not formed and repaired by homologous recombination, as occurs in *Spo11-/-* mice, (Baudat et al. 2000, Romanienko and Camerini-Otero 2000), chromosomes do not get tethered together which would lead to aneuploidy (Burgoyne et al. 2009). To prevent this oocytes undergo apoptosis (Di Giacomo et al. 2005). Therefore, programmed DSBs are signalled by the phosphorylation of H2AX (Mahadevaiah et al. 2001) and require other DDR proteins, such as ATM, RAD51 and DMC1, to be activated in order to be repaired (Baudat et al. 2013). If repair of programmed DSBs is aberrant, as in DMC1-/- and ATM-/- mice, a checkpoint exists to eliminate these oocytes through apoptosis (Di Giacomo et al. 2005).

Having this ability to deal with programmed DSBs made it reasonable to assume that oocytes are likely to be able to signal DNA DSBs induced by exogenous factors as well. Indeed it had been shown that GV stage oocytes could detect and signal DNA damage through the phosphorylation of H2AX. Oocytes treated with as little as 5µg/ml Etoposide for 3 hours had a significant increase in γH2AX (Marangos and Carroll 2012). Also the percentage of oocytes positive for γH2AX signal, when examined by immunofluorescence, was increased when treated with NCS for 1 hour (Yuen et al. 2012).

The extensive investigation into γH2AX signalling I have presented here supports the previously published work mentioned above. Here 25µg/ml Etoposide for 15 minutes,

1µM Bleomycin for 15 minutes and exposure to 4.5Gy all significantly increased the mean nuclear γH2AX fluorescence (Figure 5.2, 5.3 and 5.4). I chose to measure γH2AX by calculating the mean nuclear fluorescence due to the huge number of foci present in the oocytes which often overlapped. Counting individual foci was far too ambiguous as overlapping foci could lead to an underrepresentation of γH2AX.

Since I began my studies several other groups have also reported that GV oocytes can detect and signal DNA damage by phosphorylating H2AX. Increases in γH2AX have been reported in mouse oocytes treated with Bleomycin (Ma et al. 2013), NCS (Mayer et al. 2016) and laser beam microdissection (UV-A) (Ma et al. 2013). This response to DNA damage is not limited to the mouse model and has been shown in porcine oocytes treated with Bleomycin (Zhang et al. 2014) or Etoposide (Wang et al. 2015a). Therefore it is now well established that oocytes can detect and signal DNA damage caused by exogenous sources. It will be interesting to find out whether DDR proteins that carry out H2AX phosphorylation in somatic cells, such as ATM or ATR, also function in oocytes.

5.3.2 Signalling of UV-induced DNA damage is delayed in GV oocytes

Ultraviolet radiation is well known for its ability to cause cyclobutane pyrimidine dimers (CPDs) and 6-4 photoproducts (Chapter 1.2.4) (Goodsell 2001, Budden and Bowden 2013). It has also been extensively shown that UV-A, UV-B and UV-C can induce the phosphorylation of H2AX in somatic cells (Halicka et al. 2005, Marti et al. 2006, Hanasoge and Ljungman 2007, Oh et al. 2011, Greinert et al. 2012), a modification associated with DNA DSBs. However, whether γH2AX is signalling the induction of DSBs in UV damaged cells has been under much debate over the last decade.

The data presented here shows that UV-B exposure can initiate the phosphorylation of H2AX in oocytes, like in somatic cells. Significant increases in nuclear γH2AX were seen, but only 1 hour after UV-B exposure had occurred (Figure 5.5) implying that the mechanism that leads to this histone modification in oocytes after UV exposure is slow or delayed. Indeed, similar kinetics of H2AX phosphorylation have been reported in a variety of human cell lines. Marti et al. (2006) showed that γH2AX could be detected 1 hour after UV irradiation of human fibroblasts, but that it did not reach its maximum until 2 hours after exposure. In this study it was suggested that individual γH2AX foci were not formed by UV and rather a pan-nuclear pattern was seen (Marti et al. 2006). However, many studies published since have shown the formation of distinct foci (Hanasoge and Ljungman 2007, Oh et al. 2011, Greinert et al. 2012), agreeing with my work presented here.

There are several possibilities that could have caused H2AX to be phosphorylated in UV-B treated oocytes, including the formation of DSBs or the production of repair intermediates during nucleotide excision repair (NER) (Chapter 1.5.3). It has been suggested that the phosphorylation of H2AX after UV-C exposure in human fibroblasts was not due to the formation of DSBs as no NBS1, a protein involved in signalling and repairing DNA DSBs, co-localised with the γH2AX staining (Marti et al. 2006). Instead H2AX was found to associate with CPD staining and was reduced or eliminated in cells that were deficient in XPC or XPA, proteins involved in NER. Therefore one possibility is that H2AX phosphorylation in UV treated oocytes may not be signalling a DSB. Instead the γH2AX could be signalling the formation of DNA repair intermediates.

However, in an interesting study by Oh et al. (2011) it was shown that H2AX was phosphorylated after UV exposure even in the absence of NER using cells deficient in XPB, another NER factor. This study also revealed that DSBs could be formed after UV treatment using the neutral comet assay, which revealed a tail consistent with DSB formation. However, the increase in tail moment was not apparent 1 hour after UV exposure, and was instead seen at the later time point tested (6 hours after UV exposure). Therefore, another possibility that delayed the phosphorylation of H2AX in UV treated oocytes could have been that DSBs were in fact formed, but that these breaks are not created directly by the UV. In somatic cells, the production of ROS has been suggested to induce DSBs after UV exposure (Greinert et al. 2012). UV-A was found to induce the phosphorylation of H2AX in skin fibroblasts, which was found to correlate with an increased production of ROS. Human skin fibroblasts pre-treated with an antioxidant called Naringin, had reduced γH2AX induction, consistent with ROS being the cause of the damage (Greinert et al. 2012). Comet assays were also used to analyse DNA fragmentation in these cells. In both the neutral (to detect DSBs) and the alkaline (detects SSBs and DSBs) assays the tail length was increased; suggesting that breaks in DNA had in fact been caused.

A different profile of DNA damage induction may have been seen if the formation of thymine dimers had been monitored instead of the phosphorylation of H2AX. It would be interesting to further investigate the cause of the delayed phosphorylation of H2AX and whether it simply signals slow forming DSBs caused by ROS, or if it represents the repair intermediates created during the repair of CPD and 6-4 photoproducts.

5.3.3 GV stage oocytes are capable of initiating DNA repair

There are many mechanisms that can be initiated to repair different types of DNA damage. For this thesis the main mechanisms of concern included the repair of DSBs that were induced by Etoposide, and potentially UV-B, by homologous recombination (HR) (Chapter 1.5.1). The second was the repair of UV-B induced damage by NER (Chapter 1.5.3).

As already mentioned, oocytes are able to repair programmed DSBs that are initiated during prophase (Chapter 1.8.1). There are some studies that have suggested that oocytes can repair DNA damage caused by exogenous sources as well (Chapter 1.8.2). Therefore, I wanted to examine whether fully grown GV oocytes were able to rid themselves of such lesions. The γH2AX assay has been used to successfully monitor the repair of ionising radiation induced DSBs in human (Mariotti et al. 2013) and swine cell lines (Moroni et al. 2013). In both studies somatic cells were shown to resolve a substantial number γH2AX foci within 10 hours of IR treatment (Mariotti et al. 2013, Moroni et al. 2013). Thus, using γH2AX to assay the repair of DSBs I have shown here that oocytes treated with Etoposide are able to initiate the repair of lesions in their DNA (Figure 5.6). A majority of the γH2AX foci disappear within 10 hours of treatment with Etoposide, suggesting that GV oocytes initiate similar repair mechanisms as somatic cells.

In support of the finding that fully grown oocytes carry out DSB repair, a very recent study has suggested that oocytes treated with NCS can resolve DNA damage throughout maturation (Mayer et al. 2016). In this study low levels of DNA damage were induced so that the progression to metaphase II was not inhibited. By examining H2AX phosphorylation throughout meiosis I, they showed a reduction in both endogenously and exogenously induced γH2AX foci between the GV and metaphase II stage, and suggested this was due to repair taking place.

Interestingly, a very different γH2AX profile was seen for UV-B treated oocytes. After the initial finding that significant increases in γH2AX fluorescence were not seen until 1 hour after treatment (Figure 5.5), extending the time that γH2AX was examined over revealed that peak γH2AX fluorescence was not reached until 3 hours post irradiation (Figure 5.7). As already discussed in 5.3.2 phosphorylation of H2AX is readily reported after UV exposure and is thought to be due to either DSBs induced by ROS, or that γH2AX is not marking DSBs, but instead marking repair intermediates created whilst cells are resolving dimers and photoproducts. Therefore the results presented here can be interpreted in two different ways. Firstly, if γH2AX represents DSBs they are not initiated immediately after

UV treatment, which supports the findings in somatic cells (Greinert et al. 2012, Oh et al. 2011). It also supports the theory that ROS could be inducing such damage (Greinert et al. 2012), and that as a result this slower induction of DSBs, repair (and decrease in γH2AX fluorescence) does not begin until 10 hours after UV exposure. If the experiment was extended and γH2AX fluorescence was assessed 24 hours after exposure I would predict that γH2AX would continue to decrease during this time.

However, several studies have suggested that γH2AX in UV treated cells may be marking repair intermediates rather than DSBs (Hanasoge and Ljungman 2007, Marti et al. 2006). If this is also the case in oocytes, the γH2AX profile suggests that high levels of repair were taking place by 3 hours after UV exposure. Similar profiles have been seen in human fibroblasts treated with UV; where peaks in γH2AX foci have been reported between 2-6h followed by a reduction between 8-12h and complete absence of γH2AX by 24 hours after exposure (Hanasoge and Ljungman 2007, Marti et al. 2006). This was studied further by Hanasoge and Ljungman (2007) where they increased the number of repair intermediates by inhibiting DNA polymerase enzymes, which are required for NER, using aphidocolin. This treatment caused further increases in H2AX phosphorylation, and their persistence after UV-C exposure. Why γH2AX marks these repair intermediates is unknown but it has been suggested to maintain cell cycle arrest during repair, as the kinetics mirror the removal of 6-4 photoproducts (Marti et al. 2006).

Without further investigation it cannot be said what γH2AX is signalling in UV-B treated oocytes. Future work could include monitoring CPD formation and its repair using established antibodies. It would also be important to find out if proteins involved in DSB repair, such as RPA or RAD51, co-localise with γH2AX in UV treated oocytes as this would suggest DSBs are being signalled in these oocytes.

Despite being a well-established biomarker of DNA DSBs there may be some limitations of using the γH2AX assay to monitor the formation and repair of DSBs (Löbrich et al. 2010). Firstly, as I have demonstrated with the UV exposed oocytes, there is the potential that γH2AX may not only represent DSBs. It has also been shown to have other roles within the cell including normal progression of the cell cycle as γH2AX is present in non-damaged cells to different extents throughout mitosis (Turinetto and Giachino 2015). Nevertheless, with the damaging agents used in this thesis it is well established that they cause DSBs that are signalled by γH2AX in somatic cells (Burma et al. 2001, Redon et al. 2009, Scarpato et al. 2013), thus I am confident that DSBs are being signalled here, excluding the results seen in UV treated oocytes. Secondly, it has also been suggested that

the timing of the loss of foci does not fully correlate with repair (Löbrich et al. 2010). Regardless of this, the assay still demonstrates that oocytes can repair DSBs over time. Other assays that can be used to monitor DNA damage include the Comet Assay and Pulse-field gel electrophoresis (PFGE). However, these methods require costly equipment and intricate protocols for use on oocytes. PFGE in particular requires 10^5–10^6 cells for analysis (Löbrich et al. 2010) a number that is not feasible when studying oocytes. Therefore, I used the γH2AX assay due to the protocol for using this antibody being well-established and known to work on oocytes, but kept in mind its possible limitations.

5.3.4 Repairing DNA DSBs subtly increases PBE in oocytes

The de-phosphorylation of γH2AX is associated with the switching off of the DNA damage response and is involved in recovery of the G2/M checkpoint (Peng 2013, Wang et al. 2015b). The recovery from DNA damage checkpoints is not yet fully understood but the de-phosphorylation of many DDR proteins by protein phosphatases is known to be important. WIP1 expression is enhanced several hours after DNA damage induction where it then facilitates the de-phosphorylation of ATM kinase, γH2AX, CHK1 and CHK2 (Peng 2013, Wang et al. 2015b). Also PP2A is required for inactivating ATM kinase and also for de-phosphorylating γH2AX (Chowdhury et al. 2005, Wang et al. 2015b). PP2A has also been found to be involved in the inactivation of CHK1 (Wang et al. 2015b). Although it is known that these proteins are required for checkpoint recovery, the timing of their activation after DNA damage is still not clear.

Due to the known involvement of γH2AX de-phosphorylation in checkpoint recovery, it was logical to predict that the reduction in γH2AX in Etoposide treated oocytes over a 10 hour period, may have allowed the oocyte to recover from the DNA damage. Therefore, oocytes were allowed to undergo a recovery period and released for maturation to see if rates of PBE could be improved. Indeed rates of PBE were subtly increased in DNA damaged oocytes when a recovery period had been permitted (Figure 5.8).

In agreement with this finding, it has been shown very recently that oocytes treated with low doses of NCS (ng/ml concentrations), to induce relatively few H2AX foci, do progress to metaphase II (Mayer et al. 2016). However, here I have only seen a small increase in PBE. These differences could be due to the levels of damage originally induced between the two studies; here I induce extensive amounts of damage that could also differ in complexity compared to the low levels of damage induced by Mayer et al. (2016). Therefore, the oocytes that remained arrested in my study could have been due to residual

DNA damage that could not be repaired. In support of this the γH2AX foci in oocytes became noticeably larger in size 10 hours after Etoposide treatment (Figure 5.6). It is well-known that the γH2AX signal spreads across DNA to flank the DSB (Kinner et al. 2008, Rogakou et al. 1998), so perhaps these larger foci represent complex double strand breaks that cannot be repaired, and therefore require more signalling. This could have possibly led to persistence in the DDR signalling and continued cell cycle arrest. If oocytes were held for 24 hours after Etoposide treatment, all DSBs may be resolved and could lead to further increases in PBE, as IR and UV-B damage continues to be repaired when examined for up to 24 hours in somatic cells (Mariotti et al. 2013, Marti et al. 2006, Moroni et al. 2013).

Even though only small increases in PBE are seen here (Figure 5.8) it would be interesting to know whether the accuracy of the first meiotic division is improved after a repair period. The work produced by Mayer et al. (2016) suggests that improvements could be seen. They showed that in oocytes treated with 10ng/ml and 100ng/ml NCS, the percentage of oocytes with segregation errors was ~25% and ~90% respectively (Mayer et al. 2016). This could be interpreted to show that if oocytes can reduce the number of DSBs, as I have shown here, the accuracy of the first meiotic division could be improved. Future work could focus on the rates of aneuploidy in DNA damaged oocytes that have either had a repair period or released from milrinone immediately after treatment. I would predict that DNA damage would lead to high levels of aneuploidy and allowing oocytes to repair DNA damage would decrease this incidence.

5.3.5 Conclusions

The findings presented in this chapter clearly demonstrate the ability of the fully grown GV oocyte to detect and signal DNA DSBs, and damage associated with UV-B irradiation. My work suggests that oocytes have the ability to repair Etoposide induced DSBs with kinetics similar to, or slightly better than, that of somatic cells treated with IR. I have also shown that maturation rates of DNA damaged oocytes can be subtly improved when oocytes are kept arrested at GV for 10 hours, to allow DNA repair to take place. It will be important to establish if the proteins required for H2AX phosphorylation in somatic cells, such as ATM and ATR, also function in the oocyte response to DNA damage. This will be addressed in Chapter 6.

Chapter 6: The role of DNA Damage Response proteins in the Oocyte DNA Damage Response

6.1 Introduction

Having established that oocytes can detect and signal DNA damage (Chapter 5), it was important to understand what proteins are required for such signalling to take place. In somatic cells ATM and ATR are critical components for DDR signalling (Chapter 1.3.1 and 1.3.2); therefore it was of interest to see whether these proteins also function in the oocyte response to DNA damage.

To examine the involvement of the kinases in oocytes with and without DNA damage, pharmacological inhibitors were used to knock down the proteins. I was interested to see if H2AX phosphorylation, and so DNA damage signalling, was affected when these kinases were inhibited. This is due to the fact that both ATM and ATR are known to carry out this histone modification after DNA damage induction (Burma et al. 2001, Hanasoge and Ljungman 2007, Ward and Chen 2001). To do this oocytes were treated with DNA damaging agent either in the presence/absence of the inhibitor, were fixed after treatment and processed for immunofluorescence. Using antibodies against γH2AX (used in Chapter 5) to quantify nuclear fluorescence levels, the relative activity of ATM and ATR signalling was inferred. As well as this, the impact on oocyte maturation was assessed for each kinase individually by adding inhibitor to the incubation media and also when using a combination of the two inhibitors. The kinase inhibitors were also added to the media during treatment. After a standard IVM oocytes were assessed for polar body extrusion.

To complement the experiments that used pharmacological inhibition, oocytes from genetically modified mice in which the *Atm* and *Atr* genes had been knocked-out were used. Mutations in ATM or complete loss of the kinase results in infertility, but can also lead to embryonic lethality in mice (Barlow et al. 1996, Barlow et al. 1998, Daniel et al. 2012). The loss of ATR function is always embryonic lethal (Brown and Baltimore 2000, de Klein et al. 2000). The production of these mice was possible due to them being conditional knockouts, specific to the oocyte, using the Cre-LoxP system. With the expression of Cre recombinase linked to that of DDX4, which is needed for meiotic activation. In these experiments fully grown GV oocytes obtained from knockout mice were treated with Etoposide and the effect on oocyte maturation was assessed.

6.2 Results

6.2.1 Experimental designs for investigating the role of common DNA Damage response proteins in the oocyte DNA Damage Response

Having established that oocytes appear to have a unique SAC-dependent DNA damage response it was of interest to begin to work out the signalling pathways that lead to SAC activation. To check that ATM and ATR function was inhibited when the inhibitors were added to media oocytes were processed using the experimental design as shown in Figure 6.1A and 6.1B. GV oocytes were treated with Bleomycin, UV-B or Etoposide, in the presence or absence of the inhibitors, and then immediately processed for immunofluorescence. Following staining with antibodies against γH2AX, nuclear fluorescence could be calculated for individual oocytes.

To examine the effect of inhibiting ATM and ATR on oocyte maturation, either ATM or ATR inhibitor was added to the culture media during treatment and throughout IVM, according to the experimental design as shown in Figure 6.1C and 6.1D. The standard 16 hour IVM was used and maturation success was scored by the presence or absence of the first polar body. The combined effect of inhibiting both ATM and ATR was studied using experimental design 6.1E and 6.1F. To monitor the effect of inhibiting both kinases on DNA damage signalling GV oocytes were treated with Etoposide in the presence of both inhibitors, and immediately fixed for immunofluorescence. Following staining with antibodies against γH2AX, nuclear fluorescence could be calculated for individual oocytes (Figure 6.1E). To examine the effect on oocyte maturation both ATM and ATR inhibitor was added to the culture media during treatment and IVM. Following a 16 hour IVM maturation success was scored (Figure 6.1F).

Finally, oocytes were collected from *Atm-/- Atr-/-* mice and treated as shown in experimental design as shown in Figure 6.1G. GV oocytes were treated with Etoposide and immediately released from milrinone. Following the standard 16 hour IVM maturation success was scored.

6.2.2 ATM kinase and the oocyte DNA Damage Response

KU55933 is one of a handful of commercially available pharmacological inhibitors of ATM kinase. It is well established as a potent and specific inhibitor that is used to study the role of ATM in somatic cells (Velic et al. 2015). Therefore I wanted to

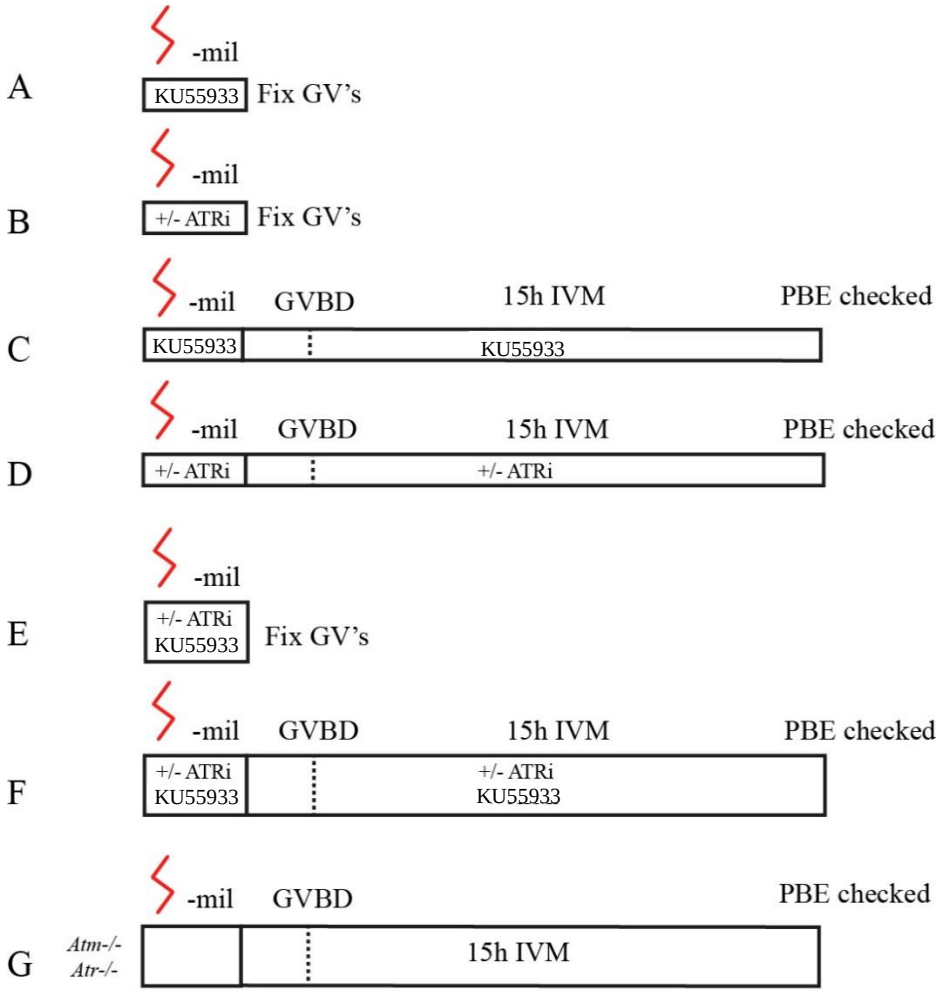

Figure 6-1 Experimental designs to study the involvement of DDR proteins in the oocyte specific DNA damage checkpoint

(A) DNA damage induced in GV arrested oocytes either in the presence or absence of KU55933. GV oocytes were fixed after treatment. (B) Same protocol as in 'A' except the inhibitor used was specific to ATR kinase. (C) DNA damage induced whilst GV arrested followed by standard 16h IVM (GVBD+15h). Media used for treatment or IVM was either supplemented with KU55933 or not. (D) Same protocol as in 'C' except the inhibitor was specific to ATR kinase. (E) Same protocol as in 'A' and 'B' except inhibitors against both ATM and ATR kinase were used. (F) Same protocol as in 'C' or 'D' except inhibitors against both ATM and ATR kinase were used. (G) GV oocytes collected from *Atm-/- Atr-/-* mice. DNA damage induced at the GV stage, followed by standard IVM (GVBD+15h).

use this inhibitor to assess the involvement of ATM in the oocyte DDR. However, some oocyte researchers anecdotally have suggested this inhibitor is problematic (personal communication – Dr Petros Marangos, Dr Elias Elinati). As a result, three different batches of KU55933 were tested in this thesis and it was indeed found that there was batch-to-batch variation in the effect of this inhibitor on oocytes both with and without DNA damage. The batches of KU55933 tested in this thesis will be described separately and will be specified to distinguish experimental findings.

6.2.3 Pharmacological inhibition of ATM kinase has variable effects on oocyte maturation

In order to use this inhibitor a suitable dose needed to be found. The dose and timing of KU55933 treatment is highly variable among oocyte studies. Marangos and Carroll used KU55933 to study the effect of DSBs on GVBD and meiotic progression in oocytes; for their experiments they used a dose of ~25μM and in a more recent publication used 40μM (Marangos and Carroll 2012, Marangos et al. 2015). In one study looking at primordial follicle apoptosis after DNA damage induction, doses of up 300μM were used (Kim and Suh 2014). Therefore, I needed to establish a dose of KU55933 that would not have a negative impact on the maturation of undamaged oocytes. Using Batch 1 I tested a variety of doses (4-100μM) on undamaged oocytes. Interestingly, none of the doses tested had a negative impact on PBE (Figure 6.2). In fact 40μM KU55933 (Batch 1) caused a significant increase in the maturation of oocytes (0μM, 73%, n=30; 40μM, 97%, n=31, P=0.0125 compared to '0', Fishers Exact test; Figure 6.2). As, a result of this 40μM was the dose of inhibitor used for the experiments involving Batch 1.

Having found that 40μM KU55933 (Batch 1) caused an increase in maturation rates in undamaged oocytes I next wanted to establish whether maturation rates could be improved by ATM inhibition in oocytes with DNA damage. This was investigated using the experimental design shown in Figure 6.1C. KU55933 (Batch 1) was added to the media during treatment and IVM; PBE was assessed after 16 hours. When 40μM KU55933 added to the media of oocytes treated with Etoposide a small increase in PBE was seen, however this did not reach a level of statistical significance (Etoposide, 48%, n=40; Etoposide+KU55933, 53%, n=40, P=0.6590 compared to Etoposide only, Fishers exact test, Figure 6.3A, blue bars). Treating oocytes with Bleomycin in the presence of KU55933 allowed for a significant increase in PBE (Bleo, 49%, n=112; Bleo+KU55933, 62%, n=119, P=0.0481 compared to

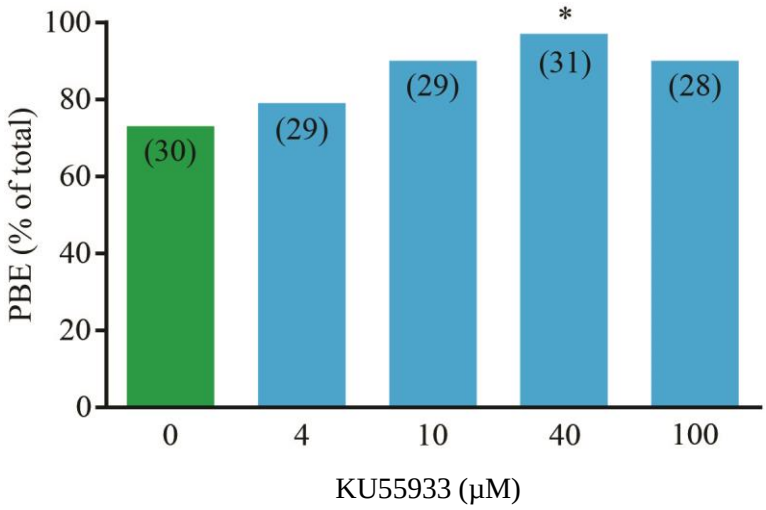

Figure 6-2 The effect of ATM kinase inhibition of PBE rates in undamaged oocytes

Maturation rates in oocytes without exposure to DNA damaging agents in the presence or absence of varying concentrations of KU55933 (Batch 1). Number of oocytes used stated. Oocytes pooled from 2 mice per treatment. *, $P<0.05$ compared to '0' (Fishers Exact test).

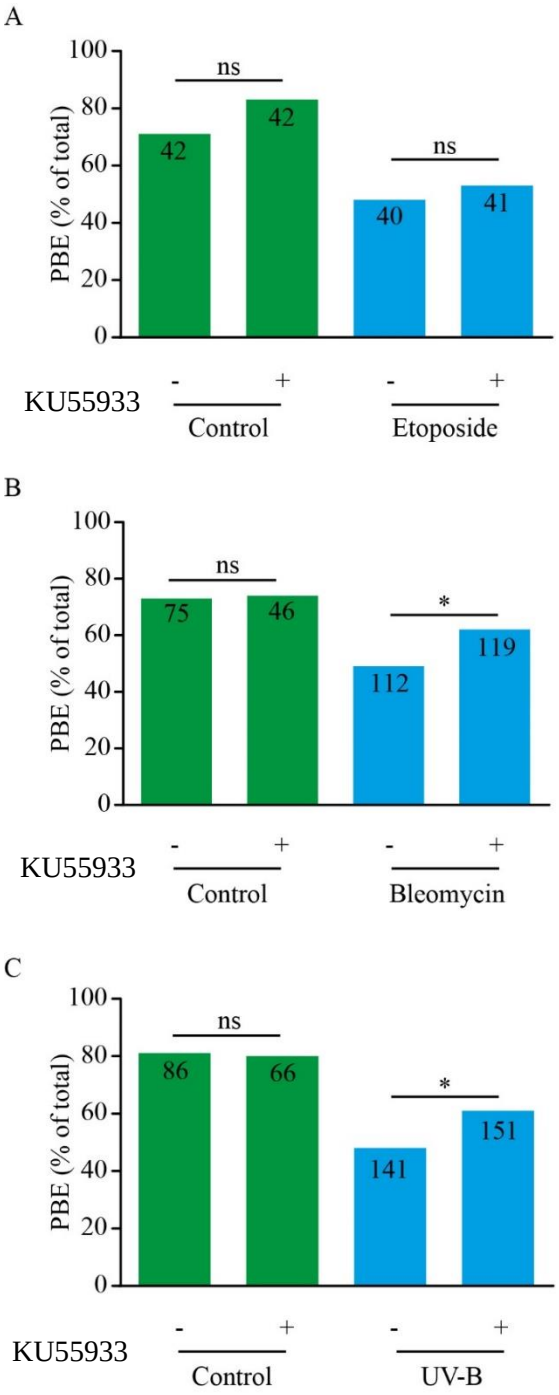

Figure 6-3 The effect of ATM kinase inhibition on PBE in DNA damaged oocytes

40µM KU55933 (Batch 1) was added to M2 media during treatment and throughout IVM. (A) Maturation rates in oocytes treated with control or 25µg/ml Etoposide, in the presence or absence of the ATM inhibitor. (B) Maturation rates in oocytes treated with 1µM Bleomycin, in the presence or absence of the ATM inhibitor.(C) Maturation rates in un-exposed or UV-B treated oocytes, in the presence or absence of the ATM inhibitor. Number of oocytes used stated. Oocytes pooled from 3-4 mice per treatment. *, $P<0.05$ compared to '-KU55933' control or treatment (Fishers Exact test).

Bleo only, Fishers exact test, Figure 6.3B, blue bars). A similar increase was also seen in oocytes exposed to UV-B when KU55933 was added to the media during treatment and IVM (UV-B, 48%, n=141; UV-B+KU55933, 61%, n=151, P=0.03 compared to UVB only, Fishers exact test; Figure 6.3B, blue bars).

To determine if the results were consistent between batches of drug, a second batch of KU55933, was tested (Batch 2). Based on the results in Figure 6.2, I used 40μM KU55933 (Batch 2) during the treatment and maturation of oocytes. In contrast to the results in Figure 6.2, the new batch of KU55933, when used at a concentration of 40μM, had a negative impact on the maturation rates of un-damaged oocytes (Control-KU55933, 85%, n=34; Control+KU55933, 50%, n=42, P=0.0015 compared to control-KU55933, Fishers exact test; Figure 6.4A, green bars). This was also seen in Etoposide treated oocytes where maturation rate was reduced to less than 10% (n =36, P<0.001 compared to Etoposide-KU55933, Fishers exact test, Figure 6.4A; blue bars). As a result of this batch-to-batch variation, I used a lower concentration of 10μM. The lower dose of KU55933 (Batch 2) only had a small effect on maturation rates (85% in –KU55933 to 82% in +KU55933, Figure 6.4B, green bars; 92% in –KU55933 to 74% in +KU55933; Figure 6.4C, green bars). However, rather than the small rescue observed in experiments using Batch 1, maturation rates in Etoposide treated oocytes were reduced further by the presence of the KU55933 (Batch 2) (Etoposide-KU55933, 52%, n=58; Etoposide+KU55933, 19%, n=59, P<0.001 compared to Etoposide-KU55933, Fishers exact test, Figure 6.4B; blue bars). KU55933 (Batch 2) was also tested on oocytes exposed to UV-B. As with Etoposide, maturation rates in UV-B exposed oocytes were further reduced by the presence of KU55933 (Batch 2) (UVB-KU55933, 38%, n= 66; UVB+KU55933, 7%, n=69, P<0.001 compared to UVB-KU55933, Fishers exact test; Figure 6.4C, blue bars).

Due to the opposite effects seen in oocytes treated with Batch 1 and 2 KU55933, a third batch of the inhibitor was tested. I tested the effects of both 10μM and 40μM KU55933 (Batch 3) on un-damaged oocyte maturation to ensure the dose selected did not inhibit PBE. Neither of these doses had a negative impact on the maturation rates of un-damaged oocytes (Figure 6.5). In fact both 10μM and 40μM KU55933 (Batch 3) caused small increases in oocyte maturation, but this increase did not reach statistical significance (0μM, 77%, n=56; 10μM, 80%, n=56, P=0.8183; 40μM, 81%, n=59, P=0.6479 compared to '0', Fishers exact test; Figure 6.5). As a result both 10μM and 40μM was tested on DNA damaged oocytes.

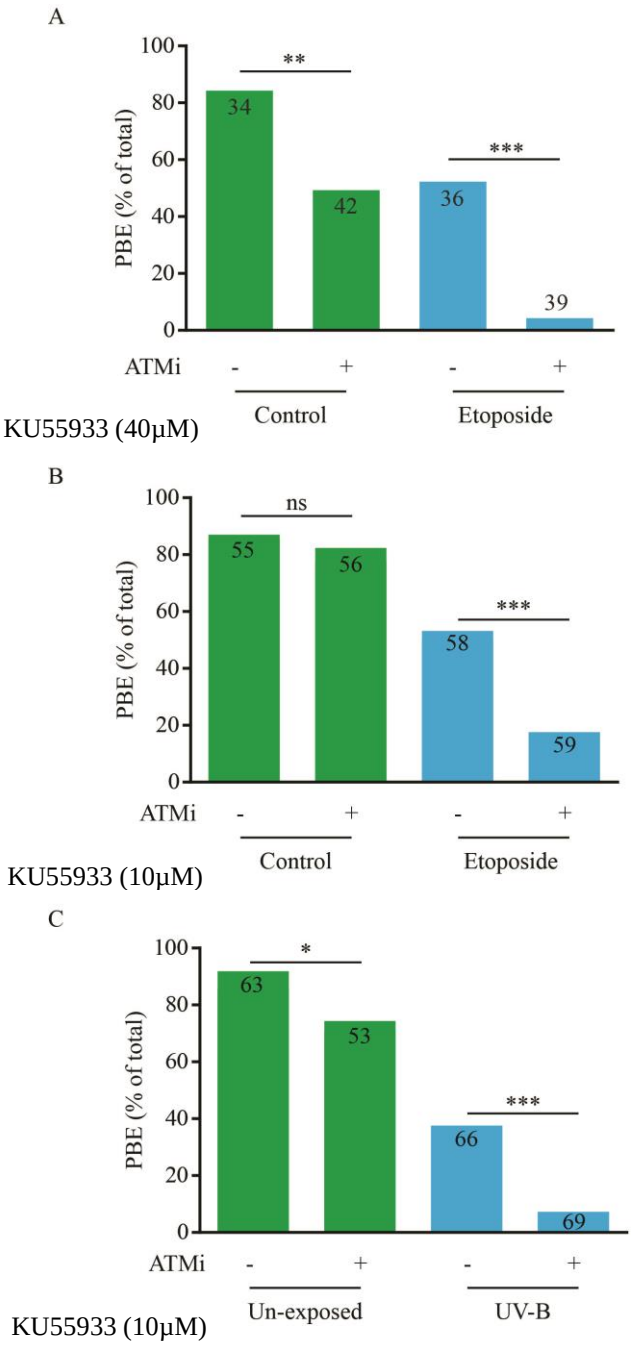

Figure 6-4 The effect of ATM kinase inhibition on PBE in DNA damaged oocytes

A second batch of KU55933 (Batch 2) was used to test for variation between lots. KU55933 was added to M2 media during treatment and IVM as in Figure 6.2 and 6.3. (A) Maturation rates in oocytes treated with vehicle or Etoposide, in the presence or absence of the 40µM ATM inhibitor. (B) Maturation rates in oocytes treated with control or 25µg/ml Etoposide, in the presence or absence of the 10µM ATM inhibitor. (C) Maturation rates in oocytes exposed to 30 seconds of UV-B, in the presence or absence of 10µM KU55933. Number of oocytes used stated. Oocytes pooled from 2-4 mice per treatment. *, $P<0.05$, **, $P<0.01$; ***, $P<0.001$ compared to '-KU55933' control or Etoposide (Fishers Exact test).

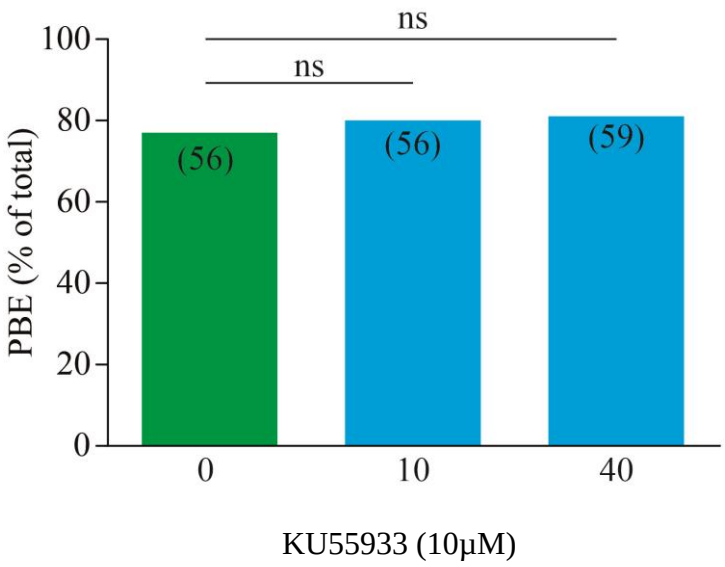

Figure 6-5 The effect of ATM kinase inhibitor on the PBE rates of undamaged oocytes

Maturation rates in oocytes without treatment with DNA damaging agents in the presence or absence of varying concentrations of KU55933 (Batch 3). Number of oocytes used stated. Oocytes pooled from 3 mice per treatment.

In agreement with the results seen using Batch 2, when 10μM KU55933 (Batch 3) was added to the media of oocytes that had been DNA damaged with Etoposide there were further decreases in maturation rates were seen (Figure 6.6). However, this decrease only reached statistical significance when 40μM KU55933 (Batch 3) was used (Etoposide-KU55933, 33%, n=80; Etoposide+ 40μM KU55933, 15%, n=54, P=0.0259 compared to 'Etoposide-KU55933', Fishers exact test; Figure 6.6, blue bars).

In summary, large variation was seen in the maturation rates when three different batches of KU55933 were used, from small amounts of rescue after DNA damage induction in Figure 6.2 and 6.3, to further decreases in PBE seen in Figure 6.4 and Figure 6.6. Therefore, the effect of ATM kinase on maturation rates in oocytes could not be properly assessed using this pharmacological inhibitor but the results suggest that ATM is not essential for the DNA damage induced arrest.

6.2.4 ATM kinase inhibition reduced the signalling of DNA damage

Despite the variable effects of KU55933 on oocyte maturation I wanted to show that the inhibitor was working and investigated whether inhibition of this kinase had any effect on the signalling of DNA damage in oocytes. In Chapter 5, it was thoroughly shown that oocytes can detect and signal DNA damage induced by a variety of agents, through the phosphorylation of H2AX. This post-translational modification is often attributed to ATM kinase, so it could be used to look into ATM activity. To examine the effect of ATM inhibition on H2AX phosphorylation the experimental design shown in Figure 6.1A was used. GV oocytes were fixed after Bleomycin, Etoposide, or UV-B treatment in the presence or absence of KU55933 (batches will be specified). Regardless of the batch used, albeit being used at different doses, KU55933 reduced the level of H2AX phosphorylation after DNA damage had been induced.

Using Batch 1 the effect of ATM inhibition on the phosphorylation of H2AX after Bleomycin treatment was assessed. In control oocytes there was very little visible γH2AX staining, whereas treating oocytes with 1μM Bleomycin led to a visible increase in the presence of γH2AX foci (Figure 6.7A). By adding 40μM KU55933 to the media during treatment caused the γH2AX staining pattern to be similar to that of controls and very few distinguishable foci could be seen (Figure 6.7A). When the mean nuclear γH2AX fluorescence was quantified it was relatively low in control treated oocytes (1750±498 Arb. Units, n=17; Figure 6.7B, green dots), whereas treatment with Bleomycin caused a

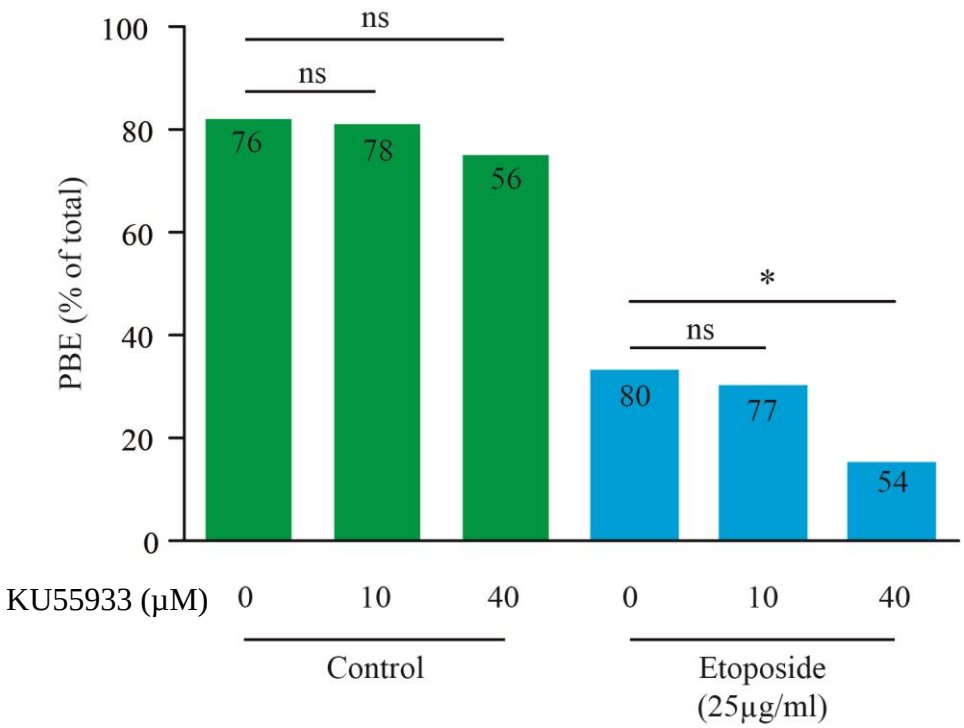

Figure 6-6 The effect of ATM kinase inhibition on PBE in DNA damaged oocytes

A third batch of KU55933 (Batch 3) was used to test for variation between lots. KU55933 (10µM or 40µM) was added to M2 media during treatment and IVM as in Figure 6.2, 6.3, 6.4 and 6.5. Maturation rates in oocytes treated with control or Etoposide, in the presence or absence of 10µM or 40µM ATM inhibitor. Number of oocytes used stated. Oocytes pooled from 4-6 mice per treatment. * $P<0.05$, compared to '-KU55933' control or Etoposide (Fishers Exact test).

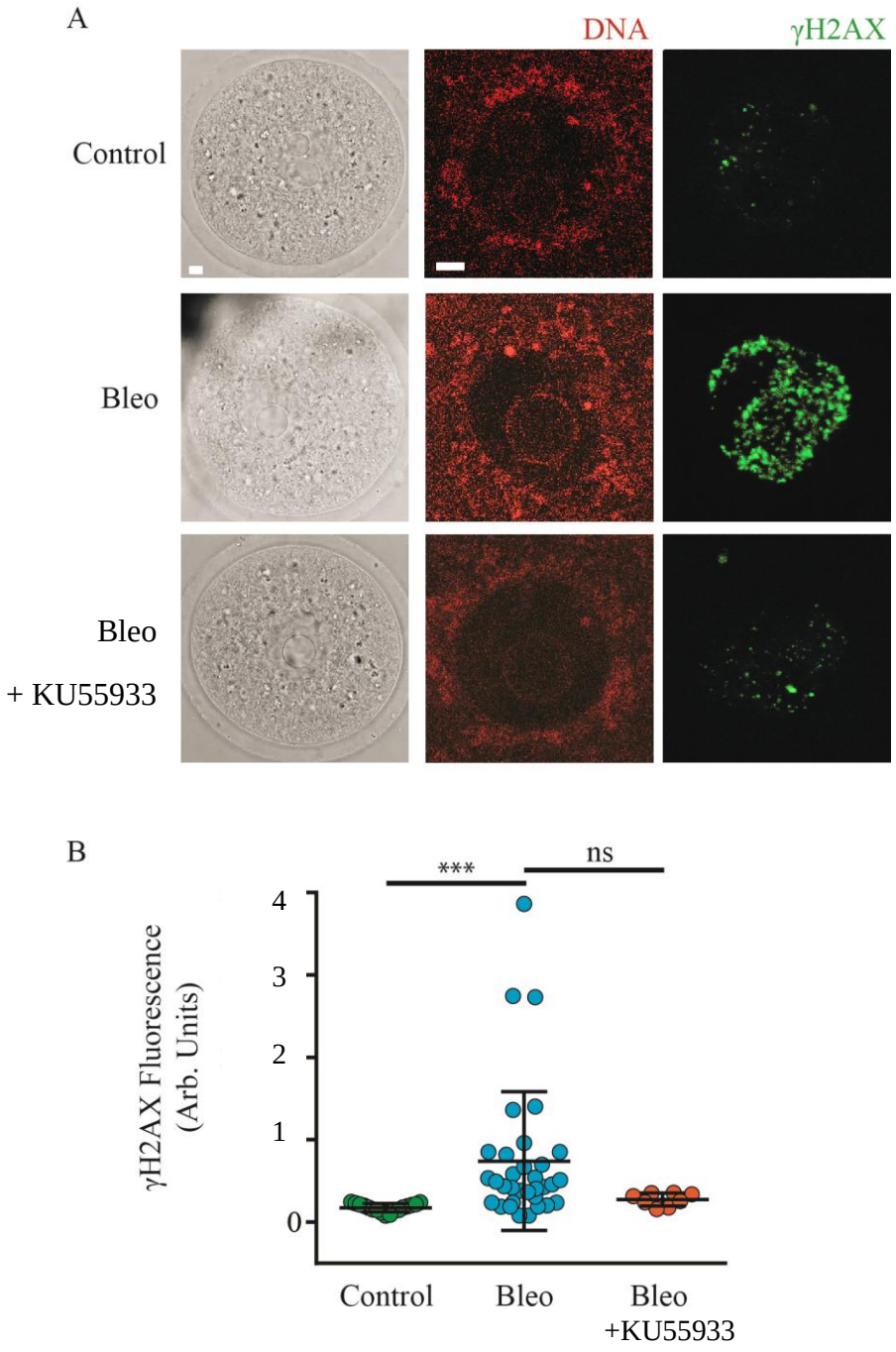

Figure 6-7 The effect of KU55933 (Batch 1) on H2AX levels in Bleomycin treated oocytes

(A) Representative γH2AX immunofluorescence in GV oocytes following control or 1μM Bleomycin in the presence or absence of 40μM KU55933. Oocytes shown here were fixed immediately after treatment. (B) Nuclear γH2AX levels in individual oocytes following either control or 1μM Bleomycin in the presence or absence of 40μM KU55933. Oocytes pooled from 3 mice. Each data point represents a single oocyte; means and s.d are represented by the horizontal lines. *** P<0.001, Kruskal-Wallis with Dunn's post hoc analysis. Scale bar, 5μm.

large increase in the mean nuclear γH2AX fluorescence (7407±8410 Arb.Units, n=33, P<0.001 compared to control, Kruskal-Wallis with Dunn's post hoc analysis; Figure 6.7B, blue dots). By adding 40μM KU55933 to the media during the treatment with Bleomycin the mean nuclear γH2AX fluorescence was greatly reduced, however this did not reach significance (2748±782 Arb.Units, n=8, P>0.05 compared to Bleomycin only, Kruskal-Wallis with Dunn's post hoc analysis; Figure 6.7B, orange dots).

KU55933 (Batch 2) was used on oocytes treated with Etoposide or exposed to UV-B. In vehicle treated oocytes there was very little visible γH2AX staining, whereas treating oocytes with 25μg/ml Etoposide led to a visible increase in the presence of γH2AX foci (Figure 6.8). Interestingly, by adding KU55933 to the media during treatment caused the γH2AX staining pattern to be similar to that of controls and very few distinguishable foci could be seen (Figure 6.8A). When the mean nuclear γH2AX fluorescence was quantified it was relatively low in control oocytes (2676±917 Arb.Units, n=31; Figure 6.8B, green dots), whereas treatment with Etoposide caused a dramatic increase in mean nuclear γH2AX fluorescence (7745±2950 Arb.Units, n=32, P<0.001 compared to control, Kruskal-Wallis with Dunn's post hoc analysis; Figure 6.8B, blue dots). By adding KU55933 to the media during the treatment with Etoposide greatly reduced mean nuclear γH2AX fluorescence (3977±1206 Arb.Units, n=29, P<0.001 compared to Etoposide only, Kruskal-Wallis with Dunn's post hoc analysis; Figure 6.8B, orange dots).

In order to test whether KU55933 affected the level of H2AX phosphorylation in oocytes exposed to UV-B, oocytes were exposed and then kept arrested at the GV stage for 1 hour prior to fixing. This was due to the delayed H2AX phosphorylation that takes place in UV-B exposed oocytes (Chapter 5.2.3). In oocytes that had not been exposed to UV-B there was very little visible γH2AX. However, oocytes exposed to UV-B had a visible increase in γH2AX foci (Figure 6.9A). Adding KU55933 to the media during UV-B exposure and for the 1 hour hold period, caused an alteration in the γH2AX staining pattern; fewer distinguishable foci could be seen (Figure 6.9A). When the mean nuclear γH2AX fluorescence was quantified it was relatively low in unexposed oocytes (3472±1030 Arb.Units, n=40; Figure 6.9B, green dots), whereas exposure to UV-B caused a dramatic increase in mean nuclear γH2AX fluorescence (12856±4382 Arb.Units, n=49, P<0.001 compared to unexposed, Kruskal-Wallis with Dunn's post hoc analysis; Figure 6.9B, blue dots). By adding KU55933 to the media during exposure to UV-B greatly reduced mean nuclear γH2AX fluorescence (8231±2096 Arb.Units, n=48, P<0.001 compared to UV-B only, Kruskal-Wallis with Dunn's post hoc analysis; Figure 6.9B, orange dots).

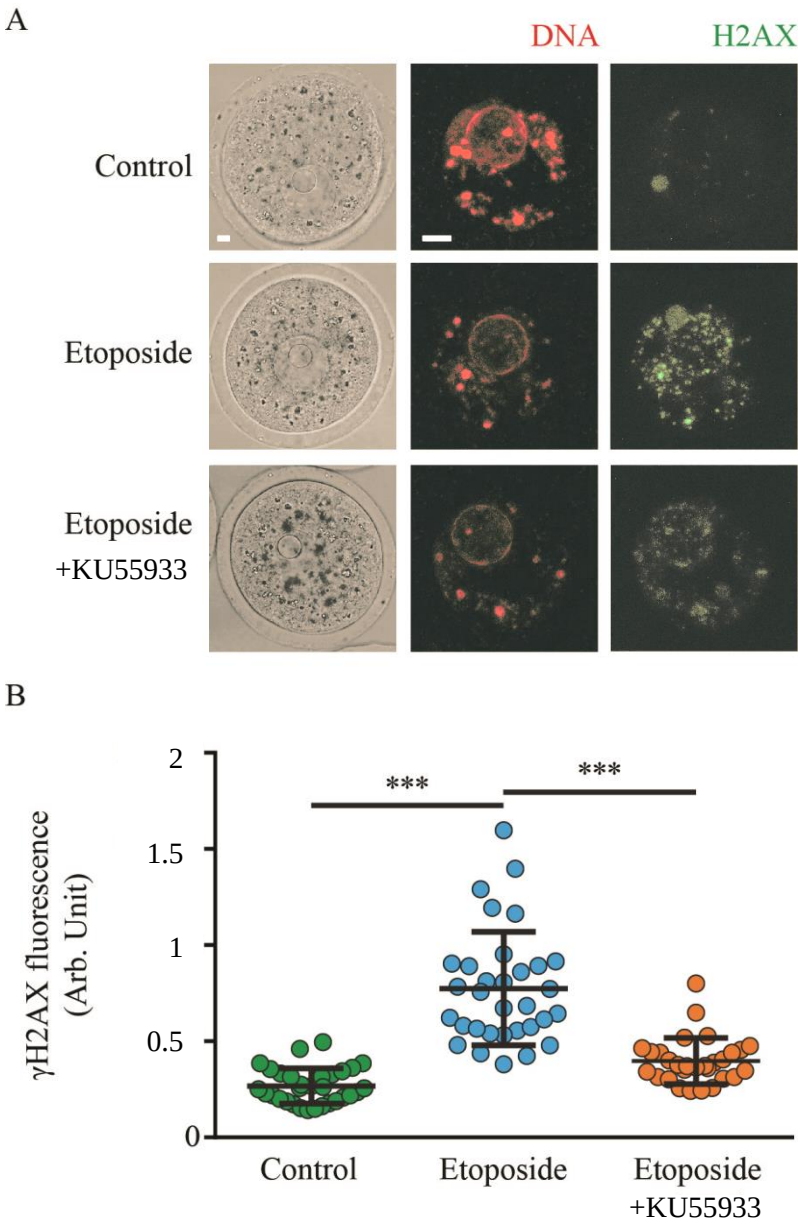

Figure 6-8 The effect of KU55933 (Batch 2) on H2AX levels in Etoposide treated GV oocytes

(A) Representative γH2AX immunofluorescence in GV oocytes following control or 25µg/ml Etoposide in the presence or absence of 10µM KU55933. Oocytes shown here were fixed immediately after treatment. (B) Nuclear γH2AX levels in individual oocytes following either control or 25µg/ml Etoposide in the presence or absence of 10µM KU55933. Oocytes pooled from 4 mice per treatment. Each data point represents a single oocyte; means and s.d are represented by the horizontal lines. *** P<0.001, Kruskal-Wallis with Dunn's post hoc analysis. Scale bar, 5µm.

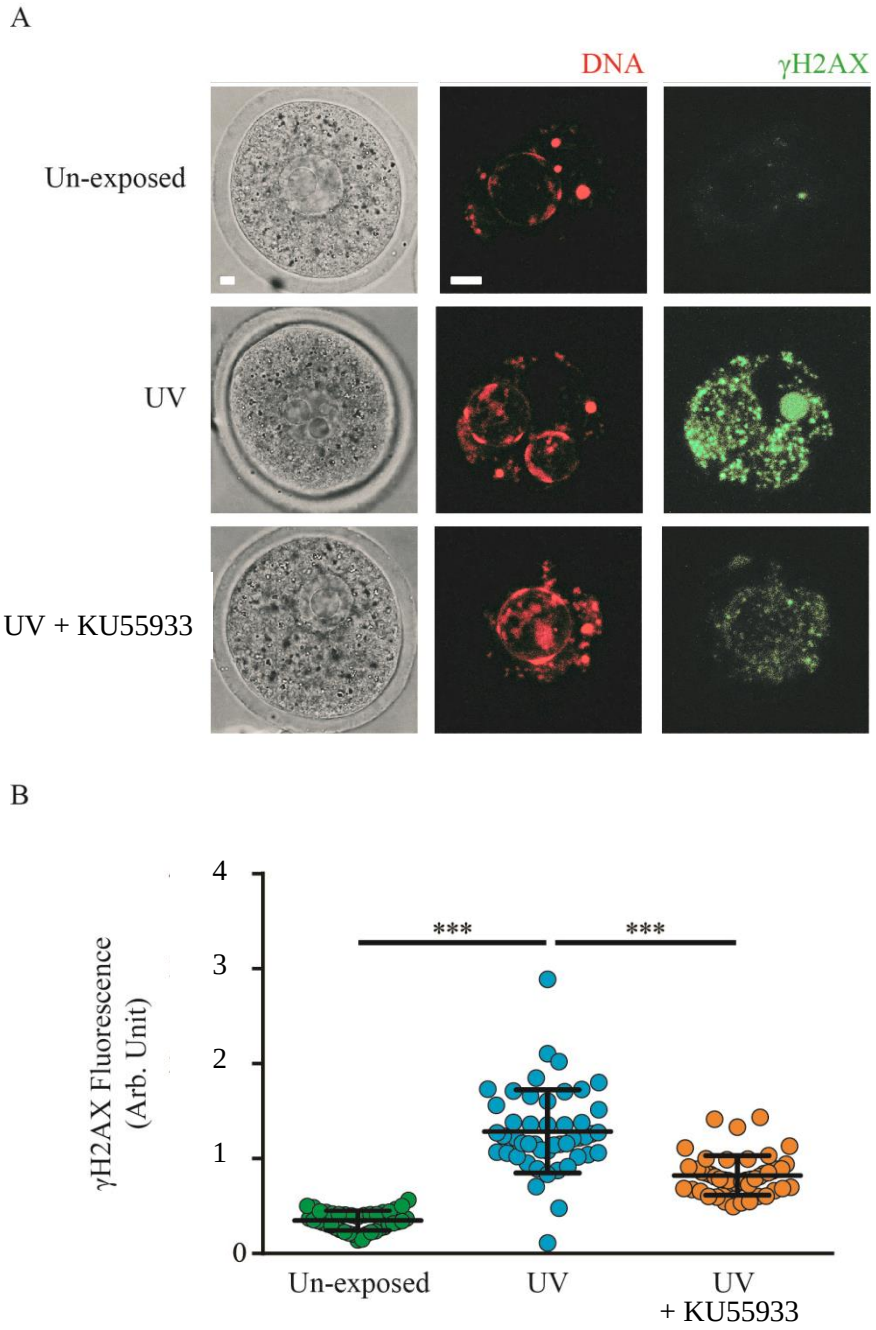

Figure 6-9 The effect of KU55933 (Batch 2) on H2AX levels in GV oocytes exposed to UV-B

(A) Representative γH2AX immunofluorescence in unexposed GV oocytes or those exposed to UV-B (30s) in the presence or absence of 10μM KU55933. Oocytes shown here were fixed 1 hour after treatment. (B) Nuclear γH2AX levels in individual unexposed oocytes or those that were exposed to UV-B in the presence or absence of 10μM KU55933. Oocytes pooled from 4 mice per treatment. Each data point represents a single oocyte; means and s.d are represented by the horizontal lines. *** P<0.001, Kruskal-Wallis with Dunn's post hoc analysis. Scale bar, 5μm.

KU55933 (Batch 3) was used on oocytes treated with Etoposide. To confirm that the inhibitor was working and whether this batch also had an effect on the signalling of DNA damage the γH2AX profile was examined. In un-damaged oocytes there was very little visible γH2AX staining, whereas treating oocytes with 25μg/ml Etoposide led to a visible increase in the presence of γH2AX foci (Figure 6.10A). By adding 10μM or 40μM KU55933 to the media during treatment there was a visible reduction in γH2AX staining (Figure 6.10A). When the mean nuclear γH2AX fluorescence was quantified it was relatively low in control treated oocytes (4083±440 Arb.Units, n=18; Figure 6.10B, green dots), whereas treatment with Etoposide caused a dramatic increase in mean nuclear γH2AX fluorescence (12770±1178 Arb.Units, n=22, $P<0.001$ compared to control, Kruskal-Wallis with Dunn's post hoc analysis; Figure 6.10B, blue dots). By adding 10μM KU55933 to the media during the treatment with Etoposide greatly reduced mean nuclear γH2AX fluorescence (6365±453 Arb.Units, n=22, $P<0.01$ compared to Etoposide only, Kruskal-Wallis with Dunn's post hoc analysis; Figure 6.10B, orange dots). By increasing the concentration of KU55933 used during treatment with Etoposide to 40μM, the mean nuclear γH2AX fluorescence was reduced further (5408±417 Arb.Units, n=18, $P<0.001$ compared to Etoposide only, Kruskal-Wallis with Dunn's post hoc analysis; Figure 6.10B, orange dots).

6.2.5 Pharmacological ATM inhibition causes cytoplasmic abnormalities in oocytes

One effect of treatment with KU55933, regardless of whether DNA damage had been induced or not, was the striking abnormalities it caused within the cytoplasm of the oocytes (Figure 6.11). This effect was also seen regardless of KU55933 batch that was used. Oocytes that had been incubated in the presence of KU55933, that had arrested at metaphase I or II, had developed circular structures that resembled, by size, nucleoli. To investigate what these structures were, oocytes were incubated with Hoechst (1:1000) for 5 minutes and then imaged using the confocal microscope. Interestingly, little or no chromatin was associated with these circular structures suggesting they were not multiple nucleoli. Further study is required to work out what exactly these structures are. The Hoechst staining also revealed that even in the presence of the ATM inhibitor oocytes had segregated their chromosomes, causing chromatin to be present in the polar body and the metaphase II egg (Figure 6.11). Polar bodies produced in the presence of the inhibitor looked similar to those produced in its absence. However, little can be said about the accuracy and fidelity of the first meiotic division in KU55933 treated oocytes. Additional experiments using time-lapse confocal microscopy would be required to do so.

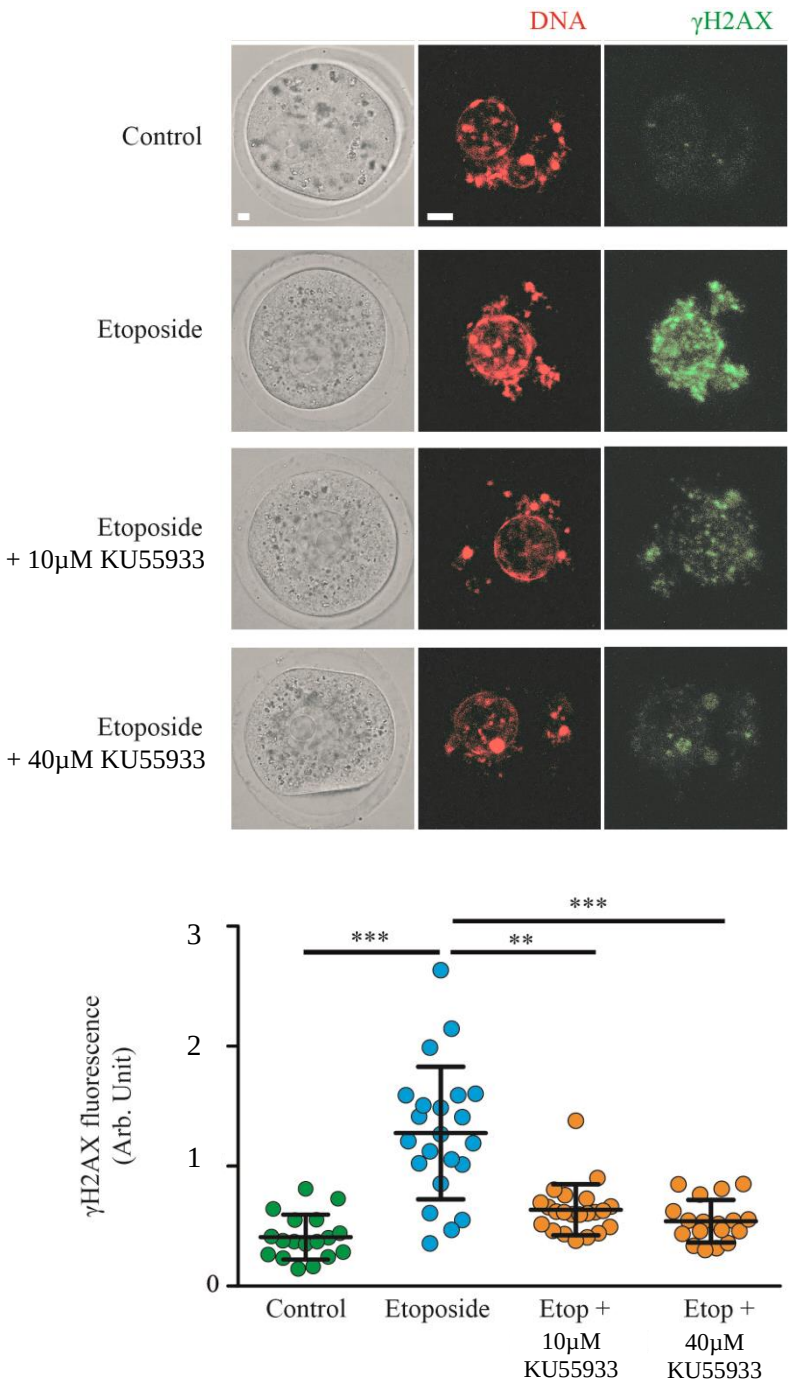

Figure 6-10 The effect of KU55933 (Batch 3) on H2AX levels in Etoposide treated GV oocytes

(A) Representative γH2AX immunofluorescence in GV oocytes following control or 25μg/ml Etoposide in the presence or absence of 10μM/40μM KU55933. Oocytes shown here were fixed immediately after treatment. (B) Nuclear γH2AX levels in individual oocytes following either control or 25μg/ml Etoposide in the presence or absence of 10μM/40μM KU55933. Oocytes pooled from 4 mice per treatment. Each data point represents a single oocyte; means and s.d are represented by the horizontal lines. *** P<0.01, *** P<0.001, Kruskal-Wallis with Dunn's post hoc analysis. Scale bar, 5μm.

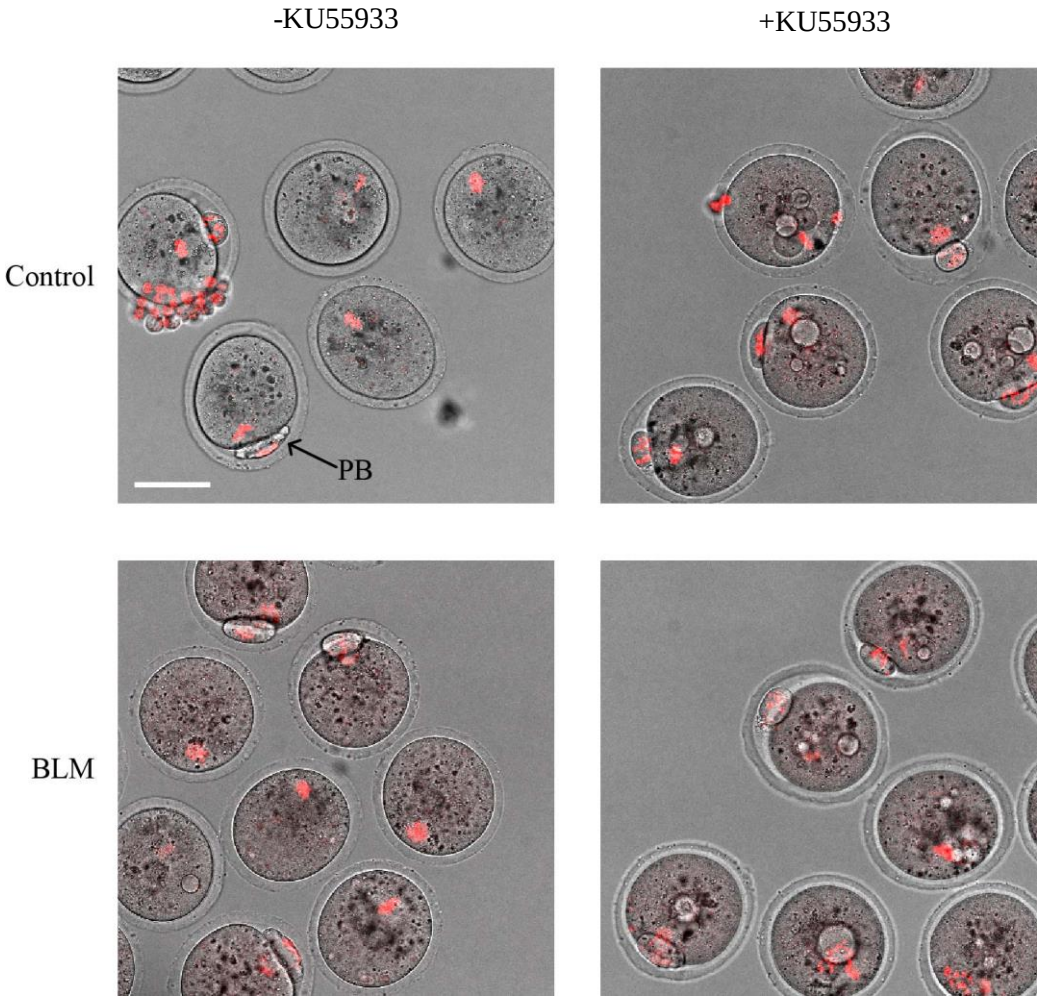

Figure 6-11 Formation of abnormal structures within the cytoplasm of mature oocytes after ATM inhibition

Images of oocytes after a variety of treatments and IVM. Example of metaphase I and II arrested oocytes are shown. Oocytes that had KU55933 in the treatment and IVM media have multiple circular structures within the oocyte cytoplasm. These structures did not appear in oocytes incubated in media without KU55933. Scale bar, 50µm.

6.2.6 ATR kinase inhibition and the oocyte DNA damage response

ATR is another kinase that is important for the DDR in somatic cells and is most commonly associated with the response to UV or replication stress (Chapter 1.3.2). Therefore, to investigate its involvement in the oocyte DNA damage response, a pharmacological inhibitor of ATR, ATR Kinase inhibitor II (ATRi), was added to media during treatment and IVM. To the best of my knowledge this inhibitor has not previously been used during oocyte studies. A dose of 10μM was used based on preliminary experiments carried out during an undergraduate student project (Aikta Sharma, University of Southampton).

6.2.7 ATR inhibition does not rescue polar body extrusion in DNA damaged oocytes

To see whether ATR inhibition would lead to improved maturation rates in DNA damaged oocytes the experimental design shown in Figure 6.1D was used. 10μM ATRi was added to media during treatment and IVM, and PBE was assessed after 16 hours. 10μM ATRi appeared to have no significant effect on the maturation rates in un-damaged oocytes (Control-ATRi, 88%, n=40; Control+ATRi, 80%, n=47, P=0.5601 compared to Control-ATRi, Fishers exact test, Figure 6.12; green bars). When added to the M2 media of oocytes treated with Etoposide a further decrease in PBE was seen (Figure 6.12; blue bars). However, this decrease did not reach significance (Etoposide-ATRi, 60%, n=40; Etoposide+ATRi, 52%, n=48, P=0.5212 compared to Etoposide-ATRi, Fishers exact test, Figure 6.12; blue bars).

6.2.8 ATR inhibition reduced the signalling of DNA damage

To demonstrate that the ATR inhibitor was working and whether it would have any effect on the phosphorylation of H2AX, the experimental design in Figure 6.1B was used. GV oocytes were fixed after either control or Etoposide treatment in the presence or absence of ATRi. γH2AX fluorescence levels were calculated according to Materials and Methods 2.16.1.

In un-treated oocytes there was very little visible γH2AX staining, whereas treating oocytes with 25μg/ml Etoposide led to a visible increase in the presence of γH2AX foci (Figure 6.13). Adding ATRi to the media during Etoposide treatment caused the γH2AX staining pattern to be similar to that of controls and very few distinguishable foci could be seen (Figure 6.13A). When the mean nuclear γH2AX fluorescence was quantified it was

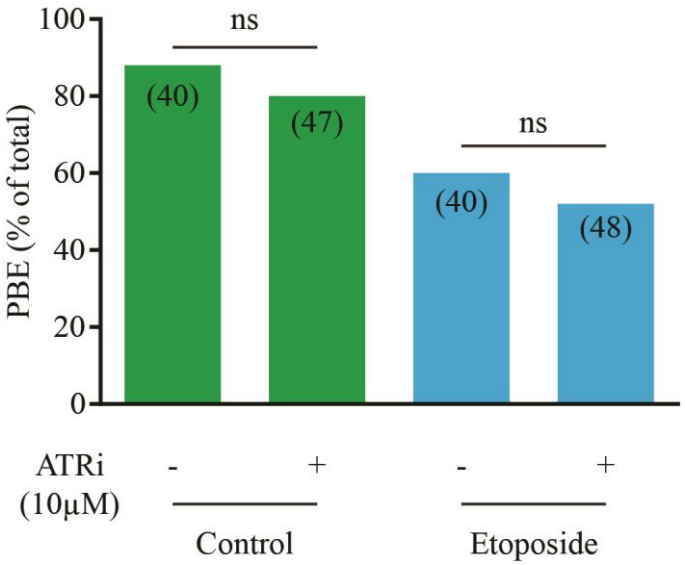

Figure 6-12 The effect of ATR kinase inhibition on PBE in Etoposide treated oocytes

10µM ATRi was added to M2 media during treatment and *in vitro* maturation. Maturation rates displayed for control or 25µg/ml Etoposide treated oocytes. Number of oocytes used stated. Oocytes pooled from 4 mice. ns, compared to '-ATRi' control or Etoposide (Fisher's Exact test).

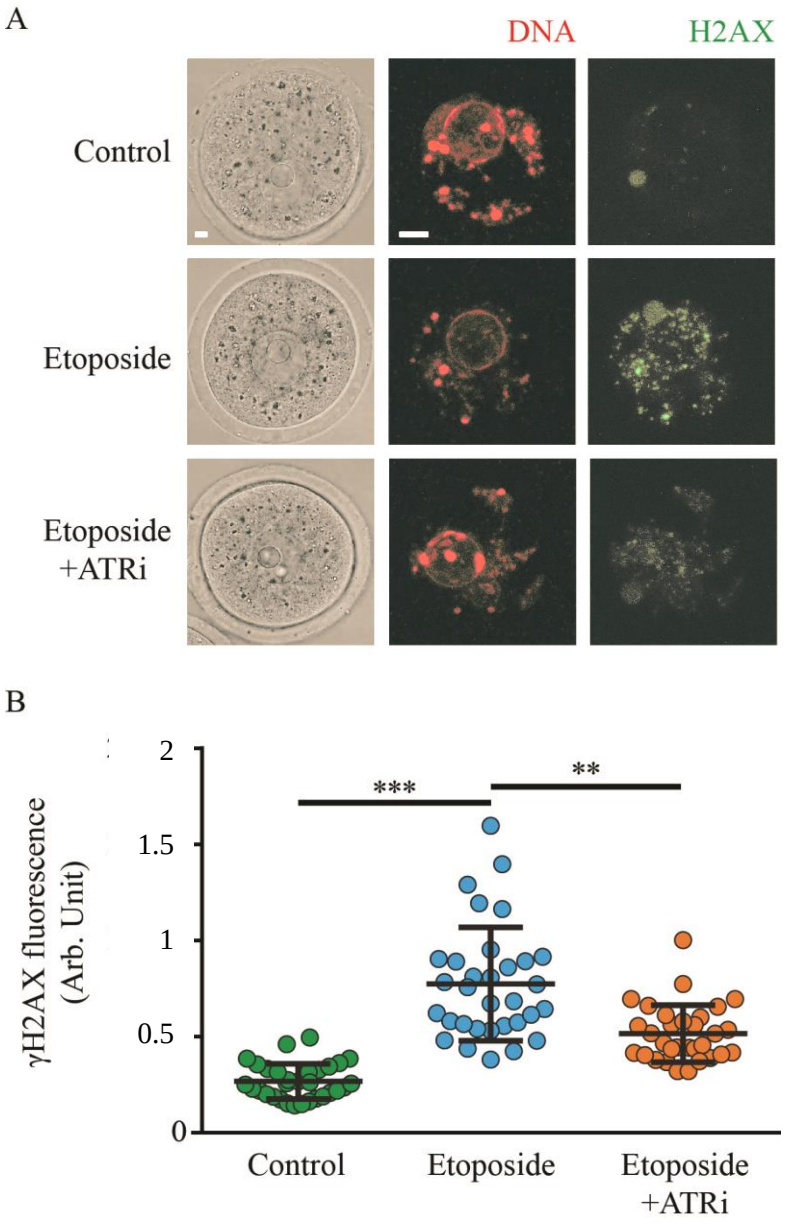

Figure 6-13 ATRi decreases H2AX phosphorylation in Etoposide treated oocytes

(A) Representative γH2AX immunofluorescence in GV oocytes following control or 25µg/ml Etoposide in the presence or absence of 10µM ATRi. Oocytes shown here were fixed immediately after treatment. (B) Nuclear γH2AX levels in individual oocytes following either control or 25µg/ml Etoposide in the presence or absence of 10µM ATRi. Oocytes pooled from 4 mice per treatment. Each data point represents a single oocyte; means and s.d are represented by the horizontal lines. **, P<0.01, ***, P<0.001, Kruskal-Wallis with Dunn's post hoc analysis. Scale bar, 5µm.

relatively low in control treated oocytes (2676±917 arb. Units, n=31; Figure 6.13B, green dots), whereas treatment with Etoposide caused a dramatic increase in mean nuclear γH2AX fluorescence (7745±2950 arb. Units, n=32, P<0.001 compared to control, Kruskal-Wallis with Dunn's post hoc analysis; Figure 6.13B, blue dots). The addition of ATRi to the media during the treatment with Etoposide did cause a reduction in the mean nuclear γH2AX fluorescence (5163±1486 arb. Units, n=31, P<0.01 compared to Etoposide only, Kruskal-Wallis with Dunn's post hoc analysis; Figure 6.13B, orange dots).

6.2.9 Combined inhibition of ATM and ATR

With the individual inhibition of ATM (Batch 2) or ATR not improving the maturation rates of DNA damaged oocytes, it was possible that just inhibiting one kinase could lead to compensation by the other. Therefore, the impact of inhibiting both kinases at the same time was assessed. Both, KU55933 (Batch 2) and ATRi were added to the M2 media during treatment and maturation. KU55933 Batch 2 was used for these experiments as KU55933 (Batch 1) was over 12 months old by the time this experiment was carried out.

6.2.10 Combined inhibition of ATM and ATR does not rescue polar body extrusion in DNA damaged oocytes

To further explore the possibility that inhibiting both ATM and ATR may improve maturation rates in DNA damaged oocytes the experimental design shown Figure 6.1F was used. Both, KU55933 (Batch 2) and ATRi were added to the M2 media during treatment and maturation. PBE was assessed after 16 hours. The concentration used for both inhibitors was 10μM.

10μM KU55933 and ATRi appeared to have no significant effect on the maturation rates in un-damaged oocytes (Control-KU55933-ATRi; 88%, n=42; Control+KU55933+ATRi, 80%, n=59, P=0.2953 compared to Control-KU55933-ATRi, Fishers exact test Figure 6.14; green bars). However, when added to the media of oocytes treated with Etoposide a further decrease in PBE was seen (Figure 6.11; blue bars). This decrease seen in Etoposide treated oocytes did not reach significance (Etoposide-KU55933-ATRi, 37%, n=41; Etoposide+KU55933+ATRi, 30%, n=60, P=0.5225 compared to Etoposide-KU55933-ATRi, Fishers exact test, Figure 6.14; blue bars). Therefore, the inhibition of both ATM and ATR kinase using pharmacological agents, does not rescue PBE in oocytes treated with 25μg/ml Etoposide.

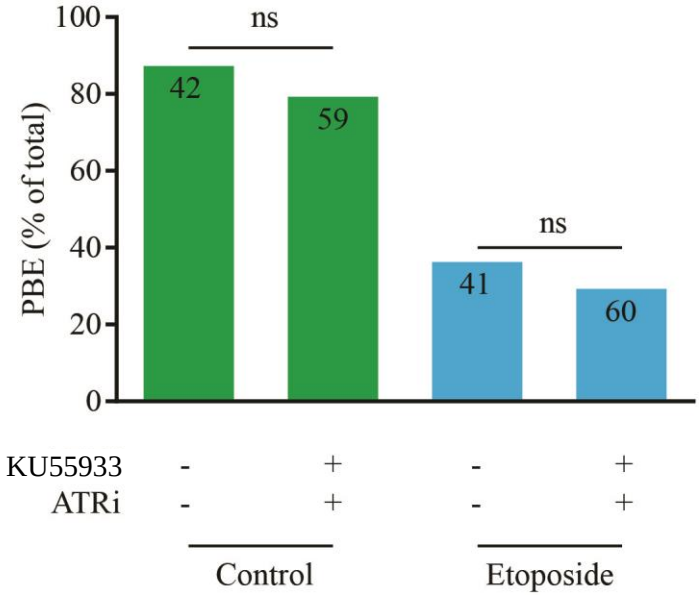

Figure 6-14 The effect of ATM and ATR kinase inhibition on PBE in Etoposide treated oocytes

10μM of KU55933 and ATRi was added to M2 media during treatment and *in vitro* maturation. Maturation rates displayed for control or 25μg/ml Etoposide treated oocytes. Number of oocytes used stated. Oocytes pooled from 4 mice in total. ns, compared to '-KU55933 and -ATRi' control or Etoposide (Fisher's Exact test).

6.2.11 Inhibition of both ATM and ATR decreased the signalling of DNA damage

I had already established that despite having no effect on maturation in DNA damaged oocytes, individually inhibiting either ATM or ATR kinases caused a decrease in the amount of H2AX that was phosphorylated when DNA had been damaged (Figure 6.7, 6.8, 6.9, 6.10 and 6.13). It was possible that inhibiting both proteins could lead to further decreases in γH2AX fluorescence if one was compensating for the other during the individual inhibition experiments. Therefore, I used the experimental design as shown in Figure 6.1E to investigate this. GV oocytes were treated with Etoposide either in the presence or absence of 10 μM KU55933 (Batch 2) and ATRi. They were then fixed and processed for immunofluorescence using the γH2AX antibody. γH2AX fluorescence levels were calculated according to Materials and Methods 2.16.1.

As already mentioned, in non-damaged oocytes there was little γH2AX staining within the nucleus, but this was greatly increased by treating oocytes with Etoposide (Figure 6.15A). Also, when oocytes were treated with Etoposide in the presence of both KU55933 and ATRi the γH2AX staining pattern was not too dissimilar to that of non-damaged oocytes. When this was quantified, the mean nuclear γH2AX fluorescence was relatively low in control treated oocytes (2676±917 arb. Units, n=31; Figure 6.15B, green dots), whereas treatment with Etoposide caused a dramatic increase in mean nuclear γH2AX fluorescence (7745±2950 arb. Units, n=32, $P<0.001$ compared to control, Kruskal-Wallis with Dunn's post hoc analysis; Figure 6.15B, blue dots). By adding both KU55933 and ATRi to the media during the treatment with Etoposide a large reduction in the mean nuclear γH2AX fluorescence was seen (3621±1281 arb. Units, n=28, $P<0.001$ compared to Etoposide only, Kruskal-Wallis with Dunn's post hoc analysis; Figure 6.15B, orange dots). However, this reduction was not different to that seen when oocytes were treated with only KU55933 during Etoposide exposure (Etoposide +KU55933, 3977±1206 arb. Units, n=29; Etoposide +KU55933 +ATRi, 3621±1281 arb. Units, n=28, $P<0.05$ when compared to Etoposide+KU55933, Kruskal-Wallis with Dunn's post hoc analysis).

6.2.12 *Atm-/- Atr-/-* mice

Due to the variability seen when using KU55933, and the lack of improvement in maturation rates when either KU55933 or ATRi were used, I wanted to be able to definitively answer whether ATM or ATR kinase are involved in the oocyte DNA damage response. The best way to ensure that ATM and ATR had been successfully knocked-out

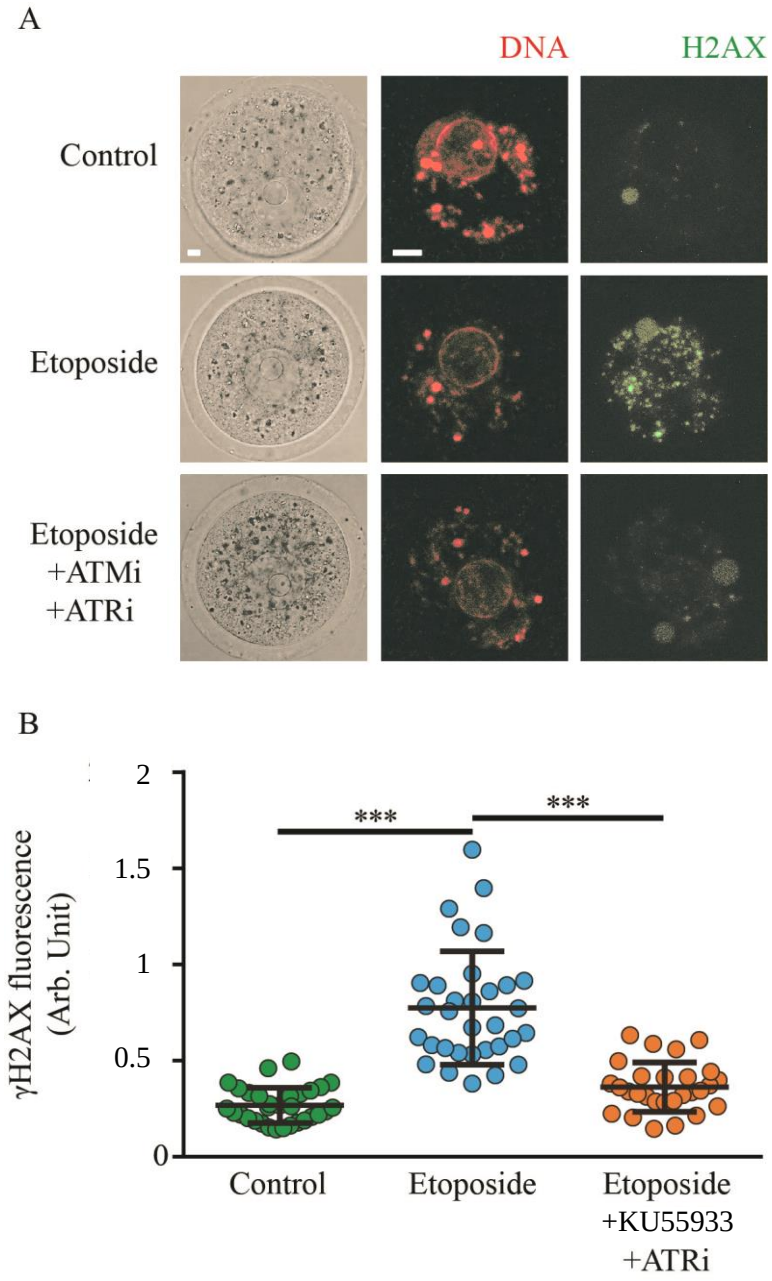

Figure 6-15 Combined KU55933 and ATRi decreases H2AX phosphorylation in Etoposide treated oocytes

(A) Representative γH2AX immunofluorescence in GV oocytes following control or 25μg/ml Etoposide in the presence or absence of 10μM KU55933 and ATRi. Oocytes shown here were fixed immediately after treatment. (B) Nuclear γH2AX levels in individual oocytes following either control or 25μg/ml Etoposide in the presence or absence of 10μM KU55933 and ATRi. Oocytes pooled from 4 mice per treatment. Each data point represents a single oocyte; means and s.d are represented by the horizontal lines. ***, P<0.001, Kruskal-Wallis with Dunn's post hoc analysis. Scale bar, 5μm.

was to use a genetically modified mouse. Therefore, *Atm-/- Atr-/-* mice were used. These were a gift of Dr James Turner (NIMR/Crick Institute London) and were genotyped in his lab. Mice were generated by the floxed deletion of the *Atm* and *Atr* genes driven by the DDX4 promoter.

6.2.13 *Atm-/- Atr-/-* oocytes arrested at MI when treated with Etoposide

To examine the effect of knocking-out the *Atm* and *Atr* genes on the oocyte DDR, the experimental design shown in Figure 6.1G was used. Oocytes were collected from the knockout mice as well as littermate controls. These were treated with either DMSO or 100µg/ml Etoposide to ensure a high arrest rate would be induced in oocytes obtained from littermate control mice.

Oocytes obtained from both littermate controls and the knockouts that were treated with DMSO had high maturation rates as expected (98% and 91% respectively; Figure 6.16, green bars). This result also revealed that ATM and ATR are not required for the progression of meiosis I as knockouts extruded polar bodies. Also as expected, the littermate control oocytes treated with Etoposide had reduced polar body extrusion rates (Etoposide ATM+/+ ATR+/+; 45%, n=31; Figure 6.16, blue bars). Interestingly, the oocytes obtained from the knockout mice had similarly low polar body extrusion rates when treated with Etoposide (Etoposide ATM-/- ATR-/-; 35%, n=31, P=0.6051 compared to Etoposide ATM+/+ ATR+/+, Fishers exact test; Figure 6.16, blue bars). This supports the results using the pharmacological inhibitors (Figure 6.4, 6.6, 6.12 and 6.14) that ATM and ATR kinase are not required for the oocyte response to DNA damage.

6.3 Discussion

In this Chapter, the pharmacological inhibition of ATM and ATR kinase had highly variable effects on maturation in oocytes. Despite this, the use of these inhibitors revealed that ATM and ATR kinases do contribute to the phosphorylation of H2AX after the induction of DNA damage in fully grown GV oocytes. Using oocytes obtained from *Atm-/- Atr-/-* mice, the variability of the pharmacological inhibitors could be avoided. It also highlighted that ATM or ATR are not crucial for the completion of meiosis I or the extrusion of the first polar body in oocytes without DNA damage. This agreed with two out of the three batches of KU55933 tested. These experiments also suggested that it is unlikely that ATM and ATR are the proteins involved in activating the SAC in response to DNA damage.

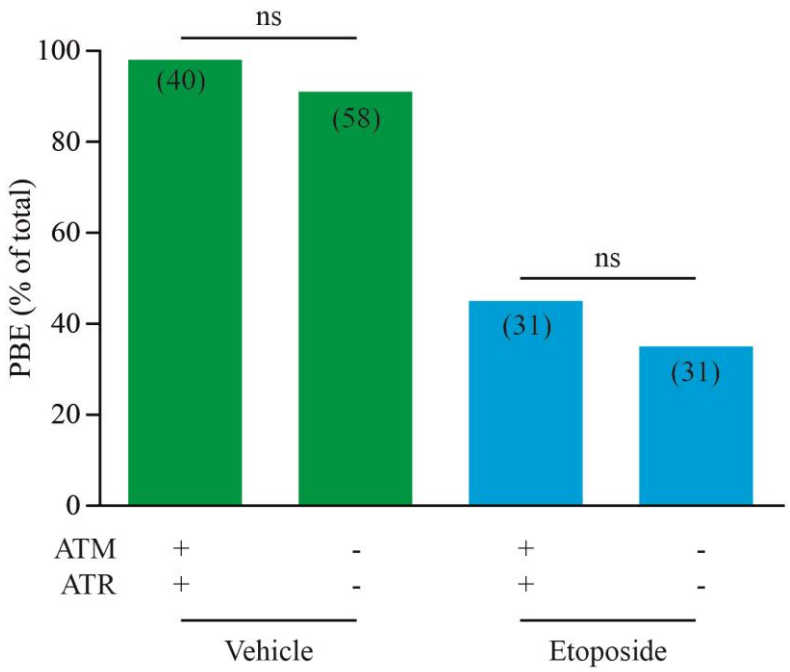

Figure 6-16 Maturation rates in *Atm-/- Atr-/-* oocytes treated with Etoposide

Maturation rates displayed for Control or Etoposide treated oocytes. Oocytes were either obtained from littermate control mice (*Atm+/+ Atr+/+*) or double knockouts (*Atm-/- Atr-/-*). Number of oocytes used stated. Oocytes pooled from between 8-9 mice in total (some mice did not receive PMSG injections). ns, compared to '+KU55933 +ATRi littermate' control or Etoposide (Fisher's Exact test).

6.3.1 ATM and ATR are involved in signalling DNA damage in oocytes

H2AX phosphorylation after DNA damage induction is important for initiating cell cycle arrest and DNA damage repair (Podhorecka et al. 2010). This histone modification is known to be one of the roles of ATM kinase after the induction of DSBs (Burma et al. 2001) and also ATR during oxidative stress or DNA replication aberrations (DeLoughery et al. 2015, Ward and Chen 2001). The role of ATM kinase in phosphorylating H2AX was specifically shown in mouse embryonic fibroblasts (MEFs). The general Phosphoinositide 3-kinase (PI3K) inhibitor, Wortmannin reduced H2AX phosphorylation in IR treated MEFs (Burma et al. 2001). Further to this ATM-/- MEFs treated with IR had near background levels of H2AX phosphorylation and this could be reinstated by ectopic expression of ATM (Burma 2001). The main role of γH2AX in the DDR is for the correct accumulation of other DDR proteins; MDC1 has been shown to bind directly to γH2AX and is also needed for the correct localisation of repair proteins like 53BP1 and NBS1 (Stucki et al. 2005).

ATM is also important in the repair of DSBs and the phosphorylation of H2AX during the induction of programmed DSBs in early prophase I in oocytes (Di Giacomo et al. 2005). More recently ATM has been shown to be involved in the phosphorylation of H2AX in exogenously damaged oocytes from primordial follicles, in both mice and humans (Soleimani et al. 2011). The activation of ATM in these oocytes is known to initiate apoptotic pathways and the loss of the pool of primordial oocytes (see Chapter 1.7.1) (Kerr et al. 2012a, Kim and Suh 2014, Soleimani et al. 2011). High concentrations of Etoposide used to treat GV oocytes has also been shown to activate ATM kinase, and this activation was strongly correlated with the phosphorylation of H2AX (Marangos and Carroll 2012). In agreement with this study I have specifically shown here that ATM and ATR are involved in signalling DNA damage in fully grown GV oocytes through the induction of γH2AX (Figure 6.7, 6.8, 6.9, 6.10, 6.13 and 6.15).

Interestingly, even in the presence of KU55933, ATRi, or a combination of the two, the levels of γH2AX were still higher than in oocytes without DNA damage. This suggests that there may be other kinases responsible and able to signal DNA damage in oocytes. The third kinase most commonly associated with the DDR is DNA-PK. It is known to be involved in DNA repair by NHEJ (see Chapter 1.5.2) (Davidson et al. 2013, Goodwin and Knudsen 2014). It has also been shown to be able to phosphorylate H2AX in a variety of situations (An et al. 2010, Mukherjee et al. 2006). The minimal H2AX phosphorylation that was seen in ATM-/- MEFs could be completely abolished by the addition of

Wortmannin, an inhibitor of ATM and DNA-PK suggesting that DNA-PK is responsible for the low levels of H2AX when ATM is absent. It has also been demonstrated in HeLa cells that have DNA-PK downregulated by siRNA that H2AX is not phosphorylated after IR (An et al. 2010). An et al. (2010) also showed that in ATM deficient cell lines some H2AX phosphorylation occurred after IR, and that this could be prevented by treating the cells with NU7026, a highly specific inhibitor of DNA-PK (Davidson et al. 2013). This could also be the case with the staining pattern seen in KU55933/ATRi treated oocytes where the residual H2AX phosphorylation is due to the activation of DNA-PK. Thus, future work could focus on the involvement of DNA-PK in signalling DNA damage in oocytes. There are now many commercially available inhibitors of this protein that could be used to study its function.

6.3.2 ATM and ATR are not required for the completion of meiosis I

Over the last decade there have been a variety of publications that show interactions between the DDR proteins and cell cycle machinery, with DDR proteins playing a role in SAC activation in cells without DNA damage, and the SAC components being involved in DNA damage checkpoints.

In Drosophila embryos, CHK1 and BUBR1 are both required to delay the metaphase to anaphase transition after exposure to high doses of x-rays (Royou et al. 2005). CHK1 is also required for mitotic spindle checkpoint function after treatment with taxol in avian lymphoma cells. This loss of checkpoint function was associated with a decreased Aurora B kinase activity and perturbations in both the phosphorylation and localisation of BUBR1 (Zachos et al. 2007). A similar situation has also been found in a mammalian cell line (Peddibhotla et al. 2009). Another SAC protein BUB1, has been implicated in the DDR in the HeLa cell line, being involved in H2AX phosphorylation after its initial activation by ATM kinase (Yang et al. 2012).

Other studies have also implicated ATM kinase to be involved in mitosis and more specifically SAC activation. Activated ATM has been shown to localise to the centromeres in mitotic cells and may have roles in regulating tubulin polymerisation (Tritarelli et al. 2004, Zhang et al. 2007). Even in the absence of DNA damage, ATM has been shown to be activated in mitotic cells (Yang et al. 2011). Yang et al. (2011) revealed that ATM is phosphorylated by Aurora-B in mitosis and that ATM is essential for the spindle checkpoint likely through its interactions with BUB1. Various cells lines deficient for ATM have been used to demonstrate that ATM is required for the metaphase arrest usually

initiated by nocodazole and that the response could be rescued by reinstating wild-type ATM (Yang et al. 2011). Cells lacking ATM have also been shown to complete mitosis much quicker than that of cells containing wild-type ATM kinase (Yang et al. 2011, Eliezer et al. 2014), similar to that of oocytes lacking SAC proteins such as MAD2. A novel interplay between DDR proteins, ATM and MDC1, and the SAC has been identified more recently (Eliezer et al. 2014). It is well documented that ATM kinase phosphorylates H2AX flanking DNA double strand breaks (Bakkenist and Kastan 2003, Burma et al. 2001) and this modification allows MDC1 to localise to the site of the damage. It has been reported that ATM also modifies H2AX at mitotic kinetochores and that this leads to the kinetochore localisation of MAD2 and CDC20 after Nocodazole treatment (Eliezer et al. 2014). It has also been suggested that MDC1 is able to interact with the APC in various human cell lines, which was also heightened in response to DNA damage (Coster et al. 2007). The SAC has also been shown to be activated in yeast in an ATM/ATR-dependant manner, which surprisingly occurs independently of the kinetochore where the SAC usually functions (Kim and Burke 2008).

ATM kinase appears to be expressed in porcine oocytes at the GV stage and that the levels of this protein increase from this stage to GVBD, followed by a decrease between metaphase I to metaphase II (Lin and Kim 2015). Also ATM was shown to localise with chromatin or the spindle at all stages of IVM.

Due to the reported interaction of DDR proteins in somatic cell cycle progression, and the expression of ATM in GV oocytes, it was logical to investigate the effect of ATM and ATR knockdown on oocytes without DNA damage. There was lots of variability in results when using the KU55933 to monitor its effects on oocyte maturation. Batch 1 slightly increased maturation rates, which would support the findings that ATM is involved with the metaphase to anaphase transition via the SAC. However, using Batch 2 KU55933 it revealed that the inhibition of this kinase had different effects on maturation at certain concentrations. The large reduction in PBE when 40µM of KU55933 (Batch 2) (Figure 6.4) mirrors the results recently reported in porcine oocytes (Lin and Kim 2015). In their study, Lin and Kim (2015) showed that IVM in the presence of 10µM KU55933 there was no significant effects on the rates of oocytes that underwent both GVBD and PBE (~90% in controls versus ~75% in KU55933 treated oocytes). However, 50µM KU55933 caused large reductions in the percentage of oocytes that underwent GVBD and PBE, from ~90% in controls versus ~50% in oocytes treated with the inhibitor. This suggests that ATM

kinase could be integral for the progression of oocytes from meiosis I to meiosis II. Batch 3 had no significant effect on the maturation rates of undamaged oocytes.

In agreement with Batch 3 KU55933, maturation rates in oocytes obtained from *Atm-/- Atr-/-* mice were no different to that of littermate controls (Figure 6.16). This suggests that the progression through meiosis I and extrusion of the polar body does not require these proteins. The difference in results seen when using KU55933/ATRi compared to the knockouts could be to do with the levels of knockdown possible between the two protocols. Also, it could be possible that the ATM and ATR inhibitors have possible off-target or toxic effects in oocytes. Therefore, these inhibitors should be used with caution in fully grown GV oocytes.

Cells lacking ATM progress through mitosis in an accelerated manner, therefore future work could involve monitoring the kinetics of meiosis I in oocytes lacking these kinases. Also, even though maturation rates in oocytes lacking active ATM or ATR were relatively normal it would be interesting to find out more about the accuracy of the division. In somatic cells lacking ATM high rates of aneuploidy have been reported (Iourov et al. 2009, Shen et al. 2005). Aneuploidy in ATM-/- MEFs was thought to be caused by misaligned chromosomes leading to defects in the metaphase to anaphase transition and cytokinesis (Shen et al. 2005). Also in neuronal cells obtained from the brains of AT patients, a condition known to be caused by a deficiency in ATM, revealed a two-fold increase in aneuploidy compared to sex- and age-matched controls (Iourov et al. 2009). Finally in a variety of human cell lines ATM knockdown caused cells to prematurely undergo anaphase despite having misaligned chromosomes, and that the occurrence of lagging chromosomes was increased. This was suggested to be due to ATM having a role in the activation of BUB1, which is known to phosphorylate H2A to regulate chromosome segregation. Yang et al. (2011) found that in ATM knockdown cells the phosphorylation of H2AX in response to spindle depolymerisation was reduced, further indicating a role of ATM in SAC activation. Taken together, this could suggest that even though oocytes appeared to be able to mature normally the quality of the oocyte may be severely impaired. It would be interesting in future to examine chromosome dynamics in non-damaged oocytes with ATM/ATR knockdown.

6.3.3 Cytoplasmic abnormalities in KU55933 treated oocytes

The presence of cytoplasmic abnormalities in oocytes treated with KU55933 agrees with the possibility that KU55933 may be toxic to fully grown GV oocytes and should be used

with caution. Having ruled out the possibility that the circular structures in KU55933 treated oocytes were multiple nucleoli, there were several other things these structures could be including clusters of organelles, such as smooth endoplasmic reticulum, or vesicles.

Oocytes obtained after ovarian stimulation can present a variety of abnormalities within the ooplasm and it is reasonably well documented in articles concerning IVF and ICSI outcomes. One possibility was that these circular structures were aggregations of smooth endoplasmic reticulum (named smooth endoplasmic reticulum clusters - sERcs). The occurrence of sERcs is reported to be limited to that of MII oocytes and were confirmed to be smooth ER using stains such as ER-Tracker (Otsuki et al. 2004). Some studies have suggested that the presence of sERcs decreased the ability of the oocyte to be fertilised and develop to the blastula stage (Ebner et al. 2008) and severely impaired pregnancy success (Akarsu et al. 2009, Ebner et al. 2008, Otsuki et al. 2004, Wallbutton and Kasraie 2010). It is well known that the smooth ER has a variety of functions; one of these functions includes detoxification (Alberts et al. 2015). One theory could be that KU55933 is toxic to GV oocytes and the ER is working get rid of the substance. If KU55933 is toxic to oocytes maybe this could account for the reduction in PBE seen when concentrations above 10μM were used (Batch 2). However, upon examination of images from the studies mentioned above it was quite clear that the structures displayed in Figure 6.11 do not resemble sERcs.

The structures seen in oocyte cytoplasm after KU55933 treatment appear to look much more like fluid filled vesicle structures (Otsuki et al. 2004). Again vacuoles have been reported as another cytoplasmic abnormality in oocytes obtained for IVF or ICSI treatment (Van Blerkom 1990, Ebner et al. 2005). As with sERcs, the presence of vacuoles in MII oocytes has been shown to correlate with lower fertilisation rates, decreased success in the formation of zygotes and severely impaired blastocyst development (Ebner et al. 2005). Ebner et al. (2005) also report that fertilisation could not occur in oocytes displaying vacuoles with a diameter larger than 14μm. Many of the vesicle structures seen in KU55933 treated oocytes were larger than this cut off size, suggesting the quality of the MII oocytes was low.

Vesicular structures are required for a variety of processes that occur within cells including endocytosis and autophagy. Of particular interest here is autophagy; a process that involves intracellular degradation. It has a variety of roles including during apoptosis, but it has also been shown to be a tactical response to extend the life of a cell under a range of stresses (Yang et al. 2005). An extensive list of proteins involved in autophagy is now known and

this includes the autophagy-related genes and the microtubule associated protein 1 light chain (LC3) (Yang et al. 2005, Noda and Inagaki 2015). These proteins are integral for the formation of the C-shaped double membrane structure in the cytoplasm, for extending this structure, and closing it to form a vacuole called the autophagosome. The autophagosome is then targeted to the lysosome where its' contents can be degraded (Yang et al. 2005).

Another possibility is that these structures are vacuoles involved in autophagy induced by increases in ROS. ATM kinase is also now known to have functions other than in the DDR. One of these roles in is in the regulation of ROS levels (Cosentino et al. 2011, Patel et al. 2011, Lin et al. 2012) and can also be activated by oxidative stress (Z. Guo et al. 2010). Cells lacking ATM, either genetically or by knockdown, display elevated levels of ROS (Barzilai et al. 2002, Lin et al. 2012). Further to this ROS has also been demonstrated to activate autophagy (Scherz-Shouval and Elazar 2011, Lin et al. 2012). More specifically addition of KU55933 to head and neck cancer cell lines increased cytoplasmic vesicles when monitored using LC3 as a marker of autophagy, and that this coincided with elevated levels of ROS (Lin et al. 2012). Further supporting this Lin et al. (2012) showed that antioxidant treatment lowered ROS and LC3 staining. Therefore, it could be that KU55933 treated oocytes have elevated levels of ROS and this induced autophagy.

Either way the presence of cytoplasmic abnormalities in MII oocytes is known to correlate with poor reproductive outcomes as already mentioned, so it would appear the health of oocytes is severely perturbed by the pharmacological inhibitor. One final note is that the vacuoles are not seen in *Atm-/- Atr-/-* oocytes which suggest that it is probably to do with toxicity rather than the inhibition of ATM/ATR.

6.3.4 ATM and ATR are not required for the activation of the oocyte specific DDR

ATM and ATR are well-documented as integral components for initiating a DNA damage checkpoint (See Chapter 1.3.1 and 1.3.2) in response to DSBs and SSBs respectively. These kinases are also necessary for the activation of proteins downstream in the DDR. For instance, ATM is needed for the phosphorylation of CHK2 in response to IR (Matsuoka et al. 2000). Whereas ATR is most commonly associated with the activation of CHK1 in response to UV or replication stress (Liu et al. 2000). It is also now accepted that there is likely to be cross-talk between the two kinases and their substrates for instance, ATM has been shown to be required for the phosphorylation of CHK1 after exposure to IR (Gatei et al. 2003).

ATM is also important in the DNA damage response of oocytes in postnatal primordial follicles, that results in widespread apoptosis (see Chapter 1.7.1). The role ATM kinase plays in this response is that it is required for the phosphorylation of TAp63 in oocytes within primordial follicles (Kim and Suh 2014). Kim and Suh (2014) identified this role by using Wortmannin and KU55933 (both of which inhibit ATM), where they prevent the phosphorylation of TAp63 after ovaries were treated with IR. Also, although fully grown GV oocytes are relatively insensitive to DNA damage, when an arrest is induced by very high exposures to Etoposide, ATM is needed to initiate this arrest (Marangos and Carroll 2012). Also, when an arrest was induced it could be partially rescued using KU55933 (KU55933). As well as this, it was found that ATM induced the activation of CHK1 and in turn this led to the inhibitory phosphorylation of CDC25B, a protein crucial for GVBD (see Chapter 1.6.4).

Therefore the main aim of this chapter was to identify whether ATM or ATR are also required for initiating the DNA damage induced M-phase arrest in oocytes. However, despite being involved in the phosphorylation of H2AX after DNA damage induction, ATM and ATR do not appear to function in the activation of the DNA damage induced metaphase arrest in fully grown oocytes. KU55933 (Batch 2 and 3), ATRi, or a combination of the two failed to improve maturation rates in oocytes with DNA damage (Figure 6.4, 6.6, 6.12 and 6.14). The results were very similar when oocytes lacking ATM or ATR (*Atm-/- Atr-/-*) were exposed to Etoposide (Figure 6.16). This agrees with previously, and very recently, published work where KU55933 did not prevent the mouse oocytes arresting at metaphase I when treated with Doxorubicin (Soleimani et al. 2011) or Etoposide (Marangos et al. 2015). This also compliments the work of Marangos and Carroll (2012) in which they show that the relative insensitivity of fully grown GV oocytes to DNA damage is due to a lack of ATM activation compared to blastomeres and also that oocytes had a lower expression of ATM in general compared to somatic cells.

The lack of rescue seen in oocytes with DNA damage when ATM and ATR are knocked out or inhibited could be due to other DDR proteins compensating for their loss. The third kinase associated with the DDR is DNA-dependant protein kinase (DNA-PK). DNA-PK is a multi-unit protein made up of a catalytic subunit called DNA-PKcs and DNA binding heterodimer of KU70 and KU80 (Davidson et al. 2013, Goodwin and Knudsen 2014). DNA-PK is known to have roles in DNA repair, specifically NHEJ (see Chapter 1.5.2) (Davidson et al. 2013, Goodwin and Knudsen 2014), as well as signalling excessive damage to initiate apoptosis (Mukherjee et al. 2006). As already discussed in section 6.3.1

DNA-PK also functions in phosphorylating H2AX after exposure of various human cell lines to ionising radiation (An et al. 2010). With this wide array of functions and its ability to signal DNA DSBs in the absence of ATM, it could play a role in the oocyte specific M-phase DDR. However, DNA-PK has is also known to have roles outside of the DNA damage response. When observed throughout mitosis it localised to centrosomes and kinetochores (Lee et al. 2011). Also DNA-PK catalytic subunit inhibition causes chromosome alignment issues, suggesting its function is needed for normal cell cycle progression (Lee et al. 2011). This could mean that DNA-PK is also needed for normal meiotic progression, which could make it difficult to untangle its role in the oocyte M-phase DDR.

Another protein that could be involved in the DDR in oocytes is CHK1; a kinase activated after UV, IR and during replication stress (Liu et al. 2000) and can be activated by both ATM (Gatei et al. 2003) and ATR (Liu et al. 2000). As already discussed in section 6.3.2 CHK1 is also implicated to have a role in the spindle assembly checkpoint in avian and mammalian cell lines (Peddibhotla et al. 2009, Zachos et al. 2007). In one paper CHK1 has also been suggested to have roles in meiosis as well (Chen et al. 2012). Chen et al. (2012) showed that CHK1 was expressed at all stages in oocytes, and was localised to the nucleus at the GV stage and to the spindle from pro-metaphase I through to metaphase II. By manipulating the levels of this protein before and after GVBD they showed that CHK1 may be involved in maintaining GV arrest and also in SAC activation. Depleting CHK1 in GV oocytes caused an increased proportion of oocytes to escape prophase arrest despite being held in milrinone (Chen et al. 2012). Also overexpression of CHK1 after GVBD, by microinjecting myc-CHK1 mRNA, decreased PBE by arresting oocytes at metaphase. BUBR1 recruitment to the kinetochore was also amplified implying that CHK1 may have a role in meiotic SAC activation (Chen et al. 2012). Therefore it could be possible that in oocytes with DNA damage, CHK1 is activated and this leads to SAC activation in oocytes.

Finally, although TAp63 is now known to protect against the formation of mature oocytes with DNA damage by inducing apoptosis in oocytes within primordial follicles (See Chapter 1), its expression is diminished in oocytes recruited for ovulation (Suh et al. 2006). There is another member of the p53 family that could possibly have a role in the DNA damage response seen in fully grown GV oocytes; TAp73. TAp73 is suggested to have a variety of roles including tumour suppression, the induction of apoptosis when DNA is damaged, and even embryonic development of the brain (Levrero et al. 2000). Of particular interest is the role of TAp73 in mitotic and meiotic SAC regulation. In a series of

publications from Tomasini et al. TAp73-/- mice were shown to be infertile due to poor oocyte quality, caused by a variety of spindle defects and most likely aneuploidy (Tomasini et al. 2008). Also TAp73 deficient cells were also unable to carry out a normal arrest response when cultured with the spindle depolymerising agent Nocodazole (Tomasini et al. 2008), further supporting that TAp73 has a role in SAC regulation. The role of TAp73 was studied further and they found that in TAp73-/- oocytes the localisation of SAC proteins BUB1 and BUBR1 were diminished. Furthermore, they showed that TAp73 can directly interact with BUBR1 using co-immunoprecipitation experiments and that the kinase activity of BUBR1 was reduced as in the absence of TAp73 (Tomasini et al. 2009). This is particularly interesting as SAC proteins such as BUB1 and BUBR1 are now known to be involved in the oocyte DDR (Marangos et al. 2015). As a final point, TAp73 expression decreases with maternal age in both mice (Guglielmino et al. 2011, Tomasini et al. 2008) and humans (Guglielmino et al. 2011), in addition the DNA damage induced MI arrest is also compromised in oocytes from aged mice (Marangos et al. 2015). Therefore it could be possible that TAp73 is integral to the DDR in fully grown GV oocytes.

Contrary to the predicted rescue, PBE was further reduced when DNA damage had been induced in *Atm*-/- *Atr*-/- oocytes (Figure 6.16) and in oocytes incubated with KU55933 (Batch 2 and 3) and/or ATRi (Figure 6.4, 6.6, 6.12, 6.14). This reduction in maturation success could be due to sensitisation of oocytes to DNA damaging agents. Cells lacking functional ATR (Kinase-dead ATR) are much more sensitive to IR and this was believed to be due to a reduction in the efficiency of HR (Wang et al. 2004) (see Chapter 1.5.1 for HR mechanism). Also various inhibitors of ATM and ATR have been shown to sensitise cancer cell lines to both radio- and chemotherapy agents (Raso et al. 2012, Toulany et al. 2014, Velic et al. 2015, Wardman 2007, Weber and Ryan 2015). Sensitisation is likely due to cells being unable to initiate efficient checkpoints or repair, leading to apoptosis. Therefore, by inhibiting and knocking-out ATM and ATR here in this study, and as a result of this inhibiting repair, could make oocytes more susceptible to undergoing a SAC-mediated arrest. This suggests that caution should be taken when inhibiting major DDR proteins, such as ATM and ATR, in oocytes with DNA damage, because even if the SAC mediated arrest can be overcome, the lack of DNA repair could severely impair the quality of the MII oocytes.

6.3.5 Conclusions

In this Chapter I have shown that ATM and ATR do not appear to be integral for the completion of meiosis I. It has also been highlighted that inhibitors against these two proteins should be used with caution as there was high variability in the results obtained using different batches of KU55933. However, inhibition of ATM and ATR did reduce the level of signalling after DNA damage was induced suggesting that they function in the detection of damage. Despite this the inhibition, or knockout, of the two kinases did not rescue PBE which suggested that they are not involved in activating the SAC after DNA damage or that perhaps other proteins are able to compensate for the action of ATM and ATR. Future work could include investigating the roles of other DDR proteins such as DNA-PK, CHK1 or TAp73.

Chapter 7: General Discussion

The overall aim of my PhD project was to characterise the effect of DNA damage on fully grown GV oocytes (see section 1.10). In Chapter 3 it was of interest to understand how DNA damage affects various stages of oocyte development including the resumption of meiosis and the progression through to meiosis II. Using various agents I have clearly demonstrated that fully grown GV oocytes obtained from C57BL/6 mice do not possess the ability to initiate a G2/M checkpoint, as had been previously demonstrated by Marangos and Carroll (2012). However, it appears that oocytes are able to initiate a unique DNA damage checkpoint during M-phase. Also, this checkpoint can be initiated even when the damage is induced during M-phase. This contrasts to somatic cells where a full DDR or repair mechanisms cannot be initiated during this phase (Figure 7.1). To the best of my knowledge this is the first report to have highlighted an oocyte-specific DNA damage checkpoint shown to be activated in response to various types of DNA damage, both physical (UV and IR) and chemical (Etoposide and Bleomycin).

Why oocytes would not initiate a G2/M checkpoint but instead choose to arrest mid-way through meiosis I is puzzling, but it could be that it gives the oocyte an opportunity to repair the damage without preventing cell cycle entry. To support this, fully grown GV oocytes ready for ovulation express a variety of factors involved in DNA damage repair (Menezo et al. 2007). It has also very recently been suggested that oocytes with levels of DNA damage low enough to permit the MI to MII transition are able to repair the damage during this progression (Mayer et al. 2016). As well as this MII arrested oocytes have been shown to be able to repair both endogenous and exogenous DNA damage (Kujjo et al. 2010), suggesting this may be another opportunity for the oocyte to repair before fertilisation. Thus this oocyte specific checkpoint may be a way of allowing all meiotically competent oocytes to re-enter the cell cycle, but acts as a barrier to those oocytes containing vast amounts of damage. Taken together I feel that the aims of Chapter 3 (Section 1.10.1) were met and has highlighted that the uniqueness of the oocyte stretches much further than just the meiotic cell cycle. Most importantly this finding suggests that there is a mechanism to prevent damaged metaphase II eggs being available for fertilisation that could propagate an embryo with lesions within its DNA. Such embryos could lead to miscarriage or developmental defects (Adriaens et al. 2009, Kirk and Lyon 1982, Meirow et al. 2001). Future work should focus on whether or not this oocyte specific checkpoint translates to the human oocyte.

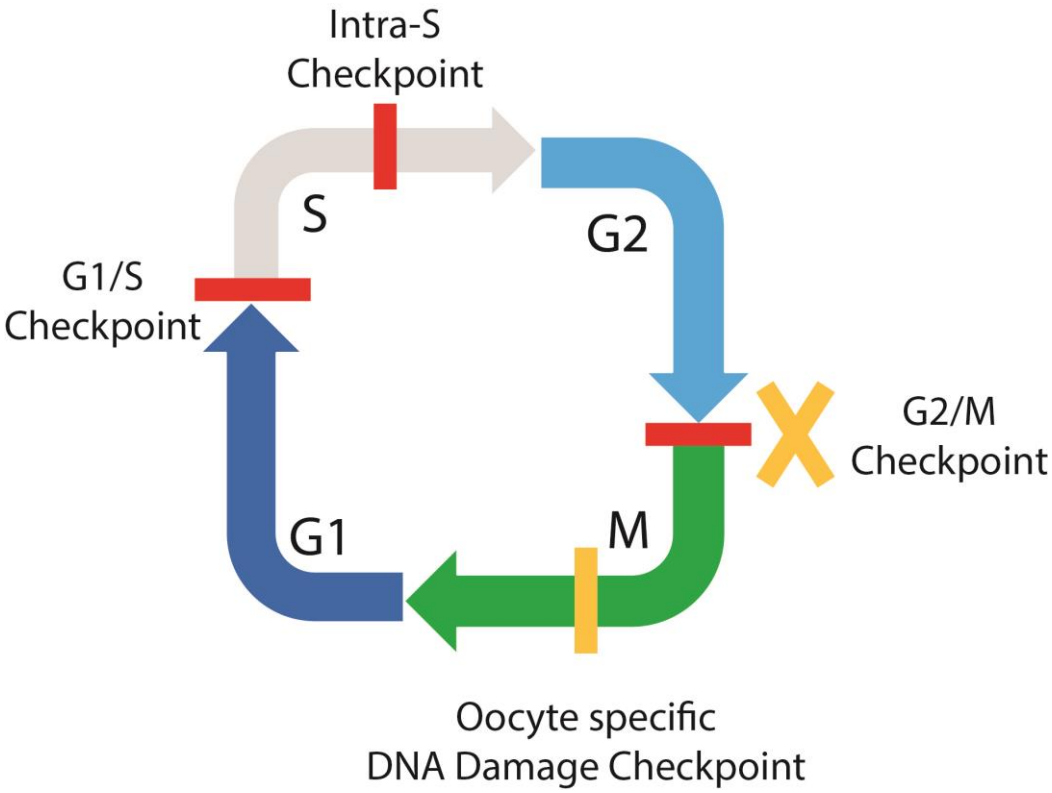

Figure 7-1 Comparison of the DNA damage checkpoints in somatic cells and oocytes

In somatic cells an arrest can be initiated at several points in the cell cycle if DNA damage is detected. This includes at the G1/S transition, during S-phase and at the G2/M transition. However, oocytes cannot initiate a checkpoint at the equivalent G2/M transition but instead have a unique checkpoint during M-phase.

The focus of Chapter 4 was to find out what mechanisms may be involved in the DNA damage induced metaphase I arrest in oocytes. Using a variety of methods I have shown that oocytes arresting at metaphase I after the induction of DNA damage do so in a SAC-dependent manner. Specifically the SAC proteins MAD2 and MPS1 have been shown to be crucial to the oocyte DNA damage response (Figure 7.2). Also, since starting my studies another research group has also highlighted the involvement of BUB1 and potentially BUBR1 in the oocyte DDR (Marangos et al. 2015) (Figure 7.2). The possibility of the SAC simply responding to non-attachment or misalignment was investigated and shown to be an unlikely instigator of the response. The works presented in Chapter 4, alongside more recently published work by another research groups (Marangos et al. 2015), has shown for the first time that the SAC may have a novel and alternative role in oocytes. Overall, I feel that the aims of this Chapter 4 were met and that it has opened a new avenue for research concerning the oocyte spindle assembly checkpoint. Future work needs to specifically address how DNA damage leads to SAC activation.

The involvement of canonical DDR proteins in the oocyte specific response to DNA damage was investigated in Chapter 6. The aim of this chapter was to show if proteins such as ATM or ATR kinase are required for the arrest. Several approaches were taken, including pharmacological inhibition and genetic knockdown. Both methods revealed that these kinases are not integral to inducing the arrest but their knockdown does impact the phosphorylation of H2AX and thus the detection of DNA damage. There were some limitations of using pharmacological inhibitors including batch to batch variability, but this was overcome by using the oocyte specific *Atm/Atr* knockout. In fact the knockout mice supported the overall findings of the inhibitors; that the DNA damage induced arrest doesn't require ATM or ATR (Figure 7.2), and that in the absence of these proteins oocytes may be further sensitised to DNA damage. Therefore, future work will need to focus on alternative proteins that could mediate the DNA damage induced arrest including CHK1, TAp73 and DNA-PK (Figure 7.2).

The aim of Chapter 5 was to establish whether fully grown GV oocytes are capable of detecting and carrying out the repair of exogenously induced DNA damage (Section 1.10). This notion seemed highly likely due to the expression of repair factors in oocytes at a variety of stages throughout maturation, alongside the ability to repair programmed DSBs (see Chapter 1.8). Indeed I have thoroughly shown that oocytes were able to detect and highlight the areas of DNA damage through the phosphorylation of H2AX. This

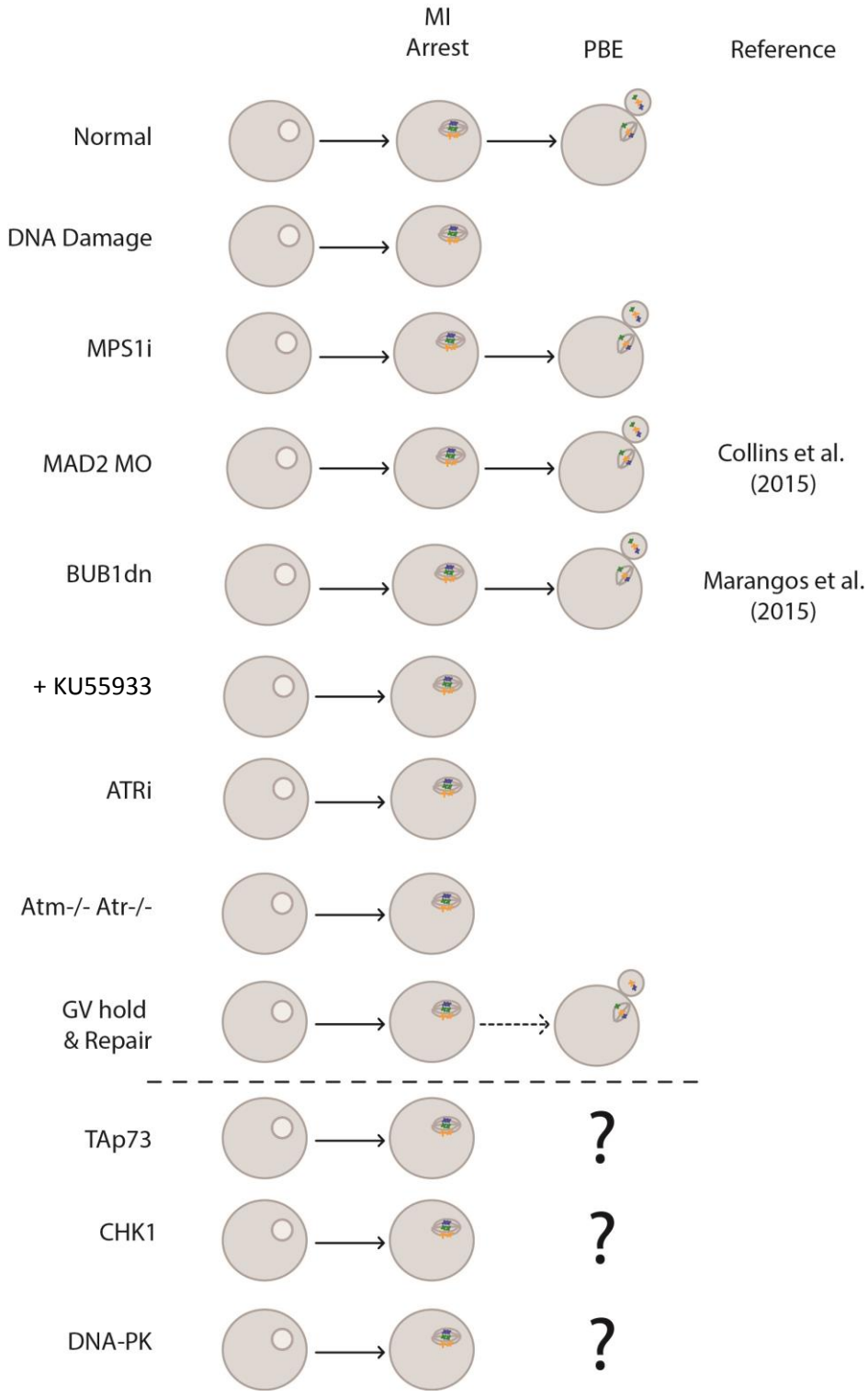

Figure 7-2 Summary of the DNA Damage Response in oocytes

Over the period of my PhD studies numerous proteins have been shown to be involved in the oocyte DNA damage response including MAD2, MSPS1 and BUB1. Unusually ATM and ATR, the major DDR proteins in somatic cells do not appear to mediate this arrest. Allowing oocytes a period of repair, after damage induction, whilst GV arrested allows for small improvements in maturation rate, which is depicted by the dashed arrow.

phosphorylation was carried out rapidly as the modification was detected immediately after treatment in oocytes treated with Etoposide, Bleomycin and IR. However, the delay in the formation of γH2AX foci in UV-B treated oocytes suggests that either the formation of DSBs after UV exposure is slow, or that γH2AX does not simply mark the site of a DSB but also other types of lesion. This will require more investigation in the future. I have also clearly demonstrated for the first time that oocytes can repair DNA damage induced by Etoposide and UV-B albeit with differing kinetics. This repair has also been shown to subtly improve maturation rates of DNA damaged oocytes (Figure 7.2), which to the best of my knowledge is the first report to do so. This finding is exciting as it may provide a way of improving and prolonging female fertility during both ageing and during the treatment of cancer. Focusing on the repair ability of oocytes would be the more favourable pathway to enhance, as knocking out the SAC or DDR signalling to bypass the arrest may still produce oocytes with DNA damage. This would increase the possibility of creating an embryo with DNA damage.

Taking into account the discoveries presented in this thesis a new model of how DNA damage causes a metaphase arrest in oocytes is presented in Figure 7.3. It is now clear that although ATM and ATR do not appear to be involved in activating the SAC after DNA damage induction, they do induce the signalling of the damage by phosphorylating H2AX.

It is also now clear that downstream of DNA damage induction several components of the SAC are required for the metaphase arrest including MPS1, MAD2 (Collins et al 2015), and BUB1 (Marangos et al 2015). As well as this it has been shown that the APC is inhibited during this times and this has been shown to be the main event in causing the arrest.

What remains unknown is the exact pathway that leads to SAC activation after DNA damage induction. There are several candidate proteins that could be involved in this signalling; CHK1, TAp73 and DNA-PK are all known to have roles in oocyte SAC regulation as well as being recognised DDR proteins. I hypothesise that one or several of these proteins is required for DNA damage induced SAC activation. Whether they are activated via ATM/ATR or by DNA damage directly remains to be seen.

Another important area is that of DNA damage repair. I hypothesise that the induction of γH2AX after exposure to DNA damaging agents leads to the activation of DNA damage repair proteins such as RAD51. If this is the case, it could be possible that upregulating

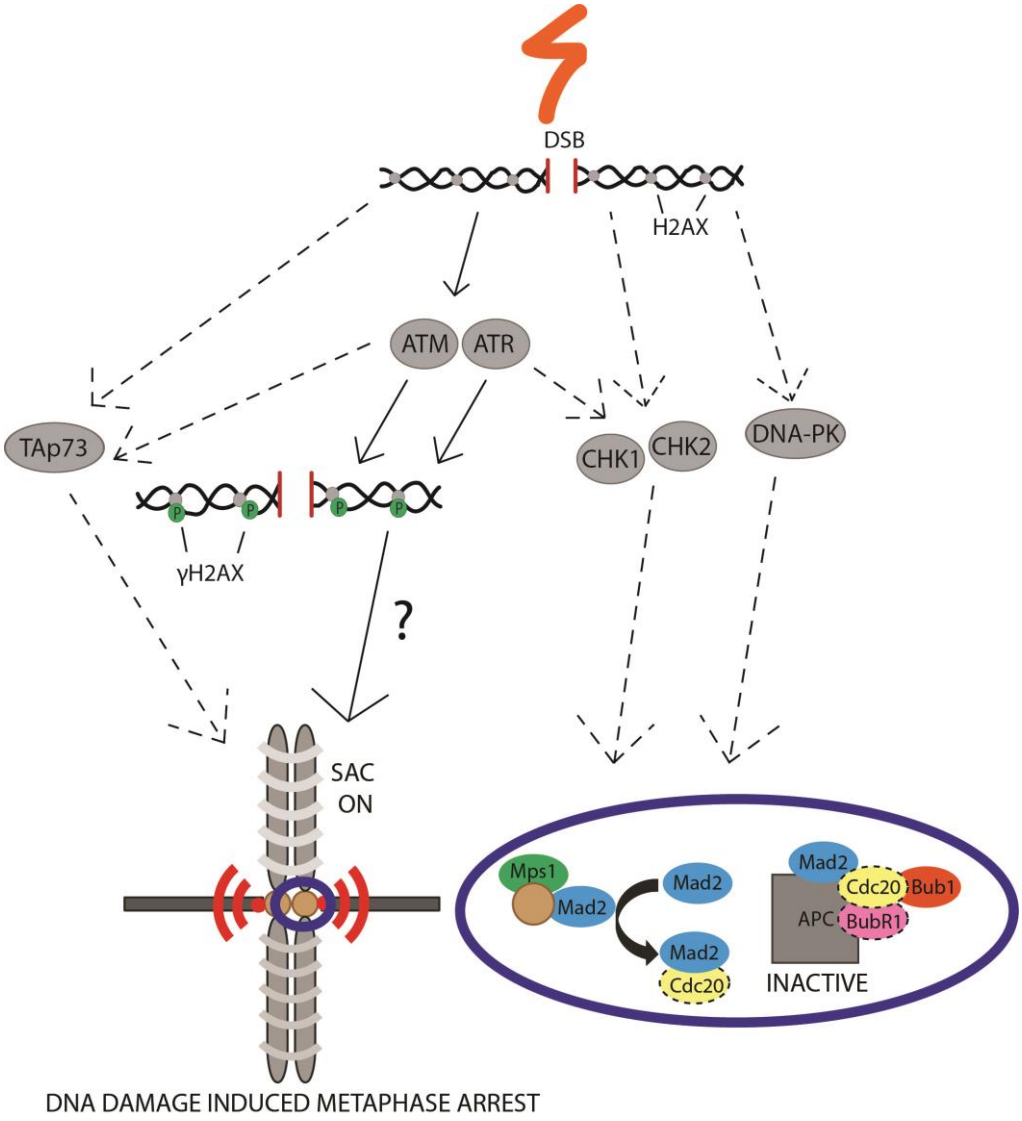

Figure 7-3 Pathways involved in the activation of the SAC after DNA damage induction in oocytes

After DNA damage is induced in oocytes ATM and ATR appeared to signal DNA damage through the phosphorylation of H2AX. This was prevented by pharmacological inhibitors of ATM (KU55933) and ATR (ATR Inhibitor II). However, these inhibitors did not allow for the metaphase arrest to be bypassed suggesting the kinases are not essential for the response. The dashed lines in this figure represent predicted proteins that could be involved in the activation of the SAC after DNA damage induction, including TAp73, CHK1/CHK2 and DNA-PK.

such proteins could increase rates of DNA repair and improve maturation rates in oocytes with DNA damage.

Appendix A Published works contained in this thesis

One publication was used in this thesis. My contributions to these publications are outlined below.

Collins, J. K., Lane, S. I. R., Merriman, J. A. and Jones, K. T. (2015) 'DNA damage induces a meiotic arrest in mouse oocytes mediated by the spindle assembly checkpoint', Nat Commun, 6.

This publication was published in November 2015 and corresponds to much of the work presented in Chapter 3 and 4 of this thesis. JC planned, carried out the experiments, statistically analysed and made figures for the data presented in the following figures: Figure 1a-c, Figure 2b-g, Figure 3a-c, Figure 4a-d, Figure 7a,c, Figure 8a,b and Supplementary Figure 1, as well as their corresponding figure legends. JC also contributed by writing the materials and methods, discussing the content of the results and discussion with the other authors of this paper and took part in the proof reading process. SL was responsible for the data presented in the remaining figures including the data collection, analysis and figure preparation. K.J. devised the study and was responsible for coordinating the research. All authors contributed to data interpretation. The manuscript was drafted by K.J., with input from all other authors.

Josie Kate Collins, Candidate Prof. Keith Jones, Principal Supervisor

Appendix B

B.1 Media

B.1.1 M2 Media

M2 media was made from several stock solutions. All volumetric flasks were cleaned by rinsing with distilled water and dried overnight in the oven.

Stock A was made every 3 months. The components in Table 7 were made in a beaker in 50ml of Fresenius water and then poured into a volumetric flask. More Fresenius water was added to make up to 100ml.

Table 7. Stock A

Chemical	g/100ml
NaCl	5.534
KCl	0.356
KH_2PO_4	0.162
$MgSO_4.7H_2O$	0.293
Na Lactate (60% syrup)	4.349
Glucose	1.000
Penicillin G	0.060
Streptomycin	0.050

Stock B was made every 2 weeks. The components in Table 8 were dissolved into 100ml of Fresenius water.

Table 8. Stock B

Chemical	g/100ml
$NaHCO_3$	2.101
Phenol Red	0.010

Stock C was also made every 2 weeks. The components in Table 9 were dissolved into 10ml of Fresenius water.

Table 9. Stock C

Chemical	g/10ml
Sodium Pyruvate	0.036

Stock D and E were made every 3 months. The components in Table 10 and Table 11 were dissolved into 100ml of Fresenius water. Stock E was made up to 50ml in a beaker and the pH adjusted to 7.6 with 1M KOH. It was then made up to 100ml in a volumetric flask.

Table 10. Stock D

Chemical	g/100ml
$CaCl_2.2H_2O$	2.52

Table 11. Stock E

Chemical	g/100ml
Hepes	5.958
Phenol Red	0.010

All stock solutions were filter sterilised into 50ml falcon tubes and kept in the fridge parafilmed.

M2 was then made up from these stock solutions according to Table 12. Osmolarity was measured to ensure it measured at 283-289. 4mg/ml of bovine serum albumin (BSA) was added and allowed to dissolve. Finally the M2 was filter sterilised into a new falcon tube and stored in the fridge at 4°c.

Table 12. Making M2 media from stock solutions

	Volume required (ml)
Stock A	5.0
Stock B	0.8
Stock C	0.5
Stock D	0.5
Stock E	4.2
Fresenius H_2O	39.0

B.1.2 MEM Media

MEM was made up fresh at least every two weeks. The MEM powder was dissolved in 900ml of Fresenius water. Then 2.2g of $NaCO_3$ was added and the pH was adjusted to 7.4. The volume was then made up to 1 litre using Fresenius water. The MEM media was stored in the fridge at 4°C until required. When needed PenStrep solution (1:200 – Life Technologies, UK) and 20% Fetal bovine serum (Life Technologies, UK) was added to the MEM. Following this the media was filter sterilised.

B.2 Buffers and Solutions

X25 PVP

Polyvinylpyrrolidone 2.5g

Dissolve in 10ml of ddH_2O.

X1 PVP-PBS

X25 PVP 1ml

PBS 24ml

1% Triton X-100

Triton X-100 0.1ml

ddH2O 9.9ml

1% Tween-20

Tween-20	0.1ml
ddH2O	9.9ml

0.05% Tween-20

1% Tween-20	1µl
ddH2O	19µl

0.5M PIPES

PIPES	3.024g

Dissolve in 10ml KOH, pH to 7, top up to 20ml with ddH2O.

0.8M HEPES

HEPES	1.906g

Dissolve in 5ml KOH, pH to 7, top up to 10ml with ddH2O.

0.1M EGTA

EGTA	0.761g

Dissolved in 10ml KOH, pH to 7, top up to 20ml with ddH20.

X3 PHEM

0.5M PIPES	3.600ml
0.8M HEPES	0.770ml
0.1M EGTA	3.000ml
0.8M MgCl2	0.075ml
ddH2O	2.555ml

X1 PHEM

X3 PHEM	1ml
ddH2O	2ml

Fixing Solution

X1 PHEM	190µl
1% Triton X-100	10µl
37% Paraformaldehyde	10.81µl

Scale up as required.

Permeabilisation Solution

X1 PVP-PBS	190µl
1% Triton X-100	10µl

Scale up as required.

Blocking Solution

PBS	880µl
Goat serum	70µl
1% Tween-20	50µl

Washing Solution

PBS	20ml
Bovine serum albumin	0.1g
0.05% Tween-20	1µl

References

Abrieu, A., Magnaghi-Jaulin, L., Kahana, J. A., Peter, M., Castro, A., Vigneron, S., Lorca, T., Cleveland, D. W. and Labbé, J.-C. (2001) 'Mps1 Is a Kinetochore-Associated Kinase Essential for the Vertebrate Mitotic Checkpoint', *Cell*, 106(1), 83-93.

Acevedo, J., Yan, S. and Michael, W. M. (2016) 'Direct Binding to RPA-Coated ssDNA Allows Recruitment of the ATR Activator TopBP1 to Sites of DNA Damage', *Journal of Biological Chemistry*.

Adriaens, I., Smitz, J. and Jacquet, P. (2009) 'The current knowledge on radiosensitivity of ovarian follicle development stages', *Human Reproduction Update*, 15(3), 359-77.

Ahn, J. Y., Li, X., Davis, H. L. and Canman, C. E. (2002) 'Phosphorylation of threonine 68 promotes oligomerization and autophosphorylation of the Chk2 protein kinase via the forkhead-associated domain', *The Journal of Biological Chemistry*, 277(22), 19389-95.

Ahn, J. Y., Schwarz, J. K., Piwnica-Worms, H. and Canman, C. E. (2000) 'Threonine 68 phosphorylation by ataxia telangiectasia mutated is required for efficient activation of Chk2 in response to ionizing radiation', *Cancer Research*, 60(21), 5934-6.

Ahnesorg, P., Smith, P. and Jackson, S. P. (2006) 'XLF interacts with the XRCC4-DNA ligase IV complex to promote DNA nonhomologous end-joining', *Cell*, 124(2), 301-13.

Akarsu, C., Caglar, G., Vicdan, K., Sozen, E. and Biberoglu, K. (2009) 'Smooth endoplasmic reticulum aggregations in all retrieved oocytes causing recurrent multiple anomalies: case report', *Fertility and Sterility*, 92(4), 1496 e1-3.

Alberts, B., Johnson, A., Lewis, J., Morgan, D., Raff, M., Roberts, K. and Walter, P. (2015) *Molecular Biology of the Cell, Sixth Edition, Molecular Biology of the Cell, Sixth Edition*, New York: Garland Science, Taylor & Francis.

An, J., Huang, Y.-C., Xu, Q.-Z., Zhou, L.-J., Shang, Z.-F., Huang, B., Wang, Y., Liu, X.-D., Wu, D.-C. and Zhou, P.-K. (2010) 'DNA-PKcs plays a dominant role in the regulation of H2AX phosphorylation in response to DNA damage and cell cycle progression', *BMC Molecular Biology*, 11(1), 1-13.

ASRM (2013) 'Mature oocyte cryopreservation: a guideline', *Fertility and Sterility*, 99(1), 37-43.

Aziz, N. M. and Rowland, J. H. (2003) 'Trends and advances in cancer survivorship research: challenge and opportunity', *Seminars in Radiation Oncology*, 13(3), 248-66.

Baker, D. J., Jeganathan, K. B., Cameron, J. D., Thompson, M., Juneja, S., Kopecka, A., Kumar, R., Jenkins, R. B., de Groen, P. C., Roche, P. and van Deursen, J. M. (2004) 'BubR1 insufficiency causes early onset of aging-associated phenotypes and infertility in mice', *Nature Genetics*, 36(7), 744-9.

Baker, S. M., Plug, A. W., Prolla, T. A., Bronner, C. E., Harris, A. C., Yao, X., Christie, D. M., Monell, C., Arnheim, N., Bradley, A., Ashley, T. and Liskay, R. M. (1996) 'Involvement of mouse Mlh1 in DNA mismatch repair and meiotic crossing over', *Nature Genetics*, 13(3), 336-42.

Bakhoum, S. F., Kabeche, L., Murnane, J. P., Zaki, B. I. and Compton, D. A. (2014) 'DNA damage response during mitosis induces whole chromosome mis-segregation', *Cancer discovery*, 4(11), 1281-1289.

Bakkenist, C. J. and Kastan, M. B. (2003) 'DNA damage activates ATM through intermolecular autophosphorylation and dimer dissociation', *Nature*, 421(6922), 499-506.

Ball, H. L., Myers, J. S. and Cortez, D. (2005) 'ATRIP binding to replication protein A-single-stranded DNA promotes ATR-ATRIP localization but is dispensable for Chk1 phosphorylation', *Molecular Biology of the Cell*, 16(5), 2372-81.

Banin, S., Moyal, L., Shieh, S., Taya, Y., Anderson, C. W., Chessa, L., Smorodinsky, N. I., Prives, C., Reiss, Y., Shiloh, Y. and Ziv, Y. (1998) 'Enhanced phosphorylation of p53 by ATM in response to DNA damage', *Science*, 281(5383), 1674-7.

Barlow, C., Hirotsune, S., Paylor, R., Liyanage, M., Eckhaus, M., Collins, F., Shiloh, Y., Crawley, J. N., Ried, T., Tagle, D. and Wynshaw-Boris, A. (1996) 'Atm-Deficient Mice: A Paradigm of Ataxia Telangiectasia', *Cell*, 86(1), 159-171.

Barlow, C., Liyanage, M., Moens, P. B., Tarsounas, M., Nagashima, K., Brown, K., Rottinghaus, S., Jackson, S. P., Tagle, D., Ried, T. and Wynshaw-Boris, A. (1998) 'Atm deficiency results in severe meiotic disruption as early as leptonema of prophase I', *Development*, 125(20), 4007-4017.

Bartek, J. and Lukas, J. (2001) 'Mammalian G1- and S-phase checkpoints in response to DNA damage', *Current Opinion in Cell Biology*, 13(6), 738-747.

Barzilai, A., Rotman, G. and Shiloh, Y. (2002) 'ATM deficiency and oxidative stress: a new dimension of defective response to DNA damage', *DNA Repair*, 1(1), 3-25.

Baskar, R., Lee, K. A., Yeo, R. and Yeoh, K.-W. (2012) 'Cancer and Radiation Therapy: Current Advances and Future Directions', *International Journal of Medical Sciences*, 9(3), 193-199.

Basu, A. and Haldar, S. (1998) 'The relationship between Bcl2, Bax and p53: consequences for cell cycle progression and cell death', *Molecular Human Reproduction*, 4(12), 1099-1109.

Baudat, F., Imai, Y. and de Massy, B. (2013) 'Meiotic recombination in mammals: localization and regulation', *Nature Reviews Genetics*, 14(11), 794-806.

Baudat, F., Manova, K., Yuen, J. P., Jasin, M. and Keeney, S. (2000) 'Chromosome Synapsis Defects and Sexually Dimorphic Meiotic Progression in Mice Lacking Spo11', *Molecular Cell*, 6(5), 989-998.

Bolcun-Filas, E., Rinaldi, V. D., White, M. E. and Schimenti, J. C. (2014) 'Reversal of Female Infertility by Chk2 Ablation Reveals the Oocyte DNA Damage Checkpoint Pathway', *Science*, 343(6170), 533-536.

Boswell-Smith, V., Spina, D. and Page, C. P. (2006) 'Phosphodiesterase inhibitors', *British Journal of Pharmacology*, 147(Suppl 1), S252-S257.

Bowles, J., Knight, D., Smith, C., Wilhelm, D., Richman, J., Mamiya, S., Yashiro, K., Chawengsaksophak, K., Wilson, M. J., Rossant, J., Hamada, H. and Koopman, P. (2006) 'Retinoid signaling determines germ cell fate in mice', *Science*, 312(5773), 596-600.

Bowles, J. and Koopman, P. (2007) 'Retinoic acid, meiosis and germ cell fate in mammals', *Development*, 134(19), 3401-11.

Breuer, M., Kolano, A., Kwon, M., Li, C.-C., Tsai, T.-F., Pellman, D., Brunet, S. and Verlhac, M.-H. (2010) 'HURP permits MTOC sorting for robust meiotic spindle bipolarity, similar to extra centrosome clustering in cancer cells', *The Journal of Cell Biology*, 191(7), 1251-1260.

Brito, D. A. and Rieder, C. L. (2006) 'Mitotic Checkpoint Slippage in Humans Occurs via Cyclin B Destruction in the Presence of an Active Checkpoint', *Current Biology*, 16(12), 1194-1200.

Britton, S., Coates, J. and Jackson, S. P. (2013) 'A new method for high-resolution imaging of Ku foci to decipher mechanisms of DNA double-strand break repair', *The Journal of Cell Biology,* 202(3), 579-595.

Brooker, A. S. and Berkowitz, K. M. (2014) 'The roles of cohesins in mitosis, meiosis, and human health and disease', *Methods in molecular biology (Clifton, N.J.),* 1170, 229-266.

Brown, E. J. and Baltimore, D. (2000) 'ATR disruption leads to chromosomal fragmentation and early embryonic lethality', *Genes & Development,* 14(4), 397-402.

Budden, T. and Bowden, N. A. (2013) 'The Role of Altered Nucleotide Excision Repair and UVB-Induced DNA Damage in Melanomagenesis', *International Journal of Molecular Sciences,* 14(1), 1132-1151.

Burden, D. A. and Osheroff, N. (1998) 'Mechanism of action of eukaryotic topoisomerase II and drugs targeted to the enzyme', *Biochimica Et Biophysica Acta-Gene Structure and Expression,* 1400(1-3), 139-154.

Burgoyne, P. S., Mahadevaiah, S. K. and Turner, J. M. (2009) 'The consequences of asynapsis for mammalian meiosis', *Nature Reviews Genetics,* 10(3), 207-16.

Burgoyne, P. S., Mahadevaiah, S. K. and Turner, J. M. A. (2007) 'The management of DNA double-strand breaks in mitotic G2, and in mammalian meiosis viewed from a mitotic G2 perspective', *Bioessays,* 29(10), 974-986.

Burma, S., Chen, B. P., Murphy, M., Kurimasa, A. and Chen, D. J. (2001) 'ATM phosphorylates histone H2AX in response to DNA double-strand breaks', *Journal of Biological Chemistry,* 276(45), 42462-42467.

Burns, K. H., Yan, C., Kumar, T. R. and Matzuk, M. M. (2001) 'Analysis of ovarian gene expression in follicle-stimulating hormone beta knockout mice', *Endocrinology,* 142(7), 2742-51.

Camlin, N. J., Sobinoff, A. P., Sutherland, J. M., Beckett, E. L., Jarnicki, A. G., Vanders, R. L., Hansbro, P. M., McLaughlin, E. A. and Holt, J. E. (2016) 'Maternal Smoke Exposure Impairs the Long-Term Fertility of Female Offspring in a Murine Model', *Biology of Reproduction,* 94(2), 39.

Capasso, H., Palermo, C., Wan, S., Rao, H., John, U. P., O'Connell, M. J. and Walworth, N. C. (2002) 'Phosphorylation activates Chk1 and is required for checkpoint-mediated cell cycle arrest', *Journal of Cell Science,* 115(23), 4555-4564.

Castrillon, D. H., Miao, L., Kollipara, R., Horner, J. W. and DePinho, R. A. (2003) 'Suppression of ovarian follicle activation in mice by the transcription factor Foxo3a', *Science*, 301(5630), 215-8.

Cesare, A. J. (2014) 'Mitosis, double strand break repair, and telomeres: A view from the end', *Bioessays*, 36(11), 1054-1061.

Chan, Y. W. and West, S. (2015) 'GEN1 promotes Holliday junction resolution by a coordinated nick and counter-nick mechanism', *Nucleic Acids Research*, 43(22), 10882-10892.

Chatterjee, G., Jimenez-Sainz, J., Presti, T., Nguyen, T. and Jensen, R. B. (2016) 'Distinct binding of BRCA2 BRC repeats to RAD51 generates differential DNA damage sensitivity', *Nucleic Acids Research*, 44(11), 5256-5270.

Chehab, N., Malikzay, A., Stavridi, E. and Halazonetis, T. D. (1999) 'Phosphorylation of Ser-20 mediates stabilization of human p53 in response to DNA damage.', *PNAS*, 96(24), 13777-13782.

Chen, J. Y. and Stubbe, J. A. (2004) 'Bleomycins: new methods will allow reinvestigation of old issues', *Current Opinion in Chemical Biology*, 8(2), 175-181.

Chen, L., Chao, S.-B., Wang, Z.-B., Qi, S.-T., Zhu, X.-L., Yang, S.-W., Yang, C.-R., Zhang, Q.-H., Ouyang, Y.-C., Hou, Y., Schatten, H. and Sun, Q.-Y. (2012) 'Checkpoint kinase 1 is essential for meiotic cell cycle regulation in mouse oocytes', *Cell Cycle*, 11(10), 1948-1955.

Chen, R. H. (2002) 'BubR1 is essential for kinetochore localization of other spindle checkpoint proteins and its phosphorylation requires Mad1', *The Journal of Cell Biology*, 158(3), 487-96.

Chiang, T., Schultz, R. M. and Lampson, M. A. (2012) 'Meiotic Origins of Maternal Age-Related Aneuploidy', *Biology of Reproduction*, 86(1), 7.

Choi, W.-J., Banerjee, J., Falcone, T., Bena, J., Agarwal, A. and Sharma, R. K. (2007) 'Oxidative stress and tumor necrosis factor–α–induced alterations in metaphase II mouse oocyte spindle structure', *Fertility and Sterility*, 88(4, Supplement), 1220-1231.

Chowdhury, D., Keogh, M.-C., Ishii, H., Peterson, C. L., Buratowski, S. and Lieberman, J. (2005) 'γ-H2AX Dephosphorylation by Protein Phosphatase 2A Facilitates DNA Double-Strand Break Repair', *Molecular Cell,* 20(5), 801-809.

Cimprich, K. A. and Cortez, D. (2008) 'ATR: an essential regulator of genome integrity', *Nature Reviews Molecular Cell Biology,* 9(8), 616-27.

Clift, D. and Schuh, M. (2013) 'Restarting life: fertilization and the transition from meiosis to mitosis', *Nature Reviews Molecular Cell Biology,* 14(9), 549-62.

Clift, D. and Schuh, M. (2015) 'A three-step MTOC fragmentation mechanism facilitates bipolar spindle assembly in mouse oocytes', *Nature Communications,* 6, 7217.

Coin, F., Oksenych, V. and Egly, J. M. (2007) 'Distinct roles for the XPB/p52 and XPD/p44 subcomplexes of TFIIH in damaged DNA opening during nucleotide excision repair', *Molecular Cell,* 26(2), 245-56.

Collins, J. K., Lane, S. I. R., Merriman, J. A. and Jones, K. T. (2015) 'DNA damage induces a meiotic arrest in mouse oocytes mediated by the spindle assembly checkpoint', *Nature Communications,* 6.

Cortes, F., Pastor, N., Mateos, S. and Dominguez, I. (2003) 'Roles of DNA topoisomerases in chromosome segregation and mitosis', *Mutation Research,* 543(1), 59-66.

Cosentino, C., Grieco, D. and Costanzo, V. (2011) 'ATM activates the pentose phosphate pathway promoting anti-oxidant defence and DNA repair', *The EMBO Journal,* 30(3), 546-555.

Costantini, S., Woodbine, L., Andreoli, L., Jeggo, P. A. and Vindigni, A. (2007) 'Interaction of the Ku heterodimer with the DNA ligase IV/Xrcc4 complex and its regulation by DNA-PK', *DNA Repair (Amst),* 6(6), 712-22.

Coster, G., Hayouka, Z., Argaman, L., Strauss, C., Friedler, A., Brandeis, M. and Goldberg, M. (2007) 'The DNA damage response mediator MDC1 directly interacts with the anaphase-promoting complex/cyclosome', *Journal of Biological Chemistry,* 282(44), 32053-32064.

Dalton, W. B. and Yang, V. W. (2009) 'The Role of Prolonged Mitotic Checkpoint Activation in the Formation and Treatment of Cancer', *Future oncology (London, England),* 5(9), 1363-1370.

Daniel, J. A., Pellegrini, M., Lee, B.-S., Guo, Z., Filsuf, D., Belkina, N. V., You, Z., Paull, T. T., Sleckman, B. P., Feigenbaum, L. and Nussenzweig, A. (2012) 'Loss of ATM kinase activity leads to embryonic lethality in mice', *The Journal of Cell Biology,* 198(3), 295-304.

Davidson, D., Amrein, L., Panasci, L. and Aloyz, R. (2013) 'Small Molecules, Inhibitors of DNA-PK, Targeting DNA Repair, and Beyond', *Frontiers in Pharmacology,* 4, 5.

Davis, A. J. and Chen, D. J. (2013) 'DNA double strand break repair via non-homologous end-joining', *Translational cancer research,* 2(3), 130-143.

De Antoni, A., Pearson, C. G., Cimini, D., Canman, J. C., Sala, V., Nezi, L., Mapelli, M., Sironi, L., Faretta, M., Salmon, E. D. and Musacchio, A. (2005) 'The Mad1/Mad2 Complex as a Template for Mad2 Activation in the Spindle Assembly Checkpoint', *Current Biology,* 15(3), 214-225.

De Felici, M. (2013) 'Origin, Migration, and Proliferation of Human Primordial Germ Cells' in Coticchio, G., Albertini, F. D. and De Santis, L., eds., *Oogenesis*, London: Springer London, 19-37.

de Gruijl, F. R., van Kranen, H. J. and Mullenders, L. H. F. (2001) 'UV-induced DNA damage, repair, mutations and oncogenic pathways in skin cancer', *Journal of Photochemistry and Photobiology B-Biology,* 63(1-3), 19-27.

de Klein, A., Muijtjens, M., van Os, R., Verhoeven, Y., Smit, B., Carr, A. M., Lehmann, A. R. and Hoeijmakers, J. H. J. (2000) 'Targeted disruption of the cell-cycle checkpoint gene ATR leads to early embryonic lethality in mice', *Current Biology,* 10(8), 479-482.

de Vries, S. S., Baart, E. B., Dekker, M., Siezen, A., de Rooij, D. G., de Boer, P. and te Riele, H. (1999) 'Mouse MutS-like protein Msh5 is required for proper chromosome synapsis in male and female meiosis', *Genes & Development,* 13(5), 523-531.

DeLoughery, Z., Luczak, M. W., Ortega-Atienza, S. and Zhitkovich, A. (2015) 'DNA Double-Strand Breaks by Cr(VI) Are Targeted to Euchromatin and Cause ATR-Dependent Phosphorylation of Histone H2AX and Its Ubiquitination', *Toxicological Sciences,* 143(1), 54-63.

Desouky, O., Ding, N. and Zhou, G. (2015) 'Targeted and non-targeted effects of ionizing radiation', *Journal of Radiation Research and Applied Sciences,* 8(2), 247-254.

deVantery, C., Gavin, A. C., Vassalli, J. D. and SchorderetSlatkine, S. (1996) 'An accumulation of p34(cdc2) at the end of mouse oocyte growth correlates with the acquisition of meiotic competence', *Developmental Biology,* 174(2), 335-344.

Dexheimer, S. T. (2013) 'DNA Repair Pathways and Mechanisms' in Mathews, A. L., Cabarcas, M. S. and Hurt, M. E., eds., *DNA Repair of Cancer Stem Cells*, Dordrecht: Springer Netherlands, 19-32.

Di Giacomo, M., Barchi, M., Baudat, F., Edelmann, W., Keeney, S. and Jasin, M. (2005) 'Distinct DNA-damage-dependent and -independent responses drive the loss of oocytes in recombination-defective mouse mutants', *Proceedings of the National Academy of Sciences of the United States of America,* 102(3), 737-742.

Dierich, A., Sairam, M. R., Monaco, L., Fimia, G. M., Gansmuller, A., LeMeur, M. and Sassone-Corsi, P. (1998) 'Impairing follicle-stimulating hormone (FSH) signaling in vivo: Targeted disruption of the FSH receptor leads to aberrant gametogenesis and hormonal imbalance', *Proceedings of the National Academy of Sciences of the United States of America,* 95(23), 13612-13617.

Digweed, M. and Sperling, K. (2004) 'Nijmegen breakage syndrome: clinical manifestation of defective response to DNA double-strand breaks', *DNA Repair,* 3(8–9), 1207-1217.

Dillman, R. O. and McClure, S. E. (2014) 'Steadily Improving Survival in Lung Cancer', *Clinical Lung Cancer,* 15(5), 331-337.

Donehower, L. A., Harvey, M., Slagle, B. L., McArthur, M. J. and Montgomery Jr, C. A. (1992) Mice deficient for p53 are developmentally normal but susceptible to spontaneous tumours., 356, *Nature*.

Donzelli, M. and Draetta, G. F. (2003) 'Regulating mammalian checkpoints through Cdc25 inactivation', *EMBO Reports,* 4(7), 671-677.

Dumont, J. and Desai, A. (2012) 'Acentrosomal spindle assembly and chromosome segregation during oocyte meiosis', *Trends in Cell Biology,* 22(5), 241-249.

Dupre, A., Boyer-Chatenet, L. and Gautier, J. (2006) 'Two-step activation of ATM by DNA and the Mre11-Rad50-Nbs1 complex', *Nature structural & molecular biology,* 13(5), 451-457.

Duro, E. and Marston, A. L. (2015) 'From equator to pole: splitting chromosomes in mitosis and meiosis', *Genes & Development,* 29(2), 109-122.

Ebner, T., Moser, M., Shebl, O., Sommerguber, M. and Tews, G. (2008) 'Prognosis of oocytes showing aggregation of smooth endoplasmic reticulum', *Reproductive biomedicine online,* 16(1), 113-8.

Ebner, T., Moser, M., Sommergruber, M., Gaiswinkler, U., Shebl, O., Jesacher, K. and Tews, G. (2005) 'Occurrence and developmental consequences of vacuoles throughout preimplantation development', *Fertility and Sterility,* 83(6), 1635-40.

Edelmann, W., Cohen, P. E., Kane, M., Lau, K., Morrow, B., Bennett, S., Umar, A., Kunkel, T., Cattoretti, G., Chaganti, R., Pollard, J. W., Kolodner, R. D. and Kucherlapati, R. (1996) 'Meiotic pachytene arrest in MLH1-deficient mice', *Cell,* 85(7), 1125-34.

Edelmann, W., Cohen, P. E., Kneitz, B., Winand, N., Lia, M., Heyer, J., Kolodner, R., Pollard, J. W. and Kucherlapati, R. (1999) 'Mammalian MutS homologue 5 is required for chromosome pairing in meiosis', *Nature Genetics,* 21(1), 123-7.

Eliezer, Y., Argaman, L., Kornowski, M., Roniger, M. and Goldberg, M. (2014) 'Interplay between the DNA Damage Proteins MDC1 and ATM in the Regulation of the Spindle Assembly Checkpoint', *Journal of Biological Chemistry,* 289(12), 8182-8193.

Elmore, S. (2007) 'Apoptosis: a review of programmed cell death', *Toxicologic Pathology,* 35(4), 495-516.

Fell, V. L. and Schild-Poulter, C. (2015) 'The Ku heterodimer: function in DNA repair and beyond', *Mutation Research/Reviews in Mutation Research,* 763, 15-29.

Ferguson, K. A., Wong, E. C., Chow, V., Nigro, M. and Ma, S. (2007) 'Abnormal meiotic recombination in infertile men and its association with sperm aneuploidy', *Human Molecular Genetics,* 16(23), 2870-9.

Filippo, J. S., Sung, P. and Klein, H. (2008) 'Mechanism of eukaryotic homologous recombination' in *Annu Rev Biochem,* Palo Alto: Annual Reviews, 229-257.

Fitch, M. E., Nakajima, S., Yasui, A. and Ford, J. M. (2003) 'In vivo recruitment of XPC to UV-induced cyclobutane pyrimidine dimers by the DDB2 gene product', *The Journal of Biological Chemistry,* 278(47), 46906-10.

Foley, E. A. and Kapoor, T. M. (2013) 'Microtubule attachment and spindle assembly checkpoint signalling at the kinetochore', *Nature Reviews Molecular Cell Biology,* 14(1), 25-37.

Forget, A. L. and Kowalczykowski, S. C. (2010) 'Single-molecule imaging brings Rad51 nucleoprotein filaments into focus', *Trends in Cell Biology*, 20(5), 269-76.

Fortune, J. E. (2003) 'The early stages of follicular development: activation of primordial follicles and growth of preantral follicles', *Animal Reproduction Science*, 78(3-4), 135-63.

Gatei, M., Sloper, K., Sorensen, C., Syljuasen, R., Falck, J., Hobson, K., Savage, K., Lukas, J., Zhou, B. B., Bartek, J. and Khanna, K. K. (2003) 'Ataxia-telangiectasia-mutated (ATM) and NBS1-dependent phosphorylation of Chk1 on Ser-317 in response to ionizing radiation', *Journal of Biological Chemistry*, 278(17), 14806-14811.

Gates, K. S. (2009) 'An Overview of Chemical Processes That Damage Cellular DNA: Spontaneous Hydrolysis, Alkylation, and Reactions with Radicals', *Chemical Research in Toxicology*, 22(11), 1747-1760.

Gavet, O. and Pines, J. (2010) 'Progressive Activation of CyclinB1-Cdk1 Coordinates Entry to Mitosis', *Developmental Cell*, 18(4), 533-543.

Giunta, S., Belotserkovskaya, R. and Jackson, S. P. (2010) 'DNA damage signaling in response to double-strand breaks during mitosis', *The Journal of Cell Biology*, 190(2), 197-207.

Goodarzi, A. A., Yu, Y., Riballo, E., Douglas, P., Walker, S. A., Ye, R., Härer, C., Marchetti, C., Morrice, N., Jeggo, P. A. and Lees-Miller, S. P. (2006) 'DNA-PK autophosphorylation facilitates Artemis endonuclease activity', *The EMBO Journal*, 25(16), 3880-3889.

Goodsell, D. S. (2001) 'The Molecular Perspective: Ultraviolet Light and Pyrimidine Dimers', *The Oncologist*, 6(3), 298-299.

Goodwin, J. F. and Knudsen, K. E. (2014) 'Beyond DNA repair: DNA-PK function in cancer', *Cancer discovery*, 4(10), 1126-39.

Gorr, I. H., Reis, A., Boos, D., Wühr, M., Madgwick, S., Jones, K. T. and Stemmann, O. (2006) 'Essential CDK1 inhibitory role for separase during meiosis I in vertebrate oocytes', *Nature Cell Biology*, 8(9), 1035-1037.

Greinert, R., Volkmer, B., Henning, S., Breitbart, E. W., Greulich, K. O., Cardoso, M. C. and Rapp, A. (2012) 'UVA-induced DNA double-strand breaks result from the repair of clustered oxidative DNA damages', *Nucleic Acids Research*, 40(20), 10263-10273.

Guglielmino, M. R., Santonocito, M., Vento, M., Ragusa, M., Barbagallo, D., Borzì, P., Casciano, I., Banelli, B., Barbieri, O., Astigiano, S., Scollo, P., Romani, M., Purrello, M. and Di Pietro, C. (2011) 'TAp73 is downregulated in oocytes from women of advanced reproductive age', *Cell Cycle,* 10(19), 3253-3256.

Gui, L. and Homer, H. (2012) 'Spindle assembly checkpoint signalling is uncoupled from chromosomal position in mouse oocytes', *Development,* 139(11), 1941-6.

Guo, X., Ward, M. D., Tiedebohl, J. B., Oden, Y. M., Nyalwidhe, J. O. and Semmes, O. J. (2010) 'Interdependent phosphorylation within the kinase domain T-loop Regulates CHK2 activity', *The Journal of Biological Chemistry*, 285(43), 33348-57.

Guo, Z., Kozlov, S., Lavin, M. F., Person, M. D. and Paull, T. T. (2010) 'ATM activation by oxidative stress', *Science,* 330(6003), 517-21.

Hached, K., Xie, S. Z., Buffin, E., Cladière, D., Rachez, C., Sacras, M., Sorger, P. K. and Wassmann, K. (2011) 'Mps1 at kinetochores is essential for female mouse meiosis I', *Development,* 138(11), 2261-2271.

Halicka, H. D., Huang, X., Traganos, F., King, M. A., Dai, W. and Darzynkiewicz, Z. (2005) 'Histone H2AX phosphorylation after cell irradiation with UV-B: relationship to cell cycle phase and induction of apoptosis', *Cell Cycle,* 4(2), 339-45.

Hanasoge, S. and Ljungman, M. (2007) 'H2AX phosphorylation after UV irradiation is triggered by DNA repair intermediates and is mediated by the ATR kinase', *Carcinogenesis,* 28(11), 2298-2304.

Hande, K. R. (1998) 'Etoposide: Four Decades of Development of a Topoisomerase II Inhibitor', *European Journal of Cancer,* 34(10), 1541-1521.

Handel, M. A. and Schimenti, J. C. (2010) 'Genetics of mammalian meiosis: regulation, dynamics and impact on fertility', *Nature Reviews Genetics,* 11(2), 124-36.

Harris, S. L. and Levine, A. J. (2005) 'The p53 pathway: positive and negative feedback loops', *Oncogene,* 24(17), 2899-2908.

Hecht, S. M. (2000) 'Bleomycin: New perspectives on the mechanism of action', *Journal of Natural Products,* 63(1), 158-168.

Heijink, A. M., Krajewska, M. and van Vugt, M. A. T. M. (2013) 'The DNA damage response during mitosis', *Mutation Research/Fundamental and Molecular Mechanisms of Mutagenesis,* 750(1–2), 45-55.

Helleday, T., Eshtad, S. and Nik-Zainal, S. (2014) 'Mechanisms underlying mutational signatures in human cancers', *Nature Reviews Genetics,* 15(9), 585-598.

Herbert, M., Levasseur, M., Homer, H., Yallop, K., Murdoch, A. and McDougall, A. (2003) 'Homologue disjunction in mouse oocytes requires proteolysis of securin and cyclin B1', *Nature Cell Biology,* 5(11), 1023-5.

Hewitt, L., Tighe, A., Santaguida, S., White, A. M., Jones, C. D., Musacchio, A., Green, S. and Taylor, S. S. (2010) 'Sustained Mps1 activity is required in mitosis to recruit O-Mad2 to the Mad1–C-Mad2 core complex', *The Journal of Cell Biology,* 190(1), 25-34.

Heyer, W. D., Ehmsen, K. T. and Liu, J. (2010) 'Regulation of Homologous Recombination in Eukaryotes' in Campbell, A., Lichten, M. and Schupbach, G., eds., *Annual Review of Genetics, Vol 44,* Palo Alto: Annual Reviews, 113-139.

Holloway, J. K., Booth, J., Edelmann, W., McGowan, C. H. and Cohen, P. E. (2008) 'MUS81 generates a subset of MLH1-MLH3-independent crossovers in mammalian meiosis', *Plos Genetics,* 4(9), e1000186.

Holloway, J. K., Morelli, M. A., Borst, P. L. and Cohen, P. E. (2010) 'Mammalian BLM helicase is critical for integrating multiple pathways of meiotic recombination', *The Journal of Cell Biology,* 188(6), 779-89.

Holt, J. E., Lane, S. I., Jennings, P., Garcia-Higuera, I., Moreno, S. and Jones, K. T. (2012) 'APC(FZR1) prevents nondisjunction in mouse oocytes by controlling meiotic spindle assembly timing', *Molecular Biology of the Cell,* 23(20), 3970-81.

Homer, H. (2013) 'The APC/C in female mammalian meiosis I', *Reproduction,* 146(2), R61-71.

Homer, H., Gui, L. and Carroll, J. (2009) 'A Spindle Assembly Checkpoint Protein Functions in Prophase I Arrest and Prometaphase Progression', *Science,* 326(5955), 991-994.

Homer, H. A., McDougall, A., Levasseur, M., Murdoch, A. P. and Herbert, M. (2005a) 'Mad2 is required for inhibiting securin and cyclin B degradation following spindle depolymerisation in meiosis I mouse oocytes', *Reproduction,* 130(6), 829-843.

Homer, H. A., McDougall, A., Levasseur, M., Yallop, K., Murdoch, A. P. and Herbert, M. (2005b) 'Mad2 prevents aneuploidy and premature proteolysis of cyclin B and securin during meiosis I in mouse oocytes', *Genes & Development,* 19(2), 202-7.

Houtgraaf, J. H., Versmissen, J. and van der Giessen, W. J. (2006) 'A concise review of DNA damage checkpoints and repair in mammalian cells', *Cardiovascular Revascularization Medicine,* 7(3), 165-72.

Hsueh, A. J., Kawamura, K., Cheng, Y. and Fauser, B. C. (2015) 'Intraovarian control of early folliculogenesis', *Endocrine Reviews,* 36(1), 1-24.

Hunter, N. (2015) 'Meiotic Recombination: The Essence of Heredity', *Cold Spring Harbor Perspectives in Biology,* 7(12).

Inoue, A., Nakajima, R., Nagata, M. and Aoki, F. (2008) 'Contribution of the oocyte nucleus and cytoplasm to the determination of meiotic and developmental competence in mice', *Human Reproduction,* 23(6), 1377-84.

Iourov, I. Y., Vorsanova, S. G., Liehr, T., Kolotii, A. D. and Yurov, Y. B. (2009) 'Increased chromosome instability dramatically disrupts neural genome integrity and mediates cerebellar degeneration in the ataxia-telangiectasia brain', *Human Molecular Genetics,* 18(14), 2656-69.

Ishiguro, T., Tanaka, K., Sakuno, T. and Watanabe, Y. (2010) 'Shugoshin-PP2A counteracts casein-kinase-1-dependent cleavage of Rec8 by separase', *Nature Cell Biology,* 12(5), 500-6.

Jaroudi, S., Kakourou, G., Cawood, S., Doshi, A., Ranieri, D. M., Serhal, P., Harper, J. C. and SenGupta, S. B. (2009) 'Expression profiling of DNA repair genes in human oocytes and blastocysts using microarrays', *Human Reproduction,* 24(10), 2649-55.

Jennings, P. C., Merriman, J. A., Beckett, E. L., Hansbro, P. M. and Jones, K. T. (2011) 'Increased zona pellucida thickness and meiotic spindle disruption in oocytes from cigarette smoking mice', *Human Reproduction,* 26(4), 878-84.

Jensen, J. T., Schwinof, K. M., Zelinski-Wooten, M. B., Conti, M., DePaolo, L. V. and Stouffer, R. L. (2002) 'Phosphodiesterase 3 inhibitors selectively block the spontaneous resumption of meiosis by macaque oocytes in vitro', *Human Reproduction,* 17(8), 2079-84.

Jones, K. T. (1998) 'Ca2+ oscillations in the activation of the egg and development of the embryo in mammals', *The International Journal of Developmental Biology,* 42(1), 1-10.

Jones, K. T. (2008) 'Meiosis in oocytes: predisposition to aneuploidy and its increased incidence with age', *Human Reproduction Update,* 14(2), 143-58.

Jones, K. T. and Lane, S. I. (2012) 'Chromosomal, metabolic, environmental, and hormonal origins of aneuploidy in mammalian oocytes', *Experimental Cell Research,* 318(12), 1394-9.

Jones, K. T. and Lane, S. I. (2013) 'Molecular causes of aneuploidy in mammalian eggs', *Development,* 140(18), 3719-30.

Katis, V. L., Lipp, J. J., Imre, R., Bogdanova, A., Okaz, E., Habermann, B., Mechtler, K., Nasmyth, K. and Zachariae, W. (2010) 'Rec8 phosphorylation by casein kinase 1 and Cdc7-Dbf4 kinase regulates cohesin cleavage by separase during meiosis', *Developmental Cell,* 18(3), 397-409.

Katsuragi, Y. and Sagata, N. (2004) 'Regulation of Chk1 Kinase by Autoinhibition and ATR-mediated Phosphorylation', *Molecular Biology of the Cell,* 15(4), 1680-1689.

Kerr, J. B., Brogan, L., Myers, M., Hutt, K. J., Mladenovska, T., Ricardo, S., Hamza, K., Scott, C. L., Strasser, A. and Findlay, J. K. (2012a) 'The primordial follicle reserve is not renewed after chemical or gamma-irradiation mediated depletion', *Reproduction,* 143(4), 469-76.

Kerr, J. B., Hutt, K. J., Michalak, E. M., Cook, M., Vandenberg, C. J., Liew, S. H., Bouillet, P., Mills, A., Scott, C. L., Findlay, J. K. and Strasser, A. (2012b) 'DNA Damage-Induced Primordial Follicle Oocyte Apoptosis and Loss of Fertility Require TAp63-Mediated Induction of Puma and Noxa', *Molecular Cell,* 48(3), 343-352.

Khodjakov, A. and Pines, J. (2010) 'Centromere tension: a divisive issue', *Nature Cell Biology,* 12(10), 919-923.

Kim, D. A. and Suh, E. K. (2014) 'Defying DNA double strand break-induced death during prophase I meiosis by temporal TAp63alpha phosphorylation regulation in developing mouse oocytes', *Molecular and Cellular Biology*.

Kim, E. M. and Burke, D. J. (2008) 'DNA damage activates the SAC in an ATM/ATR-dependent manner, independently of the kinetochore', *Plos Genetics,* 4(2), 9.

Kinner, A., Wu, W., Staudt, C. and Iliakis, G. (2008) 'γ-H2AX in recognition and signaling of DNA double-strand breaks in the context of chromatin', *Nucleic Acids Research,* 36(17), 5678-5694.

Kirk, M. and Lyon, M. F. (1982) 'Induction of congenital anomalies in offspring of female mice exposed to varying doses of X-rays', *Mutation Research/Fundamental and Molecular Mechanisms of Mutagenesis,* 106(1), 73-83.

Kitajima, T. S., Ohsugi, M. and Ellenberg, J. (2011) 'Complete kinetochore tracking reveals error-prone homologous chromosome biorientation in mammalian oocytes', *Cell,* 146(4), 568-81.

Kitajima, T. S., Sakuno, T., Ishiguro, K.-i., Iemura, S.-i., Natsume, T., Kawashima, S. A. and Watanabe, Y. (2006) 'Shugoshin collaborates with protein phosphatase 2A to protect cohesin', *Nature,* 441(7089), 46-52.

Kneitz, B., Cohen, P. E., Avdievich, E., Zhu, L., Kane, M. F., Hou, H., Jr., Kolodner, R. D., Kucherlapati, R., Pollard, J. W. and Edelmann, W. (2000) 'MutS homolog 4 localization to meiotic chromosomes is required for chromosome pairing during meiosis in male and female mice', *Genes & Development,* 14(9), 1085-97.

Kodama, M., Otsubo, C., Hirota, T., Yokota, J., Enari, M. and Taya, Y. (2010) 'Requirement of ATM for Rapid p53 Phosphorylation at Ser46 without Ser/Thr-Gln Sequences', *Molecular and Cellular Biology,* 30(7), 1620-1633.

Kolano, A., Brunet, S., Silk, A. D., Cleveland, D. W. and Verlhac, M. H. (2012) 'Error-prone mammalian female meiosis from silencing the spindle assembly checkpoint without normal interkinetochore tension', *PNAS,* 109(27), E1858-E1867.

Koubova, J., Hu, Y.-C., Bhattacharyya, T., Soh, Y. Q. S., Gill, M. E., Goodheart, M. L., Hogarth, C. A., Griswold, M. D. and Page, D. C. (2014) 'Retinoic Acid Activates Two Pathways Required for Meiosis in Mice', *Plos Genetics,* 10(8), e1004541.

Koubova, J., Menke, D. B., Zhou, Q., Capel, B., Griswold, M. D. and Page, D. C. (2006) 'Retinoic acid regulates sex-specific timing of meiotic initiation in mice', *Proceedings of the National Academy of Sciences of the United States of America,* 103(8), 2474-2479.

Kouznetsova, A., Lister, L., Nordenskjold, M., Herbert, M. and Hoog, C. (2007) 'Bi-orientation of achiasmatic chromosomes in meiosis I oocytes contributes to aneuploidy in mice', *Nature Genetics,* 39(8), 966-8.

Krejci, L., Altmannova, V., Spirek, M. and Zhao, X. L. (2012) 'Homologous recombination and its regulation', *Nucleic Acids Research,* 40(13), 5795-5818.

Kryston, T. B., Georgiev, A. B., Pissis, P. and Georgakilas, A. G. (2011) 'Role of oxidative stress and DNA damage in human carcinogenesis', *Mutation Research/Fundamental and Molecular Mechanisms of Mutagenesis,* 711(1–2), 193-201.

Kudo, N. R., Anger, M., Peters, A. H., Stemmann, O., Theussl, H. C., Helmhart, W., Kudo, H., Heyting, C. and Nasmyth, K. (2009) 'Role of cleavage by separase of the Rec8 kleisin subunit of cohesin during mammalian meiosis I', *Journal of Cell Science,* 122(Pt 15), 2686-98.

Kudo, N. R., Wassmann, K., Anger, M., Schuh, M., Wirth, K. G., Xu, H., Helmhart, W., Kudo, H., McKay, M., Maro, B., Ellenberg, J., de Boer, P. and Nasmyth, K. (2006) 'Resolution of chiasmata in oocytes requires separase-mediated proteolysis', *Cell,* 126(1), 135-146.

Kujjo, L. L., Laine, T., Pereira, R. J. G., Kagawa, W., Kurumizaka, H., Yokoyama, S. and Perez, G. I. (2010) 'Enhancing Survival of Mouse Oocytes Following Chemotherapy or Aging by Targeting Bax and Rad51', *Plos One,* 5(2), 10.

Kulukian, A., Han, J. S. and Cleveland, D. W. (2009) 'Unattached Kinetochores Catalyze Production of an Anaphase Inhibitor that Requires a Mad2 Template to Prime Cdc20 for BubR1 Binding', *Developmental Cell,* 16(1), 105-117.

Kumagai, A., Kim, S. M. and Dunphy, W. G. (2004) 'Claspin and the activated form of ATR-ATRIP collaborate in the activation of Chk1', *The Journal of Biological Chemistry,* 279(48), 49599-608.

Kumagai, A., Lee, J., Yoo, H. Y. and Dunphy, W. G. (2006) 'TopBP1 Activates the ATR-ATRIP Complex', *Cell,* 124(5), 943-955.

Kumar, R., Bourbon, H. M. and de Massy, B. (2010) 'Functional conservation of Mei4 for meiotic DNA double-strand break formation from yeasts to mice', *Genes & Development,* 24(12), 1266-80.

Kumar, R., Ghyselinck, N., Ishiguro, K. i., Watanabe, Y., Kouznetsova, A., Höög, C., Strong, E., Schimenti, J., Daniel, K., Toth, A. and de Massy, B. (2015) 'MEI4 – a central player in the regulation of meiotic DNA double-strand break formation in the mouse', *Journal of Cell Science,* 128(9), 1800-1811.

Lamarche, B. J., Orazio, N. I. and Weitzman, M. D. (2010) 'The MRN complex in Double-Strand Break Repair and Telomere Maintenance', *FEBS letters,* 584(17), 3682-3695.

Lane, S. I., Chang, H. Y., Jennings, P. C. and Jones, K. T. (2010) 'The Aurora kinase inhibitor ZM447439 accelerates first meiosis in mouse oocytes by overriding the spindle assembly checkpoint', *Reproduction,* 140(4), 521-30.

Lane, S. I., Yun, Y. and Jones, K. T. (2012) 'Timing of anaphase-promoting complex activation in mouse oocytes is predicted by microtubule-kinetochore attachment but not by bivalent alignment or tension', *Development,* 139(11), 1947-55.

Lee, C. H. and Chung, J. H. (2001) 'The hCds1 (Chk2)-FHA domain is essential for a chain of phosphorylation events on hCds1 that is induced by ionizing radiation', *The Journal of Biological Chemistry,* 276(32), 30537-41.

Lee, J.-H. and Paull, T. T. (2005) 'ATM Activation by DNA Double-Strand Breaks Through the Mre11-Rad50-Nbs1 Complex', *Science,* 308(5721), 551-554.

Lee, J. H. and Paull, T. T. (2007) 'Activation and regulation of ATM kinase activity in response to DNA double-strand breaks', *Oncogene,* 26(56), 7741-8.

Lee, K. J., Lin, Y. F., Chou, H. Y., Yajima, H., Fattah, K. R., Lee, S. C. and Chen, B. P. (2011) 'Involvement of DNA-dependent protein kinase in normal cell cycle progression through mitosis', *The Journal of Biological Chemistry,* 286(14), 12796-802.

LeMaire-Adkins, R., Radke, K. and Hunt, P. A. (1997) 'Lack of checkpoint control at the metaphase/anaphase transition: a mechanism of meiotic nondisjunction in mammalian females', *The Journal of Cell Biology,* 139(7), 1611-9.

Levrero, M., De Laurenzi, V., Constanzo, A., Sabatini, S., Gong, J., Wang, J. Y. J. and Melino, G. (2000) 'The p53/p63/p73 family of transcription factors: overlapping and distinct functions', *Journal of Cell Science,* 113, 1161-1670.

Li, L., Lu, X., Peterson, C. A. and Legerski, R. J. (1995) 'An interaction between the DNA repair factor XPA and replication protein A appears essential for nucleotide excision repair', *Molecular and Cellular Biology,* 15(10), 5396-402.

Li, X. M., Yu, C., Wang, Z. W., Zhang, Y. L., Liu, X. M., Zhou, D., Sun, Q. Y. and Fan, H. Y. (2013) 'DNA topoisomerase II is dispensable for oocyte meiotic resumption but is essential for meiotic chromosome condensation and separation in mice', *Biology of Reproduction,* 89(5), 118.

Libby, B. J., Reinholdt, L. G. and Schimenti, J. C. (2003) 'Positional cloning and characterization of Mei1, a vertebrate-specific gene required for normal meiotic chromosome synapsis in mice', *PNAS,* 100(26), 15706-11.

Lin, C. S., Wang, Y. C., Huang, J. L., Hung, C. C. and Chen, J. Y. (2012) 'Autophagy and reactive oxygen species modulate cytotoxicity induced by suppression of ATM kinase activity in head and neck cancer cells', *Oral Oncology,* 48(11), 1152-8.

Lin, Z.-L. and Kim, N.-H. (2015) 'Role of ataxia-telangiectasia mutated (ATM) in porcine oocyte in vitro maturation', *Cell Biology International,* 39(6), 710-720.

Lipkin, S. M., Moens, P. B., Wang, V., Lenzi, M., Shanmugarajah, D., Gilgeous, A., Thomas, J., Cheng, J., Touchman, J. W., Green, E. D., Schwartzberg, P., Collins, F. S. and Cohen, P. E. (2002) 'Meiotic arrest and aneuploidy in MLH3-deficient mice', *Nature Genetics,* 31(4), 385-90.

Lister, L. M., Kouznetsova, A., Hyslop, L. A., Kalleas, D., Pace, S. L., Barel, J. C., Nathan, A., Floros, V., Adelfalk, C., Watanabe, Y., Jessberger, R., Kirkwood, T. B., Höög, C. and Herbert, M. (2010) 'Age-Related Meiotic Segregation Errors in Mammalian Oocytes Are Preceded by Depletion of Cohesin and Sgo2', *Current Biology,* 20(17), 1511-1521.

Liu, J., Doty, T., Gibson, B. and Heyer, W.-D. (2010) 'Human BRCA2 protein promotes RAD51 filament formation on RPA-covered ssDNA', *Nature structural & molecular biology,* 17(10), 1260-1262.

Liu, Q., Guntuku, S., Cui, X.-S., Matsuoka, S., Cortez, D., Tamai, K., Luo, G., Carattini-Rivera, S., DeMayo, F., Bradley, A., Donehower, L. A. and Elledge, S. J. (2000) 'Chk1 is an essential kinase that is regulated by Atr and required for the G(2)/M DNA damage checkpoint', *Genes & Development,* 14(12), 1448-1459.

Liu, S., Bekker-Jensen, S., Mailand, N., Lukas, C., Bartek, J. and Lukas, J. (2006) 'Claspin operates downstream of TopBP1 to direct ATR signaling towards Chk1 activation', *Molecular and Cellular Biology,* 26(16), 6056-64.

Livera, G., Petre-Lazar, B., Guerquin, M. J., Trautmann, E., Coffigny, H. and Habert, R. (2008) 'p63 null mutation protects mouse oocytes from radio-induced apoptosis', *Reproduction,* 135(1), 3-12.

Löbrich, M., Shibata, A., Beucher, A., Fisher, A., Ensminger, M., Goodarzi, A. A., Barton, O. and Jeggo, P. A. (2010) 'γH2AX foci analysis for monitoring DNA double-strand break repair: Strengths, limitations and optimization', *Cell Cycle,* 9(4), 662-669.

Lord, T. and Aitken, R. J. (2013) 'Oxidative stress and ageing of the post-ovulatory oocyte', *Reproduction,* 146(6), R217-27.

Ma, J.-Y., Yang, Y.-C. O., Wang, Z.-W., Wang, Z.-B., Jiang, Z.-Z., Luo, S.-M., Hou, Y., Liu, Z.-H., Schatten, H. and Sun, Q.-Y. (2013) 'The effects of DNA double-strand breaks on mouse oocyte meiotic maturation', *Cell Cycle,* 12(8), 1233-1241.

Ma, W., Baumann, C. and Viveiros, M. M. (2010) 'NEDD1 is crucial for meiotic spindle stability and accurate chromosome segregation in mammalian oocytes', *Developmental Biology,* 339(2), 439-50.

Madgwick, S. and Jones, K. T. (2007) 'How eggs arrest at metaphase II: MPF stabilisation plus APC/C inhibition equals Cytostatic Factor', *Cell Division,* 2(1), 1-7.

Mahadevaiah, S. K., Turner, J. M. A., Baudat, F., Rogakou, E. P., de Boer, P., Blanco-Rodriguez, J., Jasin, M., Keeney, S., Bonner, W. M. and Burgoyne, P. S. (2001) 'Recombinational DNA double-strand breaks in mice precede synapsis', *Nature Genetics,* 27(3), 271-276.

Maltaris, T., Seufert, R., Fischl, F., Schaffrath, M., Pollow, K., Koelbl, H. and Dittrich, R. (2007) 'The effect of cancer treatment on female fertility and strategies for preserving fertility', *European Journal of Obstetrics Gynecology and Reproductive Biology,* 130(2), 148-155.

Marangos, P. and Carroll, J. (2012) 'Oocytes Progress beyond Prophase in the Presence of DNA Damage', *Current Biology,* 22(11), 989-994.

Marangos, P., Stevense, M., Niaka, K., Lagoudaki, M., Nabti, I., Jessberger, R. and Carroll, J. (2015) 'DNA damage-induced metaphase I arrest is mediated by the spindle assembly checkpoint and maternal age', *Nature Communications,* 6.

Marechal, A. and Zou, L. (2013) 'DNA damage sensing by the ATM and ATR kinases', *Cold Spring Harbor Perspectives in Biology,* 5(9).

Marechal, A. and Zou, L. (2015) 'RPA-coated single-stranded DNA as a platform for post-translational modifications in the DNA damage response', *Cell Research,* 25(1), 9-23.

Mari, P. O., Florea, B. I., Persengiev, S. P., Verkaik, N. S., Bruggenwirth, H. T., Modesti, M., Giglia-Mari, G., Bezstarosti, K., Demmers, J. A., Luider, T. M., Houtsmuller, A. B. and van Gent, D. C. (2006) 'Dynamic assembly of end-joining complexes requires interaction between Ku70/80 and XRCC4', *PNAS,* 103(49), 18597-602.

Mariotti, L. G., Pirovano, G., Savage, K. I., Ghita, M., Ottolenghi, A., Prise, K. M. and Schettino, G. (2013) 'Use of the γ-H2AX Assay to Investigate DNA Repair Dynamics Following Multiple Radiation Exposures', *Plos One*, 8(11), e79541.

Maro, B. and Verlhac, M. H. (2002) 'Polar body formation: new rules for asymmetric divisions', *Nature Cell Biology*, 4(12), E281-E283.

Marti, T. M., Hefner, E., Feeney, L., Natale, V. and Cleaver, J. E. (2006) 'H2AX phosphorylation within the G1 phase after UV irradiation depends on nucleotide excision repair and not DNA double-strand breaks', *PNAS*, 103(26), 9891-9896.

Masciarelli, S., Horner, K., Liu, C. Y., Park, S. H., Hinckley, M., Hockman, S., Nedachi, T., Jin, C., Conti, M. and Manganiello, V. (2004) 'Cyclic nucleotide phosphodiesterase 3A-deficient mice as a model of female infertility', *Journal of Clinical Investigation*, 114(2), 196-205.

Masui, Y. and Pedersen, R. A. (1975) 'Ultraviolet light-induced unscheduled DNA synthesis in mouse oocytes during meiotic maturation', *Nature*, 257(5528), 705-706.

Matos, J. and West, S. C. (2014) 'Holliday junction resolution: Regulation in space and time', *DNA Repair*, 19(100), 176-181.

Matsuda, T., Saijo, M., Kuraoka, I., Kobayashi, T., Nakatsu, Y., Nagai, A., Enjoji, T., Masutani, C., Sugasawa, K., Hanaoka, F. and et al. (1995) 'DNA repair protein XPA binds replication protein A (RPA)', *The Journal of Biological Chemistry*, 270(8), 4152-7.

Matsumoto, Y. and Bogenhagen, D. F. (1991) 'Repair of a synthetic abasic site involves concerted reactions of DNA synthesis followed by excision and ligation', *Molecular and Cellular Biology*, 11(9), 4441-4447.

Matsuoka, S., Huang, M. and Elledge, S. J. (1998) 'Linkage of ATM to cell cycle regulation by the Chk2 protein kinase', *Science*, 282(5395), 1893-7.

Matsuoka, S., Rotman, G., Ogawa, A., Shiloh, Y., Tamai, K. and Elledge, S. J. (2000) 'Ataxia telangiectasia-mutated phosphorylates Chk2 in vivo and in vitro', *PNAS*, 97(19), 10389-10394.

Mayer, A., Baran, V., Sakakibara, Y., Brzakova, A., Ferencova, I., Motlik, J., Kitajima, T. S., Schultz, R. M. and Solc, P. (2016) 'DNA damage response during mouse oocyte maturation', *Cell Cycle*, 15(4), 546-558.

McGuinness, B. E., Anger, M., Kouznetsova, A., Gil-Bernabé, A. M., Helmhart, W., Kudo, N. R., Wuensche, A., Taylor, S., Hoog, C., Novak, B. and Nasmyth, K. (2009) 'Regulation of APC/C Activity in Oocytes by a Bub1-Dependent Spindle Assembly Checkpoint', *Current Biology*, 19(5), 369-380.

McKinnon, P. J. (2004) 'ATM and ataxia telangiectasia', *EMBO Reports*, 5(8), 772-776.

McKinnon, P. J. (2012) 'ATM and the Molecular Pathogenesis of Ataxia Telangiectasia' in Abbas, A. K., Galli, S. J. and Howley, P. M., eds., *Annual Review of Pathology: Mechanisms of Disease, Vol 7*, 303-321.

Mehlmann, L. M. (2005) 'Stops and starts in mammalian oocytes: recent advances in understanding the regulation of meiotic arrest and oocyte maturation', *Reproduction*, 130(6), 791-9.

Mehlmann, L. M., Jones, T. L. Z. and Jaffe, L. A. (2002) 'Meiotic arrest in the mouse follicle maintained by a G(s) protein in the oocyte', *Science*, 297(5585), 1343-1345.

Mehlmann, L. M., Saeki, Y., Tanaka, S., Brennan, T. J., Evsikov, A. V., Pendola, F. L., Knowles, B. B., Eppig, J. J. and Jaffe, L. A. (2004) 'The G(s)-linked receptor GPR3 maintains meiotic arrest in mammalian oocytes', *Science*, 306(5703), 1947-1950.

Meirow, D., Epstein, M., Lewis, H., Nugent, D. and Gosden, R. G. (2001) 'Administration of cyclophosphamide at different stages of follicular maturation in mice: effects on reproductive performance and fetal malformations', *Human Reproduction*, 16(4), 632-7.

Menezo, Y., Jr., Russo, G., Tosti, E., El Mouatassim, S. and Benkhalifa, M. (2007) 'Expression profile of genes coding for DNA repair in human oocytes using pangenomic microarrays, with a special focus on ROS linked decays', *Journal of Assisted Reproduction and Genetics*, 24(11), 513-20.

Molinari, M., Mercurio, C., Dominguez, J., Goubin, F. and Draetta, G. F. (2000) 'Hunan Cdc25 A inactivation in response to S phase inhibition and its role in preventing prematrure mitosis', *EMBO Reports*, 1(1), 71-79.

Monti, M., Zanoni, M., Calligaro, A., Ko, M. S. H., Mauri, P. and Redi, C. A. (2013) 'Developmental Arrest and Mouse Antral Not-Surrounded Nucleolus Oocytes', *Biology of Reproduction*, 88(1), 2.

Moroni, M., Maeda, D., Whitnall, M. H., Bonner, W. M. and Redon, C. E. (2013) 'Evaluation of the Gamma-H2AX Assay for Radiation Biodosimetry in a Swine Model', *International Journal of Molecular Sciences*, 14(7), 14119-14135.

Mukherjee, B., Kessinger, C., Kobayashi, J., Chen, B. P. C., Chen, D. J., Chatterjee, A. and Burma, S. (2006) 'DNA-PK phosphorylates histone H2AX during apoptotic DNA fragmentation in mammalian cells', *DNA Repair*, 5(5), 575-590.

Musacchio, A. (2015) 'The Molecular Biology of Spindle Assembly Checkpoint Signaling Dynamics', *Current Biology*, 25(20), R1002-R1018.

Nagaoka, S. I., Hodges, C. A., Albertini, D. F. and Hunt, P. A. (2011) 'Oocyte-specific differences in cell-cycle control create an innate susceptibility to meiotic errors', *Current Biology*, 21(8), 651-7.

Namiki, Y. and Zou, L. (2006) 'ATRIP associates with replication protein A-coated ssDNA through multiple interactions', *PNAS*, 103(3), 580-5.

Nasmyth, K. and Haering, C. H. (2009) 'Cohesin: its roles and mechanisms', *Annual Review of Genetics*, 43, 525-58.

Neale, M. J., Pan, J. and Keeney, S. (2005) 'Endonucleolytic processing of covalent protein-linked DNA double-strand breaks', *Nature*, 436(7053), 1053-1057.

Niault, T., Hached, K., Sotillo, R., Sorger, P. K., Maro, B., Benezra, R. and Wassmann, K. (2007) 'Changing Mad2 Levels Affects Chromosome Segregation and Spindle Assembly Checkpoint Control in Female Mouse Meiosis I', *Plos One*, 2(11).

Nishi, R., Okuda, Y., Watanabe, E., Mori, T., Iwai, S., Masutani, C., Sugasawa, K. and Hanaoka, F. (2005) 'Centrin 2 stimulates nucleotide excision repair by interacting with xeroderma pigmentosum group C protein', *Molecular and Cellular Biology*, 25(13), 5664-74.

Nitiss, J. L. (2009) 'Targeting DNA topoisomerase II in cancer chemotherapy', *Nature Reviews Cancer*, 9(5), 338-350.

Noda, N. N. and Inagaki, F. (2015) 'Mechanisms of Autophagy', *Annual Review of Biophysics*, 44(1), 101-122.

Nouspikel, T. (2009) 'DNA repair in mammalian cells : Nucleotide excision repair: variations on versatility', *Cellular and Molecular Life Sciences*, 66(6), 994-1009.

Nowsheen, S. and Yang, E. S. (2012) 'The intersection between DNA damage response and cell death pathways', *Experimental oncology*, 34(3), 243-54.

O'Driscoll, M., Ruiz-Perez, V. L., Woods, C. G., Jeggo, P. A. and Goodship, J. A. (2003) 'A splicing mutation affecting expression of ataxia-telangiectasia and Rad3-related protein (ATR) results in Seckel syndrome', *Nature Genetics*, 33(4), 497-501.

Oh, K.-S., Bustin, M., Mazur, S. J., Appella, E. and Kraemer, K. H. (2011) 'UV-induced histone H2AX phosphorylation and DNA damage related proteins accumulate and persist in nucleotide excision repair-deficient XP-B cells', *DNA Repair*, 10(1), 5-15.

Oktay, K., Turan, V., Titus, S., Stobezki, R. and Liu, L. (2015) 'BRCA Mutations, DNA Repair Deficiency, and Ovarian Aging', *Biology of Reproduction*, 93(3).

Orthwein, A., Fradet-Turcotte, A., Noordermeer, S. M., Canny, M. D., Brun, C. M., Strecker, J., Escribano-Diaz, C. and Durocher, D. (2014) 'Mitosis inhibits DNA double-strand break repair to guard against telomere fusions', *Science*, 344(6180), 189-93.

Otsuki, J., Okada, A., Morimoto, K., Nagai, Y. and Kubo, H. (2004) 'The relationship between pregnancy outcome and smooth endoplasmic reticulum clusters in MII human oocytes', *Human Reproduction*, 19(7), 1591-1597.

Palen, W. J., Williamson, C. E., Clauser, A. A. and Schindler, D. E. (2005) 'Impact of UV-B exposure on amphibian embryos: linking species physiology and oviposition behaviour', *Proceedings of the Royal Society of London B: Biological Sciences*, 272(1569), 1227-1234.

Pangas, S. A., Choi, Y., Ballow, D. J., Zhao, Y., Westphal, H., Matzuk, M. M. and Rajkovic, A. (2006) 'Oogenesis requires germ cell-specific transcriptional regulators Sohlh1 and Lhx8', *PNAS*, 103(21), 8090-5.

Patel, A. Y., McDonald, T. M., Spears, L. D., Ching, J. K. and Fisher, J. S. (2011) 'Ataxia telangiectasia mutated influences cytochrome c oxidase activity', *Biochemical and Biophysical Research Communications*, 405(4), 599-603.

Peddibhotla, S., Lam, M. H., Gonzalez-Rimbau, M. and Rosen, J. M. (2009) 'The DNA-damage effector checkpoint kinase 1 is essential for chromosome segregation and cytokinesis', *PNAS*, 106(13), 5159-5164.

Peng, A. (2013) 'Working hard for recovery: mitotic kinases in the DNA damage checkpoint', *Cell & Bioscience*, 3, 20-20.

Pepling, M. E. and Spradling, A. C. (2001) 'Mouse Ovarian Germ Cell Cysts Undergo Programmed Breakdown to Form Primordial Follicles', *Developmental Biology*, 234(2), 339-351.

Perez, G. I., Acton, B. M., Jurisicova, A., Perkins, G. A., White, A., Brown, J., Trbovich, A. M., Kim, M. R., Fissore, R., Xu, J., Ahmady, A., D'Estaing, S. D., Li, H., Kagawa, W., Kurumizaka, H., Yokoyama, S., Okada, H., Mak, T. W., Ellisman, M. H., Casper, R. F. and Tilly, J. L. (2007) 'Genetic variance modifies apoptosis susceptibility in mature oocytes via alterations in DNA repair capacity and mitochondrial ultrastructure', *Cell Death and Differentiation*, 14(3), 524-533.

Petruseva, I. O., Evdokimov, A. N. and Lavrik, O. I. (2014) 'Molecular Mechanism of Global Genome Nucleotide Excision Repair', *Acta Naturae*, 6(1), 23-34.

Petukhova, G. V., Pezza, R. J., Vanevski, F., Ploquin, M., Masson, J. Y. and Camerini-Otero, R. D. (2005) 'The Hop2 and Mnd1 proteins act in concert with Rad51 and Dmc1 in meiotic recombination', *Nature structural & molecular biology*, 12(5), 449-53.

Petukhova, G. V., Romanienko, P. J. and Camerini-Otero, R. D. (2003) 'The Hop2 Protein Has a Direct Role in Promoting Interhomolog Interactions during Mouse Meiosis', *Developmental Cell*, 5(6), 927-936.

Pezza, R. J., Voloshin, O. N., Volodin, A. A., Boateng, K. A., Bellani, M. A., Mazin, A. V. and Camerini-Otero, R. D. (2014) 'The dual role of HOP2 in mammalian meiotic homologous recombination', *Nucleic Acids Research*, 42(4), 2346-2357.

Pines, J. (2011) 'Cubism and the cell cycle: the many faces of the APC/C', *Nature Reviews Molecular Cell Biology*, 12(7), 427-438.

Pittman, D. L., Cobb, J., Schimenti, K. J., Wilson, L. A., Cooper, D. M., Brignull, E., Handel, M. A. and Schimenti, J. C. (1998) 'Meiotic prophase arrest with failure of chromosome synapsis in mice deficient for Dmc1, a germline-specific RecA homolog', *Molecular Cell*, 1(5), 697-705.

Podhorecka, M., Skladanowski, A. and Bozko, P. (2010) 'H2AX Phosphorylation: Its Role in DNA Damage Response and Cancer Therapy', *Journal of nucleic acids*, 2010.

Povirk, L. F. (1996) 'DNA damage and mutagenesis by radiomimetic DNA-cleaving agents: Bleomycin, neocarzinostatin and other enediynes', *Mutation Research-Fundamental and Molecular Mechanisms of Mutagenesis,* 355(1-2), 71-89.

Rajkovic, A., Pangas, S. A., Ballow, D., Suzumori, N. and Matzuk, M. M. (2004) 'NOBOX deficiency disrupts early folliculogenesis and oocyte-specific gene expression', *Science,* 305(5687), 1157-9.

Ramamoorthy, M., Tadokoro, T., Rybanska, I., Ghosh, A. K., Wersto, R., May, A., Kulikowicz, T., Sykora, P., Croteau, D. L. and Bohr, V. A. (2012) 'RECQL5 cooperates with Topoisomerase II alpha in DNA decatenation and cell cycle progression', *Nucleic Acids Research,* 40(4), 1621-35.

Raso, A., Vecchio, D., Cappelli, E., Ropolo, M., Poggi, A., Nozza, P., Biassoni, R., Mascelli, S., Capra, V., Kalfas, F., Severi, P. and Frosina, G. (2012) 'Characterization of Glioma Stem Cells Through Multiple Stem Cell Markers and Their Specific Sensitization to Double-Strand Break-Inducing Agents by Pharmacological Inhibition of Ataxia Telangiectasia Mutated Protein', *Brain Pathology,* 22(5), 677-688.

Rastogi, R. P., Richa, Kumar, A., Tyagi, M. B. and Sinha, R. P. (2010) 'Molecular mechanisms of ultraviolet radiation-induced DNA damage and repair', *Journal of nucleic acids,* 2010, 592980-592980.

Reddy, P., Liu, L., Adhikari, D., Jagarlamudi, K., Rajareddy, S., Shen, Y., Du, C., Tang, W., Hamalainen, T., Peng, S. L., Lan, Z. J., Cooney, A. J., Huhtaniemi, I. and Liu, K. (2008) 'Oocyte-specific deletion of Pten causes premature activation of the primordial follicle pool', *Science,* 319(5863), 611-3.

Redon, C. E., Dickey, J. S., Bonner, W. M. and Sedelnikova, O. A. (2009) 'γ-H2AX as a biomarker of DNA damage induced by ionizing radiation in human peripheral blood lymphocytes and artificial skin', *Advances in space research : the official journal of the Committee on Space Research (COSPAR),* 43(8), 1171-1178.

Reis, A., Chang, H.-Y., Levasseur, M. and Jones, K. T. (2006) 'APCcdh1 activity in mouse oocytes prevents entry into the first meiotic division', *Nature Cell Biology,* 8, 539-540.

Reis, A., Madgwick, S., Chang, H.-Y., Nabti, I., Levasseur, M. and Jones, K. T. (2007) 'Prometaphase APC(cdh1) activity prevents non-disjunction in mammalian oocytes', *Nature Cell Biology,* 9(10), 1192-1198.

Reynolds, A., Qiao, H., Yang, Y., Chen, J. K., Jackson, N., Biswas, K., Holloway, J. K., Baudat, F., de Massy, B., Wang, J., Hoog, C., Cohen, P. E. and Hunter, N. (2013) 'RNF212 is a

dosage-sensitive regulator of crossing-over during mammalian meiosis', *Nature Genetics*, 45(3), 269-78.

Richard, S. and Baltz, J. M. (2014) 'Prophase I Arrest of Mouse Oocytes Mediated by Natriuretic Peptide Precursor C Requires GJA1 (connexin-43) and GJA4 (connexin-37) Gap Junctions in the Antral Follicle and Cumulus-Oocyte Complex', *Biology of Reproduction*, 90(6), 137.

Robinson, J. W., Shuhaibar, L. C., Eppig, J. J., Potter, L. R. and Jaffe, L. A. (2011) 'Luteinizing Hormone Reduces Guanylyl Cyclase Activity in the Granulosa Cells of the Mouse Ovary, Leading to the Resumption of Meiosis in the Oocyte', *Molecular Biology of the Cell*, 22, 1.

Rogakou, E. P., Pilch, D. R., Orr, A. H., Ivanova, V. S. and Bonner, W. M. (1998) 'DNA Double-stranded Breaks Induce Histone H2AX Phosphorylation on Serine 139', *Journal of Biological Chemistry*, 273(10), 5858-5868.

Romanienko, P. J. and Camerini-Otero, R. D. (2000) 'The Mouse Spo11 Gene Is Required for Meiotic Chromosome Synapsis', *Molecular Cell*, 6(5), 975-987.

Roness, H., Kalich-Philosoph, L. and Meirow, D. (2014) 'Prevention of chemotherapy-induced ovarian damage: possible roles for hormonal and non-hormonal attenuating agents', *Human Reproduction Update*, 20(5), 759-774.

Roos, W. P. and Kaina, B. (2006) 'DNA damage-induced cell death by apoptosis', *Trends in Molecular Medicine*, 12(9), 440-450.

Roos, W. P. and Kaina, B. (2013) 'DNA damage-induced cell death: From specific DNA lesions to the DNA damage response and apoptosis', *Cancer Letters*, 332(2), 237-248.

Royou, A., Macias, H. and Sullivan, W. (2005) 'The Drosophila Grp/Chk1 DNA damage checkpoint controls entry into anaphase', *Current Biology*, 15(4), 334-339.

Saito, S. i., Goodarzi, A. A., Higashimoto, Y., Noda, Y., Lees-Miller, S. P., Appella, E. and Anderson, C. W. (2002) 'ATM Mediates Phosphorylation at Multiple p53 Sites, Including Ser46, in Response to Ionizing Radiation', *Journal of Biological Chemistry*, 277(15), 12491-12494.

Sancar, A., Lindsey-Boltz, L. A., Unsal-Kacmaz, K. and Linn, S. (2004) 'Molecular mechanisms of mammalian DNA repair and the DNA damage checkpoints', *Annual Review of Biochemistry*, 73, 39-85.

Sánchez, F. and Smitz, J. (2012) 'Molecular control of oogenesis', *Biochimica et Biophysica Acta (BBA) - Molecular Basis of Disease,* 1822(12), 1896-1912.

Santaguida, S., Tighe, A., D'Alise, A. M., Taylor, S. S. and Musacchio, A. (2010) 'Dissecting the role of MPS1 in chromosome biorientation and the spindle checkpoint through the small molecule inhibitor reversine', *The Journal of Cell Biology,* 190(1), 73-87.

Sartori, A. A., Lukas, C., Coates, J., Mistrik, M., Fu, S., Bartek, J., Baer, R., Lukas, J. and Jackson, S. P. (2007) 'Human CtIP promotes DNA end resection', *Nature,* 450(7169), 509-514.

Scarpato, R., Castagna, S., Aliotta, R., Azzara, A., Ghetti, F., Filomeni, E., Giovannini, C., Pirillo, C., Testi, S., Lombardi, S. and Tomei, A. (2013) 'Kinetics of nuclear phosphorylation (gamma-H2AX) in human lymphocytes treated in vitro with UVB, bleomycin and mitomycin C', *Mutagenesis,* 28(4), 465-73.

Scharer, O. D. (2013) 'Nucleotide excision repair in eukaryotes', *Cold Spring Harbor Perspectives in Biology,* 5(10), a012609.

Scherz-Shouval, R. and Elazar, Z. (2011) 'Regulation of autophagy by ROS: physiology and pathology', *Trends in Biochemical Sciences,* 36(1), 30-8.

Schuh, M. and Ellenberg, J. (2007) 'Self-organization of MTOCs replaces centrosome function during acentrosomal spindle assembly in live mouse oocytes', *Cell,* 130(3), 484-98.

Sebestova, J., Danylevska, A., Novakova, L., Kubelka, M. and Anger, M. (2012) 'Lack of response to unaligned chromosomes in mammalian female gametes', *Cell Cycle,* 11(16), 3011-8.

Seki, M., Nakagawa, T., Seki, T., Kato, G., Tada, S., Takahashi, Y., Yoshimura, A., Kobayashi, T., Aoki, A., Otsuki, M., Habermann, F. A., Tanabe, H., Ishii, Y. and Enomoto, T. (2006) 'Bloom helicase and DNA topoisomerase IIIalpha are involved in the dissolution of sister chromatids', *Molecular Cell Biology,* 26(16), 6299-307.

Severson, A. F., von Dassow, G. and Bowerman, B. (2016) 'Chapter Five - Oocyte Meiotic Spindle Assembly and Function' in Paul, M. W., ed. *Current Topics in Developmental Biology*, Academic Press, 65-98.

Sharan, S. K., Pyle, A., Coppola, V., Babus, J., Swaminathan, S., Benedict, J., Swing, D., Martin, B. K., Tessarollo, L., Evans, J. P., Flaws, J. A. and Handel, M. A. (2004) 'BRCA2 deficiency in mice leads to meiotic impairment and infertility', *Development,* 131(1), 131-42.

Shelling, A. N. (2010) 'Premature ovarian failure', *Reproduction*, 140(5), 633-641.

Shen, K. C., Heng, H., Wang, Y., Lu, S., Liu, G., Deng, C. X., Brooks, S. C. and Wang, Y. A. (2005) 'ATM and p21 cooperate to suppress aneuploidy and subsequent tumor development', *Cancer Research*, 65(19), 8747-53.

Shiloh, Y. (2003) 'ATM and related protein kinases: safeguarding genome integrity', *Nature Reviews Cancer*, 3(3), 155-68.

Shiloh, Y. and Ziv, Y. (2013) 'The ATM protein kinase: regulating the cellular response to genotoxic stress, and more', *Nature Reviews Molecular Cell Biology*, 14(4), 197-210.

Shiotani, B. and Zou, L. (2009) 'ATR signaling at a glance', *Journal of Cell Science*, 122(3), 301-304.

Sinha, R. P. and Hader, D. P. (2002) 'UV-induced DNA damage and repair: a review', *Photochemical & Photobiological Sciences*, 1(4), 225-236.

Sivasakthivel, T. and Reddy, K. K. S. K. (2011) 'Ozone Layer Depletion and Its Effects: A Review', *International Journal of Environmental Science and Development*, 2(1), 30-37.

Skaznik-Wikiel, M. E., Gilbert, S. B., Meacham, R. B. and Kondapalli, L. A. (2015) 'Fertility Preservation Options for Men and Women With Cancer', *Reviews in Urology*, 17(4), 211-219.

So, S., Davis, A. J. and Chen, D. J. (2009) 'Autophosphorylation at serine 1981 stabilizes ATM at DNA damage sites', *The Journal of Cell Biology*, 187(7), 977-990.

Solc, P., Schultz, R. M. and Motlik, J. (2010) 'Prophase I arrest and progression to metaphase I in mouse oocytes: comparison of resumption of meiosis and recovery from G2-arrest in somatic cells', *Molecular Human Reproduction*, 16(9), 654-64.

Soleimani, R., Heytens, E., Darzynkiewicz, Z. and Oktay, K. (2011) 'Mechanisms of chemotherapy-induced human ovarian aging: double strand DNA breaks and microvascular compromise', *Aging (Albany NY)*, 3(8), 782-793.

Soutoglou, E., Dorn, J. F., Sengupta, K., Jasin, M., Nussenzweig, A., Ried, T., Danuser, G. and Misteli, T. (2007) 'Positional stability of single double-strand breaks in mammalian cells', *Nature Cell Biology,* 9(6), 675-82.

Stark, G. R. and Taylor, W. R. (2004) 'Analyzing the G2/M checkpoint', *Methods in Molecular Biology,* 280, 51-82.

Strome, S. and Updike, D. (2015) 'Specifying and protecting germ cell fate', *Nature Reviews Molecular Cell Biology,* 16(7), 406-416.

Stucki, M., Clapperton, J. A., Mohammad, D., Yaffe, M. B., Smerdon, S. J. and Jackson, S. P. (2005) 'MDC1 Directly Binds Phosphorylated Histone H2AX to Regulate Cellular Responses to DNA Double-Strand Breaks', *Cell,* 123(7), 1213-1226.

Sudakin, V., Chan, G. K. T. and Yen, T. J. (2001) 'Checkpoint inhibition of the APC/C in HeLa cells is mediated by a complex of BUBR1, BUB3, CDC20, and MAD2', *The Journal of Cell Biology,* 154(5), 925-936.

Sugasawa, K., Masutani, C., Uchida, A., Maekawa, T., van der Spek, P. J., Bootsma, D., Hoeijmakers, J. H. and Hanaoka, F. (1996) 'HHR23B, a human Rad23 homolog, stimulates XPC protein in nucleotide excision repair in vitro', *Molecular and Cellular Biology,* 16(9), 4852-61.

Suh, E. K., Yang, A., Kettenbach, A., Bamberger, C., Michaelis, A. H., Zhu, Z., Elvin, J. A., Bronson, R. T., Crum, C. P. and McKeon, F. (2006) 'p63 protects the female germ line during meiotic arrest', *Nature,* 444(7119), 624-8.

Sun, M.-H., Zheng, J., Xie, F.-Y., Shen, W., Yin, S. and Ma, J.-Y. (2015) 'Cumulus Cells Block Oocyte Meiotic Resumption via Gap Junctions in Cumulus Oocyte Complexes Subjected to DNA Double-Strand Breaks', *Plos One,* 10(11), e0143223.

Sun, S.-C. and Kim, N.-H. (2012) 'Spindle assembly checkpoint and its regulators in meiosis', *Human Reproduction Update,* 18(1), 60-72.

Sung, P., Krejci, L., Van Komen, S. and Sehorn, M. G. (2003) 'Rad51 recombinase and recombination mediators', *Journal of Biological Chemistry,* 278(44), 42729-42732.

Sweigert, S. E. and Carroll, D. (1990) 'Repair and recombination of X-irradiated plasmids in Xenopus laevis oocytes', *Molecular and Cellular Biology,* 10(11), 5849-56.

Swuec, P. and Costa, A. (2014) 'Molecular mechanism of double Holliday junction dissolution', *Cell & Bioscience*, 4, 36-36.

Taccioli, G. E., Amatucci, A. G., Beamish, H. J., Gell, D., Xiang, X. H., Torres Arzayus, M. I., Priestley, A., Jackson, S. P., Marshak Rothstein, A., Jeggo, P. A. and Herrera, V. L. (1998) 'Targeted disruption of the catalytic subunit of the DNA-PK gene in mice confers severe combined immunodeficiency and radiosensitivity', *Immunity*, 9(3), 355-66.

Tachibana-Konwalski, K., Godwin, J., van der Weyden, L., Champion, L., Kudo, N. R., Adams, D. J. and Nasmyth, K. (2010) 'Rec8-containing cohesin maintains bivalents without turnover during the growing phase of mouse oocytes', *Genes & Development*, 24(22), 2505-16.

Tamura, H., Takasaki, A., Miwa, I., Taniguchi, K., Maekawa, R., Asada, H., Taketani, T., Matsuoka, A., Yamagata, Y., Shimamura, K., Morioka, H., Ishikawa, H., Reiter, R. J. and Sugino, N. (2008) 'Oxidative stress impairs oocyte quality and melatonin protects oocytes from free radical damage and improves fertilization rate', *Journal of Pineal Research*, 44(3), 280-7.

Tapia-Alveal, C., Calonge, T. M. and O'Connell, M. J. (2009) 'Regulation of Chk1', *Cell Division*, 4(1), 1-7.

Taylor, A. M. R., Groom, A. and Byrd, P. J. (2004) 'Ataxia-telangiectasia-like disorder (ATLD)—its clinical presentation and molecular basis', *DNA Repair*, 3(8–9), 1219-1225.

Terasawa, M., Shinohara, A. and Shinohara, M. (2014) 'Canonical Non-Homologous End Joining in Mitosis Induces Genome Instability and Is Suppressed by M-phase-Specific Phosphorylation of XRCC4', *Plos Genetics*, 10(8), e1004563.

Terret, M.-E. and Jallepalli, P. V. (2006) 'Meiosis: separase strikes twice', *Nature Cell Biology*, 8(9), 910-911.

Terret, M. E., Wassmann, K., Waizenegger, I., Maro, B., Peters, J.-M. and Verlhac, M.-H. (2003) 'The Meiosis I-to-Meiosis II Transition in Mouse Oocytes Requires Separase Activity', *Current Biology*, 13(20), 1797-1802.

Thornton, B. R. and Toczyski, D. P. (2003) 'Securin and B-cyclin/CDK are the only essential targets of the APC', *Nature Cell Biology*, 5(12), 1090-1094.

Thorslund, T., Esashi, F. and West, S. C. (2007) 'Interactions between human BRCA2 protein and the meiosis-specific recombinase DMC1', *The EMBO Journal*, 26(12), 2915-22.

Timofeev, O., Cizmecioglu, O., Settele, F., Kempf, T. and Hoffmann, I. (2010) 'Cdc25 phosphatases are required for timely assembly of CDK1-cyclin B at the G2/M transition', *The Journal of Biological Chemistry*, 285(22), 16978-90.

Tipton, A. R., Ji, W., Sturt-Gillespie, B., Bekier, M. E., 2nd, Wang, K., Taylor, W. R. and Liu, S. T. (2013) 'Monopolar spindle 1 (MPS1) kinase promotes production of closed MAD2 (C-MAD2) conformer and assembly of the mitotic checkpoint complex', *The Journal of Biological Chemistry*, 288(49), 35149-58.

Titus, S., Li, F., Stobezki, R., Akula, K., Unsal, E., Jeong, K., Dickler, M., Robson, M., Moy, F., Goswami, S. and Oktay, K. (2013) 'Impairment of BRCA1-related DNA double-strand break repair leads to ovarian aging in mice and humans', *Science Translational Medicine*, 5(172), 172ra21.

Tomasini, R., Tsuchihara, K., Tsuda, C., Lau, S. K., Wilhelm, M., Ruffini, A., Tsao, M.-s., Iovanna, J. L., Jurisicova, A., Melino, G. and Mak, T. W. (2009) 'TAp73 regulates the spindle assembly checkpoint by modulating BubR1 activity', *PNAS*, 106(3), 797-802.

Tomasini, R., Tsuchihara, K., Wilhelm, M., Fujitani, M., Rufini, A., Cheung, C. C., Khan, F., Itie-Youten, A., Wakeham, A., Tsao, M.-s., Iovanna, J. L., Squire, J., Jurisica, I., Kaplan, D., Melino, G., Jurisicova, A. and Mak, T. W. (2008) 'TAp73 knockout shows genomic instability with infertility and tumor suppressor functions', *Genes & Development*, 22(19), 2677-2691.

Touati, S. A., Buffin, E., Cladiere, D., Hached, K., Rachez, C., van Deursen, J. M. and Wassmann, K. (2015) 'Mouse oocytes depend on BubR1 for proper chromosome segregation but not for prophase I arrest', *Nature Communications*, 6.

Toulany, M., Mihatsch, J., Holler, M., Chaachouay, H. and Rodemann, H. P. (2014) 'Cisplatin-mediated radiosensitization of non-small cell lung cancer cells is stimulated by ATM inhibition', *Radiotherapy and Oncology*, 111(2), 228-236.

Tritarelli, A., Oricchio, E., Ciciarello, M., Mangiacasale, R., Palena, A., Lavia, P., Soddu, S. and Cundari, E. (2004) 'p53 Localization at Centrosomes during Mitosis and Postmitotic Checkpoint Are ATM-dependent and Require Serine 15 Phosphorylation', *Molecular Biology of the Cell*, 15(8), 3751-3757.

Tsutsumi, M., Fujiwara, R., Nishizawa, H., Ito, M., Kogo, H., Inagaki, H., Ohye, T., Kato, T., Fujii, T. and Kurahashi, H. (2014) 'Age-Related Decrease of Meiotic Cohesins in Human Oocytes', *Plos One*, 9(5), 8.

Turinetto, V. and Giachino, C. (2015) 'Multiple facets of histone variant H2AX: a DNA double-strand-break marker with several biological functions', *Nucleic Acids Research*, 43(5), 2489-2498.

Uziel, T., Lerenthal, Y., Moyal, L., Andegeko, Y., Mittelman, L. and Shiloh, Y. (2003) 'Requirement of the MRN complex for ATM activation by DNA damage', *Embo Journal*, 22(20), 5612-5621.

Vakifahmetoglu, H., Olsson, M. and Zhivotovsky, B. (2008) 'Death through a tragedy: mitotic catastrophe', *Cell Death & Differentiation*, 15(7), 1153-1162.

Van Blerkom, J. (1990) 'Occurrence and developmental consequences of aberrant cellular organization in meiotically mature human oocytes after exogenous ovarian hyperstimulation', *Journal of Electron Microscopy Technique*, 16(4), 324-46.

van den Bosch, M., Bree, R. T. and Lowndes, N. F. (2003) 'The MRN complex: coordinating and mediating the response to broken chromosomes', *EMBO Reports*, 4(9), 844-849.

Velic, D., Couturier, A. M., Ferreira, M. T., Rodrigue, A., Poirier, G. G., Fleury, F. and Masson, J.-Y. (2015) 'DNA Damage Signalling and Repair Inhibitors: The Long-Sought-After Achilles' Heel of Cancer', *Biomolecules*, 5(4), 3204-3259.

Wallbutton, S. and Kasraie, J. (2010) 'Vacuolated oocytes: fertilization and embryonic arrest following intra-cytoplasmic sperm injection in a patient exhibiting persistent oocyte macro vacuolization—Case report', *Journal of Assisted Reproduction and Genetics*, 27(4), 183-188.

Wang, H., Luo, Y., Zhao, M. H., Lin, Z., Kwon, J., Cui, X. S. and Kim, N. H. (2015a) 'DNA double-strand breaks disrupted the spindle assembly in porcine oocytes', *Molecular Reproduction and Development*.

Wang, H., Zhang, X., Teng, L. and Legerski, R. J. (2015b) 'DNA damage checkpoint recovery and cancer development', *Experimental Cell Research*, 334(2), 350-358.

Wang, H. Y., Wang, H. C., Powell, S. N., Iliakis, G. and Wang, Y. (2004) 'ATR affecting cell radiosensitivity is dependent on homologous recombination repair but independent of nonhomologous end joining', *Cancer Research*, 64(19), 7139-7143.

Ward, I. M. and Chen, J. (2001) 'Histone H2AX Is Phosphorylated in an ATR-dependent Manner in Response to Replicational Stress', *Journal of Biological Chemistry*, 276(51), 47759-47762.

Wardman, P. (2007) 'Chemical Radiosensitizers for Use in Radiotherapy', *Clinical Oncology,* 19(6), 397-417.

Wassmann, K., Niault, T. and Maro, B. (2003) 'Metaphase I Arrest upon Activation of the Mad2-Dependent Spindle Checkpoint in Mouse Oocytes', *Current Biology,* 13(18), 1596-1608.

Watanabe, Y. (2012) 'Geometry and force behind kinetochore orientation: lessons from meiosis', *Nature Reviews Molecular Cell Biology,* 13(6), 370-382.

Waters, J. C., Chen, R.-H., Murray, A. W. and Salmon, E. D. (1998) 'Localization of Mad2 to Kinetochores Depends on Microtubule Attachment, Not Tension', *The Journal of Cell Biology,* 141(5), 1181-1191.

Weber, A. M. and Ryan, A. J. (2015) 'ATM and ATR as therapeutic targets in cancer', *Pharmacology & Therapeutics,* 149, 124-138.

Wei, L., Liang, X.-W., Zhang, Q.-H., Li, M., Yuan, J., Li, S., Sun, S.-C., Ouyang, Y.-C., Schatten, H. and Sun, Q.-Y. (2010) 'BubR1 is a spindle assembly checkpoint protein regulating meiotic cell cycle progression of mouse oocyte', *Cell Cycle,* 9(6), 1112-1121.

Willis, N. and Rhind, N. (2009) 'Regulation of DNA replication by the S-phase DNA damage checkpoint', *Cell Division,* 4(1), 1-10.

Woodbine, L., Brunton, H., Goodarzi, A. A., Shibata, A. and Jeggo, P. A. (2011) 'Endogenously induced DNA double strand breaks arise in heterochromatic DNA regions and require ataxia telangiectasia mutated and Artemis for their repair', *Nucleic Acids Research,* 39(16), 6986-97.

Wyatt, Haley D. M., Sarbajna, S., Matos, J. and West, Stephen C. (2013) 'Coordinated Actions of SLX1-SLX4 and MUS81-EME1 for Holliday Junction Resolution in Human Cells', *Molecular Cell,* 52(2), 234-247.

Xu, X., Tsvetkov, L. M. and Stern, D. F. (2002) 'Chk2 activation and phosphorylation-dependent oligomerization', *Molecular and Cellular Biology,* 22(12), 4419-32.

Yamagishi, Y., Yang, C. H., Tanno, Y. and Watanabe, Y. (2012) 'MPS1/Mph1 phosphorylates the kinetochore protein KNL1/Spc7 to recruit SAC components', *Nature Cell Biology,* 14(7), 746-52.

Yang, C., Tang, X., Guo, X., Niikura, Y., Kitagawa, K., Cui, K., Wong, S. T., Fu, L. and Xu, B. (2011) 'Aurora-B mediated ATM serine 1403 phosphorylation is required for mitotic ATM activation and the spindle checkpoint', *Molecular Cell,* 44(4), 597-608.

Yang, C., Wang, H., Xu, Y., Brinkman, K. L., Ishiyama, H., Wong, S. T. C. and Xu, B. (2012) 'The kinetochore protein Bub1 participates in the DNA damage response', *DNA Repair,* 11(2), 185-191.

Yang, Y. P., Liang, Z. Q., Gu, Z. L. and Qin, Z. H. (2005) 'Molecular mechanism and regulation of autophagy', *Acta Pharmacologica Sinica,* 26(12), 1421-34.

Yano, K.-i., Morotomi-Yano, K., Wang, S.-Y., Uematsu, N., Lee, K.-J., Asaithamby, A., Weterings, E. and Chen, D. J. (2008) 'Ku recruits XLF to DNA double-strand breaks', *EMBO Reports,* 9(1), 91-96.

Yin, S., Wang, Q., Liu, J.-H., Ai, J.-S., Liang, C.-G., Hou, Y., Chen, D.-Y., Schatten, H. and Sun, Q.-Y. (2006) 'Bub1 prevents chromosome misalignment and precocious anaphase during mouse oocyte meiosis', *Cell Cycle,* 5(18), 2130-2137.

Youds, J. L. and Boulton, S. J. (2011) 'The choice in meiosis – defining the factors that influence crossover or non-crossover formation', *Journal of Cell Science,* 124(4), 501-513.

Yuen, W. S., Merriman, J. A., O'Bryan, M. K. and Jones, K. T. (2012) 'DNA Double Strand Breaks but Not Interstrand Crosslinks Prevent Progress through Meiosis in Fully Grown Mouse Oocytes', *Plos One,* 7(8).

Zachos, G., Black, E. J., Walker, M., Scott, M. T., Vagnarelli, P., Earnshaw, W. C. and Gillespie, D. A. F. (2007) 'Chk1 is required for spindle checkpoint function', *Developmental Cell,* 12(2), 247-260.

Zannini, L., Delia, D. and Buscemi, G. (2014) 'CHK2 kinase in the DNA damage response and beyond', *Journal of Molecular Cell Biology,* 6(6), 442-457.

Zaremba, T. G., LeBon, T. R., Millar, D. B., Smejkal, R. M. and Hawley, R. J. (1984) 'Effects of ultraviolet light on the in vitro assembly of microtubules', *Biochemistry,* 23(6), 1073-1080.

Zhang, D., Ma, W., Li, Y.-H., Hou, Y., Li, S.-W., Meng, X.-Q., Sun, X.-F., Sun, Q.-Y. and Wang, W.-H. (2004) 'Intra-oocyte Localization of MAD2 and Its Relationship with Kinetochores, Microtubules, and Chromosomes in Rat Oocytes During Meiosis', *Biology of Reproduction,* 71(3), 740-748.

Zhang, M., Su, Y.-Q., Sugiura, K., Xia, G. and Eppig, J. J. (2010) 'Granulosa Cell Ligand NPPC and Its Receptor NPR2 Maintain Meiotic Arrest in Mouse Oocytes', *Science Signaling*, 3(144).

Zhang, S., Hemmerich, P. and Grosse, F. (2007) 'Centrosomal localization of DNA damage checkpoint proteins', *Journal of Cellular Biochemistry*, 101(2), 451-65.

Zhang, T., Zhang, G. L., Ma, J. Y., Qi, S. T., Wang, Z. B., Wang, Z. W., Luo, Y. B., Jiang, Z. Z., Schatten, H. and Sun, Q. Y. (2014) 'Effects of DNA damage and short-term spindle disruption on oocyte meiotic maturation', *Histochemistry and Cell Biology*, 142(2), 185-194.

Zhang, Y. and Hunter, T. (2014) 'Roles of Chk1 in cell biology and cancer therapy', *International Journal of Cancer*, 134(5), 1013-23.

Zhao, H. and Piwnica-Worms, H. (2001) 'ATR-mediated checkpoint pathways regulate phosphorylation and activation of human Chk1', *Molecular and Cellular Biology*, 21(13), 4129-39.

Zhou, B. S. and Elledge, S. J. (2000) 'The DNA damage response: putting checkpoints in perspective', *Nature*, 408, 433-439.

Zuccotti, M., Garagna, S., Merico, V., Monti, M. and Alberto Redi, C. (2005) 'Chromatin organisation and nuclear architecture in growing mouse oocytes', *Molecular and Cellular Endocrinology*, 234(1–2), 11-17.